On the Analysis of Mouse Behavior

Laura Bethany Murdaugh

Dissertation submitted to the faculty of the Virginia Polytechnic Institute and State University in partial fulfillment of the requirements for the degree of

Doctor of Philosophy

In

Translational Biology, Medicine, and Health

Matthew W. Buczynski, Chair

Michelle H. Theus

Sujith Vijayan

Susan L. Campbell

Carla V. Finkelstein

1.1.2023

Keywords: rodent models, behavior, goal-directed, affective, operant,

On the Analysis of Mouse Behavior

Laura Bethany Murdaugh

ABSTRACT

Accurate and high throughput methods of measuring animal behavior are critical for many branches of neuroscience, allowing for mechanistic studies and preclinical drug testing. Methodological limitations contribute to narrow investigations, which may overlook the interplay between distinct but related behaviors, like affective behaviors and executive function (EF). To prevent such oversight, researchers can perform test batteries, or multiple assessments in one study. However, test batteries often exclude cognitive behaviors due to their lengthy testing period. This dissertation first reviews current evidence related to the investigation and relation of affective, pain-like, and operant behaviors in rodent models. Then, I demonstrate the use of traditional and novel test batteries to investigate these behavioral changes in multiple mouse models.

First, I investigated affective and pain-like behavior in mice lacking *Nape-pld,* a key enzyme that synthesizes lipid mediators which activate receptors in the endocannabinoid system. I found that these mice displayed reduced sucrose preference, but otherwise normal anxiety- and depression-like behavior, and had baseline differences in thermal nociception and inflammation response. Then, I investigated the affective, pain-like, and operant effects of chronic vapor exposure (CVE) to vehicle or nicotine (NIC). Regardless of NIC content, acute abstinence from CVE increased mechanical sensitivity and self-grooming, while chronic abstinence from NIC CVE resulted in motor stimulation. Other traditional anxiety- and depression-like behaviors were unchanged by CVE. In an operant test battery, acute abstinence from NIC CVE impaired acquisition, decreased sucrose motivation, and impaired the response to aversive rewards. Finally, I developed a protocol for the high throughput analysis of six operant tests which can be completed in as few as nineteen sessions, significantly fewer sessions than traditional operant tests. This battery investigates multiple aspects of goal-directed behavior and EF including operant acquisition, cognitive flexibility, reward devaluation, motivation via response to increased instrumental effort, cue devaluation or the extinction of learned behavior, and reacquisition. I validated several of these tests by demonstrating that lesions to specific subregions of the orbitofrontal cortex impaired cognitive flexibility and altered response to instrumental effort as observed in traditional operant tests. I then used this battery to investigate the effects of the P129T

mutation, which results in a mutated version of the Fatty Acid Amide Hydrolase (FAAH) enzyme that is associated with addiction, in male and female mice. Knock-in animals displayed reduced activity in response to increasing instrumental effort, and reduced activity on the first day of an extinction test. Then, to encourage others to use this new operant battery I outlined how to efficiently collect data, shared a database for customizable analysis, and described common issues and how to solve them. This protocol has potential implications for many aspects of neuroscience including the investigation of novel therapeutics and the neural circuitry underlying behaviors.

Together, the information in this dissertation demonstrates the utility of multi-faceted behavioral assays and the combination of traditional and novel approaches to collect more comprehensive behavioral data, which will allow researchers to better investigate neural circuitry underlying behaviors or the behavioral changes associated with novel therapeutics.

On the Analysis of Mouse Behavior

Laura Bethany Murdaugh

GENERAL AUDIENCE ABSTRACT

By measuring animal behavior researchers can gain insight into how specific brain regions interact to influence choice and action. Limitations in testing methods mean that researchers may fail to investigate the relationship between distinct aspects of behavior, like the influence of emotional state or pain on cognition. To prevent such oversight researchers can perform a test battery, a specific series of multiple tests that measures several different aspects of behavior. Traditional test batteries often overlook cognitive or operant (learning to perform an action for reward) behaviors due to time constraints, which limits their translational potential. This dissertation provides a brief overview of the ways that researchers investigate affective (emotional), pain-like (physical discomfort), and goal-directed behaviors. It further has a broad focus on mouse models related to addiction or the endocannabinoid system (ECS), which is shown to play a role in mood, pain (e.g., perception, relief, and inflammation), and cognition. Using a traditional test battery, we demonstrate that mice lacking a key enzyme in the ECS have altered responses to sugar, heat, and inflammation, but display otherwise normal performance in anxiety-, depression-, and pain-like tests. Next, we used a combined traditional and operant battery to investigate the effects of chronic vapor exposure (CVE) and nicotine in mice. We found that regardless of nicotine content, acute abstinence from CVE increased physical sensitivity and self-grooming but spared other anxiety- and depression-like behaviors. Acute abstinence from nicotine CVE resulted in motor stimulation, impaired operant learning, lower motivation for sucrose reward, and an impaired ability to withhold responding when presented with a bitter reward. Finally, I outline a novel operant test battery that addresses the limitations of current operant chamber- or place-based batteries. Using this battery, I first demonstrate that it captures similar behavioral changes to those seen in traditional operant chambers. Then, I demonstrate that mice containing an ECS mutation associated with problem drug use in humans display less motivation for food reward in response to increased effort, and more quickly inhibit a learned behavior when reward delivery is interrupted. I also found that in response to increased effort for reward or bitter rewards, male mice are more likely to alter their behavioral strategy. To

encourage others to use this new operant battery I outlined how to efficiently collect data, shared a database for customizable analysis, and described common issues and how to solve them. This protocol has the potential to improve upon traditional tasks while opening cognitive research to more scientists. This has implications for many fields of neuroscience, especially the investigation of novel therapeutics and investigation of the neural circuitry underlying various disorders.

DEDICATION

This dissertation is dedicated to my late mother (Lois Walthall Murdaugh) and my father (William Oscar Murdaugh III). I would not be who I am without them. Guess I was wrong when I said that “mys” was not going to “be a scientist”.

ACKNOWLEDGEMENTS

I would like to thank my advisor, Dr. Matthew Buczynski, for his most important contribution to my graduate career: the lab espresso machine. I would also like to thank him for his assistance and encouragement over the years, project failures, and successes. This work could not have been completed without the Buczynski-Gregus lab, and the friendship, support, and assistance of its current and former members, including PI Dr. Ann Gregus, Research Scientist Dr. Cristina Miliano, Previous Research Technician Irene Chen, and Graduate Students Brieann Brown, and Yuyang Dong. I truly cannot put into words the impact you all have had on my life and graduate career. Without your collective help, encouragement, and shenanigans I would not have stayed sane through these projects. I would like to extend an enormous thanks to my family, especially my partner (Justin Stone McFail) and my cousin (Scott Andrew Cast Jr.). Without the help and support of you all, I could not have made it through this journey. Truly, words cannot express how much each and every single one of you contributed to my success.

Further, I extend my thanks to our two 3D printers, Primo and Twain, for the work they have done, the trouble they have caused, and the pranks they have helped me commit.

TABLE OF CONTENTS

LIST OF ABBREVIATIONS AND ACRONYMS

AEA	Anandamide (N-arachidonoylethanolamine)
AIR	Passive Air Flow
AUC	Area Under the Curve
BLA	Basolateral Amygdala
CAD	Computer-aided design
CB1	Cannabinoid Receptor 1
CB2	Cannabinoid Receptor 2
CFA	Complete Freund's Adjuvant
CIPN	Chemotherapy-Induced Peripheral Neuropathy
cm	Centimeters
Cmax	Maximum Observed Plasma Concentration
CPP	Conditioned Place Preference
CVE	Chronic Vapor Exposure
CZ	Center Zone
DL	Discrimination Learning
DL/RL	Discrimination and Reversal Learning
EPM	Elevated Plus Maze
ENDS	Electronic Nicotine Delivery System
EF	Executive Function/ Functions/ Functioning
EX	Extinction
EZ	Edge Zone
FAAH	Fatty Acid Amide Hydrolase
FED	Feeding Experimentation Device
FED3	Feeding Experimentation Device v3
FF	Free Feed/Free Feeding
FR	Fixed Ratio
FR1	Fixed Ratio 1
FR1R	Fixed Ratio 1 Reverse/d
FR3	Fixed Ratio 3
FR3R	Fixed Ratio 3 Reverse/d

FR5	Fixed Ratio 5
FST	Forced Swim Test
g	Grams
h	Hours
Het	Heterozygous
HPA	Hypothalamic-Pituitary-Adrenocortical
IACUC	Institutional Animal Care and Use Committee
IBO	Ibotenic Acid
IR	Infra-red
IZ	Intermediary Zone
KI	Knock-In
KO	Knockout
LDT	Light/Dark Test
L/min	Liters/Minute
lOFC	Lateral Orbitofrontal cortex
LOD	Limit of Detection
LOQ	Limit of Quantification
m	Meters
mg	Milligrams
min	Minutes or Minimum
mm	Millimeters
mM	Millimolar
mOFC	Medial Orbitofrontal cortex
mPFC	Medial Prefrontal Cortex
MRM	Multiple Reaction Monitoring
MTBE	Methyl Tert-butyl Ether
MWM	Morris Water Maze
NAcc	Nucleus Accumbens
NAE	N-acyl-ethanolamine
NaOH	Sodium Hydroxide
NAPE-PLD	N-acylphosphatidylethanolamine Phospholipase D

NIC	Nicotine
ng/ml	Nanograms/Milliliter
ng*hr/ml	Nanograms per hour/milliliter
OEA	N-oleoylethanolamine
OFC	Orbitofrontal Cortex
OFT	Open Field Test
PBS	Phosphate Buffered Saline
PEA	N-palmitoylethanolamine
PFC	Prefrontal Cortex
PG	Propylene Glycol
PPARα	Peroxisome Proliferator-activated Receptor α
PR	Progressive Ratio
PWT/s	Paw Withdrawal Threshold/s
QU	Quinine
RE	Reinstatement
RL	Reversal Learning
s	Seconds
SAL	Saline
SEM	Standard Error of the Mean
SPT	Sucrose Preference Test
ST	Spray/Splash Test
$t^{1/2}$	Half-life
TST	Tail Suspension Test
TRPV1	Transient Receptor Potential Vanilloid 1
UPLC-MS/MS	Ultra Performance Liquid Chromatography/Tandem Mass Spectrometry
VEH	Vehicle
VG	Vegetable Glycerin
vOFC	Ventral Orbitofrontal cortex
VTA	Ventral Tegmental Area
WT	Wild type
µL	microliters

CHAPTER 1 INTRODUCTION

1.1 ON BEHAVIOR AND ITS IMPORTANCE TO RESEARCH

Despite the relative simplicity of the word, agreeing on one scientific definition of the word "behavior" is challenging[1,2]. Broadly speaking, behavior refers to the actions an organism makes in response to some stimulus, whether that stimulus is the environment, the action of another, or a change in its internal state. The term 'behavior' thus encompasses broad categories of actions including observable actions like movement, unobservable actions like internal decision-making, actions performed alone, actions performed in social settings, actions performed with intent, or actions performed reflexively [3–6]. However, were you to ask ten researchers which specific actions are included or excluded from the definition of 'behavior' you may receive ten different answers.

Regardless of which actions fall within the definition of behavior, it is well understood that human and animal behavior can be shaped by numerous interacting influences including genetics[7,8], prior experience or learning[9–13], bodily processes[14,15], and the current environment[16,17]. Understanding how, why, and when animals, including humans, perform a behavior are fundamental questions at the heart of multiple related disciplines including ethology (the science of animal behavior), sociology (the study of human society, social relationships, individual and group behavior), psychology (the science of the human and non-human mind and behaviors), and neuroscience (the study of the nervous system and brain).

The experimental analysis of animal behavior[6,9–11,18] allows researchers to answer the preceding questions. By performing empirical and controlled studies using animal subjects, researchers can come to understand what specific criteria may influence the likelihood of an action occurring, how specific brain regions contribute to behavior, or the behavioral effects of a novel therapeutic treatment. Indeed, the information gained from the experimental analysis of animal behavior has informed and influenced vast aspects of daily life including, but not limited to, economic theories[19,20], education[21,22], and the understanding and treatment of psychiatric disorders[23–25]. The analysis of animal behavior is of paramount importance for the latter, as a compound that alters an identified molecular target but fails to result in behavioral changes in an animal model will likely not progress to clinical trials[26–28].

While various sub-categories of behavior can be measured, this paper will focus on three: affective (emotional) behavior, pain-like behavior, and cognitive or goal-directed behavior in rodent models. Though seemingly disparate, there is much research demonstrating that changes in

the underlying structures and systems associated with affective[29–31] and pain[32,33] behaviors contribute to cognition, and that affective[34–36] and pain disorders[37,38] can result in altered cognition.

For each of these sub-categories, I will provide a brief description of the behavioral domain, an overview of common methods of measurement, and some of the major regions associated with them. These are intended as an introductory background on these topics rather than an exhaustive list. Then, I further describe limitations associated with traditional methods of measuring operant or goal-directed behavior, and the utility of a novel open-source operant device. Finally, in three manuscripts I describe the use of traditional and novel test batteries to investigate behavioral changes in multiple mouse models broadly related to pain and addiction.

1.2 AFFECTIVE BEHAVIOR

1.2a Description:

Regarding behavior, affect refers to the subjective experience, expression, or influence of feelings or emotions. Affect thus includes (but is not limited to) the perception and response to physiological states like hunger and the emotional or neurochemical response to an external force[30,31,39]. While this broad category encompasses various moods and physical states (e.g., anger, sorrow, hunger, thirst) this section will primarily focus on anxiety-like and depression-like behaviors as these are a traditional focus of rodent-based measures of affective behavior and are some of the most commonly diagnosed psychiatric disorders[40–44].

Broadly, the human experience of anxiety refers to a negative affect associated with a perceived ambiguous threat or a negative outcome and is related to the broader mechanisms of both fear and stress. While such experiences are inherently unpleasant, they arise from a system which likely provided an evolutionary benefit[45,46], as the priming of the sympathetic nervous system may allow one to react to a threat more quickly thus resulting in successful escape from a dangerous situation. However, an overactive anxiety response can be maladaptive, leading to persistent feelings of anxiety after or in the absence of ambiguous threat. This in turn leads to further feelings of distress and impaired functioning, may lead to avoidance of normal situations, and negatively impact quality of life [47,48]. In the context of affective disorders depression refers to a persistent negative or flat affect, anhedonia (lack of pleasure), or state of fatigue, which is absent of rational cause (e.g., grief)[41,43,49–51]. There are various sub-types or sub-classifications of

depression (major depressive disorder, dysthymic disorder, etc.), the specific diagnosis of which relies on the number, strength, and duration of symptoms. Like anxiety, the experienced symptoms can negatively impact functioning and quality of life[40,43,47,51].

While humans can self-report feelings of anxiety or depression, rodents are unable to verbalize internal feelings. Instead, researchers must use models, described below, in order to investigate similar behaviors in rodents. Understanding rodent-based models of anxiety- and depression-like behaviors is important, as such models often serve as the foundation for demonstrating efficacy of therapeutic targets and the basis for investigation of the neural mechanisms underlying psychiatric disorders[52–55].

1.2b Common Methods:

Whereas we can directly ask a person how they feel to correlate mood and feelings with physiological or behavioral changes, we lack the ability to do so for non-human animals and must therefore make inferences about their internal state. Rather than measuring *anxiety* or *depression* in rodents, researchers measure changes in specific *anxiety-like* or *depression-like* behaviors. These are more narrowly defined behaviors which correlate with or mimic symptoms of the disease in question, where a single test may measure one or two specific aspects of that behavioral domain. Because of this, there has been a push for researchers to perform several complementary tests before drawing any conclusions regarding genetic or molecular contributions to anxiety- and depression-like behaviors[56–58].

Some of the most common methods for measuring rodent models of anxiety-like behaviors capture unconditioned changes in exploratory behavior[57–60], and although there is ongoing debate on the validity[61] of these tests, they remain a gold standard as they demonstrate sensitivity to traditional anxiolytics like benzodiazepines. A human given benzodiazepines may report a decrease in anxiety symptoms, while rodents demonstrate reduced hiding behavior. This pharmacological validity has made such tests a popular tool for screening novel drug targets. These exploration-based models rely on two inherent and competing needs that contribute to a rodent's biological success: the need to explore and thus find resources or mates, and the need to hide and avoid predators for survival. An animal which spends too much time performing either activity may have reduced biological success.

The devices and setups used to examine changes in exploratory behavior take advantage of these dueling needs for exploration or perceived safety. The Elevated Plus Maze (EPM)[58,62] apparatus is a four-armed platform elevated from the ground. Two opposing arms have walls, while the other two arms do not have walls and are thus open to the environment. The apparatus used for the Open Field Test (OFT)[63,64] is a large area, typically square or rectangular, with an open top. The box used for the Light/Dark Test (LDT)[65] consists of two connecting areas or sides, one of which is covered and unlit, the other of which is uncovered and lit.

To measure anxiety-like behavior an animal is placed in the apparatus and allowed to freely move about. Rodents typically show a natural preference for the 'safe' walled or covered spaces (walled arms of the EPM, walls of the OFT, dark side of the LDT) but do perform some degree of exploratory behavior and engage with the 'unsafe' side (open arm of the EPM, center of the OFT, light side of the LDT). An increase in the amount of time spent on the 'safe' side relative to baseline or other animals is interpreted as an increase in anxiety-like behavior, while an increase in the amount of time spent on the 'unsafe' side is considered a decrease in anxiety-like behavior.

Some of the most common methods for measuring rodent models of depression-like behaviors investigate behaviors related to consummatory anhedonia (decreased consumption of hedonic or pleasurable rewards), apathy-like behavior, and despondency/despair. Depression is correlated with alterations to the motivation and reward pathways, such that there may be diminished motivation to pursue rewards or activities, or deficits in the subjective pleasure associated with previously enjoyed foods or activities [40,41,66].

Consummatory anhedonia is typically measured using a sweetened sucrose solution in what is aptly called the Sucrose Preference Test (SPT)[67]. In this test animals are given access to a sweetened sucrose solution and/or plain water. Typically, animals will show a preference for the sucrose solution, drinking more of it than plain water. A reduction in sucrose consumption is interpreted as consummatory anhedonia and thought to indicate alterations to the natural reward system.

Apathy refers to a reduction in voluntary and goal-directed behavior, with common human symptoms including decreases in self-care like bathing or brushing of the hair and teeth. Like humans, rodents typically engage in self-care behaviors like grooming. Increases or decreases in spontaneous or stress-induced grooming can be measured by observing the frequency or duration an animal spends grooming itself in response to some mild stressor, like novelty. In the Splash or

Spray Test (ST)[68] a small amount of sucrose solution or water is sprayed, squirted, or misted onto the back of an animal, and the frequency or duration of grooming behavior is measured. A decrease in these measures is correlated with both stress and a decrease in motivated behavior, and thus interpreted as an increase in apathy-like behavior.

Tests measuring despondency or despair investigate the behavioral response an animal has to being placed in an inescapable unpleasant situation. In these situations, an animal can engage in an active coping strategy, where they attempt to escape, or a passive strategy, where they reduce their activity and conserve energy. In the Forced Swim Test (FST)[69] an animal is placed into a container of water, while in the Tail Suspension Test (TST)[70,71] an animal is suspended by its tail. A quicker switch to or an increase in duration of passive behavior is interpreted as the animal demonstrating despondency or despair. Like the exploratory tests utilized for anxiety-like behaviors, these tasks have historically been used because they demonstrate pharmacological or predictive validity; drugs that are effective antidepressants are likely to reduce passive behaviors, and drugs which reduce passive behaviors in these tests may have efficacy as an antidepressant.

1.2c Regions:

Mood and behavior are influenced by the interaction of multiple brain regions, and molecular, cellular, and structural changes are associated with anxiety- and depression-like behavior[34,41,72–82] in humans and rodents. For the sake of brevity, this section will only cover some of the major systems involved in both. In both anxiety and depression changes to the frontal cortex, including the input received from other regions, result in altered cognitive processes[35,36,83]. In humans, the prefrontal cortex (PFC) is associated with so-called higher order cognitive processes or executive functions (EFs) like planning, decision-making, and understanding social behavior[84,85]. While scientists do not fully agree on which regions and subregions of the rodent brain are considered the PFC[86], most agree that cortical regions contribute to similar cognitive behaviors[87,88]. The OFC is involved in the encoding of information, mood regulation, and impulse control[89,90]. Alterations to such cortical regions during affective states may thus contribute to altered decision making. The limbic system refers to a collection of brain structures that are involved in the processing of emotion and include the hippocampus, the amygdala, the thalamus, and the hypothalamic-pituitary-adrenocortical (HPA) axis[91]. The limbic system integrates sensory input, affective information, homeostatic information, cognitive information, and stress-related

information. Limbic dysregulation is associated with anxiety and depression in humans, and increased anxiety- and depression-like behaviors in rodents[91–93]. Dysregulation of the so-called reward circuit, which involves mesocortical, mesolimbic, and nigrostriatal pathways connecting the ventral tegmental area (VTA), the Nucleus Accumbens (NAcc), the limbic system, and the frontal cortex, result in altered perception of or seeking of rewards[94–97]. Thus, behaviors associated with affective disorders may result from dysregulation of one or many distinct brain regions.

Both anxiety and depression involve changes in numerous neurotransmitter systems; canonically the monoaminergic systems including serotonin, norepinephrine, and dopamine are highly implicated in the disease symptomology of both. However, alterations in neuropeptides are also associated with psychiatric symptoms[98]. Additionally, the endocannabinoid system is implicated in the regulation of the stress response[99–101] and symptoms of neuropsychiatric disorders[25,29,102–104].

Despite our knowledge on affective behavior and disorders in both humans and rodents, further research is still needed. Rodent models remain an early step for the validation of novel therapeutics for such disorders, which are still a major focus of research[98].

1.3 PAIN-LIKE BEHAVIOR

1.3a Description

Pain refers to the emotional and/or sensory experience associated with a negative or noxious stimulus or the potential for tissue damage[105,106]. This typically unpleasant experience serves an evolutionary benefit, allowing organisms to avoid activities or items which have the potential to cause bodily damage [citation?]. Pain encompasses both the short-term response to a noxious stimulus (acute pain) and maladaptive long-term changes (chronic pain) which persists after the resolution of any primary injury. Chronic pain can present as spontaneous pain[107] (pain in the absence of stimulus), allodynia (pain in response to an otherwise non-noxious stimulus), or hyperalgesia (increased pain in response to a noxious stimulus). The perception of pain relies on both the initial activation of peripheral pain mechanisms, the transmission of these signals, and the modulation and response to these signals [citation?]. As the modulation and response differs from person-to-person, the overall experience of pain is incredibly subjective. As pain involves a subjective component and reporting of the experienced stimulus, we cannot directly measure pain in rodents. Instead, we infer a pain-like behavior from nociception (peripheral neuronal

response to noxious stimuli and the ability to perceive them) and the behavioral response to noxious stimuli (withdrawal, flinching, etc.). Measuring pain-like behaviors in rodents is important, as it allows for the investigation of pain perception and other disorders. For instance, human studies demonstrate a potential link between depression and altered pain perception[108,109] and chronic pain disorders can result in affective and cognitive changes[32,33,54,110].

1.3b Common Methods

As nociception relies on central nervous system processing, many clinical tests for humans have direct rodent correlations[111]. Stimulus-evoked pain-like behaviors (allodynia, hyperalgesia) are further divided into categories based on the specific stimulus used (heat, cold, mechanical, etc.). In both humans[112] and rodents[113] punctate (touch-triggered) mechanical allodynia or hyperalgesia can be measured using von Frey filaments which are calibrated to impart a specific amount of force when applied to the skin. By applying varying filaments to the hand or bottom of the paw, and then observing for reflexive removal from the stimulus, researchers can investigate the force required to mount a nociceptive response[113]. A decrease in the force required to elicit a response is considered a measure of mechanical allodynia or having a decreased pain threshold is interpreted as an increased pain state in humans and rodents.

Heat or cold thresholds, the specific temperature or duration of exposure to a temperature stimulus required to mount a reflexive response, can be measured through the application of a warm/hot or cool/cold stimulus to the hand or bottom of the paw. Heat thresholds in rodents rely on exposing the animal to controlled heat or warmth and measuring the latency to a nocifensive response. This can be done by applying heat to the tail and observing a flicking withdrawal (tail flick test[114]), applying a radiant or infrared heat stimulus to the bottom of the paw and observing nocifensive behavior (hot plate test[115], Hargreaves test[116]). Cold thresholds in rodents rely on exposing animals to a controlled cool or cold temperature and measuring the latency to a nocifensive response[117]. This can be done by applying acetone to the bottom of the paw, which evaporates and causes cooling, or by applying dry- or wet ice to a glass plate the animal is standing on. In both hot and cold tests, a decrease in response latency is considered thermal allodynia or hyperalgesia, indicating decreased tolerance and increased pain state.

While these stimulus-evoked pain models are important, the relative ease of performing such tests may have contributed to an overreliance on these testing methods[107,118]. While chronic

pain disorders result in alterations to such measures, patients primary concern is spontaneous pain (pain that occurs without an apparent stimulus)[107] which results in significant impairments in quality of life and reductions in voluntary behavior. Due to a historical reliance on evoked pain measures, possibly due to their ease of use and interpretation or technical limitations to high-throughput testing of other methods, there exist fewer tests of spontaneous pain-like behavior in rodents. Non-reflexive measures of pain-like behavior can broadly be placed into one of two groups: observational or free-choice/operant tests.

Similar to humans, when experiencing pain rodents engage in several somatic (bodily) behaviors absent of an external stimulus. For instance, animals may lift, lick, flinch their paw or alter their gait[107,119]. Just like humans in pain, rodents will also engage in specific stereotyped facial expressions, or grimace[106,120]. An increase in either of these behaviors absent the application of an acute or chronic external stimulus is interpreted as the animal being in a spontaneous pain-like state. Just as humans in pain may choose to forego otherwise typical or rewarding behaviors (e.g., attending a social event, grocery shopping), rodents in pain may avoid participating in otherwise typical or rewarding behaviors. Free-choice or operant tests instead measure an animals willingness to engage in some behavior to receive reward or to escape an aversive stimulus. In the conditioned place preference (CPP) test to measure spontaneous pain animals are given access to a chamber with two distinct sides or areas; one side of which was repeatedly paired with delivery of a rewarding substance like an analgesic or drug of abuse. They are then given free access to both sides of the chamber absent of analgesics, and a preference for the analgesic-paired side is interpreted as a measure of ongoing pain[120]. Conflict assays are another operant choice-based assay [121,122]. In these tasks animals are placed in a chamber and one aversive stimulus is presented (e.g., bright light). Animals are allowed to escape this stimulus, but doing so requires crossing over another aversive stimulus (e.g., heat, probes). An increased latency to escape or cross the chamber is interpreted as the animal being in a pain-like state.

1.3c Regions

Pain perception is a complex mechanism that relies on both sub- and supraspinal mechanisms, multiple brain regions and neurotransmitter systems[123,124]. Broadly speaking, tissue damage or nerve injury results in activation of peripheral sensory neurons whose signals are transmitted through the spinal cord and to the brain. From here signals sent to and from

numerous regions including the parietal cortex[123,125], frontal cortex[33], and areas of the limbic[92] system contribute to the subjective perception of pain. Spontaneous[107] and chronic pain instead relate to changes in the peripheral and central nervous system that can result in activation of these pathways absent of a stimulus, or activation at previously non-noxious stimuli, spinal or supraspinal central sensitization. Changes in peripheral receptor expression can lead to hyperexcitability of sensory neurons, which may contribute to allodynia or hyperalgesia. Additionally, the rate of spontaneous firing of c-fiber nociceptors is positively correlated with observational measures of spontaneous pain in mice.

However, as stated previously, a historic reliance on rodent measures of acute or reflexive pain means that more is known about that aspect of pain than spontaneous pain. Due to that, and inherent differences in their neurobiology, therapeutics which target acute pain often fail to treat chronic pain. As such, rodent models will continue to be important as we seek to further understand the underlying mechanisms and create better therapeutics.

1.4 OPERANT AND GOAL-DIRECTED BEHAVIOR

1.4a Description

Broadly speaking operant conditioning refers to an associative learning process whereby the frequency of a voluntary action is modified by the application of a reinforcer, which increases behavior frequency, or a punishment, which decreases it[126–130]. This focus on voluntary action differentiates it from classical conditioning, where with repeated pairings a previously neutral cue comes to elicit an unconditioned or involuntary response. By measuring operant performance researchers can investigate aspects of learning, memory, and goal-directed behaviors, or behaviors performed with intentionality or in the pursuit of some goal. As such, operant tests can be used to measure an aspect of goal-directed behavior important for translational studies: executive functioning (EF). While there is not one exact definition of what EF entails, it generally refers to a cluster of cognitive abilities or processes that allow an organism to split its attention, plan, perform, alter, adapt, or inhibit goal-directed behavior in response to an altered environment. Executive dysfunction, or impairments to some aspect of those abilities or behaviors, is implicated in or results from numerous psychiatric diseases[131–133], neurodegenerative disorders[134,135], and neurological[136] disorders.

1.4b Common Methods

As EF and goal-directed behaviors entail a broad collection of processes, many tests can be used to measure them. Traditional methods of measuring operant behavior and EF have relied on operant chambers, which is discussed in its own section. Other common methods of measuring learning and memory are spatial assays, like the Morris Water Maze (MWM). In the MWM an animal is placed into opaque water where there is a hidden platform and external cues (shapes on the wall of the maze, etc.). Through trial-and-error the animal will find the platform, and through repeated sessions come to find the platform more quickly by orienting themselves via the external cues. While spatial learning tests like the MWM allow for investigation of discrimination learning, reversal learning, and set-shifting behavior, they are heavily reliant on the hippocampus rather than cortical regions, which are more heavily associated with higher order cognitive processes.

1.4c Regions

Operant conditioning and EF rely on the interaction of multiple brain regions and neurotransmitter systems [133,137–139]. No one brain region can be said to control decision-making, rather, they work in tandem to produce desired outcomes. Similarly, no one aspect of decision-making is truly under the control of a single brain region. For instance, the dorsolateral prefrontal cortex, lateral orbitofrontal cortex, and hippocampus are all involved in decision-making based on experienced and remembered value of a reward.

Broadly, the frontal cortex (prefrontal cortex, orbitofrontal cortex, anterior cingulate cortex etc.) is involved in the evaluation, representation, or encoding of value of a reward or stimuli, as well as sustained attention, decision-making, and inhibitory control of actions[84,85,89,90,140,141]. They are informed by subcortical regions, like the striatum, which is associated with habitual/conditioned responses, reward prediction, and incentive salience of a reward[142–144]. Other subcortical regions that are highly involved in EF and goal-directed behavior include the hippocampus[145–147] (associated with aspects of memory including long-term, episodic, and working memory), the thalamus[148–151] (working memory, behavioral flexibility), and the basal ganglia[152–154] (motor control, working memory).

1.5 TRADITIONAL OPERANT CHAMBERS AND THEIR LIMITATIONS:

Nearly a century has passed since the operant conditioning chamber was first developed by B. F. Skinner in the 1930s[127,128,130,155]. Building upon the ideas of E. L. Thorndike, Skinner created the operant chambers to perform controlled empirical studies on the intentional behavior in animals. Broadly, he introduced the idea of operant conditioning, an associative learning process whereby the frequency of a voluntary action is modified by the application of a reinforcer, which increases behavior frequency, or a punishment, which decreases it[126–130]. This focus on voluntary action differentiates it from classical conditioning, where with repeated pairings a previously neutral cue comes to elicit an unconditioned or involuntary response. Due to his contributions to behavioral studies, he is considered one of the fathers of both operant conditioning and the field of experimental behavioral analysis[9–11,130,156,157].

The operant chamber formed the foundation of his experiments, allowing for controlled, empirical, replicable studies on learning rates and reinforcers. Research using operant chambers has had broad impacts on various fields, including psychology[128,130,156], economics[19,158], and neuroscience[159–161]. The results of studies using these chambers have shaped our understanding of childhood learning and influenced education[21,22] and have been used to elucidate the neural mechanisms underlying altered decision-making related to psychiatric disorders [23,162–166].

To be considered an operant chamber or device an item must meet a minimum of two criteria. There must be an operandum, an item that can automatically detect when an animal has interacted with it, such as a lever or button. And there must be a method to deliver a reinforcer, such as a chute to deliver food. Through repeated pairings of an action, like lever pressing, and an outcome, like food dispensation, an animal comes to form an association between lever pressing and food. By analyzing how many actions an animal made before consistently making the correct choice one can create a learning curve and make inferences on associative learning. By modifying aspects of the test, such as including multiple operanda or stimuli to act as cues, the difficulty can be altered and changes to the learning curve can be measured. Such additions have allowed for the investigation of more complex behaviors, including reversal learning or set-shifting[24,167–169], where an animal must inhibit a previously learned response while also creating a new association, and delay-discounting[170], where an animal must choose between a small reward now or a larger reward later. Ultimately, an operant chamber or device is used to investigate behavioral adaptation in

response to altered or novel action-outcome associations. Understanding such behaviors is incredibly important, as it forms the foundation for understanding human decision-making.

However, in the decades since Skinner's original design was released, few alterations have been made. Many researchers rely on commercially available operant chambers whose overall designs are largely unchanged from Skinner's original design[163,171–173]. These are typically large (~1' x 1' x 1') chambers, costing a minimum of several thousand dollars for the base version, with additional features like liquid dispensers or attachments for synchronization with other devices increasing the cost of the chamber. This limits the number of chambers a researcher may have at their disposal, especially for newer labs with less capital or space to run experiments. To combat this limitation researchers often test animals in rounds of short (~2h) daily sessions[174–176] so they may collect data from enough animals to perform a well-powered study with a limited number of chambers. In such a design researchers must repeatedly clean the chambers and check they are working between each round of testing, and repeatedly transfer groups of animals to and from the testing room. As such, this is a labor-intensive project where researchers devote their entire day to collecting behavioral data for weeks to months in a row. To study one or two operant behaviors researchers may be running daily sessions for a month. This may prevent them from investigating models that resolve quickly, like acute pain models, or may mean that researchers can only investigate the effect of the model on a single portion of operant behavior.

In addition to having drawbacks for the researcher, the limitations associated with traditional operant chambers may influence the results collected from the research subject. Animals are placed into a semi-novel environment for each round of testing, which has unclear effects on stress. Further, even with repeated handling, animals may not truly habituate to the stress of handling. A meta-analysis[177] of 80 studies investigating common minimally invasive laboratory procedures, like brief handling or transport, found that animals demonstrated significant increases in stress-related measures including increased corticosterone levels, heart rate, and blood pressure. Further, they found that these changes were observable for more than 30 minutes after testing. Thus, in a short 2-hour test, a quarter of an animal's performance may be impacted by stress. There is a large body of research demonstrating that stress alters normal operant and cognitive performance[178], and thus the collected results may be less translatable to the generalized human condition. In addition, a testing schedule where animals are tested in different rounds separated by ~2 hours means that animals will be tested at different points in their circadian cycle, with up to 6

hours between the first and last animals tested. Research has demonstrated that performance may be impacted by circadian cycle and rhythm[179,180].

In summary, while the operant chamber has revolutionized multiple fields of research, the devices have remained largely unchanged since their initial design. As such, the chambers are expensive and time-consuming to use, which limits how researchers perform experiments and what models they may use when investigating decision-making. Because of these limitations, the typical operant study is designed such that the collected results may be influenced by the effects of stress or circadian rhythm. These confounds may limit the translatability of the results. As such, novel methods of measuring operant behavior are necessary which reduce the impact of these confounds and allow for testing on shorter time scales. Such methods would allow for the investigation of altered decision-making during more acute changes, such as pain models, where symptoms may only be observed for several weeks. As traditional operant chambers have inherent limitations, this novel method should make use of a different operant device.

1.6 THE FED3

Multiple researchers have developed novel alternatives to traditional operant chambers to address these limitations and concerns[174,181,182]. Such devices are typically built with a focus on off-the-shelf or 3D-printed parts, are run on Arduino or Raspberry Pi, and require limited engineering knowledge to produce. Furthermore, there is a heavy focus on being open source to encourage uptake, modification, and innovation, while also allowing for custom experimental programs. However, many of such devices have seen limited uptake since their publication or release. While factors including cost, size, and ease of set-up can influence uptake, it may also be influenced by outreach and partnerships with existing companies or services such as JOVE.

In 2016 Drs Katrina Nguyen and Alexxai Kravitz published the design for a device for performing feeding studies called the Feeding Experimentation Device (FED)[183,184]. This device was intended as an improvement to the labor-intensive and temporally imprecise methods of measuring food intake[185]; as such it lacked any operanda and its main function was to record timestamped data regarding pellet release and retrieval, allowing for precise measurements of food intake and meal patterns. To encourage the uptake of the device, their design prioritized the use of off-the-shelf materials and minimized the amount of engineering knowledge needed for construction. Over multiple iterations, additional features were added to the device that

transformed it from a food-intake tracking device to one capable of performing operant studies[186], such that it could be used to investigate aspects of food intake and motivation, including the neural circuitry underlying food consumption and motivation[187,188].

The current version of the device, the Feeding Experimentation Device v3 (FED3), has all the necessary tools to be considered a robust operant feeding device: two nose poke operanda containing infra-red (IR) beam break sensors, a pellet dispenser, a pellet well containing an IR beam break sensor, a buzzer for audio cues, and LEDs on the outside of the device (and optionally inside the operanda) for visual cues. In addition, the device has an output allowing for synchronization with other equipment like optogenetics and fiber phtometry[187]. Unlike traditional operant chambers, the FED3 is a small (<5" x 4" x 4") device, allowing for the investigation of behaviors in the home-cage or a home-cage-like environment, which may reduce stress. In addition, the device is extremely low-cost, being approximately 10 to 100 times less expensive than a traditional operant chamber. The device can be purchased pre-made from open-ephys[189] for about $500, purchased from open-ephys as parts and assembled in-house for under $250, or made fully in-house by purchasing electronic components in bulk for considerably less (<$150). Regardless of the option chosen, a researcher could acquire a minimum of 10 FED3 devices for the cost of a basic traditional operant chamber.

In addition to a lower cost, the FED3 is easily modifiable. The 3D printed files are made freely available through Tinkercad, an easy-to-use online computer-aided design (CAD) program. Using these files users have made modifications to optimize the devices for specific applications. For example, our lab is in the process of modifying the FED3 to enable operant liquid dispensation. Further, the FED3 is based on an Arduino microcontroller, and the Kravitz lab has written an Arduino library to allow users to create custom behavioral paradigms using the FED3. Standard functions include Fixed, Progressive Ratio, or Timed Feeding schedules, while more advanced functions including Go/No-Go and Probabilistic Reversal tests have been created[190]. The Kravitz lab has further maintained a Google Groups-based 'FEDforum' where 200+ registered users readily interact to request help and share novel programs. According to Dr. Kravitz himself, more than 2,000+ FED3 devices are being used in 200+ labs around the world[191].

Despite the immense potential of the FED3 to perform operant tests, no one has yet designed a test battery to investigate multiple operant behaviors by posting a protocol on the FEDforum or publishing a paper. In Manuscript 3 I will demonstrate the utility of the FED3 for

investigating operant conditioning and outline a protocol for performing a 6-test operant test battery to investigate multiple aspects of operant behavior in a shorter time than could be done using traditional operant chambers. To encourage the uptake of this protocol I will also introduce a customizable pipeline for data analysis. Through these findings, I hope to contribute to our understanding of goal-directed behavior and encourage a more comprehensive investigation of behavior.

1.7 REFERENCES

1. Baum, W. M. What counts as behavior? The molar multiscale view. *Behavior Analyst* **36**, 283–293 (2013).
2. WHAT IS BEHAVIOR? *The JOURNAL OF PHILOSOPHY, PSYCHOLOGY, AND SCIENTIFIC METHODS* **XXVIII**, 373-b-377 (1919).
3. Eible-Eibesfeldt, I. & Kramer, S. Ethology, the Comparative Study of Animal Behavior. *Q Rev Biol* **33**, 181–211 (1958).
4. Richter, C. P. Animal Behavior and Internal Drives. *Q Rev Biol* **2**, 307–343 (1927).
5. Lehrman, D. S. Comparative Physiology (Behavior). *Annu Rev Physiol* **18**, 527–542 (1956).
6. Lehner, P. N. Design and execution of animal behavior research: an overview. *Journal of animal science* vol. 65 1213–1219 Preprint at https://doi.org/10.2527/jas1987.6551213x (1987).
7. Wimer, R. E. & Wimer, C. C. Animal behavior genetics: a search for the biological foundations of behavior. *Annu Rev Psychol* **36**, 171–218 (1985).
8. Parmigiani, S., Palanza, P., Rodgers, J. & Ferrari, P. F. Selection, evolution of behavior and animal models in behavioral neuroscience. *Neurosci Biobehav Rev* **23**, 957–970 (1999).
9. Skinner, B. F. The experimental analysis of behavior. *Am Sci* **45**, 343–371 (1957).
10. Skinner, B. F. WHAT IS THE EXPERIMENTAL ANALYSIS OF BEHAVIOR? 1. *J Exp Anal Behav* **9**, 213–218 (1966).
11. Skinner, B. F. Can the Experimental Analysis of Behavior Rescue Psychology? *Behav Anal* **6**, 9–17 (1983).
12. Castro, L. & Wasserman, E. A. Animal learning. *Wiley Interdiscip Rev Cogn Sci* **1**, 89–98 (2010).
13. Rescorla, R. A. & Holland, P. C. Behavioral Studies of Associative Learning in Animals. *Annu Rev Psychol* **33**, 265–308 (1982).

14. Riley, A. L., Zellner, D. A. & Duncan, H. J. The role of endorphins in animal learning and behavior. *Neurosci Biobehav Rev* **4**, 69–76 (1980).

15. Friend, T. E. D. H. Behavioral Aspects of Stress '. (1991) doi:10.3168/jds.S0022-0302(91)78173-3.

16. Russart, K. L. G. & Nelson, R. J. Artificial light at night alters behavior in laboratory and wild animals. 401–408 (2018) doi:10.1002/jez.2173.

17. Burt, C. S. *et al.* Ecology & Evolution The effects of light pollution on migratory animal behavior. *Trends Ecol Evol* **38**, 355–368 (2022).

18. Mench, J. Why it is important to understand animal behavior. *ILAR J* **39**, 20–26 (1998).

19. Furrebøe, E. F. & Sandaker, I. Contributions of Behavior Analysis to Behavioral Economics. *Behavior Analyst* **40**, 315–327 (2017).

20. Gardner, M. P. H. *et al.* Medial orbitofrontal inactivation does not affect economic choice. *Elife* **7**, 1–22 (2018).

21. Schlinger, H. D. The impact of B. F. Skinner's science of operant learning on early childhood research, theory, treatment, and care. *Early Child Dev Care* **191**, 1089–1106 (2021).

22. Altman, K. I. & Linton, T. E. Operant conditioning in the classroom setting: A review of the research. *Journal of Educational Research* **64**, 277–286 (1971).

23. Martín-García, E., Domingo-Rodriguez, L. & Maldonado, R. An Operant Conditioning Model Combined with a Chemogenetic Approach to Study the Neurobiology of Food Addiction in Mice. *Bio Protoc* **10**, 1–23 (2020).

24. Izquierdo, A. & Jentsch, J. D. Reversal learning as a measure of impulsive and compulsive behavior in addictions. *Psychopharmacology (Berl)* **219**, 607–620 (2012).

25. Navarro, D. *et al.* Molecular Alterations of the Endocannabinoid System in Psychiatric Disorders. *Int J Mol Sci* **23**, (2022).

26. Belzung, C. Innovative drugs to treat depression: Did animal models fail to be predictive or did clinical trials fail to detect effects. *Neuropsychopharmacology* **39**, 1041–1051 (2014).

27. Pound, P. & Ritskes-Hoitinga, M. Is it possible to overcome issues of external validity in preclinical animal research? Why most animal models are bound to fail. *J Transl Med* **16**, 1–8 (2018).

28. Bespalov, A. *et al.* Failed trials for central nervous system disorders do not necessarily invalidate preclinical models and drug targets. *Nat Rev Drug Discov* **15**, 516 (2016).

29. Campolongo, P. & Trezza, V. The endocannabinoid system: a key modulator of emotions and cognition. *Front Behav Neurosci* (2012) doi:10.3389/fnbeh.2012.00073.

30. Panksepp, J. Affective consciousness: Core emotional feelings in animals and humans. *Conscious Cogn* **14**, 30–80 (2005).

31. Panksepp, J. At the interface of the affective, behavioral, and cognitive neurosciences: Decoding the emotional feelings of the brain. *Brain Cogn* **52**, 4–14 (2003).

32. Low, L. A. The impact of pain upon cognition: What have rodent studies told us? *Pain* **154**, 2603–2605 (2013).

33. W.-Y., O., C.S., S. & D.R., H. Role of the Prefrontal Cortex in Pain Processing. *Mol Neurobiol* **56**, 1137–1166 (2019).

34. Kim, J. & Gorman, J. The psychobiology of anxiety. *Clin Neurosci Res* **4**, 335–347 (2005).

35. Medalla, A. & Lim, R. Treatment of Cognitive Dysfunction in Psychiatric Disorders. *J Psychiatr Pract* **10**, 17–25 (2004).

36. Gonda, X. *et al.* The role of cognitive dysfunction in the symptoms and remission from depression. *Ann Gen Psychiatry* **14**, 1–7 (2015).

37. Milutinovic, B. & Singh, A. K. Editorial: Cognitive Impairment and Peripheral Neuropathy From Chemotherapy: Molecular Mechanisms and Therapeutic Approaches. *Front Mol Biosci* **9**, 1–3 (2022).

38. Ibrahim, E. Y. *et al.* A preliminary, prospective study of peripheral neuropathy and cognitive function in patients with breast cancer during taxane therapy. *PLoS One* **17**, e0275648 (2022).

39. Ostrom, T. M. The relationship between the affective, behavioral, and cognitive components of attitude. *J Exp Soc Psychol* **5**, 12–30 (1969).

40. Richards, D. Prevalence and clinical course of depression: A review. *Clin Psychol Rev* **31**, 1117–1125 (2011).

41. Ruscio, A. M. & Khazanov, G. K. Anxiety and depression. *The Oxford Handbook of Mood Disorders* 313–324 (2015) doi:10.1093/oxfordhb/9780199973965.013.27.

42. Wittchen, H. U. Generalized anxiety disorder: Prevalence, burden, and cost to society. *Depress Anxiety* **16**, 162–171 (2002).

43. Lehtinen, V. & Joukamaa, M. Epidemiology of depression: Prevalence, risk factors and treatment situation. *Acta Psychiatr Scand* **89**, 7–10 (1994).

44. Baxter, A. J., Scott, K. M., Vos, T. & Whiteford, H. A. Global prevalence of anxiety disorders: A systematic review and meta-regression. *Psychol Med* **43**, 897–910 (2013).

45. Bateson, M., Brilot, B. & Nettle, D. Anxiety: An evolutionary approach. *Canadian Journal of Psychiatry* **56**, 707–715 (2011).

46. Price, J. S. Evolutionary aspects of anxiety disorders. *Dialogues Clin Neurosci* **5**, 223–236 (2003).

47. Brenes, G. A. Anxiety, depression, and quality of life in primary care patients. *Prim Care Companion J Clin Psychiatry* **9**, 437–443 (2007).

48. Rapaport, M. H., Clary, C., Fayyad, R. & Endicott, J. Quality-of-life impairment in depressive and anxiety disorders. *American Journal of Psychiatry* **162**, 1171–1178 (2005).

49. Gilbert, P. Evolution and depression: Issues and implications. *Psychol Med* **36**, 287–297 (2006).

50. Nettle, D. Evolutionary origins of depression: A review and reformulation. *J Affect Disord* **81**, 91–102 (2004).

51. Holtzheimer, P. E. & Mayberg, H. S. Stuck in a rut: Rethinking depression and its treatment. *Trends Neurosci* **34**, 1–9 (2011).

52. Rubinow, D. R. & Schmidt, P. J. Sex differences and the neurobiology of affective disorders. *Neuropsychopharmacology* **44**, 111–128 (2019).

53. Palmer, R. H. C., McGeary, J. E., Knopik, V. S., Bidwell, L. C. & Metrik, J. M. CNR1 and FAAH variation and affective states induced by marijuana smoking. *American Journal of Drug and Alcohol Abuse* **45**, 514–526 (2019).

54. Johansen, J. P., Fields, H. L. & Manning, B. H. The affective component of pain in rodents: Direct evidence for a contribution of the anterior cingulate cortex. *Proc Natl Acad Sci U S A* **98**, 8077–8082 (2001).

55. Marquardt, K. & Brigman, J. L. The impact of prenatal alcohol exposure on social, cognitive and affective behavioral domains: Insights from rodent models. *Alcohol* **51**, 1–15 (2016).

56. Blokland, A. *et al.* The use of a test battery assessing affective behavior in rats: Order effects. *Behavioural Brain Research* **228**, 16–21 (2012).

57. Kalueff, A. V., Wheaton, M. & Murphy, D. L. What's wrong with my mouse model?. Advances and strategies in animal modeling of anxiety and depression. *Behavioural Brain Research* **179**, 1–18 (2007).

58. Carola, V., D'Olimpio, F., Brunamonti, E., Mangia, F. & Renzi, P. Evaluation of the elevated plus-maze and open-field tests for the assessment of anxiety-related behaviour in inbred mice. *Behavioural Brain Research* (2002) doi:10.1016/S0166-4328(01)00452-1.

59. Prut, L. & Belzung, C. The open field as a paradigm to measure the effects of drugs on anxiety-like behaviors: A review. *European Journal of Pharmacology* Preprint at https://doi.org/10.1016/S0014-2999(03)01272-X (2003).

60. Belzung, C. & Le Pape, G. Comparison of different behavioral test situations used in psychopharmacology for measurement of anxiety. *Physiol Behav* **56**, 623–8 (1994).

61. Ennaceur, A. Tests of unconditioned anxiety - Pitfalls and disappointments. *Physiol Behav* **135**, 55–71 (2014).

62. Ramos, A., Pereira, E., Martins, G. C., Wehrmeister, T. D. & Izídio, G. S. Integrating the open field, elevated plus maze and light/dark box to assess different types of emotional behaviors in one single trial. *Behavioural Brain Research* **193**, 277–288 (2008).

63. Walsh, R. N. & Cummins, R. A. The open-field test: A critical review. *Psychol Bull* (1976) doi:10.1037/0033-2909.83.3.482.

64. Perals, D., Griffin, A. S., Bartomeus, I. & Sol, D. Revisiting the open-field test: what does it really tell us about animal personality? *Anim Behav* (2017) doi:10.1016/j.anbehav.2016.10.006.

65. Bourin, M. & Hascoët, M. The mouse light/dark box test. *Eur J Pharmacol* **463**, 55–65 (2003).

66. Keedwell, P. A., Andrew, C., Williams, S. C. R., Brammer, M. J. & Phillips, M. L. The neural correlates of anhedonia in major depressive disorder. *Biol Psychiatry* **58**, 843–853 (2005).

67. Issues, O. brain sciences Sucrose Preference Test as a Measure of Anhedonic Behavior in a Chronic Unpredictable Mild Stress Model of Depression : (2022).

68. Becker, M., Pinhasov, A. & Ornoy, A. Animal Models of Depression: What Can They Teach Us about the Human Disease? *Diagnostics* **11**, 123 (2021).

69. Armario, A. The forced swim test: Historical, conceptual and methodological considerations and its relationship with individual behavioral traits. *Neurosci Biobehav Rev* **128**, 74–86 (2021).

70. Can, A. *et al.* The tail suspension test. *Journal of Visualized Experiments* 3–7 (2011) doi:10.3791/3769.

71. Steru, L., Chermat, R., Thierry, B. & Simon, P. The tail suspension test: A new method for screening antidepressants in mice. *Psychopharmacology (Berl)* **85**, 367–370 (1985).

72. Bowers, M. E. & Ressler, K. J. Sex-dependence of anxiety-like behavior in cannabinoid receptor 1 (Cnr1) knockout mice. *Behavioural Brain Research* **300**, 65–69 (2016).

73. Bouter, Y. *et al.* Chronic Psychosocial Stress Causes Increased Anxiety-Like Behavior and Alters Endocannabinoid Levels in the Brain of C57Bl/6J Mice. *Cannabis Cannabinoid Res* **5**, 51–61 (2020).

74. Morgan, M. A. & Pfaff, D. W. Estrogen's effects on activity, anxiety, and fear in two mouse strains. *Behavioural Brain Research* **132**, 85–93 (2002).

75. Gray, J. A. The neuropsychology of anxiety. *Issues Ment Health Nurs* (1985) doi:10.3109/01612848509009455.

76. Kathuria, S. *et al.* Modulation of anxiety through blockade of anandamide hydrolysis. *Nat Med* **9**, 76–81 (2003).

77. Logan, R. W. *et al.* Chronic Stress Induces Brain Region-Specific Alterations of Molecular Rhythms that Correlate with Depression-like Behavior in Mice. *Biol Psychiatry* **78**, 249–258 (2015).

78. Hill, M. N. & Gorzalka, B. B. Is there a role for the endocannabinoid system in the etiology and treatment of melancholic depression? *Behavioural Pharmacology* **16**, 333–352 (2005).

79. Stepanichev, M., Dygalo, N. N., Grigoryan, G., Shishkina, G. T. & Gulyaeva, N. Rodent models of depression: Neurotrophic and neuroinflammatory biomarkers. *Biomed Res Int* **2014**, (2014).

80. Chaudhury, D., Liu, H. & Han, M.-H. Neuronal correlates of depression. *Cellular and Molecular Life Sciences* **72**, 4825–4848 (2015).

81. Bangasser, D. A. & Cuarenta, A. Sex differences in anxiety and depression: circuits and mechanisms. *Nat Rev Neurosci* **22**, 674–684 (2021).

82. Beuke, C. J., Fischer, R. & McDowall, J. Anxiety and depression: Why and how to measure their separate effects. *Clin Psychol Rev* **23**, 831–848 (2003).

83. Kessing, L. V. Cognitive impairment in the euthymic phase of affective disorder. *Psychol Med* **28**, 1027–1038 (1998).

84. Teffer, K. & Semendeferi, K. *Human prefrontal cortex. Evolution, development, and pathology. Progress in Brain Research* vol. 195 (Elsevier B.V., 2012).

85. Dixon, M. L., Thiruchselvam, R., Todd, R. & Christoff, K. Emotion and the prefrontal cortex: An integrative review. *Psychol Bull* **143**, 1033–1081 (2017).

86. Laubach, M., Amarante, L. M., Swanson, K. & White, S. R. Cognition and Behavior What, If Anything, Is Rodent Prefrontal Cortex? *eNeuro* **5**, 315–333 (2018).

87. Chudasama, Y. Animal models of prefrontal-executive function. *Behavioral Neuroscience* **125**, 327–343 (2011).

88. Dalley, J. W., Cardinal, R. N. & Robbins, T. W. Prefrontal executive and cognitive functions in rodents : neural and neurochemical substrates. **28**, 771–784 (2004).

89. Rolls, E. T. The functions of the orbitofrontal cortex. *Brain Cogn* **55**, 11–29 (2004).

90. Rolls, E. T. & Grabenhorst, F. The orbitofrontal cortex and beyond: From affect to decision-making. *Prog Neurobiol* **86**, 216–244 (2008).

91. Roxo, M. R., Franceschini, P. R., Zubaran, C., Kleber, F. D. & Sander, J. W. The limbic system conception and its historical evolution. *ScientificWorldJournal* **11**, 2427–2440 (2011).

92. Rolls, E. T. Limbic systems for emotion and for memory, but no single limbic system. *Cortex* **62**, 119–157 (2015).

93. Kötter, R. & Meyer, N. The limbic system: a review of its empirical foundation. *Behavioural Brain Research* **52**, 105–127 (1992).

94. Bissonette, G. B. & Roesch, M. R. Neurophysiology of Reward-Guided Behavior: Correlates Related to Predictions, Value, Motivation, Errors, Attention, and Action. in *Brain Imaging in Behavioral Neuroscience* 199–230 (2015). doi:10.1007/7854_2015_382.

95. Wassum, K. M. Amygdala-cortical collaboration in reward learning and decision making. *Elife* **11**, 1–29 (2022).

96. Damme, K. S. F. *et al.* Emotional content impacts how executive function ability relates to willingness to wait and to work for reward. *Cogn Affect Behav Neurosci* **19**, 637–652 (2019).

97. Lichtenberg, N. T. *et al.* The medial orbitofrontal cortex-basolateral amygdala circuit regulates the influence of reward cues on adaptive behavior and choice. *Journal of Neuroscience* **41**, 7267–7277 (2021).

98. Wong, M. & Licinio, J. Research and treatment approaches to depression. *Nat Rev Neurosci* **2**, 343–351 (2001).

99. Morena, M., Patel, S., Bains, J. S. & Hill, M. N. Neurobiological Interactions Between Stress and the Endocannabinoid System. *Neuropsychopharmacology* **41**, 80–102 (2016).

100. Spohrs, J. *et al.* Endocannabinoid system reactivity during stress processing in healthy humans. *Biol Psychol* **169**, 108281 (2022).

101. Jenniches, I. *et al.* Anxiety, Stress, and Fear Response in Mice with Reduced Endocannabinoid Levels. *Biol Psychiatry* **79**, 858–868 (2016).

102. Di Marzo, V. The endocannabinoidome as a substrate for noneuphoric phytocannabinoid action and gut microbiome dysfunction in neuropsychiatric disorders. *Dialogues Clin Neurosci* **22**, 259–269 (2020).

103. Scheyer, A., Yasmin, F., Naskar, S. & Patel, S. Endocannabinoids at the synapse and beyond: implications for neuropsychiatric disease pathophysiology and treatment. *Neuropsychopharmacology* 1–17 (2022) doi:10.1038/s41386-022-01438-7.

104. Gao, W., Walther, A., Wekenborg, M., Penz, M. & Kirschbaum, C. Determination of endocannabinoids and N-acylethanolamines in human hair with LC-MS/MS and their relation to symptoms of depression, burnout, and anxiety. *Talanta* **217**, 121006 (2020).

105. Woolf, C. J. Review series introduction What is this thing called pain ? *J Clin Invest* **120**, 10–12 (2010).

106. Yam, M. F., Loh, Y. C., Oo, C. W. & Basir, R. Overview of neurological mechanism of pain profile used for animal “pain-like” behavioral study with proposed analgesic pathways. *Int J Mol Sci* **21**, 1–26 (2020).

107. Ma, L., Liu, S., Yi, M. & Wan, Y. Spontaneous pain as a challenge of research and management in chronic pain. *Medical Review* **2**, 308–319 (2022).

108. Lautenbacher, S. & Krieg, J. C. Pain perception in psychiatric disorders: A review of the literature. *J Psychiatr Res* **28**, 109–122 (1994).

109. Schlereth, T. *et al.* Association between pain, central sensitization and anxiety in postherpetic neuralgia. *European Journal of Pain (United Kingdom)* **19**, 193–201 (2015).

110. Wiech, K. Deconstructing the sensation of pain: The influence of cognitive processes on pain perception. *Science (1979)* **354**, 584–587 (2016).

111. Deuis, J. R., Dvorakova, L. S. & Vetter, I. Methods used to evaluate pain behaviors in rodents. *Front Mol Neurosci* **10**, 1–17 (2017).

112. Krumova, E. K., Geber, C., Westermann, A. & Maier, C. Neuropathic pain: Is quantitative sensory testing helpful? *Curr Diab Rep* **12**, 393–402 (2012).

113. Chaplan, S. R., Bach, F. W., Pogrel, J. W., Chung, J. M. & Yaksh, T. L. Quantitative assessment of tactile allodynia in the rat paw. *J Neurosci Methods* **53**, 55–63 (1994).

114. Elhabazi, K., Ayachi, S., Ilien, B. & Simonin, F. Assessment of morphine-induced hyperalgesia and analgesic tolerance in mice using thermal and mechanical nociceptive modalities. *Journal of Visualized Experiments* 25–30 (2014) doi:10.3791/51264.

115. Chen, I. *et al.* NAPE-PLD regulates specific baseline affective behaviors but is dispensable for inflammatory hyperalgesia. *Neurobiology of Pain* **14**, 100135 (2023).

116. Christianson, C. A. *et al.* Spinal TLR4 mediates the transition to a persistent mechanical hypersensitivity after the resolution of inflammation in serum-transferred arthritis. *Pain* **152**, 2881–2891 (2011).

117. Brenner, D. S., Golden, J. P., Vogt, S. K. & Gereau, R. W. A simple and inexpensive method for determining cold sensitivity and adaptation in mice. *Journal of Visualized Experiments* **2015**, 1–12 (2015).

118. Mogil, J. S. & Crager, S. E. What should we be measuring in behavioral studies of chronic pain in animals? *Pain* **112**, 12–15 (2004).

119. Shepherd, A. J. & Mohapatra, D. P. Pharmacological validation of voluntary gait and mechanical sensitivity assays associated with inflammatory and neuropathic pain in mice. *Neuropharmacology* **130**, 18–29 (2018).

120. Abboud, C. *et al.* Animal models of pain: Diversity and benefits. *J Neurosci Methods* **348**, (2021).

121. Gaffney, C. M., Muwanga, G., Shen, H., Tawfik, V. L. & Shepherd, A. J. Mechanical Conflict-Avoidance Assay to Measure Pain Behavior in Mice. *Journal of Visualized Experiments* **2022**, 1–11 (2022).

122. Harte, S. E., Meyers, J. B., Donahue, R. R., Taylor, B. K. & Morrow, T. J. Mechanical conflict system: A novel operant method for the assessment of nociceptive behavior. *PLoS One* **11**, 1–20 (2016).

123. Apkarian, A. V., Bushnell, M. C., Treede, R. D. & Zubieta, J. K. Human brain mechanisms of pain perception and regulation in health and disease. *European Journal of Pain* **9**, 463 (2005).

124. Das, V. *An introduction to pain pathways and pain 'targets'*. *Progress in Molecular Biology and Translational Science* vol. 131 (Elsevier Inc., 2015).

125. Wiech, K., Ploner, M. & Tracey, I. Neurocognitive aspects of pain perception. *Trends Cogn Sci* **12**, 306–313 (2008).

126. Staddon, J. E. R. & Cerutti, D. T. Operant Conditioning. *Annu Rev Psychol* **54**, 115–144 (2003).

127. Fantino, E. & Stolarz-Fantino, S. Operant Conditioning. *Encyclopedia of Human Behavior: Second Edition* 749–756 (2012) doi:10.1016/B978-0-12-375000-6.00262-7.

128. Iversen, I. H. Skinner's Early Research Reflexology to Operant Conditioning. *American Psychologist* **47**, 1318–1328 (1992).

129. Kirsch, I., Lynn, S. J., Vigorito, M. & Miller, R. R. The Role of Cognition in Classical and Operant Conditioning. *J Clin Psychol* **60**, 369–392 (2004).

130. Catania, A. C. The operant behaviorism of B. F. Skinner. *Behavioral and Brain Sciences* **7**, 473–475 (1984).

131. Warren, S. L., Heller, W. & Miller, G. A. The Structure of Executive Dysfunction in Depression and Anxiety. *J Affect Disord* **279**, 208–216 (2021).

132. Hill, E. L. Executive dysfunction in autism Elisabeth. *Trends Cogn Sci* **8**, 26–32 (2006).

133. Goldstein, R. Z. & Volkow, N. D. Dysfunction of the prefrontal cortex in addiction: neuroimaging findings and clinical implications. *Nat Rev Neurosci* **12**, 652–669 (2011).

134. Dirnberger, G. & Jahanshahi, M. Executive dysfunction in Parkinson's disease: A review. *J Neuropsychol* **7**, 193–224 (2013).

135. Binetti, G. *et al.* Executive dysfunction in early Alzheimer's disease. *J Neurol Neurosurg Psychiatry* **60**, 91–93 (1996).

136. B.C., M., L.A., F. & A.J., S. Executive dysfunction following traumatic brain injury: Neural substrates and treatment strategies. *NeuroRehabilitation* **17**, 333–344 (2002).

137. Rabinovici, G. D., Stephens, M. L. & Possin, K. L. Executive Dysfunction. *CONTINUUM: Lifelong Learning in Neurology* **21**, 646–659 (2015).

138. Uddin, L. Q. Cognitive and behavioural flexibility: neural mechanisms and clinical considerations. *Nat Rev Neurosci* **22**, 167–179 (2021).

139. Fried, P. A. & Smith, A. M. A literature review of the consequences of prenatal marihuana exposure - An emerging theme of a deficiency in aspects of executive function. *Neurotoxicology and Teratology* vol. 23 1–11 Preprint at https://doi.org/10.1016/S0892-0362(00)00119-7 (2001).

140. Rolls, E. T., Everitt, B. J. & Roberts, A. The Orbitofrontal Cortex [and Discussion] Linked references are available on JSTOR for this article : The orbitofrontal cortex. **351**, 1433–1444 (1996).

141. Miller, E. K., Freedman, D. J. & Wallis, J. D. The prefrontal cortex: Categories, concepts and cognition. *Philosophical Transactions of the Royal Society B: Biological Sciences* **357**, 1123–1136 (2002).

142. Minogianis, E.-A., Servonnet, A., Filion, M.-P. & Samaha, A.-N. Role of the orbitofrontal cortex and the dorsal striatum in incentive motivation for cocaine. *Behavioural Brain Research* **372**, 112026 (2019).

143. Ragozzino, M. E. The Contribution of the Medial Prefrontal Cortex, Orbitofrontal Cortex, and Dorsomedial Striatum to Behavioral Flexibility. *Ann. N.Y. Acad. Sci* **1121**, 355–375 (2007).

144. Lucantonio, F., Caprioli, D. & Schoenbaum, G. Transition from 'model-based' to 'model-free' behavioral control in addiction: Involvement of the orbitofrontal cortex and dorsolateral striatum. *Neuropharmacology* **76**, 407–415 (2014).

145. Pennartz, C. M. A., Ito, R., Verschure, P. F. M. J., Battaglia, F. P. & Robbins, T. W. The hippocampal – striatal axis in learning , prediction and goal-directed behavior. **34**, (2011).

146. Neuroscience, H., Rubin, R. D., Watson, P. D., Duff, M. C. & Cohen, N. J. The role of the hippocampus in flexible cognition and social behavior. **8**, 1–15 (2014).

147. Numan, R. A Prefrontal-Hippocampal Comparator for Goal-Directed Behavior : The Intentional Self and Episodic Memory. **9**, 1–19 (2015).

148. Ouhaz, Z., Fleming, H. & Mitchell, A. S. Cognitive Functions and Neurodevelopmental Disorders Involving the Prefrontal Cortex and Mediodorsal Thalamus. **12**, 1–18 (2018).

149. Parnaudeau, S. *et al.* Archival Report Mediodorsal Thalamus Hypofunction Impairs Flexible Goal-Directed Behavior. *Biol Psychiatry* **77**, 445–453 (2015).

150. Werf, Y. D. Van Der *et al.* Deficits of memory , executive functioning and attention following infarction in the thalamus ; a study of 22 cases with localised lesions. **41**, 1330–1344 (2003).

151. Parnaudeau, S., Bolkan, S. S. & Kellendonk, C. Review The Mediodorsal Thalamus : An Essential Partner of the Prefrontal Cortex for Cognition. *Biol Psychiatry* **83**, 648–656 (2018).

152. Middleton, F. A. & Strick, P. L. Basal ganglia and cerebellar loops: Motor and cognitive circuits. *Brain Res Rev* **31**, 236–250 (2000).

153. Middleton, F. A. & Strick, P. L. Anatomical Evidence for Cerebellar and Basal Ganglia Involvement in Higher Cognitive Function Author (s): Frank A . Middleton and Peter L . Strick Published by : American Association for the Advancement of Science Stable URL : http://www.jstor.org/stabl. *Science (1979)* **266**, 458–461 (1994).

154. Middleton, F. A. & Strick, P. L. Basal ganglia output and cognition: Evidence from anatomical, behavioral, and clinical studies. *Brain Cogn* **42**, 183–200 (2000).

155. Donahoe, J. W. & Palmer, D. C. The behavior of organisms - Skinner , BF years earlier in The Behavior of Organisms. *Journal of the Experimental Analysis f Behavior* **50**, 333–341 (1988).

156. Diller, J. W. *B. F. Skinner and Behaviorism*. *Encyclopedia of Evolutionary Psychological Science* (2021). doi:10.1007/978-3-319-19650-3_1306.

157. Skinner, B. E. The experimental analysis of behavior. *Am Sci* **100**, 54–59 (2012).

158. Lea, S. E. G. Animal experiments in economic psychology. *J Econ Psychol* **1**, 245–271 (1981).

159. Zilio, D. Filling the Gaps : Skinner on The Role of Neuroscience in The Explanation of Behavior. *Behavior and Philosophy* **41**, 33–59 (2013).

160. Skinner, B. F. Behaviorism at fifty. *Science (1979)* **140**, 951–958 (1963).

161. Donahoe, J. W. Behavior analysis and neuroscience: Complementary disciplines. *J Exp Anal Behav* **107**, 301–320 (2017).

162. Arinze, I. & Moorman, D. E. Selective impact of lateral orbitofrontal cortex inactivation on reinstatement of alcohol seeking in male Long-Evans rats. *Neuropharmacology* **168**, 108007 (2020).

163. Lederle, L. *et al.* Reward-related behavioral paradigms for addiction research in the mouse: Performance of common inbred strains. *PLoS One* **6**, (2011).

164. Golden, S. A., Jin, M. & Shaham, Y. Animal models of (or for) aggression reward, addiction, and relapse: Behavior and circuits. *Journal of Neuroscience* **39**, 3996–4008 (2019).

165. Dolan, S. B., Chen, Z., Huang, R. & Gatch, M. B. "Ecstasy" to addiction: Mechanisms and reinforcing effects of three synthetic cathinone analogs of MDMA. *Neuropharmacology* **133**, 171–180 (2018).

166. Radke, A. K., Sneddon, E. A. & Monroe, S. C. Studying Sex Differences in Rodent Models of Addictive Behavior. *Curr Protoc* **1**, 1–18 (2021).

167. Izquierdo, A., Brigman, J. L., Radke, A. K., Rudebeck, P. H. & Holmes, A. The neural basis of reversal learning: An updated perspective. *Neuroscience* **345**, 12–26 (2017).

168. Laughlin, R. E., Grant, T. L., Williams, R. W. & Jentsch, J. D. Genetic dissection of behavioral flexibility: Reversal learning in mice. *Biol Psychiatry* **69**, 1109–1116 (2011).

169. Bissonette, G. B. & Powell, E. M. Reversal learning and attentional set-shifting in mice. *Neuropharmacology* **62**, 1168–1174 (2012).

170. Adriani, W., Koot, S., Saso, L., Van Den Bos, R. & Laviola, G. Home cage testing of delay discounting in rats. *Behav Res Methods* **41**, 1169–1176 (2009).

171. Zeeb, F. D. & Winstanley, C. A. Functional disconnection of the orbitofrontal cortex and basolateral amygdala impairs acquisition of a rat gambling task and disrupts animals' ability to alter decision-making behavior after reinforcer devaluation. *Journal of Neuroscience* **33**, 6434–6443 (2013).

172. Diester, C. M., Lichtman, A. H. & Negus, S. S. Behavioral battery for testing candidate analgesics in mice. II. Effects of endocannabinoid catabolic enzyme inhibitors and Δ9-tetrahydrocannabinol. *Journal of Pharmacology and Experimental Therapeutics* **377**, 242–253 (2021).

173. Brigman, J. L. *et al.* Impaired discrimination learning in mice lacking the NMDA receptor NR2A subunit. *Learning and Memory* **15**, 50–54 (2008).

174. Buscher, N. *et al.* Open-source raspberry Pi-based operant box for translational behavioral testing in rodents. *J Neurosci Methods* **342**, 108761 (2020).

175. Lewon, M. *et al.* Assessment of operant learning and memory in mice born through ICSI. *Human Reproduction* **35**, 2058–2071 (2020).

176. Heyser, C. J., Fienberg, A. A., Greengard, P. & Gold, L. H. DARPP-32 knockout mice exhibit impaired reversal learning in a discriminated operant task. *Brain Res* **867**, 122–130 (2000).

177. Balcombe, J. P., Barnard, N. D. & Sandusky, C. Laboratory routines cause animal stress. *Contemp Top Lab Anim Sci* **43**, 42–51 (2004).

178. KIM, J. J. & HALLER, J. Glucocorticoid Hyper- and Hypofunction. *Ann N Y Acad Sci* **1113**, 291–303 (2007).

179. Gritton, H. J., Sutton, B. C., Martinez, V., Sarter, M. & Lee, T. M. Interactions Between Cognition and Circadian Rhythms: Attentional Demands Modify Circadian Entrainment. *Behavioral Neuroscience* **123**, 937–948 (2009).

180. Valentinuzzi, V. S., Menna-Barreto, L. & Xavier, G. F. Effect of circadian phase on performance of rats in the Morris water maze task. *J Biol Rhythms* **19**, 312–324 (2004).

181. O'Leary, J. D., O'Leary, O. F., Cryan, J. F. & Nolan, Y. M. A low-cost touchscreen operant chamber using a Raspberry Pi^{TM}. *Behav Res Methods* **50**, 2523–2530 (2018).

182. Devarakonda, K., Nguyen, K. P. & Kravitz, A. V. ROBucket: A low cost operant chamber based on the Arduino microcontroller. *Behav Res Methods* **48**, 503–509 (2016).

183. Nguyen, K. P. *et al.* Feeding Experimentation Device (FED): A flexible open-source device for measuring feeding behavior. *J Neurosci Methods* **267**, 108–114 (2016).

184. Nguyen, K. P. *et al.* Feeding experimentation device (FED): Construction and validation of an open-source device for measuring food intake in rodents. *Journal of Visualized Experiments* **2017**, (2017).

185. Ali, M. A. & Kravitz, A. V. Challenges in quantifying food intake in rodents. *Brain Res* **1693**, 188–191 (2018).

186. Matikainen-Ankney, B. A. *et al.* An open-source device for measuring food intake and operant behavior in rodent home-cages. *Elife* **10**, (2021).

187. London, T. D. *et al.* Coordinated ramping of dorsal striatal pathways preceding food approach and consumption. *Journal of Neuroscience* **38**, 3547–3558 (2018).

188. Matikainen-Ankney, B. A. *et al.* Weight Loss After Obesity is Associated with Increased Food Motivation and Faster Weight Regain in Mice. *Obesity* **28**, 851–856 (2020).

189. Open-ephys. New FED3.1. https://open-ephys.org/fed3/fed3.

190. Kravitz, A. V. FED3_library. https://github.com/KravitzLabDevices/FED3_library/wiki.

191. Kravitz, A. V. Custom coding help available. *Google* https://groups.google.com/g/fedforum/c/VhECQbSBG2k/m/otmwT61xAQAJ.

CHAPTER 2

NAPE-PLD regulates specific baseline affective behaviors but is dispensable for inflammatory hyperalgesia

The text represented herein was published in Neurobiology of Pain, Available online from 14 June 2023 at the following location: https://doi.org/10.1016/j.ynpai.2023.100135
Authorship as follows:

Chen I[1#], Murdaugh LB[1,2#], Miliano C[1], Dong Y[1], Gregus AM[1†], and Buczynski MW[1,3†]

Affiliations:
[1]School of Neuroscience, Virginia Polytechnic Institute and State University, Blacksburg, Virginia
[2]Translational Biology, Medicine, and Health, Virginia Polytechnic Institute and State University, Blacksburg, Virginia
[3]Department of Chemistry, Virginia Polytechnic Institute and State University, Blacksburg, Virginia
# These primary authors contributed equally to the paper

2.1 ABSTRACT

N-acyl-ethanolamine (NAEs) serve as key endogenous lipid mediators as revealed by manipulation of fatty acid amide hydrolase (FAAH), the primary enzyme responsible for metabolizing NAEs. Preclinical studies focused on FAAH or NAE receptors indicate an important role for NAE signaling in nociception and affective behaviors. However, there is limited information on the role of NAE biosynthesis in these same behavioral paradigms. Biosynthesis of NAEs has been attributed largely to the enzyme *N*-acylphosphatidylethanolamine Phospholipase D (NAPE-PLD), one of three pathways capable of producing these bioactive lipids in the brain. In this report, we demonstrate that *Nape-pld* knockout (KO) mice displayed reduced sucrose preference and consumption, but other

baseline anxiety-like or depression-like behaviors were unaltered. Additionally, we observed sex-dependent responses in thermal nociception and other baseline measures in wildtype (WT) mice that were absent in *Nape-pld* KO mice. In the Complete Freund's Adjuvant (CFA) model of inflammatory arthritis, WT mice exhibited sex-dependent changes in paw edema that were lost in *Nape-pld* KO mice. However, there was no effect of *Nape-pld* deletion on arthritic pain-like behaviors (grip force deficit and tactile allodynia) in either sex, indicating that while NAPE-PLD may alter local inflammation, it does not contribute to pain-like behaviors associated with inflammatory arthritis. Collectively, these findings indicate that chronic and systemic NAPE-PLD inactivation will likely be well-tolerated, warranting further pharmacological evaluation of this target in other disease indications.

2.2 KEYWORDS

Endocannabinoids ; Lipids ; Sex difference ; Depression ; Hyperalgesia ; Arthritis

2.3 INTRODUCTION

Bioactive lipids have been widely recognized as important neuromodulators in the central nervous system. In contrast to traditional neurotransmitters that are stored and released from presynaptic vesicles, lipids signals are synthesized "on demand" and rapidly metabolized to terminate signaling *in vivo*. *N*-acyl-ethanolamines (NAEs) serve as key endogenous lipid mediators as revealed by manipulating fatty acid amide hydrolase (FAAH), the primary enzyme responsible for metabolizing NAEs. Accordingly, global inactivation of FAAH elevates multiple bioactive NAEs including *N*-oleoylethanolamine (OEA), *N*-palmitoylethanolamine (PEA), and the endocannabinoid anandamide (*N*-arachidonoylethanolamine, AEA) (Leung et al., 2006, Mock et al., 2020, Nyilas et al., 2008, Simon and Cravatt, 2010). NAE biosynthesis has been attributed largely to the enzyme *N*-acylphosphatidylethanolamine Phospholipase D (NAPE-PLD), supported by multiple studies showing reduced NAE levels in the brain following genetic or pharmacological inactivation (Leishman et al., 2016, Leung et al., 2006, Mock et al., 2020, Simon and Cravatt, 2010). However, NAPE-PLD represents one of at least three identified enzymatic pathways in the central nervous system that control NAE production (Leung et al., 2006, Mock et al., 2020, Nyilas et al., 2008, Simon and Cravatt, 2010), hence the contributions of NAEs produced specifically by NAPE-PLD to nociceptive and affective behaviors remains unclear. NAEs mediate their effects through a number of receptors in the central nervous system

(Gregus and Buczynski, 2020, Mock et al., 2023, Pistis and Melis, 2010). For example, AEA can activate cannabinoid receptor 1 (CB1) and cannabinoid receptor 2 (CB2), OEA and PEA can activate peroxisome proliferator-activated receptor α (PPARα), and all three of these NAEs can potentiate transient receptor potential vanilloid 1 (TRPV1) activity. Thus, alterations in endogenous NAE levels may influence numerous central nervous system signaling pathways. Preclinical studies focused on FAAH or NAE receptors indicate an important role for NAE signaling during nociception and affective behaviors. Both rats and mice with elevated FAAH activity subsequently have diminished AEA levels in the amygdala, a critical control hub in the brain for nociception and affective behaviors (Gray et al., 2016, Natividad et al., 2017). Accordingly, long-term FAAH inactivation reduces anxiety-like behaviors in Wistar-Kyoto rats (chronic FAAH inhibitor treatment) and C57BL6/J mice (genetic FAAH knockout) as measured by increased center time in the open field test (Bambico et al., 2010, Vinod et al., 2012). Similar to models of anxiety, elevated FAAH also induces depression-like phenotypes in multiple output modalities including increased sucrose preference and increased forced swim test immobility time (Blanton et al., 2021), while conversely FAAH inhibitors reduce forced swim immobility time in both species (Gobbi et al., 2005, Griebel et al., 2018, Jankovic et al., 2020). These behavioral effects may be mediated by multiple NAE signaling pathways, as pharmacological activation of CB1 and PPARα produces anti-depressant effects in rodents. Administration of synthetic cannabinoids decreases immobility during the forced swim test in rats (15916883), and restores sucrose preference following chronic restraint stress in male mice (Rademacher and Hillard, 2007). Following chronic social defeat stress in male mice, treatment with a PPARα agonist restores sucrose preference and decreases immobility in the forced swim test (Jiang et al., 2017, Jiang et al., 2015). Affective dysfunction exhibits co-morbidity with the emergence of pain hypersensitivity, and systemic inactivation of FAAH produces antinociceptive responses in multiple mouse preclinical pain models including neuropathy, gastrointestinal inflammation, and inflammatory arthritis (Schlosburg et al., 2009). The carrageenan paw inflammation model produces tactile pain hypersensitivity that is reversed by systemic treatment with a FAAH inhibitor in rats and mice (Holt et al., 2005, Sagar et al., 2008). This antihyperalgesic effect of FAAH inactivation is blocked by antagonists of PPARα but not of CB1 in rats (Sagar et al., 2008), and is recapitulated by OEA and PEA in mice (Lo Verme et al., 2005). In the Complete Freund's Adjuvant (CFA) model of inflammatory arthritis, inactivation of FAAH reduces tactile

pain hypersensitivity in rats (Ahn et al., 2011) and in mice through CB1- and CB2-dependent mechanisms (Jayamanne et al., 2006). These studies highlight the need to elucidate specific endogenous NAE signaling mechanisms underlying affective and nociceptive behavioral responses.

While many of these studies were performed in males, accumulating evidence indicates that NAE signaling pathways exhibit sex differences in rodents. For example, female rats express higher levels of FAAH activity and lower AEA levels in the amygdala as compared to males (Krebs-Kraft et al., 2010). Conversely, male rodents express higher levels of CB1 receptors than females in this region, which may be attributed in part to the influence of ovarian hormones in the latter (Castelli et al., 2014). Males also express higher levels of PPARα in T-cells (Dunn et al., 2007) and in the hippocampus (Pierrot et al., 2019), where pharmacological activation of PPARα enhances synaptic plasticity in males but not female mice. These findings reflect the established role of sex in the behavioral responses to nociception (Gregus et al., 2021), anxiety (Hodes and Epperson, 2019), and depression (Kropp and Hodes, 2023) suggesting that behavioral evaluations of NAE signaling should incorporate sex as a biological variable.

Despite the importance attributed to NAEs in nociception and affective disorders as revealed by investigation of FAAH, there is limited information on the role of NAE biosynthesis in these same behavioral paradigms. A recent study using acute dosing of the NAPE-PLD selective inhibitor LEI-401 attributes NAEs from this pathway in fear conditioning in male mice (Mock et al., 2020). However, the role of NAPE-PLD in nociceptive and other affective behaviors has not been broadly evaluated. In this paper, we describe the effects of constitutive deletion of *Nape-pld* on multiple nociceptive and affective behaviors in mice of both sexes. We utilized an extensive test battery that includes exploratory (open field, light–dark box), stress-coping (forced swim, splash), natural reward (sucrose preference), nociceptive (tactile paw withdrawal, thermal escape) and motor function (rotarod, locomotor activity). Finally, we measured nociceptive responses following intraplantar CFA including peripheral inflammation (paw edema), tactile sensitization (tactile paw withdrawal), and functional pain-like (grip force) behavioral assessments to evaluate NAPE-PLD as a target for inflammatory arthritis.

2.4 METHODS

2.4a Reagents and consumables

Materials were purchased as follows: Sigma Aldrich: Ultrapure sucrose (#RES0928S-A102X), Fatty acid-free BSA (#A7030), Tween-20 (#P9416), Tris-HCl (#T5941), Complete Freund's Adjuvant (#F5881, Lot number SLCF1289); Viagen: DirectPCR Lysis Reagent (Mouse Tail, #102-T); Integrated DNA Technologies (Bishay et al.): *Nape-pld* primers; Lonza: Seakem-LE Agarose (#50002); Thermo: SuperSignal West Pico PLUS Chemiluminescent Substrate (#34579), Phusion Hi-Fidelity DNA polymerase (#F530S), Bolt 4–12% Bis-Tris gels (#NW04120BOX), iBlot2 PVDF transfer stacks (#IB24002); BioRad: blotting grade blocker (#1706404); Cayman Chemical: anti-NAPE-PLD rabbit polyclonal antibody (#10306); Cell Signaling: goat anti-rabbit HRP-linked secondary antibody (#7074); Braintree Scientific: Iso Pads, 6″x10″ (#ISO); MWI: Isoflurane (#NDC 13985–528-60), Saline (#NDC 0990–7983-02).

2.4b Animals

All mice were bred in-house using heterozygous × heterozygous breeding pairs of *Nape-pld* mutant mice kindly provided by Benjamin Cravatt (Leung et al., 2006). These mice were generated from 129SvJ-C57BL/6J and backcrossed for at least 10 generations onto a C57BL/6J background and validated using PCR, qPCR, and Western Blot (Supplemental Information Fig. 1). Wildtype (WT), heterozygous (HET) and *Nape-pld* knockout (KO) weanlings were housed 2 to 5 per cage under a 12-hour reverse light cycle (21:00 on/09:00 off) with ad-libitum access to standard chow and water, except when otherwise stated for specific experimental procedures. A total of 75 (36 male and 39 female) WT or *Nape-pld* KO mice 10–20 weeks of age were entered into the study. All behaviors were performed during the dark cycle and measured under controlled light conditions. All behavioral testing was performed by the same observers who were blinded to the genotype and treatment condition by another investigator, and the observers were unblinded at the conclusion of the experiment. All protocols and experiments were approved by the Virginia Tech (Blacksburg, VA, USA) Institutional Animal Care and Use Committee (IACUC) and complied with the ARRIVE guidelines (Percie du Sert et al., 2020).

2.4c Behavoral testing

Affective behavioral battery

Mice were evaluated in a behavioral battery to investigate the effects of sex (male vs. female) and genotype (WT vs. NAPE-PLD KO) on baseline affective behavior (Fig. 1), with one test per week over the course of 9 weeks. In order, mice were evaluated for anxiety-like behavior

(Open Field Test, Light-Dark Box), nociceptive responses (Thermal Escape Latency, Tactile Allodynia), depression-like behavior (Splash Test, Sucrose-Preference Test, Forced Swim Test), and motor function (Rotarod Test). Locomotor activity was determined from data collected during Open Field Test.

Open field test

Mice were tested as previously described (Johnson et al., 2021). Briefly, mice were acclimated to the testing room in their home cage with cage lids open for a minimum of 30 min. At the start of testing, mice were placed in the corner of an opaque testing arena (43 cm × 43 cm × 43 cm) under illuminated conditions (200 lx) and their movements were recorded for 10 min with an overhead camera. The latency to first enter the center space, amount of time spent in the center space (20 cm × 20 cm) and edge (3.5 cm from each wall) spaces, the total number of entries into the edge and center spaces, and the total distance traveled were measured using ANY-maze tracking software (Stoelting Co., version 5.25).

Light dark box

Mice were tested as previously described (Alkhlaif et al., 2017). Briefly, mice were acclimated to the testing room in their home cage with cage lids open for a minimum of 30 min. A black acrylic rectangular insert (43 cm × 15 cm × 43 cm) was placed into an opaque testing arena (43 cm × 43 cm × 43 cm) to create a division of light (25–30 lx) and dark space (<3 lx), with a small opening in one wall that permitted mice to cross between these spaces. At the start of testing, mice were placed into the dark space and their movements were recorded for 10 min with an overhead camera. The amount of time spent in the light and dark spaces, the number of entries into the light and dark spaces, and the mean light and dark space visit lengths were measured using ANY-maze tracking software (Stoelting Co., version 5.25).

Thermal escape latency (hotplate)

Thermal thresholds were tested as previously described (Naidu et al., 2010). Briefly, mice were habituated to the testing room in their home cages for a minimum of 1 h with cage lids open. They were then individually acclimated to the hot plate apparatus (IITC, Part #39) within an acrylic cylinder (IITC, Part #39ME, 9 cm diameter, 30 cm height) for a minimum of 10 min while turned off, and baseline measurements were taken once before experimental evaluation. For all testing procedures, the hot plate was set to 53˚C with a cutoff time of 20 s to prevent

tissue damage, and then mice were placed into the cylinder. Each mouse was measured three times and then averaged to report mean thermal paw withdrawal latency (*i.e.* shaking, lifting or licking the paw, or jumping) using a hand timer.

Tactile allodynia

Tactile allodynia was evaluated using manual von Frey filaments with buckling forces between 0.02 and 2 g (Touch Test, Stoelting Co.) applied to the mid-plantar surface of each hindpaw using the up-down method (Chaplan et al., 1994, Gregus et al., 2018). Mice were habituated to the testing room and apparatus once before collecting data. Prior to testing, mice were acclimated to the testing room in a 4-sided acrylic chamber with only one transparent wall (3 × 3 × 7.5 in.) placed on a metal mesh grid under controlled lighting conditions (~100 lx) for a minimum of 60 min (baseline measurements) or 15 min (experimental timepoints). Any mouse with a basal 50% paw withdrawal threshold (PWT) ≤ 0.79 g was excluded from the study. For baseline measurements, PWTs from both hindpaws were averaged; for CFA, PWTs from the hindpaw ipsilateral to injection (left) were reported. Data were expressed as 50% gram thresholds vs time or as area under the curve (hyperalgesic index % change from baseline).

Splash test

Mice were tested as previously described (Hodes et al., 2015). Briefly, mice were acclimated in a 4-sided acrylic chamber with only one transparent wall (12.5 × 7 × 7.25 in.) containing a mirror opposite to the high-resolution video camera (Logitech C920) for a minimum of 30 min under controlled lighting conditions (25–30 lx). At the start of testing, mice were sprayed three times with water on the backside with a 4 oz spray bottle, then returned to the chamber for evaluation of grooming behavior (20 min). The latency to the first grooming episode and total time spent grooming was recorded.

Forced swim test

Mice were tested as previously described (Can et al., 2012). Briefly, mice were acclimated to the testing room in their home cage with cage lids open for a minimum of 30 min. At the start of testing, mice were placed in a 5000 mL beaker filled with 2500 mL of water (25 ± 0.5 ˚C) and recorded for 6 min. The latency to the first immobile episode (during all 6 min) and total immobility time amount (during the last 4 min) was recorded.

Sucrose preference test

Mice were tested using an open source two-bottle choice apparatus with infrared sensors to detect real-time interactions as previously described (Godynyuk et al., 2019). One sipper tube contained 1% sucrose (1 g of sucrose mixed with 100 g of tap water, made fresh daily) and the other sipper tube contained tap water (prepared fresh daily). Mice were habituated to the two-bottle choice apparatus in their home cages for 48 h, with position of the sucrose tube switched at 24 h. During training, mice were individually placed into a standard home cage with IsoPad bedding and two-bottle choice apparatus for a 2-hour session on three consecutive days. During testing, mice were deprived of water for 24 h and subsequently tested as done during training. Any cage that exhibited substantial liquid below the apparatus indicated a technical malfunction of the sipper tube(s), so these mice were excluded from the final analysis. Each bottle was weighed before and after testing, and the sucrose preference was calculated as the percentage of sucrose consumed relative to the total amount of liquid consumed. Additionally, the total number of sucrose sips during the session was determined by infrared sensor reporting.

Rotarod test

Mice were tested for motor function as previously described (Brickler et al., 2016). Mice were habituated to the testing room in their home cage with cage lids open for a minimum of 30 min. During testing, mice were placed on the Rotarod apparatus (Economex Rotarod, Columbus Instruments, Part# 0201–003 M) set to an initial velocity (10 rpm) with an acceleration of 0.1 rpm/sec. The latency to fall from the rotarod was measured using a hand timer. All animals were tested 3 times with at least a 2-minute resting period after each test. Any mice that fell initially within 20 s were immediately placed back on the rotarod for continued testing.

2.4d Complete freunds adjuvant model of arthritis

The Complete Freund's Adjuvant (CFA) model of arthritis was induced as previously described (Urban et al., 2011). Mice were briefly anesthetized with isoflurane via low-flow vaporizer (Somnosuite, Kent Scientific) and injected with 10 µl of vehicle (saline) or 100% CFA into the left hind paw (day 0), and subsequently tested for clinical and behavioral signs of arthritis for up to 16 days including grip strength, paw edema, and tactile allodynia. Paw edema was measured using digital calipers (Mitutoyo Corporation Digimatic Caliper #500–196-30) in the ipsilateral and contralateral paw (Ghosh et al., 2013), where each paw was measured three

times (reported as the mean of respective paw). Grip strength was evaluated using a grip force meter (BIOSEB #BIO-GS3) using BIO-CIS response analysis software according to a previous report (Montilla-García et al., 2017). Briefly, mice were allowed to grasp a metal grid (BIOSEB #BIO-GRIPGS) and their tails were gently pulled by hand for 3 s to measure the maximal force exerted by the mouse before releasing the grid. Each mouse was measured three times and then averaged to report mean grip force. A systematic review and *meta*-analysis of behavioral outcome measures for intraplantar CFA model of arthritis demonstrates that open field, light–dark box, forced swim test, and sucrose preference test exhibit weak or no correlation with significant effects, so we elected not to examine these parameters in this model (Burek et al., 2022).

2.5 STATISTICAL ANALYSIS

Statistical analyses were performed using GraphPad Prism (version 9.4.1). All data are reported as mean ± SEM, and individual data points are indicated where applicable. All baseline behavioral tests were analyzed using 2-way ANOVA (sex × genotype) and Bonferroni post hoc, with all ANOVA statistics and post hoc p-values reported in Table 1. For the CFA experiments, CFA pain study was analyzed by 3-way repeated measures ANOVA (sex × genotype × time) followed by Tukey's post hoc with all ANOVA statistics and post hoc p-values reported in Table 2. Statistical outliers were determined using Grubb's Test. In the event of multiple outliers within the same genotype and sex, the individual with the higher z-value was removed. The criteria for significance were as follows: *P < 0.05, **P < 0.01, ***P < 0.001.

2.6 RESULTS

2.6a Sex-dependent effects on some baseline anxiety-like behaviors

To evaluate the role of both sex and *Nape-pld* genotype in anxiety-like behavior, we examined WT and KO mice of both sexes in the open field and light–dark box tests. The complete statistical results for these experiments can be found in Table 1. In the open field test, two-way ANOVA revealed that there were no significant effects of *Nape-pld* genotype or sex on the time spent in the center of the apparatus (Fig. 2**A**), latency to the first entry into the center (Fig. 2**B**) or the total number of times the mice crossed between the center and edge of the apparatus (Supplemental Fig. 2**A**). In the light–dark box test, there was an effect of sex, but not genotype, in the total amount of time (Fig. 2**C**) and mean visit length in the light side of the box (Fig. 2**D**), with male *Nape-pld KO* spending significantly more time in and making longer visits

to the light than female *Nape-pld KO* mice. In contrast, there were no differences in the total number of crossings between light and dark (Supplemental Fig. 2**B**). Collectively, these observations indicate that deletion of *Nape-pld* unmasks a phenotypic sex difference wherein males exhibit less of some anxiety-like behaviors than their female counterparts.

2.6b Sex-dependent effects on baseline nociceptive behaviors

Next, we evaluated baseline nociception in WT and KO mice of both sexes in the hotplate (thermal) and von Frey tests (tactile). Two-way ANOVA revealed an effect of sex and an interaction between genotype and sex in thermal thresholds at 53 °C, wherein WT males exhibited significantly lower response latencies than WT females, an effect not observed in *Nape-pld* KO mice (Fig. 3**A**). However, there was no significant effect of sex or genotype on tactile withdrawal thresholds (Fig. 3**B**). These results show that WT female mice exhibit increased thresholds to a 53˚C thermal stimulus compared WT male mice, and this effect was lost in *Nape-pld* KOs as males and females had similar thermal response thresholds.

2.6c Sex- and Nape-pld-dependent effects on baseline depression-like behaviors

To evaluate the role of NAPE-PLD in depression-like behaviors, we examined WT and Nape-pld KO mice in the splash test, forced swim test, and sucrose preference test. In the splash test, two-way ANOVA revealed no significant effect of genotype or sex on the time spent grooming (Fig. 4A). However, we observed an effect of sex as well as an interaction between sex and genotype for latency to initiate grooming behaviors, in which WT males exhibited reduced latency relative to WT females. This sex difference is not present in Nape-pld KO mice (Fig. 4B). For the forced swim test, while there were no significant effects of genotype or sex on total immobility time (Fig. 4C), we noted a sex difference in latency to immobility wherein Nape-pld KO males initiated floating behaviors earlier than isogenic females (Fig. 4D). In contrast, in the sucrose preference test there was a significant effect of genotype (Fig. 4E), with male Nape-pld KO mice showing a trend towards reduced preference for 1% sucrose compared with male WT mice ($p = 0.08$). Similarly, we observed an effect of genotype as well as an interaction between genotype and sex in the number of sips of sucrose solution (Fig. 4F), wherein male Nape-pld KO mice took fewer sips of 1% sucrose compared with WT males. Taken together, these results indicate that Nape-pld contributes to some motivational depression-like behaviors.

2.6d No sex- or Nape-pld-dependent effects on motor function

To evaluate motor coordination and function, we examined WT and Nape-pld KO mice for performance in the rotarod test and locomotor activity from the open field test. We observed no Nape-pld genotype- or sex-dependent differences in locomotor activity based on total distance traveled in the open field arena (Supplemental Fig. 2C) or in total time spent on the rotarod (Supplemental Fig. 2D) as revealed by two-way ANOVA. Overall, these results indicate intact motor function in all groups regardless of sex or expression of NAPE-PLD.

2.6e Sex-specific differences in peripheral inflammation and pain-like behaviors

To evaluate the role of NAPE-PLD in inflammatory hyperalgesia, CFA-induced arthritis was examined in WT and Nape-pld KO mice of both sexes. The complete statistical results for these experiments can be found in Table 2. We measured local inflammation (paw edema), von Frey (tactile allodynia), and grip strength deficit (grip force), a common rheumatological measure of functionality. Measurements of paw edema revealed a significant effect of time and sex (but not genotype), in which maximal swelling was evident on Days 1 and 3 in all groups post-injection by 3-way repeated measures ANOVA (Fig. 5A). Additionally, there was a significant interaction between time and sex, as well as genotype and sex, showing that inflammation in WT females was more pronounced and lasted longer compared with WT males, and this sex-dependent response was lost in Nape-pld KO mice.

Next, we determined the effects of *Nape-pld* on inflammatory hyperalgesia in both sexes using the clinically relevant rheumatological outputs of tactile allodynia and grip force. There was a significant effect of time and sex (but not genotype) on the development of CFA-induced tactile allodynia in which WT and *Nape-pld* KO mice of both sexes exhibited reduced paw withdrawal thresholds within 1 day following CFA (Fig. 5**B**). In addition, we observed an interaction between time and sex, as the resolution of allodynia is expedited in *Nape-pld* KO females versus isogenic male littermates. Similarly, we detected a significant effect of time as well as an interaction between time and genotype on the development of grip force strength deficits, which emerged on Day 1 post-CFA and peaked at day 7 in males and trended toward a peak between days 5 and 10 for females (Fig. 5**C**). Collectively, these results demonstrate that while paw inflammation in *Nape-pld* KO mice is not different between sexes, pain-like behaviors began to resolve more quickly in females regardless of genotype.

2.7 DISCUSSION

Multiple studies have investigated the physiological roles of NAE signaling by targeting metabolism via FAAH inactivation or downstream receptor activity, but the current work is the first to comprehensively evaluate the behavioral effects of long-term inactivation of NAE biosynthesis by *Nape-pld* KO in mice. Accordingly, our findings reveal that *Nape-pld* KO mice exhibit a subset of behavioral changes previously identified as a result of manipulation of FAAH. Specifically, deletion of *Nape-pld* reduced sucrose preference, but not other baseline anxiety-like or depression-like behaviors in naïve mice. In addition, we observed sex differences in multiple baseline measures in WT mice that were absent in *Nape-pld* KO mice. We did not identify any genotypic changes on baseline motor function. Finally, while CFA-induced inflammatory arthritis developed differently in male and female mice, we did not observe any specific effect of *Nape-pld* KO.

The principal genotypic effect of *Nape-pld* inactivation we observed was altered sucrose preference behavior. We found that *Nape-pld* KO mice exhibited less preference for sucrose and less sucrose drinking behavior, consistent with previous studies implicating endocannabinoid signaling in anhedonic aspects of depression-like behavior. Exogenous administration of AEA increased sucrose consumption, whereas systemic administration of a CB1 receptor antagonist decreased sucrose intake in male rats (Higgs et al., 2003). Non-cannabinergic receptor signaling is unlikely to facilitate this aspect of anhedonic behavior as neither TRPV1 (male or female) nor PPARα (male) knockout mice exhibited a difference in sucrose preference (Ellingson et al., 2009, Middleton et al., 1988). Anhedonic differences may also be mediated by stress, as systemic inactivation of FAAH failed to alter sucrose preference in unstressed animals (Bortolato et al., 2007, Rademacher and Hillard, 2007), suggesting that basal endogenous NAE tone is sufficient to support typical hedonic behaviors in naïve mice. However, FAAH inhibitors reduced sucrose preference following social isolation (Carnevali et al., 2020) or stress (Bortolato et al., 2007, Rademacher and Hillard, 2007). Collectively, these studies suggest that anxiogenic or depressive states may be mediated by other NAEs, since exogenous OEA and PEA also prevent stress-induced changes in sucrose preference (Jin et al., 2015, Li et al., 2019). Despite our findings that NAPE-PLD inactivation had no effect on immobility time during the forced swim test, multiple lines of evidence suggest that pharmacological activation of NAE signaling elicits anti-depressive effects during this test. FAAH inhibitors elevate endogenous

NAE levels, and subsequently reduce forced swim immobility time in mice (Gobbi et al., 2005, Griebel et al., 2018, Jankovic et al., 2020). These effects can be recapitulated by activation of CB1 with HU-210 in rats (Hill and Gorzalka, 2005) as well as central activation of PPARα with fenofibrate (Jiang et al., 2017). Thus, pharmacological activation of NAE signaling reduces depression-like behavior during the forced swim test that is not induced by inactivation of NAPE-PLD and thus may rely on other NAE biosynthetic pathways. Collectively, these findings support an important role for *Nape-pld* in mediating the interaction between stress and anhedonic behavior.

Additionally, our findings showed that WT male mice were more sensitive to noxious heat than females in the hotplate test, corroborating findings in rats (Vierck et al., 2008) but in contrast with previous work in mice showing no sex differences in hotplate response latency (Leo et al., 2008). This sex-dependent thermal response sensitivity is lost in *Nape-pld* KO mice, suggesting that NAEs contribute to basal thermal nociception. Males have higher NAE levels and lower expression of FAAH in the amygdala, a key hub for nociceptive processing (Gray et al., 2016, Krebs-Kraft et al., 2010, Natividad et al., 2017). Thus, enhanced thermal sensitivity in males may result from increased NAE activation of pronociceptive signaling via TRPV1, as TRPV1 KO mice (Bolcskei et al., 2005) and rats (Huda et al., 2018) both have increased thermal latency in the hotplate test, and FAAH KO mice unmask endogenous NAE-dependent TRPV1 thermal nociception (Carey et al., 2016). It is also possible that this sex-dependent thermal response could be explained by decreased CB1 and/or CB2 sensitivity, as multiple studies indicate that the analgesic effect of cannabinoids on thermal response latency may have more efficacy in female rats using the tail flick assay (Craft and Leitl, 2008, Craft et al., 2012, Marusich et al., 2015). However, it is less likely that this sex difference results from disparities in PPARα-mediated signaling, as multiple studies assessing the role of sex indicate that this receptor produces pro-nociceptive responses mainly in male rodents. Chemotherapy-induced peripheral neuropathy results in persistent allodynia in male mice that can be reversed by systemic PEA administration, an effect that is blocked by co-administration of the PPARα antagonist GW6471 (Donvito et al., 2016). In a mouse model of spinal nerve injury, fenofibrate produces anti-allodynic effects in males – but not females – that are reversed by administration of the PPARα antagonist GW6471 (Sorge et al., 2015). However, since these studies evaluated

tactile pain hypersensitivity, a role for PPARα in baseline thermal response latency cannot be ruled out.

Our findings suggest that NAPE-PLD does not play a critical role in the development of inflammatory arthritis. We found no impact of *Nape-pld* KO on clinically relevant evoked (tactile) and functional (grip force) measures of pain-like behaviors during inflammatory arthritis, as genetic inactivation did not alter the intensity or duration of allodynia following induction of CFA arthritis. In contrast, acute treatment with a FAAH inhibitor following CFA arthritis increases NAE levels to produce robust anti-allodynia in male mice (Holt et al., 2005) and rats (Ahn et al., 2009). Similar effects were seen in the Collagen-Induced Arthritis model, where long-term chemical or genetic inactivation of FAAH attenuates allodynia in male mice (Kinsey et al., 2011). These studies all indicate that CB1, and possibly CB2, mediate therapeutic actions of FAAH-produced NAE signaling, as FAAH actions are mitigated by treatment with CB1 antagonists. In the Collagen-Induced Arthritis model, daily administration of PEA reverses allodynia after five days of treatment, suggesting that PPARα may also help mitigate arthritis-induced nociception (Impellizzeri et al., 2013). Accordingly, multiple studies indicate that the PPARα agonist fenofibrate may have clinical efficacy in treating pain in patients with rheumatoid arthritis (van Eekeren et al., 2013). In the carrageenan model, the anti-allodynic effects of FAAH inhibitor are blocked by GW647 suggesting a potential role for NAE signaling via PPARα during treatment of arthritis (Jhaveri et al., 2008). These findings indicate that NAEs produced by NAPE-PLD have a therapeutic but not causative role in the development of nociception during arthritis.

We did observe sex-dependent effects in CFA-induced arthritis, wherein females exhibited greater edema during arthritis induction, yet their allodynia resolved earlier than male counterparts. These results are congruent with clinical studies reporting that women with rheumatoid arthritis develop more severe swelling than men (Intriago et al., 2019), yet similar studies examining mice of both sexes during arthritis show mixed results. A murine model of psoriatic arthritis produces more significant paw edema in females (Haley et al., 2021), whereas other studies in mice using either CFA- (Bryant et al., 2019, Chillingworth et al., 2006) or K/BxN-induced arthritis (Woller et al., 2019) displayed no sex differences in mice. Our study used higher animal numbers per group with greater statistical power than previous studies, which may explain the difference in our findings. We observed no effect of NAPE-PLD inactivation on

paw edema, consistent with findings showing that FAAH inhibitors also fail to alter paw swelling following intraplantar carrageenan injection in rats (Okine et al., 2012). Taken together, these results suggest that endogenous NAEs do not play a critical role in the development of global inflammation during arthritis. Likewise, prior literature examining time courses of arthritis-induced allodynia in male and female rodents also reports conflicting findings. The K/BxN model of arthritis produces longer lasting allodynia in male mice (Woller et al., 2019), whereas similar studies using CFA in mice show no significant sex differences in nociception (Bryant et al., 2019, Cook and Nickerson, 2005). Our study showing that allodynia resolves faster in wild-type female mice incorporated greater statistical power, and replicated these results in NAPE-PLD knockout mice that showed the same sex-specific effect. While these findings indicate that endogenous NAEs do not play a critical role in the resolution of pain hypersensitivity during CFA arthritis, they suggest that future studies using this model should be performed with appropriately powered male and female cohorts instead of a mixed-sex design.

Taken together, our findings suggest that NAPE-PLD likely would not be a high value target for treating inflammatory arthritis. However, our results do not preclude involvement of NAPE-PLD in the development of neuropathic pain states following chemotherapy (Noya-Riobó et al., 2023) or nerve injury (Bishay et al., 2010, Jee Kim et al., 2018, Palazzo et al., 2012). It also is possible that deletion of *Nape-pld* may alter other aspects of pain hypersensitivity including spontaneous, affective, or cognitive functions using additional output measures, which could be a focus of future research. Importantly, the lack of deficits in motor function or anxiety-like behaviors in KO mice indicates that chronic pharmacological inactivation of NAPE-PLD likely will be well-tolerated, warranting further evaluation of this target in other appropriate disease indications (Mock et al., 2020).

2.8 REFERENCES

Ahn, K., Johnson, D. S., Mileni, M., Beidler, D., Long, J. Z., McKinney, M. K., Weerapana, E., Sadagopan, N., Liimatta, M., Smith, S. E., Lazerwith, S., Stiff, C., Kamtekar, S., Bhattacharya, K., Zhang, Y., Swaney, S., Van Becelaere, K., Stevens, R. C., Cravatt, B. F., 2009. Discovery and characterization of a highly selective FAAH inhibitor that reduces inflammatory pain. Chem Biol 16, 411-420.

Ahn, K., Smith, S. E., Liimatta, M. B., Beidler, D., Sadagopan, N., Dudley, D. T., Young, T., Wren, P., Zhang, Y., Swaney, S., Van Becelaere, K., Blankman, J. L., Nomura, D. K., Bhattachar, S. N., Stiff, C., Nomanbhoy, T. K., Weerapana, E., Johnson, D. S., Cravatt, B. F., 2011. Mechanistic and pharmacological characterization of PF-04457845: a highly potent and selective fatty acid amide hydrolase inhibitor that reduces inflammatory and noninflammatory pain. J Pharmacol Exp Ther 338, 114-124.

Alkhlaif, Y., Bagdas, D., Jackson, A., Park, A. J., Damaj, I. M., 2017. Assessment of nicotine withdrawal-induced changes in sucrose preference in mice. Pharmacol Biochem Behav 161, 47-52.

Bambico, F. R., Cassano, T., Dominguez-Lopez, S., Katz, N., Walker, C. D., Piomelli, D., Gobbi, G., 2010. Genetic deletion of fatty acid amide hydrolase alters emotional behavior and serotonergic transmission in the dorsal raphe, prefrontal cortex, and hippocampus. Neuropsychopharmacology 35, 2083-2100.

Bishay, P., Schmidt, H., Marian, C., Häussler, A., Wijnvoord, N., Ziebell, S., Metzner, J., Koch, M., Myrczek, T., Bechmann, I., Kuner, R., Costigan, M., Dehghani, F., Geisslinger, G., Tegeder, I., 2010. R-flurbiprofen reduces neuropathic pain in rodents by restoring endogenous cannabinoids. PLoS One 5, e10628.

Blanton, H. L., Barnes, R. C., McHann, M. C., Bilbrey, J. A., Wilkerson, J. L., Guindon, J., 2021. Sex differences and the endocannabinoid system in pain. Pharmacol Biochem Behav 202, 173107.

Bolcskei, K., Helyes, Z., Szabo, A., Sandor, K., Elekes, K., Nemeth, J., Almasi, R., Pinter, E., Petho, G., Szolcsanyi, J., 2005. Investigation of the role of TRPV1 receptors in acute and chronic nociceptive processes using gene-deficient mice. Pain 117, 368-376.

Bortolato, M., Mangieri, R. A., Fu, J., Kim, J. H., Arguello, O., Duranti, A., Tontini, A., Mor, M., Tarzia, G., Piomelli, D., 2007. Antidepressant-like activity of the fatty acid amide hydrolase inhibitor URB597 in a rat model of chronic mild stress. Biol Psychiatry 62, 1103-1110.

Brickler, T., Gresham, K., Meza, A., Coutermarsh-Ott, S., Williams, T. M., Rothschild, D. E., Allen, I. C., Theus, M. H., 2016. Nonessential Role for the NLRP1 Inflammasome Complex in a Murine Model of Traumatic Brain Injury. Mediators Inflamm 2016, 6373506.

Britch, S. C., Goodman, A. G., Wiley, J. L., Pondelick, A. M., Craft, R. M., 2020. Antinociceptive and Immune Effects of Delta-9-Tetrahydrocannabinol or Cannabidiol in Male Versus Female Rats with Persistent Inflammatory Pain. J Pharmacol Exp Ther 373, 416-428.

Bryant, C. D., Bagdas, D., Goldberg, L. R., Khalefa, T., Reed, E. R., Kirkpatrick, S. L., Kelliher, J. C., Chen, M. M., Johnson, W. E., Mulligan, M. K., Imad Damaj, M., 2019. C57BL/6 substrain differences in inflammatory and neuropathic nociception and genetic mapping of a major quantitative trait locus underlying acute thermal nociception. Mol Pain 15, 1744806918825046.

Burek, D. J., Massaly, N., Yoon, H. J., Doering, M., Morón, J. A., 2022. Behavioral outcomes of complete Freund adjuvant-induced inflammatory pain in the rodent hind paw: a systematic review and meta-analysis. Pain 163, 809-819.

Can, A., Dao, D. T., Arad, M., Terrillion, C. E., Piantadosi, S. C., Gould, T. D., 2012. The mouse forced swim test. J Vis Exp, e3638.
Carey, L. M., Slivicki, R. A., Leishman, E., Cornett, B., Mackie, K., Bradshaw, H., Hohmann, A. G., 2016. A pro-nociceptive phenotype unmasked in mice lacking fatty-acid amide hydrolase. Mol Pain 12.
Carnevali, L., Statello, R., Vacondio, F., Ferlenghi, F., Spadoni, G., Rivara, S., Mor, M., Sgoifo, A., 2020. Antidepressant-like effects of pharmacological inhibition of FAAH activity in socially isolated female rats. Eur Neuropsychopharmacol 32, 77-87.
Castelli, M. P., Fadda, P., Casu, A., Spano, M. S., Casti, A., Fratta, W., Fattore, L., 2014. Male and female rats differ in brain cannabinoid CB1 receptor density and function and in behavioural traits predisposing to drug addiction: effect of ovarian hormones. Curr Pharm Des 20, 2100-2113.
Chaplan, S. R., Bach, F. W., Pogrel, J. W., Chung, J. M., Yaksh, T. L., 1994. Quantitative assessment of tactile allodynia in the rat paw. J Neurosci Methods 53, 55-63.
Chillingworth, N. L., Morham, S. G., Donaldson, L. F., 2006. Sex differences in inflammation and inflammatory pain in cyclooxygenase-deficient mice. Am J Physiol Regul Integr Comp Physiol 291, R327-334.
Cook, C. D., Nickerson, M. D., 2005. Nociceptive sensitivity and opioid antinociception and antihyperalgesia in Freund's adjuvant-induced arthritic male and female rats. J Pharmacol Exp Ther 313, 449-459.
Craft, R. M., Leitl, M. D., 2008. Gonadal hormone modulation of the behavioral effects of Delta9-tetrahydrocannabinol in male and female rats. Eur J Pharmacol 578, 37-42.
Craft, R. M., Wakley, A. A., Tsutsui, K. T., Laggart, J. D., 2012. Sex differences in cannabinoid 1 vs. cannabinoid 2 receptor-selective antagonism of antinociception produced by delta9-tetrahydrocannabinol and CP55,940 in the rat. J Pharmacol Exp Ther 340, 787-800.
Croci, T., Zarini, E., 2007. Effect of the cannabinoid CB1 receptor antagonist rimonabant on nociceptive responses and adjuvant-induced arthritis in obese and lean rats. Br J Pharmacol 150, 559-566.
Donvito, G., Wilkerson, J. L., Damaj, M. I., Lichtman, A. H., 2016. Palmitoylethanolamide Reverses Paclitaxel-Induced Allodynia in Mice. J Pharmacol Exp Ther 359, 310-318.
Dunn, S. E., Ousman, S. S., Sobel, R. A., Zuniga, L., Baranzini, S. E., Youssef, S., Crowell, A., Loh, J., Oksenberg, J., Steinman, L., 2007. Peroxisome proliferator-activated receptor (PPAR)alpha expression in T cells mediates gender differences in development of T cell-mediated autoimmunity. J Exp Med 204, 321-330.
Ellingson, J. M., Silbaugh, B. C., Brasser, S. M., 2009. Reduced oral ethanol avoidance in mice lacking transient receptor potential channel vanilloid receptor 1. Behav Genet 39, 62-72.
Ghosh, S., Wise, L. E., Chen, Y., Gujjar, R., Mahadevan, A., Cravatt, B. F., Lichtman, A. H., 2013. The monoacylglycerol lipase inhibitor JZL184 suppresses inflammatory pain in the mouse carrageenan model. Life Sci 92, 498-505.
Gobbi, G., Bambico, F. R., Mangieri, R., Bortolato, M., Campolongo, P., Solinas, M., Cassano, T., Morgese, M. G., Debonnel, G., Duranti, A., Tontini, A., Tarzia, G., Mor, M., Trezza, V., Goldberg, S. R., Cuomo, V., Piomelli, D., 2005. Antidepressant-like activity and modulation of brain monoaminergic transmission by blockade of anandamide hydrolysis. Proc Natl Acad Sci U S A 102, 18620-18625.

Godynyuk, E., Bluitt, M. N., Tooley, J. R., Kravitz, A. V., Creed, M. C., 2019. An Open-Source, Automated Home-Cage Sipper Device for Monitoring Liquid Ingestive Behavior in Rodents. eNeuro 6.
Gray, J. M., Wilson, C. D., Lee, T. T., Pittman, Q. J., Deussing, J. M., Hillard, C. J., McEwen, B. S., Schulkin, J., Karatsoreos, I. N., Patel, S., Hill, M. N., 2016. Sustained glucocorticoid exposure recruits cortico-limbic CRH signaling to modulate endocannabinoid function. Psychoneuroendocrinology 66, 151-158.
Gregus, A. M., Buczynski, M. W., 2020. Druggable Targets in Endocannabinoid Signaling. Adv Exp Med Biol 1274, 177-201.
Gregus, A. M., Buczynski, M. W., Dumlao, D. S., Norris, P. C., Rai, G., Simeonov, A., Maloney, D. J., Jadhav, A., Xu, Q., Wei, S. C., Fitzsimmons, B. L., Dennis, E. A., Yaksh, T. L., 2018. Inhibition of spinal 15-LOX-1 attenuates TLR4-dependent, nonsteroidal anti-inflammatory drug-unresponsive hyperalgesia in male rats. Pain 159, 2620-2629.
Gregus, A. M., Levine, I. S., Eddinger, K. A., Yaksh, T. L., Buczynski, M. W., 2021. Sex differences in neuroimmune and glial mechanisms of pain. Pain 162, 2186-2200.
Griebel, G., Stemmelin, J., Lopez-Grancha, M., Fauchey, V., Slowinski, F., Pichat, P., Dargazanli, G., Abouabdellah, A., Cohen, C., Bergis, O. E., 2018. The selective reversible FAAH inhibitor, SSR411298, restores the development of maladaptive behaviors to acute and chronic stress in rodents. Sci Rep 8, 2416.
Haley, E. K., Matmusaev, M., Hossain, I. N., Davin, S., Martin, T. M., Ermann, J., 2021. The impact of genetic background and sex on the phenotype of IL-23 induced murine spondyloarthritis. PLoS One 16, e0247149.
Higgs, S., Williams, C. M., Kirkham, T. C., 2003. Cannabinoid influences on palatability: microstructural analysis of sucrose drinking after delta(9)-tetrahydrocannabinol, anandamide, 2-arachidonoyl glycerol and SR141716. Psychopharmacology (Berl) 165, 370-377.
Hill, M. N., Gorzalka, B. B., 2005. Pharmacological enhancement of cannabinoid CB1 receptor activity elicits an antidepressant-like response in the rat forced swim test. Eur Neuropsychopharmacol 15, 593-599.
Hodes, G. E., Epperson, C. N., 2019. Sex Differences in Vulnerability and Resilience to Stress Across the Life Span. Biol Psychiatry 86, 421-432.
Hodes, G. E., Pfau, M. L., Purushothaman, I., Ahn, H. F., Golden, S. A., Christoffel, D. J., Magida, J., Brancato, A., Takahashi, A., Flanigan, M. E., Ménard, C., Aleyasin, H., Koo, J. W., Lorsch, Z. S., Feng, J., Heshmati, M., Wang, M., Turecki, G., Neve, R., Zhang, B., Shen, L., Nestler, E. J., Russo, S. J., 2015. Sex Differences in Nucleus Accumbens Transcriptome Profiles Associated with Susceptibility versus Resilience to Subchronic Variable Stress. J Neurosci 35, 16362-16376.
Holt, S., Comelli, F., Costa, B., Fowler, C. J., 2005. Inhibitors of fatty acid amide hydrolase reduce carrageenan-induced hind paw inflammation in pentobarbital-treated mice: comparison with indomethacin and possible involvement of cannabinoid receptors. Br J Pharmacol 146, 467-476.
Huda, R., Chang, Z., Do, J., McCrimmon, D. R., Martina, M., 2018. Activation of astrocytic PAR1 receptors in the rat nucleus of the solitary tract regulates breathing through modulation of presynaptic TRPV1. J Physiol 596, 497-513.
Impellizzeri, D., Esposito, E., Di Paola, R., Ahmad, A., Campolo, M., Peli, A., Morittu, V. M., Britti, D., Cuzzocrea, S., 2013. Palmitoylethanolamide and luteolin ameliorate development of arthritis caused by injection of collagen type II in mice. Arthritis Res Ther 15, R192.

Intriago, M., Maldonado, G., Cardenas, J., Rios, C., 2019. Clinical Characteristics in Patients with Rheumatoid Arthritis: Differences between Genders. ScientificWorldJournal 2019, 8103812.
Jankovic, M., Spasojevic, N., Ferizovic, H., Stefanovic, B., Dronjak, S., 2020. Inhibition of the fatty acid amide hydrolase changes behaviors and brain catecholamines in a sex-specific manner in rats exposed to chronic unpredictable stress. Physiol Behav 227, 113174.
Jayamanne, A., Greenwood, R., Mitchell, V. A., Aslan, S., Piomelli, D., Vaughan, C. W., 2006. Actions of the FAAH inhibitor URB597 in neuropathic and inflammatory chronic pain models. Br J Pharmacol 147, 281-288.
Jee Kim, M., Tanioka, M., Woo Um, S., Hong, S. K., Hwan Lee, B., 2018. Analgesic effects of FAAH inhibitor in the insular cortex of nerve-injured rats. Mol Pain 14, 1744806918814345.
Jhaveri, M. D., Richardson, D., Robinson, I., Garle, M. J., Patel, A., Sun, Y., Sagar, D. R., Bennett, A. J., Alexander, S. P., Kendall, D. A., Barrett, D. A., Chapman, V., 2008. Inhibition of fatty acid amide hydrolase and cyclooxygenase-2 increases levels of endocannabinoid related molecules and produces analgesia via peroxisome proliferator-activated receptor-alpha in a model of inflammatory pain. Neuropharmacology 55, 85-93.
Jiang, B., Wang, Y. J., Wang, H., Song, L., Huang, C., Zhu, Q., Wu, F., Zhang, W., 2017. Antidepressant-like effects of fenofibrate in mice via the hippocampal brain-derived neurotrophic factor signalling pathway. Br J Pharmacol 174, 177-194.
Jin, P., Yu, H. L., Tian, L., Zhang, F., Quan, Z. S., 2015. Antidepressant-like effects of oleoylethanolamide in a mouse model of chronic unpredictable mild stress. Pharmacol Biochem Behav 133, 146-154.
Johnson, A., Rainville, J. R., Rivero-Ballon, G. N., Dhimitri, K., Hodes, G. E., 2021. Testing the Limits of Sex Differences Using Variable Stress. Neuroscience 454, 72-84.
Kinsey, S. G., Naidu, P. S., Cravatt, B. F., Dudley, D. T., Lichtman, A. H., 2011. Fatty acid amide hydrolase blockade attenuates the development of collagen-induced arthritis and related thermal hyperalgesia in mice. Pharmacol Biochem Behav 99, 718-725.
Krebs-Kraft, D. L., Hill, M. N., Hillard, C. J., McCarthy, M. M., 2010. Sex difference in cell proliferation in developing rat amygdala mediated by endocannabinoids has implications for social behavior. Proc Natl Acad Sci U S A 107, 20535-20540.
Kropp, D. R., Hodes, G. E., 2023. Sex differences in depression: An immunological perspective. Brain Res Bull 196, 34-45.
Leishman, E., Mackie, K., Luquet, S., Bradshaw, H. B., 2016. Lipidomics profile of a NAPE-PLD KO mouse provides evidence of a broader role of this enzyme in lipid metabolism in the brain. Biochim Biophys Acta 1861, 491-500.
Leo, S., Straetemans, R., D'Hooge, R., Meert, T., 2008. Differences in nociceptive behavioral performance between C57BL/6J, 129S6/SvEv, B6 129 F1 and NMRI mice. Behav Brain Res 190, 233-242.
Leung, D., Saghatelian, A., Simon, G. M., Cravatt, B. F., 2006. Inactivation of N-acyl phosphatidylethanolamine phospholipase D reveals multiple mechanisms for the biosynthesis of endocannabinoids. Biochemistry 45, 4720-4726.
Li, M., Wang, D., Bi, W., Jiang, Z. E., Piao, R., Yu, H., 2019. N-Palmitoylethanolamide Exerts Antidepressant-Like Effects in Rats: Involvement of PPARα Pathway in the Hippocampus. J Pharmacol Exp Ther 369, 163-172.

Lo Verme, J., Fu, J., Astarita, G., La Rana, G., Russo, R., Calignano, A., Piomelli, D., 2005. The nuclear receptor peroxisome proliferator-activated receptor-alpha mediates the anti-inflammatory actions of palmitoylethanolamide. Mol Pharmacol 67, 15-19.
Marusich, J. A., Craft, R. M., Lefever, T. W., Wiley, J. L., 2015. The impact of gonadal hormones on cannabinoid dependence. Exp Clin Psychopharmacol 23, 206-216.
Middleton, W. D., Dodds, W. J., Lawson, T. L., Foley, W. D., 1988. Renal calculi: sensitivity for detection with US. Radiology 167, 239-244.
Mock, E. D., Gagestein, B., van der Stelt, M., 2023. Anandamide and other N-acylethanolamines: A class of signaling lipids with therapeutic opportunities. Prog Lipid Res 89, 101194.
Mock, E. D., Mustafa, M., Gunduz-Cinar, O., Cinar, R., Petrie, G. N., Kantae, V., Di, X., Ogasawara, D., Varga, Z. V., Paloczi, J., Miliano, C., Donvito, G., van Esbroeck, A. C. M., van der Gracht, A. M. F., Kotsogianni, I., Park, J. K., Martella, A., van der Wel, T., Soethoudt, M., Jiang, M., Wendel, T. J., Janssen, A. P. A., Bakker, A. T., Donovan, C. M., Castillo, L. I., Florea, B. I., Wat, J., van den Hurk, H., Wittwer, M., Grether, U., Holmes, A., van Boeckel, C. A. A., Hankemeier, T., Cravatt, B. F., Buczynski, M. W., Hill, M. N., Pacher, P., Lichtman, A. H., van der Stelt, M., 2020. Discovery of a NAPE-PLD inhibitor that modulates emotional behavior in mice. Nat Chem Biol 16, 667-675.
Montilla-García, Á., Tejada, M., Perazzoli, G., Entrena, J. M., Portillo-Salido, E., Fernández-Segura, E., Cañizares, F. J., Cobos, E. J., 2017. Grip strength in mice with joint inflammation: A rheumatology function test sensitive to pain and analgesia. Neuropharmacology 125, 231-242.
Naidu, P. S., Kinsey, S. G., Guo, T. L., Cravatt, B. F., Lichtman, A. H., 2010. Regulation of inflammatory pain by inhibition of fatty acid amide hydrolase. J Pharmacol Exp Ther 334, 182-190.
Natividad, L. A., Buczynski, M. W., Herman, M. A., Kirson, D., Oleata, C. S., Irimia, C., Polis, I., Ciccocioppo, R., Roberto, M., Parsons, L. H., 2017. Constitutive Increases in Amygdalar Corticotropin-Releasing Factor and Fatty Acid Amide Hydrolase Drive an Anxious Phenotype. Biol Psychiatry 82, 500-510.
Noya-Riobó, M. V., Miguel, C., Soriano, D. B., Brumovsky, P. R., Villar, M. J., Coronel, M. F., 2023. Changes in the expression of endocannabinoid system components in an experimental model of chemotherapy-induced peripheral neuropathic pain: Evaluation of sex-related differences. Exp Neurol 359, 114232.
Nyilas, R., Dudok, B., Urbán, G. M., Mackie, K., Watanabe, M., Cravatt, B. F., Freund, T. F., Katona, I., 2008. Enzymatic machinery for endocannabinoid biosynthesis associated with calcium stores in glutamatergic axon terminals. J Neurosci 28, 1058-1063.
Okine, B. N., Norris, L. M., Woodhams, S., Burston, J., Patel, A., Alexander, S. P., Barrett, D. A., Kendall, D. A., Bennett, A. J., Chapman, V., 2012. Lack of effect of chronic pre-treatment with the FAAH inhibitor URB597 on inflammatory pain behaviour: evidence for plastic changes in the endocannabinoid system. Br J Pharmacol 167, 627-640.
Palazzo, E., Luongo, L., Bellini, G., Guida, F., Marabese, I., Boccella, S., Rossi, F., Maione, S., de Novellis, V., 2012. Changes in cannabinoid receptor subtype 1 activity and interaction with metabotropic glutamate subtype 5 receptors in the periaqueductal gray-rostral ventromedial medulla pathway in a rodent neuropathic pain model. CNS Neurol Disord Drug Targets 11, 148-161.
Percie du Sert, N., Hurst, V., Ahluwalia, A., Alam, S., Avey, M. T., Baker, M., Browne, W. J., Clark, A., Cuthill, I. C., Dirnagl, U., Emerson, M., Garner, P., Holgate, S. T., Howells, D. W.,

Karp, N. A., Lazic, S. E., Lidster, K., MacCallum, C. J., Macleod, M., Pearl, E. J., Petersen, O. H., Rawle, F., Reynolds, P., Rooney, K., Sena, E. S., Silberberg, S. D., Steckler, T., Wurbel, H., 2020. The ARRIVE guidelines 2.0: Updated guidelines for reporting animal research. PLoS Biol 18, e3000410.
Pierrot, N., Ris, L., Stancu, I. C., Doshina, A., Ribeiro, F., Tyteca, D., Bauge, E., Lalloyer, F., Malong, L., Schakman, O., Leroy, K., Kienlen-Campard, P., Gailly, P., Brion, J. P., Dewachter, I., Staels, B., Octave, J. N., 2019. Sex-regulated gene dosage effect of PPARalpha on synaptic plasticity. Life Sci Alliance 2.
Pistis, M., Melis, M., 2010. From surface to nuclear receptors: the endocannabinoid family extends its assets. Curr Med Chem 17, 1450-1467.
Rademacher, D. J., Hillard, C. J., 2007. Interactions between endocannabinoids and stress-induced decreased sensitivity to natural reward. Prog Neuropsychopharmacol Biol Psychiatry 31, 633-641.
Sagar, D. R., Kendall, D. A., Chapman, V., 2008. Inhibition of fatty acid amide hydrolase produces PPAR-alpha-mediated analgesia in a rat model of inflammatory pain. Br J Pharmacol 155, 1297-1306.
Sagar, D. R., Staniaszek, L. E., Okine, B. N., Woodhams, S., Norris, L. M., Pearson, R. G., Garle, M. J., Alexander, S. P., Bennett, A. J., Barrett, D. A., Kendall, D. A., Scammell, B. E., Chapman, V., 2010. Tonic modulation of spinal hyperexcitability by the endocannabinoid receptor system in a rat model of osteoarthritis pain. Arthritis Rheum 62, 3666-3676.
Schlosburg, J. E., Kinsey, S. G., Lichtman, A. H., 2009. Targeting fatty acid amide hydrolase (FAAH) to treat pain and inflammation. AAPS J 11, 39-44.
Simon, G. M., Cravatt, B. F., 2010. Characterization of mice lacking candidate N-acyl ethanolamine biosynthetic enzymes provides evidence for multiple pathways that contribute to endocannabinoid production in vivo. Mol Biosyst 6, 1411-1418.
Sorge, R. E., Mapplebeck, J. C., Rosen, S., Beggs, S., Taves, S., Alexander, J. K., Martin, L. J., Austin, J. S., Sotocinal, S. G., Chen, D., Yang, M., Shi, X. Q., Huang, H., Pillon, N. J., Bilan, P. J., Tu, Y., Klip, A., Ji, R. R., Zhang, J., Salter, M. W., Mogil, J. S., 2015. Different immune cells mediate mechanical pain hypersensitivity in male and female mice. Nat Neurosci 18, 1081-1083.
Urban, R., Scherrer, G., Goulding, E. H., Tecott, L. H., Basbaum, A. I., 2011. Behavioral indices of ongoing pain are largely unchanged in male mice with tissue or nerve injury-induced mechanical hypersensitivity. Pain 152, 990-1000.
van Eekeren, I. C., Clockaerts, S., Bastiaansen-Jenniskens, Y. M., Lubberts, E., Verhaar, J. A., van Osch, G. J., Bierma-Zeinstra, S. M., 2013. Fibrates as therapy for osteoarthritis and rheumatoid arthritis? A systematic review. Ther Adv Musculoskelet Dis 5, 33-44.
Vierck, C. J., Acosta-Rua, A. J., Rossi, H. L., Neubert, J. K., 2008. Sex differences in thermal pain sensitivity and sympathetic reactivity for two strains of rat. J Pain 9, 739-749.
Vinod, K. Y., Xie, S., Psychoyos, D., Hungund, B. L., Cooper, T. B., Tejani-Butt, S. M., 2012. Dysfunction in fatty acid amide hydrolase is associated with depressive-like behavior in Wistar Kyoto rats. PLoS One 7, e36743.
Woller, S. A., Ocheltree, C., Wong, S. Y., Bui, A., Fujita, Y., Goncalves Dos Santos, G., Yaksh, T. L., Corr, M., 2019. Neuraxial TNF and IFN-beta co-modulate persistent allodynia in arthritic mice. Brain Behav Immun 76, 151-158.

2.9 TABLES

2.9a Table 1. Statistics for all behavioral evaluations using 2-way ANOVA.

Figure	Behavioral Test	Factor	F-Value	P-value	Bonferroni
2A	Open Field Test (Center Time)	Genotype	F(1, 71) = 0.2378	0.6273	–
		Sex	F(1, 71) = 3.409	0.0690	–
		Genotype*Sex	F(1, 71) = 0.0179	0.8940	–
2B	Open Field Test (Center Latency)	Genotype	F(1, 71) = 0.8624	0.3562	–
		Sex	F(1, 71) = 0.1005	0.7521	–
		Genotype*Sex	F(1, 71) = 0.2163	0.6433	–
2C	Light Dark Box (Light Time)	Genotype	F(1, 68) = 0.4881	0.4871	WT (M vs F) = 0.8147
		Sex	F(1, 68) = 5.049	0.0279	KO (M vs F) = 0.0294
		Genotype*Sex	F(1, 68) = 0.9386	0.3361	
2D	Light Dark Box (Light Mean Visit)	Genotype	F(1, 67) = 0.2080	0.6498	WT (M vs F) = 0.9678
		Sex	F(1, 67) = 5.126	0.0268	KO (M vs F) = 0.0190
		Genotype*Sex	F(1, 67) = 1.417	0.2381	
3A	Hotplate Test (Response Latency)	Genotype	F(1, 70) = 0.7027	0.4047	WT (M vs F) = 0.0007
		Sex	F(1, 70) = 10.29	0.0020	KO (M vs F) = 0.9999
		Genotype*Sex	F(1, 70) = 6.391	0.0137	
3B	Von Frey Test (Tactile Threshold)	Genotype	F(1, 71) = 0.0076	0.9308	–

Figure	Behavioral Test	Factor	F-Value	P-value	Bonferroni
		Sex	F(1, 71) = 0.0731	0.7876	–
		Genotype*Sex	F(1, 71) = 0.2135	0.6455	–
4A	Splash Test (Grooming Time)	Genotype	F(1, 74) = 2.599	0.1112	–
		Sex	F(1, 74) = 2.516	0.1170	–
		Genotype*Sex	F(1, 74) = 1.445	0.2332	–
4B	Splash Test (Grooming Latency)	Genotype	F(1, 69) = 0.5876	0.4459	WT (M vs F) = 0.0064
		Sex	F(1, 69) = 6.936	0.0104	KO (M vs F) = 0.9999
		Genotype*Sex	F(1, 69) = 4.109	0.0465	
4C	Forced Swim Test (Immobility Time)	Genotype	F(1, 73) = 0.2544	0.6155	–
		Sex	F(1, 73) = 0.3903	0.5341	–
		Genotype*Sex	F(1, 73) = 0.1056	0.7461	–
4D	Forced Swim Test (Immobility Latency)	Genotype	F(1, 70) = 0.1357	0.7137	WT (M vs F) = 0.1868
		Sex	F(1, 70) = 11.66	0.0011	KO (M vs F) = 0.0032
		Genotype*Sex	F(1, 70) = 0.6553	0.4210	
4E	Sucrose Preference (% Sucrose)	Genotype	F(1, 70) = 5.609	0.0206	M (WT vs KO) = 0.0817
		Sex	F(1, 70) = 0.3316	0.5665	F (WT vs KO) = 0.4439
		Genotype*Sex	F(1, 70) = 0.4918	0.4855	

Figure	Behavioral Test	Factor	F-Value	P-value	Bonferroni
4F	Sucrose Preference (# of Sips)	Genotype	F(1, 70) = 5.670	0.0200	M (WT vs KO) = 0.0043
		Sex	F(1, 70) = 0.0009	0.9767	F (WT vs KO) = 0.9999
		Genotype*Sex	F(1, 70) = 5.330	0.0239	
S2A	Open Field Test (Center Crossings)	Genotype	F(1, 71) = 0.0031	0.9555	–
		Sex	F(1, 71) = 0.0704	0.7915	–
		Genotype*Sex	F(1, 71) = 0.5486	0.4614	–
S2B	Locomotor Activity (Total Distance)	Genotype	F(1, 71) = 0.1784	0.6740	–
		Sex	F(1, 71) = 1.550	0.2172	–
		Genotype*Sex	F(1, 71) = 0.1597	0.6906	–
S2C	Light Dark Box (Light Dark Crossings)	Genotype	F(1, 67) = 0.0004	0.9849	–
		Sex	F(1, 67) = 1.748	0.1906	–
		Genotype*Sex	F(1, 67) = 0.4477	0.5057	–
S2D	Rotarod Test (Fall Latency)	Genotype	F(1, 71) = 3.657	0.0599	
		Sex	F(1, 71) = 0.3280	0.5687	–
		Genotype*Sex	F(1, 71) = 0.5377	0.4658	–

2.9b Table 2. Statistics for all behavioral evaluations using 3-way ANOVA.

Figure	Behavioral Test	Factor	F-Value	P-value
5A	Paw Edema (Ispilateral)	Time	F(4.541, 172.6) = 39.66	<0.0001
		Genotype	F(1, 38) = 0.04884	0.8263
		Sex	F(1, 38) = 4.927	0.0325
		Time*Genotype	F(8, 304) = 0.5793	0.7948
		Time*Sex	F(8, 304) = 3.232	0.0015
		Genotype*Sex	F(1,38) = 5.227	0.0279
		Time*Genotype*Sex	F(8, 304) = 2.785	0.0055
5B	Tactile Allodynia (Ipsilateral)	Time	F(8, 552) = 138.4	<0.0001
		Genotype	F(1, 69) = 1.187	0.2796
		Sex	F(1, 69) = 9.040	0.0037
		Time*Genotype	F(8, 552) = 0.5749	0.7988
		Time*Sex	F(8, 552) = 4.678	<0.0001
		Genotype*Sex	F(1, 69) = 0.05516	0.8150
		Time*Genotype*Sex	F(8, 552) = 0.6125	0.7677
5C	Grip Force (change from baseline)	Time	F(6.357, 451.4) = 17.01	<0.0001
		Genotype	F(1, 71) = 0.9521	0.3325
		Sex	F(1, 71) = 0.005372	0.9418
		Time*Genotype	F(8, 568) = 3.647	0.0004
		Time*Sex	F(8, 568) = 1.435	0.1787
		Genotype*Sex	F(1, 71) = 0.07860	0.7800
		Time*Genotype*Sex	F(8, 568) = 0.8642	0.5466

2.10 FIGURES

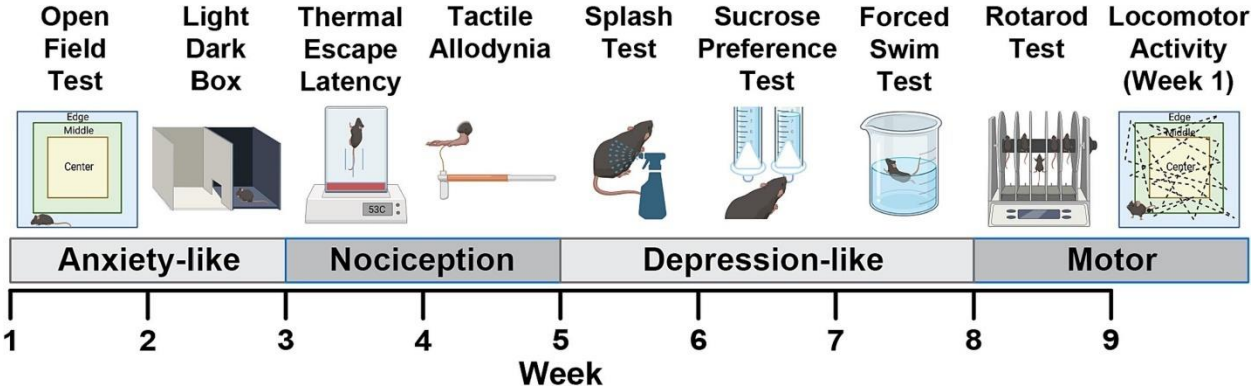

Fig. 1. Experimental timeline for behavioral characterization of male and female *Nape-pld* KO mice. All images were generated using BioRender.

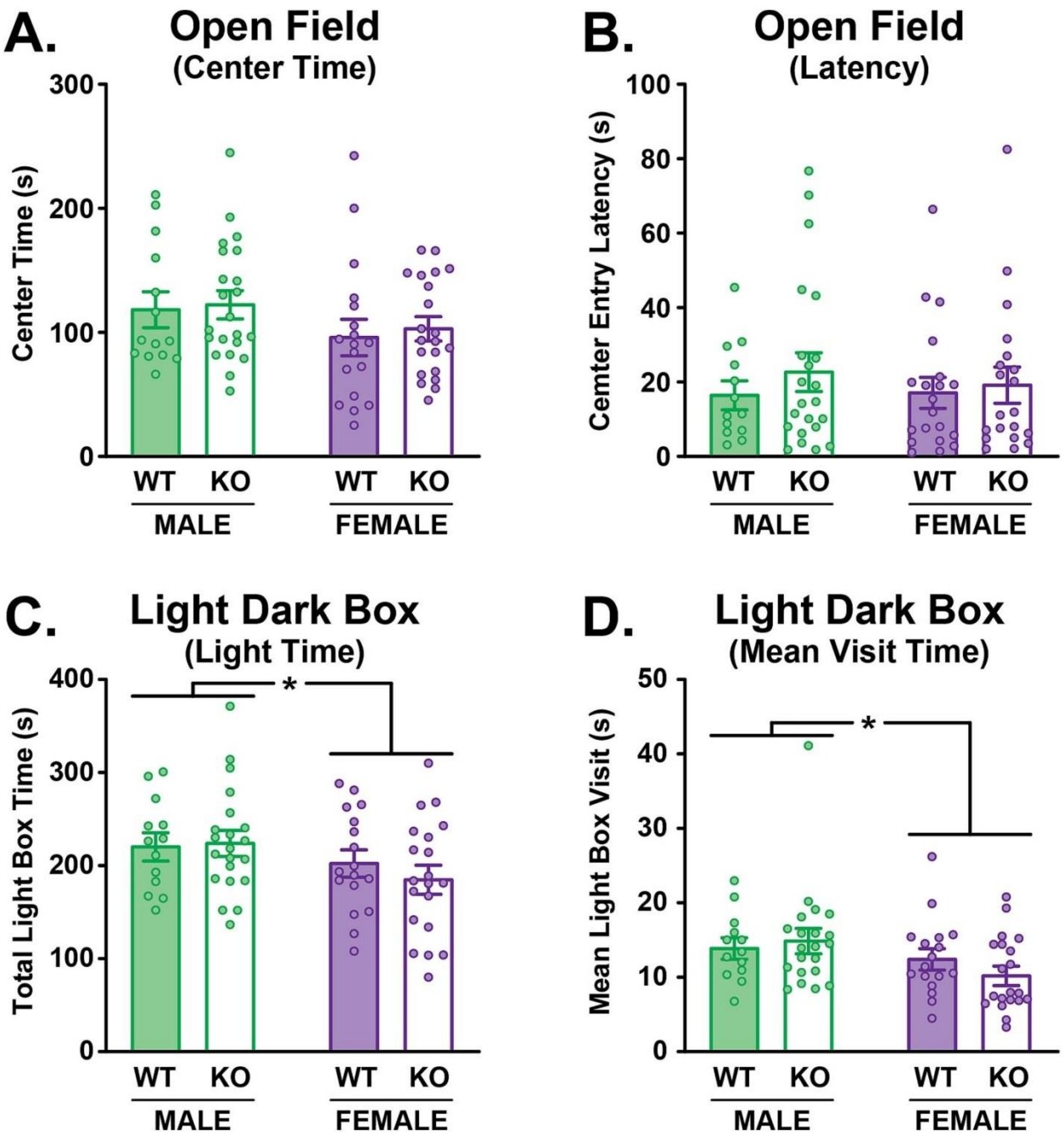

Fig. 2. Contribution of NAPE-PLD to baseline anxiety-like behaviors in males and females. (A) Time spent in the center of the open field test. (B) Latency to first enter the center of the open field apparatus. (C) Total time spent in the light side during the light–dark box test. (D) Mean time spent in a single light side visit during the light–dark box test. Data are presented as mean ± SEM, with WT (filled bars: males in green, n = 14–16; females in purple, n = 14–15) and *Nape-pld* KO mice (open bars: males in green, n = 14–16; females in purple n = 14–15).

Statistical significance indicated by *P < 0.05. (For interpretation of the references to colour in this figure legend, the reader is referred to the web version of this article.)

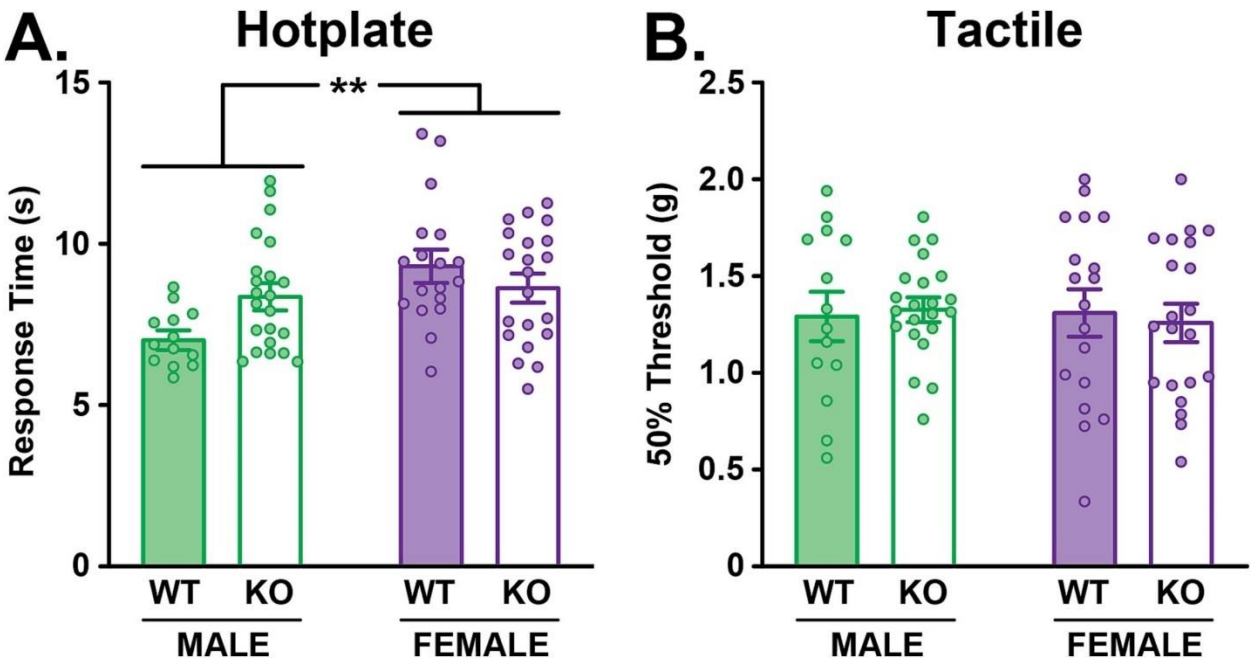

Fig. 3. Contribution of NAPE-PLD to baseline nociceptive thresholds in males and females. (A) Baseline average latency to withdrawal response in the hot plate test at 53 °C. (B) Baseline 50% tactile paw withdrawal threshold in the von Frey test. Data are presented as mean ± SEM, with WT (filled bars: males in green, n = 14; females in purple, n = 18) and *Nape-pld* KO mice (open bars: males in green, n = 22; females in purple n = 21). Statistical significance indicated by **P < 0.01. (For interpretation of the references to colour in this figure legend, the reader is referred to the web version of this article.)

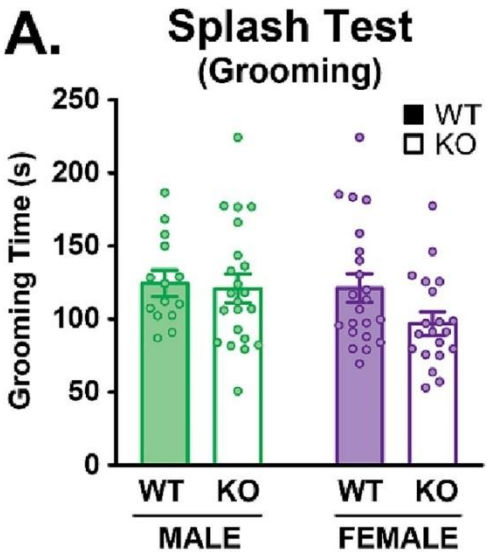
A.
Splash Test
(Grooming)
Grooming Time (s)
250
200
150
100
50
0
WT
KO
WT KO WT KO
MALE FEMALE

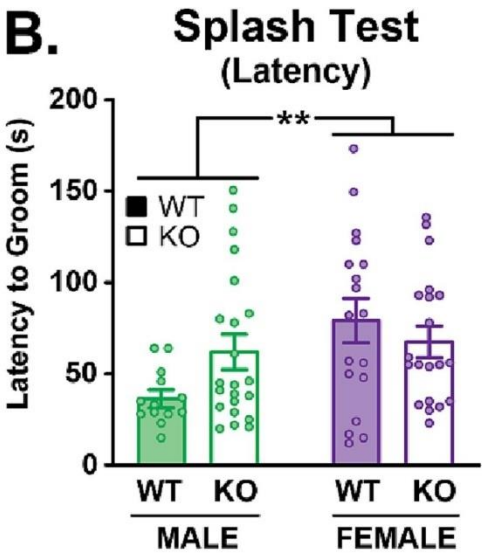
B.
Splash Test
(Latency)
Latency to Groom (s)
200
150
100
50
0
**
WT
KO
WT KO WT KO
MALE FEMALE

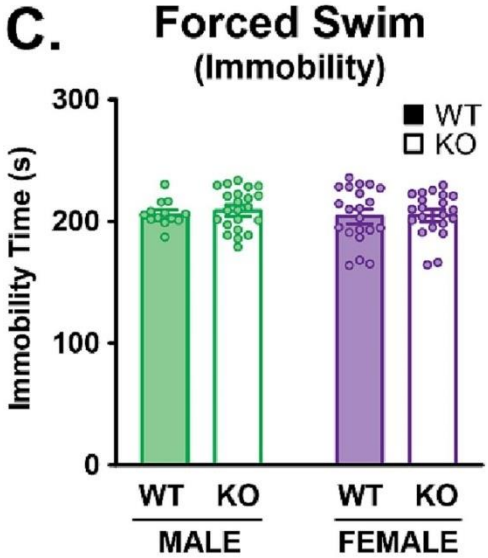
C.
Forced Swim
(Immobility)
Immobility Time (s)
300
200
100
0
WT
KO
WT KO WT KO
MALE FEMALE

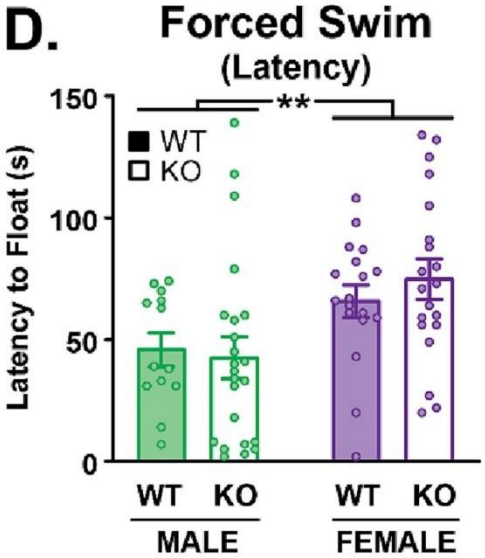
D.
Forced Swim
(Latency)
Latency to Float (s)
150
100
50
0
**
WT
KO
WT KO WT KO
MALE FEMALE

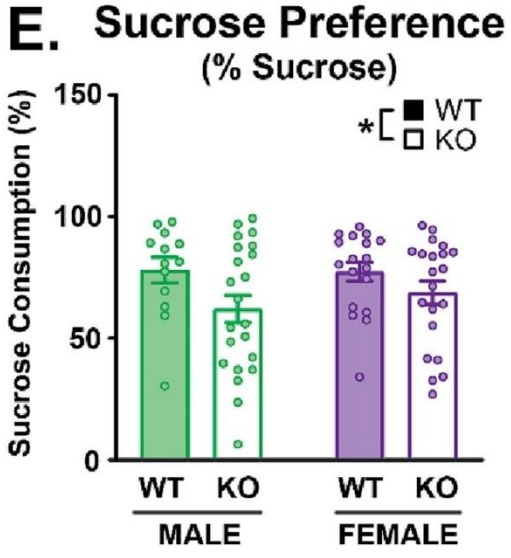
E.
Sucrose Preference
(% Sucrose)
Sucrose Consumption (%)
150
100
50
0
*
WT
KO
WT KO WT KO
MALE FEMALE

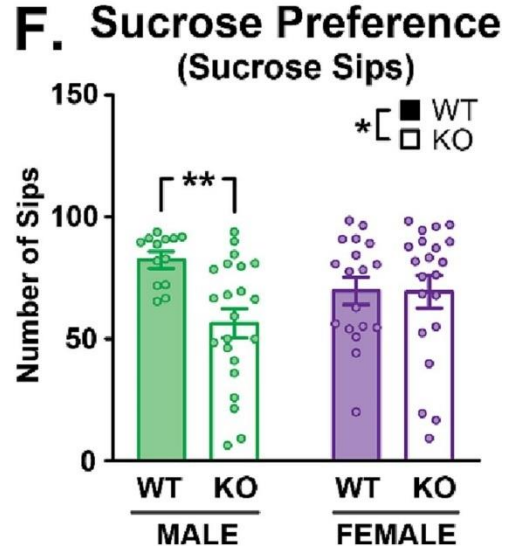
F.
Sucrose Preference
(Sucrose Sips)
Number of Sips
150
100
50
0
**
*
WT
KO
WT KO WT KO
MALE FEMALE

Fig. 4. Contribution of NAPE-PLD to depression-like behaviors in males and females. (A) Time spent grooming (s) and (B) Latency to first grooming (s) in the splash test. (C) Total immobility time (s) and (D) Latency to first immobility time (s) in the forced swim test. (E) Sucrose preference based on total grams consumed and (F) Number of sips of 1% sucrose solution during the sucrose preference test. Data are presented as mean ± SEM, with WT (filled bars: males in green, n = 13–14; females in purple, n = 18) and *Nape-pld* KO mice (open bars: males in green, n = 22; females in purple n = 20–21). Statistical significance indicated by *P < 0.05, **P < 0.01. (For interpretation of the references to colour in this figure legend, the reader is referred to the web version of this article.)

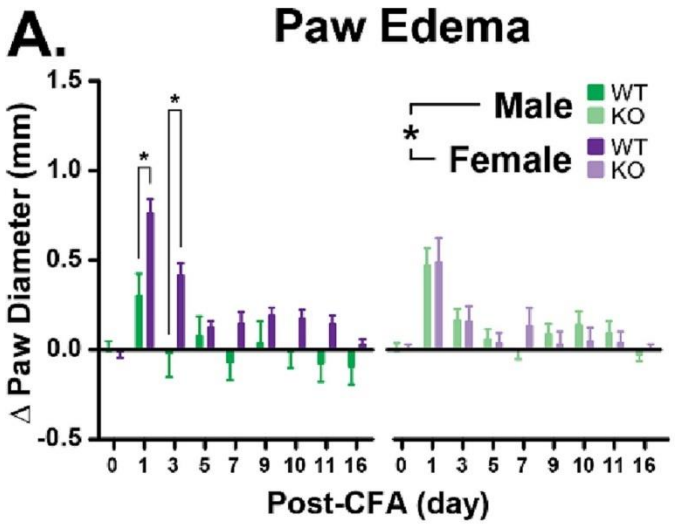
A.
Paw Edema
Male
WT
KO
Female
WT
KO
*
*
*
Δ Paw Diameter (mm)
1.5
1.0
0.5
0.0
-0.5
0 1 3 5 7 9 10 11 16
0 1 3 5 7 9 10 11 16
Post-CFA (day)

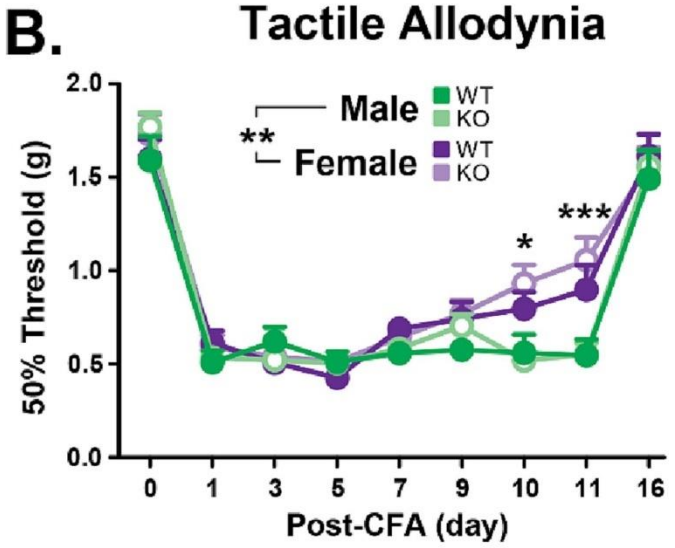
B.
Tactile Allodynia
Male
WT
KO
Female
WT
KO
**
*
***
50% Threshold (g)
2.0
1.5
1.0
0.5
0.0
0 1 3 5 7 9 10 11 16
Post-CFA (day)

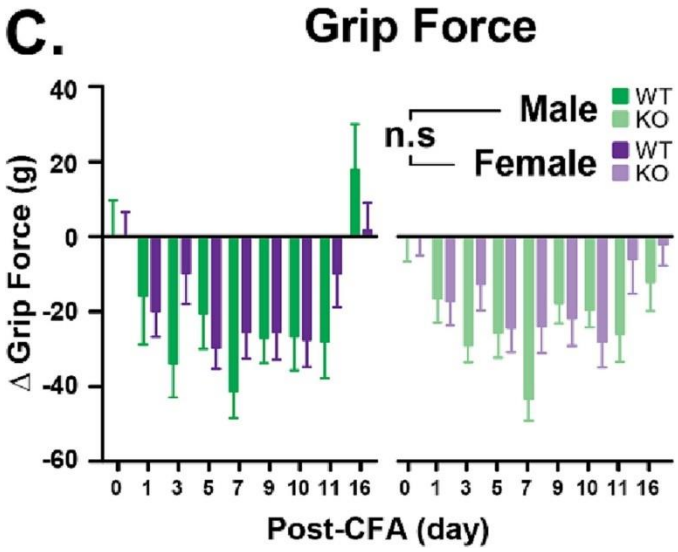
C.
Grip Force
Male
WT
KO
n.s
Female
WT
KO
Δ Grip Force (g)
40
20
0
-20
-40
-60
0 1 3 5 7 9 10 11 16
0 1 3 5 7 9 10 11 16
Post-CFA (day)

Fig. 5. Evaluation of arthritis pain model using CFA in *Nape-pld* KO male and female mice. Time courses of changes in (A) Ipsilateral paw diameter (mm), (B) 50% tactile withdrawal threshold (g) and (C) Grip force (g) from the mean following induction of CFA. Data are presented as mean ± SEM, with WT (left: males in dark green, n = 10–23; females in dark purple, n = 12–18) and NAPE-PLD KO mice (right: males in light green, n = 13–22; females in light purple n = 17–21); the lower # in the range represents n for paw edema experiment. Statistical significance indicated by *P < 0.05, **P < 0.01, ***P < 0.001. (For interpretation of the references to colour in this figure legend, the reader is referred to the web version of this article.)

2.11 SUPPLEMENTAL MATERIAL

2.11a Supplemental Methods

2.11a i Genotyping:

Colony genotyping was conducted by Transnetyx (Cordova, TN) and validated in-house by PCR and western blot (**Supplemental Figure 1**). DNA extraction was performed with Viagen DirectPCR Lysis Reagent (Mouse Tail) according to the manufacturer's instructions. PCR for *Nape-pld* WT, HET, and KO mice was conducted using Phusion Hi-Fidelity DNA polymerase according to the manufacturer's instructions and previously published procedures with primer sets listed below (Leung et al., 2006). Product sizes were 1 band at 245 bp for WT, 1 band at 385 bp for KO, and 2 bands at 245 and 385 bp for HET.

PLD+/+ primer set:

5'-GAGCTGGACTGGTGGGAGGAG-3', 5'-GCTCCGATGGGAATGGCCGC-3'

PLD-/- primer set:

5'-CTGCACACTTGTTCCCCGAGC-3', 5'-GCTGCTATTGGCCGCTGC-3'

2.11a ii qPCR:

Total RNA was extracted using RNeasy Lipid Tissue Mini Kit (Qiagen #74804) and cDNA libraries generated by iScript cDNA synthesis kit (BioRad #1708891) according to the manufacturer's instructions. qPCR was performed in Life Technologies MicroAmp Fast Optical 96-Well Reaction Plates (#4346906) on an ABI PRISM® 7700 using Taqman Fast Advanced Master Mix and primer/probe sets for mouse *Nape-pld* (Mm00724596_m1 FAM_MGB) and *Gapdh* (Mm99999915_g1 VIC_MGB) as a loading control.

2.11a iii Western Blotting:

Total protein was extracted and processed according to previously published procedures with modifications (Leung et al., 2006). Membrane proteins (30 ug) from brain of WT or *Nape-pld* KO mice were resolved by Bolt 4-12% Bis-Tris SDS-PAGE gel, transferred to membranes using iBlot2 PVDF transfer stacks (7 min, 20V) and blocked with 5% blotting grade blocker in TBST. Membranes were probed with anti-NAPE-PLD antibody in rabbit (1:200 dilution in 3% fatty-acid free BSA in TBST) followed by anti-rabbit HRP-linked secondary antibody (1:5000 dilution in 5% blotting grade blocker in TBST), and then developed using SuperSignal West Pico PLUS Chemiluminescent Substrate according to the manufacturer's instructions. NAPE-PLD KO was confirmed by absence of a single protein band at 46 kDa.

2.11b Supplemental Figures

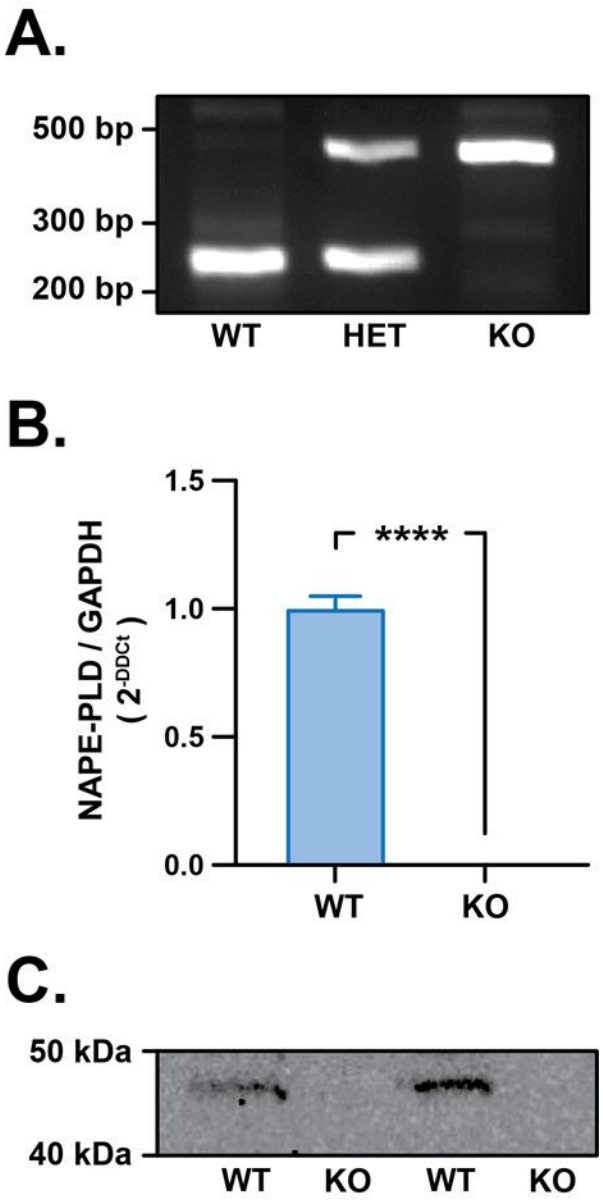

Supplemental Figure 1: Biochemical confirmation of *Nape-pld* KO mice. (A) PCR analysis of mouse genomic DNA from wild-type (WT), heterozygous (HET) and homozygous *Nape-pld* knockout (KO) mice resulting from HETxHET breeding. The lower (245 bp) and upper (385 bp) band correspond to WT and KO genotypes, respectively. Both bands are detected in HET mice. **(B) (B)** Quantitative PCR analysis of brain tissue from WT and *Nape-pld* KO mice. **(C)** Western blot of brain tissue (30 µg) from WT and *Nape-pld* KO mice. Statistical significance indicated by ****P < 0.001.

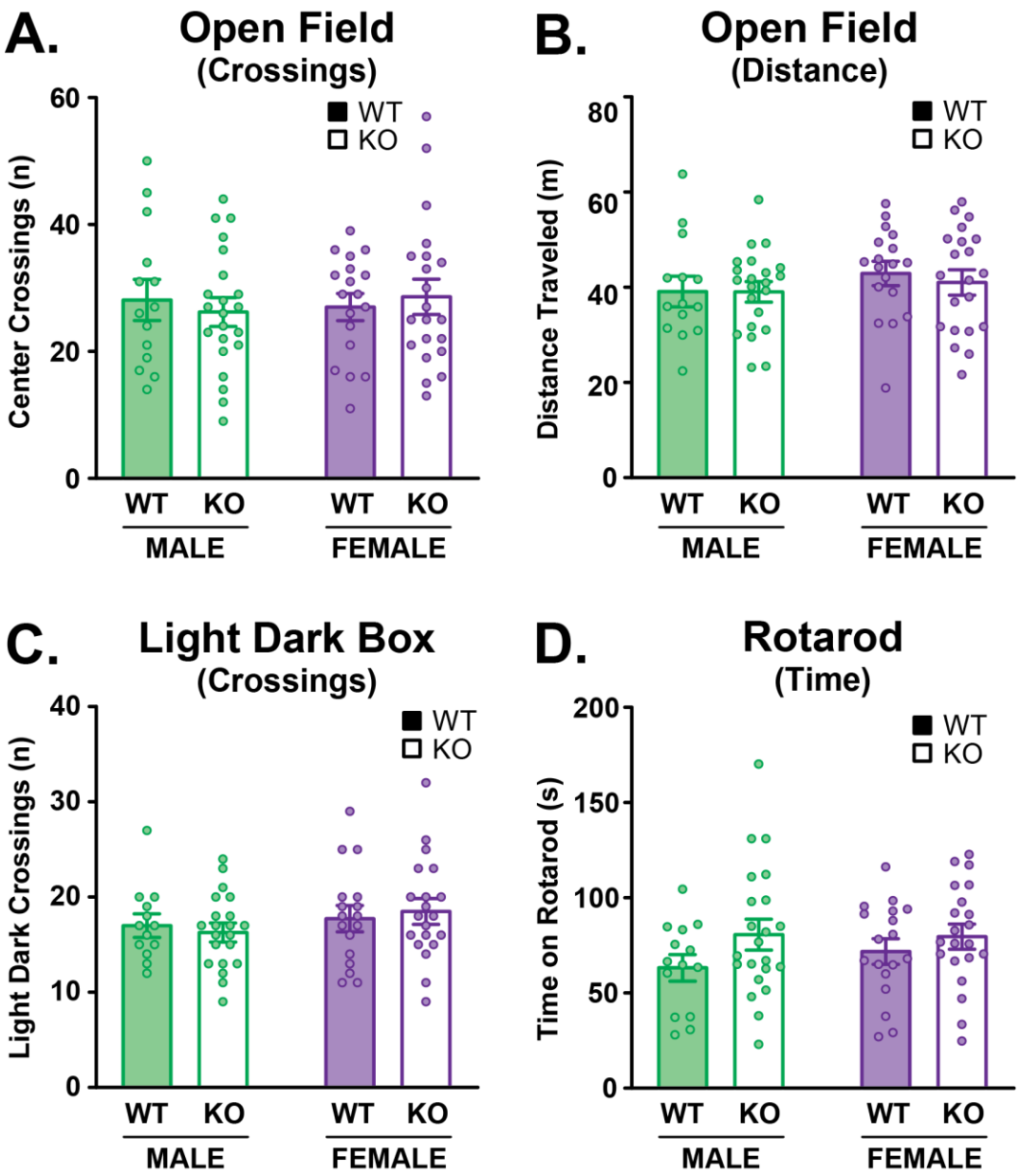

Supplemental Figure 2: Evaluation of motor function in *Nape-pld* KO males and females. (A) Number of crossings between center and edge zones during the open field test. **(B)** Total distance traveled (m) during the Open Field Test. **(C)** Number of crossings between the light and dark side during the light dark box. **(D)** Latencies (s) to fall from the rotarod. Data are presented as mean ± SEM, with WT (filled bars: males in green, n=14-16; females in purple, n=14-18) and *Nape-pld* KO mice (open bars: males in green, n=14-22; females in purple n=14-21).

CHAPTER 3

Effect of chronic vapor nicotine exposure on affective and cognitive behavior in male mice

Number of figures: 7; Number of tables: 1

3.1 ABSTRACT

Nicotine use is a leading cause of preventable deaths both in the US and worldwide, and a majority of those who attempt to quit will relapse. While electronic cigarettes and other electronic nicotine delivery systems (ENDS) were presented as a safer alternative to traditional cigarettes and promoted as devices to help traditional tobacco smokers reduce or quit smoking, they have instead contributed to increasing nicotine use among youths. Despite this, ENDS also represent a useful tool to create novel preclinical animal models of nicotine exposure that more accurately represent human nicotine use. In this study, we validated a chronic, intermittent, ENDS-based passive vapor exposure model in mice, and then measured changes in multiple behaviors related to nicotine abstinence. First, we performed a behavioral dose curve to investigate the effect of different nicotine inter-vape intervals on various measures including body weight, and locomotor activity. Next, we performed a pharmacokinetic study to measure plasma levels of nicotine and cotinine following chronic exposure for each inter-vape interval. Finally, we utilized a behavior test battery at a single dosing regimen to investigate the effects of chronic exposure to nicotine, vehicle, or passive airflow on affective and cognitive behaviors.

3.2 KEYWORDS

ENDS, e-cigarette, nicotine, vaping, affective behavior, cognitive behavior,

3.3 INTRODUCTION

While a half-century of effort has successfully reduced overall nicotine use from its highest levels, 18.7% of US adults [1] and 10.0% of US middle- and high-school youths [2] report

current tobacco use. Despite progress in reducing their consumption, tobacco and nicotine use remains a leading cause of preventable death in the US. Since the advent of electronic cigarettes (e-cigarettes) and electronic nicotine delivery systems (ENDS), many users have shifted away from using traditional combustible cigarettes and towards these novel methods of nicotine delivery [3,4]. ENDS are typically small battery-powered devices that heat and deliver a mixture of a liquid vehicle, drug (e.g., nicotine, Δ9-tetrahydrocannabinol), and/or flavors for user inhalation [5]. Despite the popularity of such devices, there is limited basic or preclinical research [6] into the physiological, behavioral, and cognitive effects of chronic vapor-based exposure (CVE) to nicotine.

The use of animal models allows researchers to perform in-depth research into the mechanisms and/or circuitry underlying the behavioral and cognitive effects of chronic vapor-based nicotine exposure, which is still under-studied. Historically, research on the health implications of chronic nicotine exposure [7–9] has used non-inhalation routes of administration (e.g., intravenous self-administration, continuous subcutaneous exposure) to recapitulate human nicotine consumption. It is well known that the route of administration strongly influences the subjective or reinforcing effects of a drug, ultimately contributing to its addictive potential [10–12]. For these reasons, intravenous self-administration of nicotine has considerable face validity[13,14] as the drug quickly crosses the blood-brain barrier to exert central nervous system effects. However, the development of ENDS allows the study of nicotine effects by using the same route of administration of clinical populations. While some researchers have begun to employ ENDS-based vapor delivery systems to study the neurobiological effects of chronic nicotine exposure [15–17], most studies to date have investigated a limited number of dosing regimens or behavioral outputs.

To address this gap, we first investigated the dose-dependent physical, behavioral, and pharmacokinetic effects of nicotine under chronic exposure conditions. Based on these experiments, we selected the chronic nicotine dosing procedure that produced pharmacokinetic and behavioral responses that best recapitulated responses observed in human smokers and performed a multi-faceted test battery to investigate the subsequent effects of CVE on affective, and cognitive behaviors.

3.4 MATERIALS AND METHODS

Animals: C57BL/6J male mice (8-10 weeks at the beginning of experiments) were obtained from Jackson labs and group housed five to a cage on a 12-hour reverse light cycle (21:00 on/9:00 off). Animals were given *ad libitum* access to standard chow and water, except when otherwise stated. Chronic Vapor Exposure and all behavioral experiments were performed during the dark cycle unless otherwise stated. All experimental procedures were conducted in accordance with the guidelines for the care and use of animals, as set by the National Institutes of Health. Protocols were approved by the Institutional Animal Care and Use Committee (IACUC) of Virginia Tech (Blacksburg, VA, USA).

Chronic Vapor Exposure (CVE) paradigm: CVE was performed using a vacuum-based vapor exposure system from La Jolla Alcohol Research [17–19]. Animals were placed into sealed home cages with their standard housing cage-mates for 8 hours a day, 5 days a week (9:00-17:00 M-F) before being returned to their standard home cages. The sealed cages continuously received clean room air from a down-stream vacuum pump (16 L/m), and a computer-controlled Electronic Nicotine Delivery System (ENDS) delivered vapor (3 sec, 200˚C) at pre-defined inter-vape intervals (2 to 60 minutes). The e-liquid vehicle (VEH) consisted of 50% propylene glycol (Sigma-Aldrich, P4347) and 50% vegetable glycerin (Sigma-Aldrich, G5516) (50/50 PGVG), and all experiments with nicotine (NIC) used a dose of 20 mg/ml (-)-nicotine (Sigma Aldrich, N3876). During all vapor exposure procedures, mice could move freely within the home cage with *ad libitum* access to food and water.

Pharmacokinetic analysis: Submandibular blood sampling was performed as previously described [20,21] by collecting blood in EDTA-coated tubes at different time points (5 minutes or 1,2,4, and 24 hours) following chronic vaping exposure. Blood samples were immediately centrifuged at 3000xg for 15 minutes at 4°C and plasma was stored at -80°C until analysis. The samples were processed and analyzed by using UPLC-MS/MS. The nicotine extraction was performed by adding 5µL of isotopically labeled nicotine-d4 and cotinine-d3 internal standards to 50 µl of plasma, followed by 100 µL Brine NaOH solution and 100 µL of Methyl tert-butyl ether (MTBE). After briefly vortexing, samples were placed in dry ice for approximately one

minute to freeze the aqueous layer[22]. The organic layer was transferred to a mass spec vial and analyzed using a 1290 Infinity II LC System (Agilent Technologies) coupled with a 6495 triple quadrupole mass detector (Agilent Technologies). The chromatographic separation was performed with an Acquity UPLC® BEH HILIC column (Waters Corporation, 2.1 mm I.D. × 100 mm, particle size 1.7 µm) at a flow rate of 400 µL/min at 35 °C, by injecting 2µL of sample. The mobile phase consisted of solvent A (0.2% formic acid, 10 mM ammonium formate in water) and solvent B (Acetonitrile, 0.2% formic acid). The analytes were eluted with the following gradient: 0–1.50 min, 99% (B); at 2.7 min, 98% (B); at 3 min, 95% (B); at 3.1 min, 70% (B); 3.10-5.10 min, 70% (B); at 5.20 min, 40% (B); 5.20-7.50 min, 40% (B); at 7.51 min, 95% (B); at 8.50 min, 99% (B); 8.50-10 min, 99% (B). The acquisition mode used was multiple reaction monitoring (MRM) in positive mode. The following transition ions were monitored for the analytes and their isotope-labeled internal standards: Nicotine (163.2 →132.4), d4-nicotine (167.2 →136.4), Cotinine (177.2 →80), d3-cotinine (180.2 →101). A 9-point calibration curve containing Nicotine (0.78-200 ng/ml) and Cotinine (2.34-600 ng/ml) was constructed using the peak area ratios of the drugs to their deuterated internal standards. Plasma control samples were run to calculate the limit of quantification (LOQ) which was 6.6 ng/ml for Nicotine and 18.7 ng/ml for Cotinine, respectively. The limit of detection (LOD) was calculated as the amount of compound able to give a 3 times higher response than noise signal and it was 0.78 ng/ml for Nicotine and 0.3 ng/ml for Cotinine. Pharmacokinetic parameters for blood level time courses such as AUC, Cmax, and t1/2 are reported in **Table 1**.

Behavioral assessments of nicotine exposure

Open Field Test: OFT was performed 2 hours after completion of vapor exposure as we have described previously[23]. The mouse's position was assessed by AnyMaze software using an overhead camera to measure the total distance traveled (m), time spent immobile (s), time spent in edge or center zone, and number of center entries.

Light/Dark Box test*:* LDT was performed at 2 and 24 hours after completion of vapor exposure as we have described previously[23]. Time spent on either side (s), latency to exit from the dark chamber (s), and average dark visits (s) were recorded.

Locomotor activity: The locomotor activity of mice was recorded in clear cages by using a video tracking system (AnyMaze) to measure the total distance traveled (m) for 1 hour prior to starting the vaping session and 1 hour immediately following the vaping session.

Tactile Allodynia: We performed a time course at 1,2,4,16, and 24 hours after vapor exposure; tactile allodynia was evaluated using manual von Frey filaments with buckling forces between 0.02 and 2 g (Touch Test, Stoelting Co.) applied to the mid-plantar surface of each hind paw using the up-down method as we have described previously[23–25.] All testing was performed under red light during the dark cycle, and the researcher was blinded to the experimental conditions. Any mouse with a basal 50% paw withdrawal threshold (PWT) ≤0.79 g was excluded from the study. For baseline measurements, PWTs from both hind paws were averaged. Data were expressed as 50% gram thresholds vs time.

Splash Test: The splash test protocol was conducted as we described previously[23] 2 hours after the last vapor exposure using tap water. The total time spent grooming was recorded.

Sucrose Preference Test: The sucrose preference test was performed by exposing the mice to two bottles with either tap water or 1% sucrose, in a 2-hour session at 2 and 24 hours after cessation of vapor exposure. Each bottle was weighed before and after testing, and sucrose preference was calculated as the % sucrose consumed relative to the total liquid intake ((sucrose consumed (g)/total liquid consumed (g))x 100) for each session.

Operant Conditioning using FED3

Equipment and Setup: Operant conditioning was performed using the Feeding Experimentation Device 3 (FED3)[26–28]. The FED3 is a small battery-powered operant device that dispenses pellet rewards (*e.g.*, grain-based diet or sucrose) according to experimenter-designed programs. For this

set of behaviors we used sucrose pellets (Dustless Precision Pellets, 20 mg Sucrose, Bio-Serv). The FED3 contains two nose pokes for operant training, a pellet well for reward retrieval, and light and sound cues upon reward delivery. All actions are timestamped and recorded in internal storage for future analysis. To habituate mice to the FED3 and increase the speed of acquisition of FR1 behavior[28] mice were given 48 hours of continuous access to a FED3 in their group-housed home cage. This device was set to the Free Feeding paradigm, where the removal of a pellet from the well triggers the release of a new pellet absent any delivery cues. For all operant conditioning sessions (2-hour sessions, starting 2 hours after completion of vapor exposure) animals were individually placed into a standard cage containing a FED3 with iso-pad bedding under red light, then returned to group housing upon completion of the session. Experimental Parameters, such as FED3 error rate, were counterbalanced between treatment groups for each experiment. If animals failed to reach stable responding before the progressive ratio test (PRT, day 10) they were excluded from that task; however, if they then reached stability in the 4 days between PRT and the quinine test (QT, day 15) they were included in the QT analysis.

Fixed Ratio 1 (FR1): To establish operant responding for sucrose pellets (Dustless Precision Pellets, 20 mg Sucrose, Bio-Serv) mice were given daily access to the FED3 under a Fixed Ratio 1 (FR1) feeding paradigm, with a pellet in the well at the start of the session. The left nose poke was set as the active operandum and correct responses were paired with brief audio and visual cues serving as conditioned reinforcers. No timeout period after pellet nose poke or pellet retrieval was used. Acquisition of stable responding was defined as when animals had 3 consecutive sessions where each of the following was met: >50% correct responding, ±20% the number of pellets retrieved on the previous day. For each session, the number of pellets obtained, number of left pokes made, number of right pokes made, % correct, latency to first pellet retrieval, average pellet retrieval time, average inter-pellet interval, and number of sessions until stability were recorded.

Progressive Ratio Test (PRT): To measure motivation for sucrose, the PRT was performed using an escalating reinforcement schedule for sucrose pellets. Animals that did not reach a stable responding by session 9 were excluded from this test. After mice established stable operant responding under an FR1 paradigm with a pellet in the well at the start of a session, progressive responding was measured over a single 4-hour session occurring 2 hours after completion of

vaping exposure. The number of responses on the active lever needed for reward dispensation increased exponentially based on the following equation: (ratio = ratio + round ((5 * exp (0.2 * PelletCount) - 5))[28,29]. Breakpoint was defined as the highest number of reinforcers earned before a 2-hour break between reinforcers. For this session, the total number of pellets obtained, number of left and right pokes made, percent correct, latency to first pellet retrieval, average pellet retrieval time, average inter-pellet interval, and breakpoint were recorded or calculated.

Quinine Test (QT): To evaluate the impact of aversive consequences on sucrose consumption, mice were given access to sucrose pellets containing quinine (Dustless Precision Pellets, 20 mg Sucrose 0.44% Quinine by weight, Bio-Serv) on an FR1 reinforcement schedule. Animals that failed to meet stable responding before day 14 were excluded from this test. After mice reached stable responding or returned to/exceeded the number of pellets retrieved at stability, they were given a single 2-hour session of access to a FED3 with a pellet in well at the start of the session. The total number of pellets obtained, number of left and right pokes made, percent correct, latency to first pellet retrieval, average pellet retrieval time, average inter-pellet interval, and number of pellets eaten (calculated as the number of pellets taken from the device minus the number of pellets found on the floor of the cage at task completion) were recorded. A negative number of pellets eaten signifies that the mouse intercepted a pellet mid-air prior to it reaching the well so that the FED3 could record the pellets' dispensation; the FED3 would then release another pellet so that the mouse could retrieve two pellets for one active nose poke.

Statistical Analyses Statistical analyses were performed using GraphPad Prism (version 10.1.0) and detailed reports are available in **Table 1** and **Supplemental Table 1**. All data are reported as mean ± SEM and individual data points are displayed where applicable. Behavioral experiments were analyzed as follows: for affective behaviors and tactile allodynia, one- or two-way ANOVA with repeated measures as appropriate and Tukey post hoc; for cognitive tests, Kruskal-Wallis followed by Dunn's post hoc. Pharmacokinetic data are presented as follows: area under the curve, AUC (ng*hr/ml); maximum plasma concentration, Cmax (ng/ml); plasma half-life, t1/2 (min). The area- AUC and its relative statistical analysis were computed by the Center for Biostatistics and Health Data Science (CBHDS), Department of Statistics at Virginia Tech using the PK package in R, which is based on the work of Wolfsegger and Jaki[30]. Statistical outliers were determined using

Grubbs' Test. In the event of multiple outliers within the same treatment group, the individual with the higher z-value was removed. The criteria for significance were as follows: *P < 0.05, **P < 0.01, ***P < 0.001, ****P < 0.0001.

3.5 RESULTS

Optimization of the CVE paradigm

To determine optimal conditions for the CVE paradigm, we first examined the effects of 5 different nicotine vapor inter-vape intervals (2, 5, 10, 15, and 60 minutes, **see Figure 1A**) on 3 validated output measures of nicotine effect: changes in body weight during each week of exposure, changes in locomotor activity, and the expression of tactile allodynia. Detailed statistical results are available in **Table 1** and **Supplemental Table** 1. While all treatment groups exhibited a body weight change compared to the air control, the 2-minute nicotine frequency produced significant body weight loss **(Figure 1B)** and did not increase locomotor activity **(Figure 1C)**, indicating that this dose was too high for further study. Accordingly, we proceeded to measure tactile thresholds to assess abstinence-induced hyperalgesia **(Figure 1D)** and performed an *in vivo* pharmacokinetic study of blood levels of nicotine and its active metabolite cotinine at different time points following the last vapor exposure in all other inter-vape intervals **(Figure 2A-B, Table 1)**. While mice exposed to the 5-minute nicotine frequency exhibited increased locomotor activity **(Figure 1B)** and abstinence-induced tactile allodynia **(Figure 2C)**, they showed a significant reduction in body weight over time **(Figure 1A)** and supraphysiological levels of nicotine and cotinine in the blood **(Figure 2A-B, Table 1)**. Despite increased locomotor activity **(Figure 1B)**, mice subjected to 15-minute or 60-minute nicotine inter-vape intervals displayed body weight gain **(Figure 1A)**, did not develop significant allodynia **(Figure 2C)** and failed to exhibit blood levels of nicotine and cotinine within range of human smokers **(Figure 2A-B)**. By contrast, mice given the 10-minute nicotine frequency exhibited increased locomotor activity without a corresponding change in body weight as well as marked abstinence-induced tactile allodynia **(Figure 1B-D)** along with predicted blood levels of nicotine and cotinine within the range of human smokers **(Figure 2A-B, Table 1)**. Collectively, these results indicate that the 10-minute nicotine frequency prevents body weight gain without producing weight loss, elicits predicted increases in locomotor activity and abstinence-induced tactile allodynia, and nicotine blood levels equivalent to human smokers.

Thus, we selected the 10-minute inter-vape interval for affective and cognitive behavioral evaluation of the nicotine CVE paradigm. A new cohort of mice were divided into three groups (n=20 per group); the first group was exposed to CVE containing nicotine (NIC, 20 mg/ml), the second group was exposed to vehicle CVE without nicotine (VEH), and the third group was exposed only to passive airflow (AIR), all delivered at a 10-minute frequency. An experimental timeline for these studies is presented in **Figure 3**.

Nicotine CVE does not elicit substantial affective behaviors

Next, we investigated the effects of nicotine CVE on affective behaviors at defined timepoints after the last vapor exposure as follows: the Open Field Test (OFT) and the Splash Test (ST) at 2 hours, the Light-Dark box Test (LDT) and Sucrose Preference Test (SPT) at 2 and 24 hours. Detailed statistical results are available in **Supplemental Table 2.** In the OFT, distance traveled, and time spent immobile represent measures of activity, while time spent on the edges and the number of center entries signify levels of anxiety-like behavior. In the LDT, the number of exits from, average length of visits to, and latency to exit from the dark area were taken as measures of activity, while time spent in the dark portion signifies levels of anxiety-like behavior. As expected, there was no significant difference between vehicle CVE and air controls at 2 hours after cessation of vapor exposure for any parameter examined in OFT **(Figure 4A-D)** or LDT **(Figure 4E-G)**, indicating that the vehicle itself did not produce effects on anxiety-like behaviors or overall locomotor activity at this time point or inter-vape interval. Compared with vehicle CVE or air controls, mice receiving nicotine CVE displayed an increase in distance traveled and a decrease in immobility time **(Figure 4A-B)**, but there was no significant difference from controls in time spent in the center or number of center entries in the OFT **(Figure 4C-D)**. Similarly, in the LDT, nicotine CVE produced an increased number of exits from the dark and decreased the average length of dark visits **(Figure 4E-F)** at 2 hours after cessation of treatment, without altering the latency to the first dark exit or time spent in the dark at either 2 hours or 24 hours after cessation of treatment **(Figure 4G-H)**. Thus, this paradigm of nicotine CVE produced hyperactivity without effect on anxiety-like behaviors as evaluated by the OFT or LDT.

To determine the effects of nicotine CVE on measures of anhedonia, the same groups of mice described above were subjected to the Splash Test 2 hours, and Sucrose Preference Test at 2 and 24 hours, after cessation of treatment. Detailed statistical results are available in

Supplemental Table 2. In the Splash Test, both vehicle and nicotine spent significantly more time grooming than air controls **(Figure 5A)**. As there was no difference between vehicle and nicotine treatment groups, increased grooming is most likely due to fur and skin exposure to the vehicle itself. The vaporized vehicle solution is viscous, and probably aversive to the mouse, possibly triggering a natural grooming response. There were no differences in sucrose preference between air and vehicle controls, and no significant effect of nicotine at 2 hours or 24 hours post vapor exposure **(Figure 5B)**, indicating that cessation from nicotine CVE did not produce anhedonia.

Nicotine CVE impairs the acquisition of discrimination learning

To examine the effects of nicotine CVE on operant learning, mice were trained to self-administer sucrose pellets using FED3 in daily 2-hour sessions as previously described[28]. Detailed statistical results are available in **Supplemental Tables 2-3.** First, we evaluated the number of active nose pokes **(Figure 6A)** and response accuracy (percentage of correct nose pokes) **(Figure 6B)** in each training session for 9 consecutive sessions to determine when mice achieved stable operant responding behavior, defined as 3 consecutive sessions where each of the following was met: >50% correct responding, ±20% the number of pellets retrieved on the previous day. With each successive training session, all groups exhibited faster pellet retrieval time after an active nose poke **(Figure 6C)** with a significant effect of time but no main effect of treatment. Interestingly, there was a significant difference between nicotine CVE and air controls in the number of sessions until stable responding **(Figure 6D)** with nicotine treated mice needing more sessions to stability, although the vehicle may contribute in part to this effect. There were no effects of time or treatment on the number of pellets retrieved at stability **(Figure 6E)**, suggesting that the delayed acquisition observed in the nicotine group is not due to sucrose palatability. Analysis of the number of inactive nose pokes per session, number of pellets retrieved per session, latency to first pellet retrieval, and inter-pellet interval revealed significant effects of time, but only latency to first pellet retrieval showed significant effects of treatment **(Figure S1)**. These data suggest that nicotine CVE may impair the acquisition of operant reinforcement behavior for sucrose rewards.

After mice reached stable responding to FED3, they were subjected to a single 4-hour session set to an escalating reinforcement schedule for 20 mg sucrose pellets (Progressive Ratio

Test, PRT) to examine the effects of nicotine CVE on sucrose motivation as described previously[29]. Motivation for sucrose was measured by breakpoint, defined as the last pellet retrieved before a 2-hour period without another pellet retrieval or the final number of pellets retrieved over the session. There was no effect of nicotine CVE on sucrose motivation **(Figure 7A)** or ability to perform the PRT as measured by response accuracy/% correct **(Figure 7B)**. There were no significant differences between treatment groups in latency to first pellet retrieval, average pellet retrieval time, or inter-pellet interval **(Figure S2D-F)** during the PRT. In contrast, we found a significant reduction in the number of active nose pokes made for vehicle CVE versus air controls **(Figure S2A)** resulting in fewer pellets retrieved at end of session **(Figure S2C)**. Conversely, there was a corresponding increase in the number of inactive nose pokes made for air controls versus vehicle CVE **(Figure S2B)**. Collectively, these data indicated that acute abstinence from nicotine CVE does not affect motivation for sucrose as a natural reward.

Abstinence from nicotine CVE does not affect sucrose motivation

After mice reached stable responding to FED3, they were subjected to a single 4h session set to an escalating reinforcement schedule for 20 mg sucrose pellets (progressive ratio test, PRT) to examine the effects of acute abstinence from nicotine CVE on sucrose motivation as described previously[32.] Motivation for sucrose was measured by breakpoint, defined as the last pellet retrieved before a 2h period without another pellet retrieval or the final number of pellets retrieved over the session. There was no effect of nicotine CVE abstinence on sucrose motivation **(Figure 7A)** or ability to perform the PRT as measured by response accuracy/% correct **(Figure 7B)**. There were no significant differences between treatment groups in latency to first pellet retrieval, average pellet retrieval time, or inter-pellet interval **(Figure S?)**. In contrast, we found a significant reduction in the number of active nosepokes made for nicotine CVE versus air controls **(Figure S2)**, although this response appears to be mediated in part by a vehicle effect. Conversely, there was a corresponding increase in the number of inactive nosepokes made for air controls versus vehicle CVE **(Figure S2)**. Collectively, these data indicated that nicotine CVE withdrawal does not affect motivation for sucrose as a natural reward.

Nicotine CVE increases consumption of quinine-infused pellets

To examine the effects of nicotine CVE on response to aversive consequences of sucrose consumption, mice were subjected to a single 2-hour session of access to a FED3 on an FR1 reinforcement schedule with pellets consisting of 0.44% quinine in sucrose. Detailed statistical results are available in **Supplemental Table 2-3.** There was a significant increase in consumption of quinine/sucrose pellets by nicotine CVE-treated versus both vehicle CVE-treated and air control mice **(Figure 7C)**. Additionally, nicotine CVE mice exhibited a greater number of active nose pokes than air controls **(Figure 7D)**. Despite an increased number of active nose pokes, there was no effect of treatment on response accuracy/% correct **(Figure 7E),** number of right (inactive) nose pokes made **(Figure 7F)**, average pellet retrieval time or the average inter-pellet interval **(Figure S3B,C)**. However, nicotine CVE-treated mice demonstrated an increased latency to first pellet retrieval versus vehicle CVE-treated mice **(Figure S3A)**. Additionally, while air and vehicle CVE mice demonstrated significant differences between sucrose and quinine/sucrose pellet consumption this effect was not observed in nicotine CVE-treated mice **(Figure S3D)**. Taken together, these results indicate nicotine CVE alters quinine taste perception.

3.6 DISCUSSION

Nicotine and tobacco use are leading causes of preventable deaths, and a majority of those who attempt to quit using nicotine or tobacco will relapse. Electronic cigarettes and other electronic nicotine delivery systems (ENDS) were presented as a safer alternative to smoking cigarettes but have instead contributed to increasing nicotine use among US youths. However, these devices represent useful tools for creating preclinical methods of chronic nicotine exposure that better model human nicotine consumption. Using an ENDS device, we demonstrate that chronic, intermittent vapor-based nicotine exposure at a 10-minute inter-vape interval produces expected changes in weight, locomotor activity, and plasma nicotine levels, as well as tactile allodynia following vaping cessation. While this dosing schedule results in deficits in operant acquisition and quinine perception, it does not produce changes in affective behavior.

Our CVE procedures produced dose-dependent pharmacokinetic and behavioral responses to nicotine. By manipulating the frequency of vapor exposure during a session (using a constant flow rate, vape time, and concentration of nicotine in the ENDS solution), we can produce dose-dependent changes in the Cmax and AUC. At exposure frequencies of 5 and 10 minutes, male mice metabolize nicotine at a similar rate as previously published work using other routes of

administration[9]. Interestingly, we discovered that the half-life was much longer at a lower exposure frequency, which suggests that in-cage CVE may exhibit non-linear pharmacokinetics in mice. This may result in part from multiple potential routes of administration using this model beyond inhalation, including oral consumption or absorption through the skin. At high-frequency dosing, we see a non-linear impact on nicotine metabolism as cotinine levels rise well beyond those typically seen in rodent or clinical studies at 1200 ng/ml. Collectively, our pharmacokinetic studies indicate that the 10-minute CVE dosing frequency produces plasma nicotine levels at levels consistent with nicotine dependence in human and rodent models[9,31].

Evaluation of multiple dosing regimens confirmed our pharmacokinetics data to support chronic dosing at a 10-minute frequency to produce relevant phenotypic changes in mice. We demonstrated that CVE to nicotine produces dose-dependent effects on body weight during the first three weeks of exposure, recapitulating a long-standing clinical observation[32,33]. These results support multiple reports that nicotine drives anorexic effects[34,35] as well as consumption-independent effects on metabolism and activity[36,37]. The emergence of pain-like behavior during abstinence has been established as a key indicator of dependence, and our data show a clear dose-dependent increase in tactile allodynia following CVE with a peak at 2 to 4 hours post-session. This supports multiple prior studies showing that nicotine abstinence or withdrawal produces increased allodynia in humans[38,39] and rodents[40–42]. In contrast, we did not observe dose-dependent effects on locomotor activity, as all frequencies of nicotine exposure (with the exception of the 2-minute inter-vape interval) produced comparable increases in locomotor activity. Elevated locomotor activity may be attributable to increased central and peripheral monoaminergic signaling, as acute nicotine exposure can elevate noradrenergic signaling in the periphery as well as facilitate dopamine release into the nucleus accumbens to drive drug reinforcement[43–45]. The minimum cumulative dose needed for dependence far exceeds the level for nicotine reinforcement behavior, suggesting that locomotor activity may serve as a poor criterion for dependence dose selection. Likewise, CVE at the 2-minute exposure frequency produced nicotine plasma levels well in excess of those typically measured in humans and rodent models, and the observed decreased locomotor activity may reflect acutely depressed respiratory function seen in other high-dose nicotine exposure paradigms[46,47] Thus, the CVE procedures and time points selected for evaluating the effect of nicotine inhalation exposure in this study were supported by multiple pharmacokinetic and behavioral output measures.

Our study revealed that nicotine CVE at a 10 minute inter-vape interval did not result in nicotine-specific changes in affective behavior as measured by an Open Field Test (OFT), Light/Dark box Test (LDT), Sucrose Preference Test, or splash test. However, we did observe vapor-specific effects during the splash test, whereby both vehicle and nicotine CVE groups demonstrated increased self-grooming at 2 hours of abstinence. While increased self-grooming during splash/spray tests can be interpreted as increased motivation and self-care behavior[48] or a reduction in depression-like behaviors[49], the absence of reduced depression-like behavior during the sucrose preference test indicates that the observed results might better reflect self-grooming after completion of the vaping session performed to remove the viscous vehicle from the fur. Upon cessation of nicotine intake humans experience a number of side effects (*e.g.*, headache, increased anxiety and depression, cognitive deficits) which can serve as powerful negative reinforcers, contributing to continued nicotine use[50–52]. While traditional models of chronic nicotine exposure generally report increased anxiety- and depression-like behaviors in response to nicotine cessation or abstinence[53,54], chronic vapor-based exposure models demonstrate mixed findings. Some studies report that cessation results in increased anxiety-like behavior as measured by a novelty-suppressed feeding[19] or by the elevated plus maze[55]. However, others have reported findings similar to ours, whereby vapor-based nicotine exposure resulted in body-weight changes and physical signs of withdrawal but did not result in significant differences between groups during the open-field test[42]. Such differences may be due to any one of several factors. For instance, while the field of nicotine research has reached a general agreement on accepted dosing and duration parameters for subcutaneously implanted osmotic pumps or oral administration, these parameters have not been established for vapor exposure. Differences between labs regarding nicotine content, puff length, inter-vape interval, chamber airflow, and session length may alter nicotine pharmacokinetics[56], confounding the direct comparison of results. Direct comparisons may be further confounded by measuring behavioral effects at different time points following treatment. For instance, we examined affective behaviors at 2 or 24 hours post-vapor cessation, while others have conducted these studies immediately following the final vapor exposure[19]. Therefore, our observations of the lack of nicotine-specific changes in affective behaviors may reflect aspects of the study design in addition to the overall effects of vapor-based nicotine exposure.

Importantly, our study revealed that nicotine CVE impaired the acquisition of operant discrimination learning for sucrose. Mice exhibited a similarly high preference for sucrose solution

in the sucrose preference test, they consumed the same number of sucrose pellets (following the acquisition of discrimination learning), and they exhibited similar motivation for sucrose pellets during the progressive ratio test. Thus, delayed acquisition of discrimination learning most likely results from nicotine-induced cognitive impairments. Downregulation of β2-containing nicotinic acetylcholine receptors following CVE may participate in this effect, as deletion of the β2-subunit slows the acquisition of auditory discrimination learning for saccharin in mice[57]. Using T-Maze, a similar deletion of the β2-subunit in the dorsal striatum slows the acquisition of discrimination learning suggesting a potential role for this brain site[58]. Both studies showed no impact on cognitive flexibility using reversal learning tests, but future studies may evaluate CVE-induced impairments of other aspects of executive function.

While nicotine CVE did not affect the palatability of sucrose, nicotine exposure did impact the devaluation of sucrose rewards by quinine. Previous studies have shown that nicotine and quinine both produce a bitter taste by activating gustatory TRPM5 receptors[59,60]. Consistent with these findings, we show that nicotine-exposed mice exhibit increased consumption and active responding for sucrose pellets containing quinine compared with control groups, suggesting nicotine CVE alters bitterness perception. However, these findings may be influenced by both sex[61] and strain[62] and thus warrant further investigation for a more complete understanding of this phenomenon.

There are some limitations of the present work that can be addressed in future studies. While our current approach of modulating the frequency of exposure to increase the cumulative dose produced pharmacologically relevant plasma levels during exposure and increased tactile allodynia during abstinence, future studies may focus on modulating other parameters to facilitate more robust negative affective during abstinence. Furthermore, we only evaluated a limited number of aspects of executive function, and future work can expand on these findings to determine the effect of CVE on cognitive flexibility, reward valuation and devaluation, attention, and response inhibition. Finally, these studies were only performed in male mice and comparative studies in female mice warrant further evaluation.

3.7 REFERENCES

1. Cornelius, M. E. *et al.* Tobacco Product Use Among Adults - United States, 2021. *MMWR Morb Mortal Wkly Rep* **72**, 475–483 (2023).

2. Birdsey, J. *et al.* Tobacco Product Use Among U.S. Middle and High School Students - National Youth Tobacco Survey, 2023. *MMWR Morb Mortal Wkly Rep* **72**, 1173–1182 (2023).

3. Pepper, J. K. & Brewer, N. T. Electronic nicotine delivery system (electronic cigarette) awareness, use, reactions and beliefs: A systematic review. *Tob Control* **23**, 375–384 (2014).

4. Gentzke, A. S. *et al.* Morbidity and Mortality Weekly Report - Vital Signs: Tobacco Product Use Among Middle and High School Students-United States, 2011-2018. *Morbidity and Mortality Weekly* **68**, 157–164 (2018).

5. Voos, N., Goniewicz, M. L. & Eissenberg, T. What is the nicotine delivery profile of electronic cigarettes? *Expert Opin Drug Deliv* **16**, 1193–1203 (2019).

6. Miliano, C. *et al.* Modeling drug exposure in rodents using e-cigarettes and other electronic nicotine delivery systems. *J Neurosci Methods* **330**, 108458 (2020).

7. Jackson, K. J., Muldoon, P. P., De Biasi, M. & Damaj, M. I. New mechanisms and perspectives in nicotine withdrawal. *Neuropharmacology* **96**, 223–234 (2015).

8. Smith, T. T. *et al.* Animal research on nicotine reduction: Current evidence and research gaps. *Nicotine and Tobacco Research* **19**, 1005–1015 (2017).

9. Matta, S. G. *et al.* Guidelines on nicotine dose selection for in vivo research. *Psychopharmacology (Berl)* **190**, 269–319 (2007).

10. Dong, Y., Zhang, T., Li, W., Doyon, W. & Dani, J. A. Route of nicotine administration influences in vivo dopamine neuron activity: Habituation, needle injection, and cannula infusion. *Journal of Molecular Neuroscience* **40**, 164–171 (2010).

11. Wiley, J. L., Lefever, T. W., Glass, M. & Thomas, B. F. Do you feel it now? Route of administration and Δ9-tetrahydrocannabinol-like discriminative stimulus effects of synthetic cannabinoids in mice. *Neurotoxicology* **73**, 161–167 (2019).

12. Lefever, T. W., Thomas, B. F., Kovach, A. L., Snyder, R. W. & Wiley, J. L. Route of administration effects on nicotine discrimination in female and male mice. *Drug Alcohol Depend* **204**, 107504 (2019).

13. Fowler, C. D. & Kenny, P. J. Intravenous nicotine self-administration and cue-induced reinstatement in mice: Effects of nicotine dose, rate of drug infusion and prior instrumental training. *Neuropharmacology* **61**, 687–698 (2011).

14. Rose, J. E. & Corrigall, W. A. Nicotine self-administration in animals and humans: Similarities and differences. *Psychopharmacology (Berl)* **130**, 28–40 (1997).

15. Garrett, P. I. *et al.* Nicotine-free vapor inhalation produces behavioral disruptions and anxiety-like behaviors in mice: Effects of puff duration, session length, sex, and flavor. *Pharmacol Biochem Behav* **206**, (2021).

16. Smith, D. *et al.* Adult Behavior in Male Mice Exposed to E-Cigarette Nicotine Vapors during Late Prenatal and Early Postnatal Life. *PLoS One* **10**, e0137953 (2015).

17. Montanari, C., Kelley, L. K., Kerr, T. M., Cole, M. & Gilpin, N. W. Nicotine e-cigarette vapor inhalation effects on nicotine & cotinine plasma levels and somatic withdrawal signs in adult male Wistar rats. *Psychopharmacology (Berl)* **237**, 613–625 (2020).

18. Miliano, C. *et al.* Modeling drug exposure in rodents using e-cigarettes and other electronic nicotine delivery systems. *J Neurosci Methods* **330**, 108458 (2020).

19. Sanchez, M. E. *et al.* Electronic Vaporization of Nicotine Salt or Freebase produces differential effects on metabolism, neuronal activity and behavior in male and female C57BL/6J mice. *Addiction Neuroscience* **6**, 100082 (2023).

20. Golde, W. T., Gollobin, P. & Rodriguez, L. L. A rapid, simple, and humane method for submandibular bleeding of mice using a lancet. *Lab Anim (NY)* **34**, 39–43 (2005).

21. Hodes, G. E. *et al.* Sex differences in nucleus accumbens transcriptome profiles associated with susceptibility versus resilience to subchronic variable stress. *Journal of Neuroscience* **35**, 16362–16376 (2015).

22. Loukotková, L., VonTungeln, L. S., Vanlandingham, M. & da Costa, G. G. A simple and highly sensitive UPLC-ESI-MS/MS method for the simultaneous quantification of nicotine, cotinine, and the tobacco-specific carcinogens N'-nitrosonornicotine and 4-(methylnitrosamino)-1-(3-pyridyl)-1-butanone in serum samples. *J Chromatogr B Analyt Technol Biomed Life Sci* **1072**, 229–234 (2018).

23. Chen, I. *et al.* NAPE-PLD regulates specific baseline affective behaviors but is dispensable for inflammatory hyperalgesia. *Neurobiology of Pain* **14**, 100135 (2023).

24. Chaplan, S. R., Bach, F. W., Pogrel, J. W., Chung, J. M. & Yaksh, T. L. Quantitative assessment of tactile allodynia in the rat paw. *J Neurosci Methods* **53**, 55–63 (1994).

25. Gregus, A. M. *et al.* Inhibition of spinal 15-LOX-1 attenuates TLR4-dependent, nonsteroidal anti-inflammatory drug–unresponsive hyperalgesia in male rats. *Pain* **159**, 2620–2629 (2018).

26. Nguyen, K. P. *et al.* Feeding experimentation device (FED): Construction and validation of an open-source device for measuring food intake in rodents. *Journal of Visualized Experiments* **2017**, (2017).

27. Nguyen, K. P. *et al.* Feeding Experimentation Device (FED): A flexible open-source device for measuring feeding behavior. *J Neurosci Methods* **267**, 108–114 (2016).

28. Matikainen-Ankney, B. A. *et al.* An open-source device for measuring food intake and operant behavior in rodent home-cages. *Elife* **10**, (2021).

29. Richardson, N. R. & Roberts, D. C. S. <1996 - Richardson & Roberts - J Neurosci Methods (Progressive Ration).pdf>. *J Neurosci Methods* **66**, 1–11 (1996).

30. Wolfsegger, M. J. & Jaki, T. Assessing systemic drug exposure in repeated dose toxicity studies in the case of complete and incomplete sampling. *Biometrical Journal* **51**, 1017–1029 (2009).

31. Kaisar, M. A., Kallem, R. R., Sajja, R. K., Sifat, A. E. & Cucullo, L. A convenient UHPLC-MS/MS method for routine monitoring of plasma and brain levels of nicotine and cotinine as a tool to validate newly developed preclinical smoking model in mouse. *BMC Neurosci* **18**, 1–13 (2017).

32. Grunberg, N. E. Nicotine, cigarette smoking, and body weight. *Br J Addict* **80**, 369–377 (1985).

33. Zoli, M. & Picciotto, M. R. Nicotinic regulation of energy homeostasis. *Nicotine Tob Res* **14**, 1270–1290 (2012).

34. Mangubat, M. *et al.* Effect of nicotine on body composition in mice. *J Endocrinol* **212**, 317–326 (2012).

35. Easwaran, M. *et al.* Effects of Short-term Electronic(e)-Cigarette Aerosol Exposure in the Mouse Larynx. *Laryngoscope* (2023) doi:10.1002/lary.31043.

36. Rupprecht, L. E., Smith, T. T., Donny, E. C. & Sved, A. F. Self-Administered Nicotine Suppresses Body Weight Gain Independent of Food Intake in Male Rats. *Nicotine Tob Res* **18**, 1869–1876 (2016).

37. Wang, R. *et al.* Four-week administration of nicotinemoderately impacts blood metabolic profile and gut microbiota in a diet-dependent manner. *Biomed Pharmacother* **115**, 108945 (2019).

38. Ditre, J. W., Zale, E. L., LaRowe, L. R., Kosiba, J. D. & De Vita, M. J. Nicotine deprivation increases pain intensity, neurogenic inflammation, and mechanical hyperalgesia among daily tobacco smokers. *J Abnorm Psychol* **127**, 578–589 (2018).

39. LaRowe, L. R. & Ditre, J. W. Pain, nicotine, and tobacco smoking: current state of the science. *Pain* **161**, 1688–1693 (2020).

40. Baiamonte, B. A. *et al.* Nicotine dependence produces hyperalgesia: role of corticotropin-releasing factor-1 receptors (CRF1Rs) in the central amygdala (CeA). *Neuropharmacology* **77**, 217–223 (2014).

41. George, O., Grieder, T. E., Cole, M. & Koob, G. F. Exposure to chronic intermittent nicotine vapor induces nicotine dependence. *Pharmacol Biochem Behav* **96**, 104–107 (2010).

42. Kallupi, M., de Guglielmo, G., Larrosa, E. & George, O. Exposure to passive nicotine vapor in male adolescent rats produces a withdrawal-like state and facilitates nicotine self-administration during adulthood. *European Neuropsychopharmacology* **29**, 1227–1234 (2019).

43. Cadoni, C. & Di Chiara, G. Differential changes in accumbens shell and core dopamine in behavioral sensitization to nicotine. *Eur J Pharmacol* **387**, R23-5 (2000).

44. Dani, J. A. Neuronal Nicotinic Acetylcholine Receptor Structure and Function and Response to Nicotine. in *International Review of Neurobiology* vol. 124 3–19 (2015).

45. Picciotto, M. R. & Mineur, Y. S. Molecules and circuits involved in nicotine addiction: The many faces of smoking. *Neuropharmacology* **76**, 545–553 (2014).

46. Bernardi, R. E. & Spanagel, R. Basal activity level in mice predicts the initial and sensitized locomotor response to nicotine only in high responders. *Behavioural brain research* **264**, 143–150 (2014).

47. Bloom, A. J. Mouse strain-specific acute respiratory effects of nicotine unrelated to nicotine metabolism. *Toxicol Mech Methods* **29**, 542–548 (2019).

48. Becker, M., Pinhasov, A. & Ornoy, A. Animal Models of Depression: What Can They Teach Us about the Human Disease? *Diagnostics* **11**, 123 (2021).

49. Shiota, N., Narikiyo, K., Masuda, A. & Aou, S. Water spray-induced grooming is negatively correlated with depressive behavior in the forced swimming test in rats. *Journal of Physiological Sciences* **66**, 265–273 (2016).

50. Chellian, R. *et al.* Rodent models for nicotine withdrawal. *Journal of Psychopharmacology* **35**, 1169–1187 (2021).

51. Besson, M. & Forget, B. Cognitive Dysfunction, Affective States, and Vulnerability to Nicotine Addiction: A Multifactorial Perspective. *Front Psychiatry* **7**, 1–24 (2016).

52. Cohen, A. & George, O. Animal Models of Nicotine Exposure: Relevance to Second-Hand Smoking, Electronic Cigarette Use, and Compulsive Smoking. *Front Psychiatry* **4**, 1–21 (2013).

53. Stoker, A. K., Semenova, S. & Markou, A. Affective and somatic aspects of spontaneous and precipitated nicotine withdrawal in C57BL/6J and BALB/cByJ mice. *Neuropharmacology* **54**, 1223–1232 (2008).

54. Bruijnzeel, A. W. & Markou, A. Adaptations in cholinergic transmission in the ventral tegmental area associated with the affective signs of nicotine withdrawal in rats. *Neuropharmacology* **47**, 572–579 (2004).

55. Smith, L. C. *et al.* Validation of a nicotine vapor self-administration model in rats with relevance to electronic cigarette use. *Neuropsychopharmacology* **45**, 1909–1919 (2020).

56. Jackson, A., Grobman, B. & Krishnan-Sarin, S. Recent findings in the pharmacology of inhaled nicotine: Preclinical and clinical in vivo studies. *Neuropharmacology* **176**, 108218 (2020).

57. Horst, N. K. *et al.* Impaired auditory discrimination learning following perinatal nicotine exposure or β2 nicotinic acetylcholine receptor subunit deletion. *Behavioural brain research* **231**, 170–180 (2012).

58. Abbondanza, A. *et al.* Nicotinic Acetylcholine Receptors Expressed by Striatal Interneurons Inhibit Striatal Activity and Control Striatal-Dependent Behaviors. *J Neurosci* **42**, 2786–2803 (2022).

59. Oliveira-Maia, A. J. *et al.* Nicotine activates TRPM5-dependent and independent taste pathways. *Proc Natl Acad Sci U S A* **106**, 1596–1601 (2009).

60. Gees, M. *et al.* Differential effects of bitter compounds on the taste transduction channels TRPM5 and IP3 receptor type 3. *Chem Senses* **39**, 295–311 (2014).

61. Nesil, T., Kanit, L. & Pogun, S. Bitter taste and nicotine preference: evidence for sex differences in rats. *Am J Drug Alcohol Abuse* **41**, 57–67 (2015).

62. Gyekis, J. P. *et al.* Gustatory, trigeminal, and olfactory aspects of nicotine intake in three mouse strains. *Behav Genet* **42**, 820–829 (2012).

3.8 TABLE

Table 1 - Pharmacokinetic parameters of Nicotine CVE (Figure 2)

	Inter-vape interval			
Parameter	**5 min$^{(+)}$**	**10 min$^{(*)}$**	**15 min$^{(\#)}$**	**60 min$^{(\^)}$**
AUC (ng*hr/ml)	661±60$^{\#\#\#\#,\^\^\^\^}$	488 ± 39$^{\#\#\#\#,\^\^\^\^}$	300 ± 14$^{\^\^\^\^}$	135 ± 6
Cmax (ng/ml)	155 ± 11	83 ± 21	24 ± 3	13 ± 0.9
t1/2 (min)	5.8	8.1	15.1	19.8

Abbreviations: AUC, the area under the plasma concentration-time curve from t=0 to t=24 h; C_{max}, maximum observed plasma concentration; $t_{1/2}$, half-life. ****P < 0.0001 vs. VEH by two-way repeated measures ANOVA followed by Tukey post-hoc. n=7 per group.

3.9 FIGURES

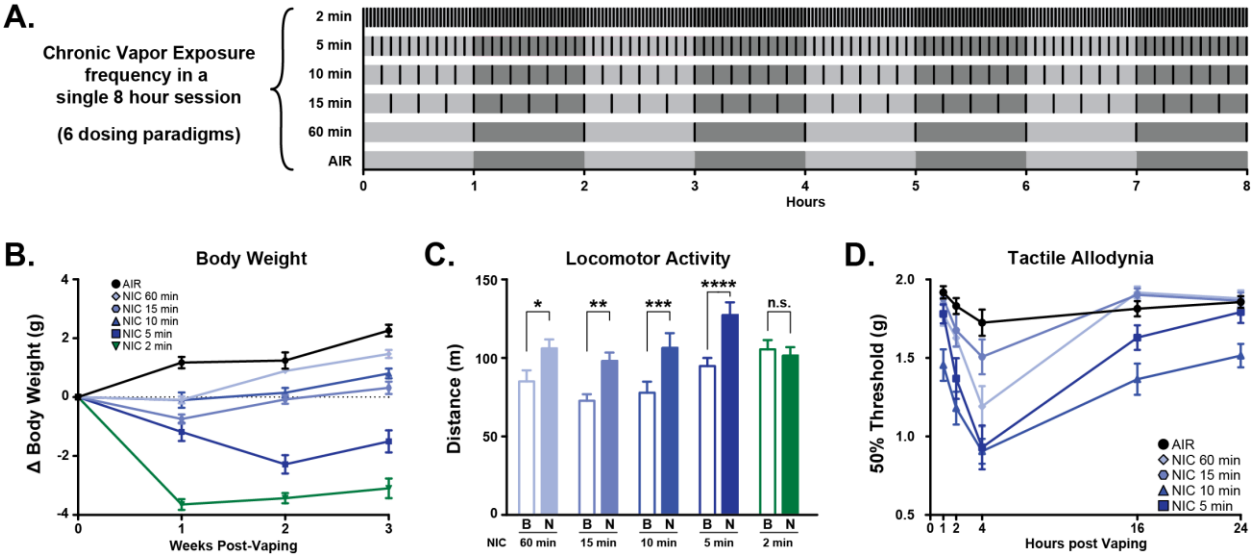

Figure 1. Dose-dependent effects of chronic vapor exposure (CVE) in mice. (A) Visualization of the chronic vapor exposure frequencies evaluated in this study during a single 8h session including air controls (AIR, 0 exposures), 60 min (8 exposures), 15 min (32 exposures), 10 min (48 exposures), 5 min (96 exposures), and 2 min (240 exposures). Exposures are shown as an esterline, with each nicotine (NIC or N) exposure indicated by a black line. **(B)** Changes in body weight (g) during the first three weeks of CVE. **(C)** Locomotor activity prior to (baseline, B) and immediately after a single nicotine exposure session collected following a minimum of five weeks CVE. **(D)** Expression of tactile allodynia measured during post-exposure abstinence following a minimum of six weeks CVE. Data expressed as mean ± s.e.m., and statistical significance indicated by *$p < 0.05$, **$p < 0.01$, ***$p < 0.001$, ****$p < 0.0001$.

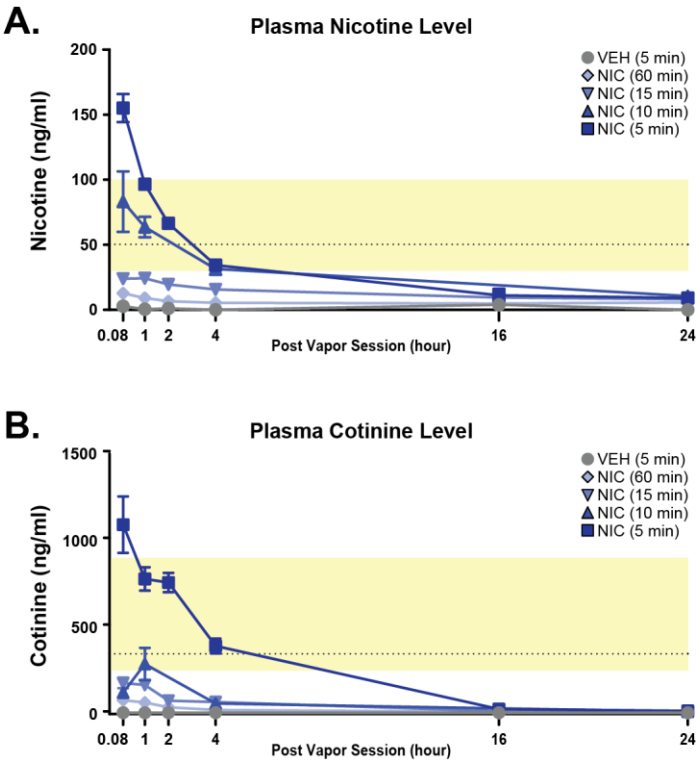

Figure 2. Pharmacokinetic analysis of plasma nicotine and cotinine following nicotine CVE. Mice exposed to different inter-vape intervals (5, 10, 15, and 60 min) were used to measure plasma levels of **(A)** nicotine (NIC) and **(B)** cotinine at 1, 2, 4, 16, and 24 hours after the last vapor exposure. The shaded yellow box indicates the expected range of plasma nicotine or cotinine for individual nicotine-dependent human users. Data expressed as mean ± s.e.m., and vehicle (VEH) results represent data compiled from all four exposure frequencies.

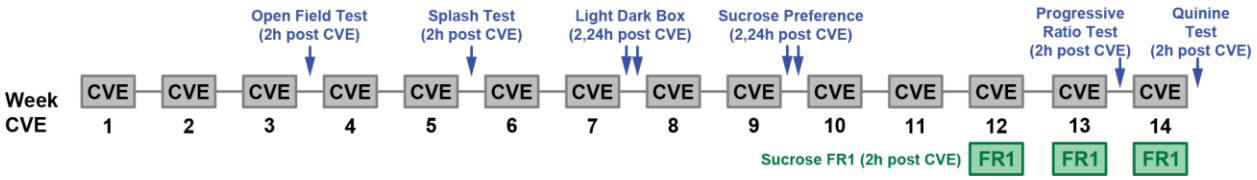

Figure 3. Timeline of the battery for affective and cognitive behavioral testing following CVE. Mice were exposed to nicotine (NIC) or vehicle (VEH) at a 10-minute CVE frequency for 8 hours daily sessions, 5 days per week, for 14 weeks. Additionally, a third group of mice were placed into chambers receiving room air (AIR) at the same time as other mice. At 3 weeks of CVE, mice were evaluated for anxiety-like behaviors (Open Field Test, Light-Dark Box), depression-like behavior (Splash Test, Sucrose Preference Test), and cognitive behavior (acquisition of Sucrose Fixed-Ratio 1 operant self-administration, Progressive Ratio Test, Quinine Test).

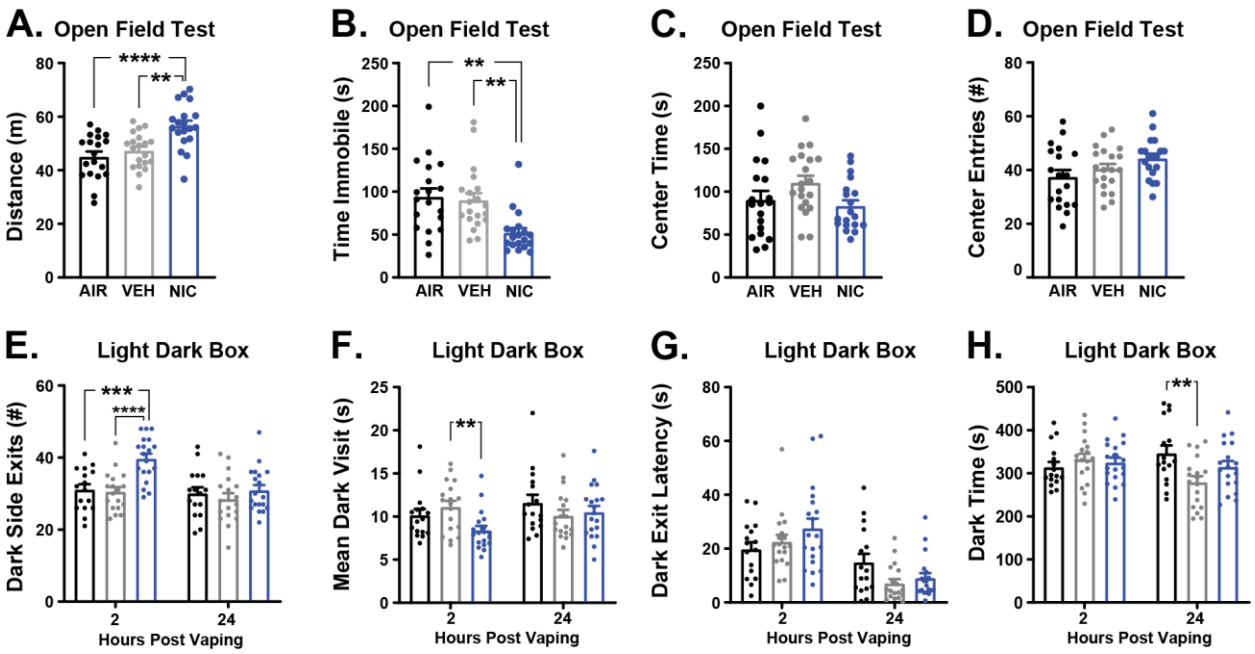

Figure 4. Effects of nicotine CVE on anxiety-like behaviors. (A-D) Open field test (OFT) at 2 hours and **(E-G)** light-dark box test (LDT) at 2 hours and 24 hours after the last vapor exposure for nicotine CVE (NIC), vehicle CVE (VEH), and air controls (AIR). Output measures from the OFT include **(A)** distance traveled, **(B)** time spent immobile, **(C)** center time, and **(D)** number of center entries. Output measures from the LDT include **(E)** number of dark side exits, **(F)** the mean dark visit time, **(G)** dark exit latency, and **(H)** the total dark side time. Data expressed as mean ± s.e.m., and statistical significance indicated by ** $p<0.01$, ***$p<0.001$, ****$p<0.0001$. n=18-20 per group.

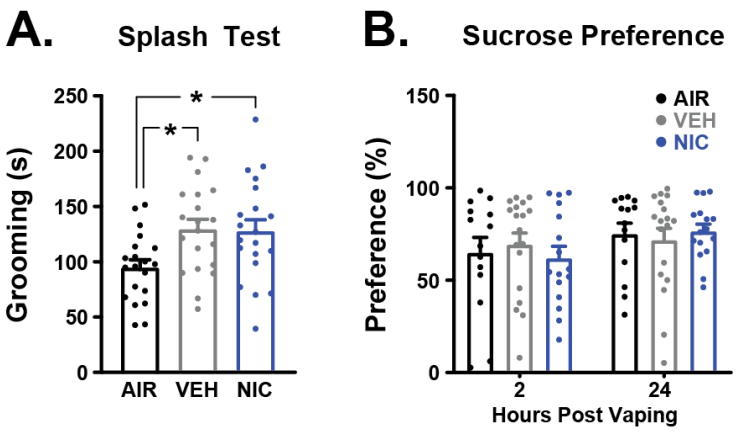

Figure 5: **Effects of nicotine CVE on depression-like behaviors.** Splash Test and Sucrose Preference Test were evaluated after the last vapor exposure for nicotine CVE (NIC), vehicle CVE (VEH), and air controls (AIR). **(A)** Total time spent grooming during the splash test at 2 hours post-CVE. **(B)** The preference for sucrose (as a percentage of total liquid consumption) during the sucrose preference test at 2 hours or 24 hours post-CVE. Data expressed as mean ± s.e.m., and statistical significance indicated by *$p<0.05$. n=14-18 per group.

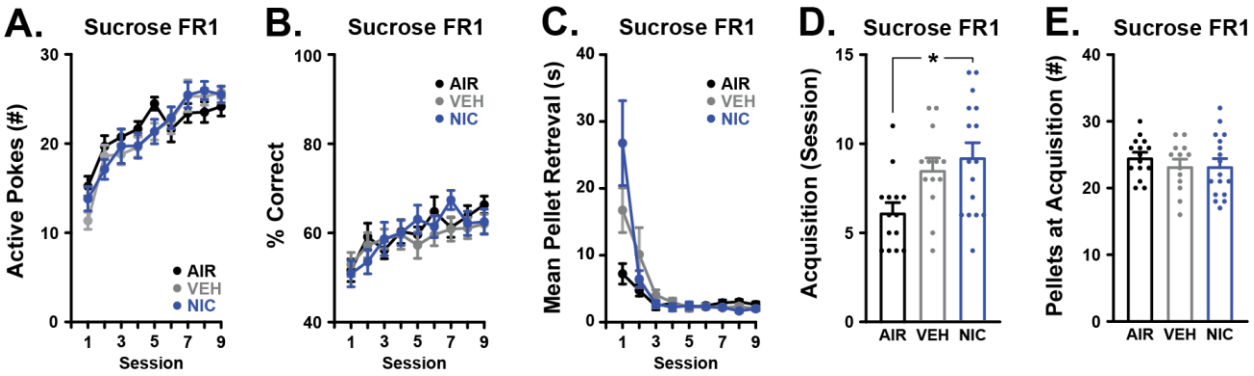

Figure 6: **Effects of nicotine CVE abstinence on operant sucrose self-administration.** Acquisition of operant self-administration of sucrose pellets was evaluated during daily 2-hour sessions immediately following the last vapor exposure for nicotine CVE (NIC), vehicle CVE (VEH), or air controls (AIR). Output measures included **(A)** active nose pokes during each of the first 9 sessions, **(B)** response accuracy during each of the first 9 sessions, **(C)** mean time between the delivery and retrieval of the pellet during each of the first 9 sessions, **(D)** number of sessions until reaching the criteria for stable goal-directed responding (acquisition), and **(E)** the total number of pellets retrieved during that session that acquisition was achieved. Data expressed as mean ± s.e.m., and statistical significance indicated by * $p<0.05$. n=13-17 per group.

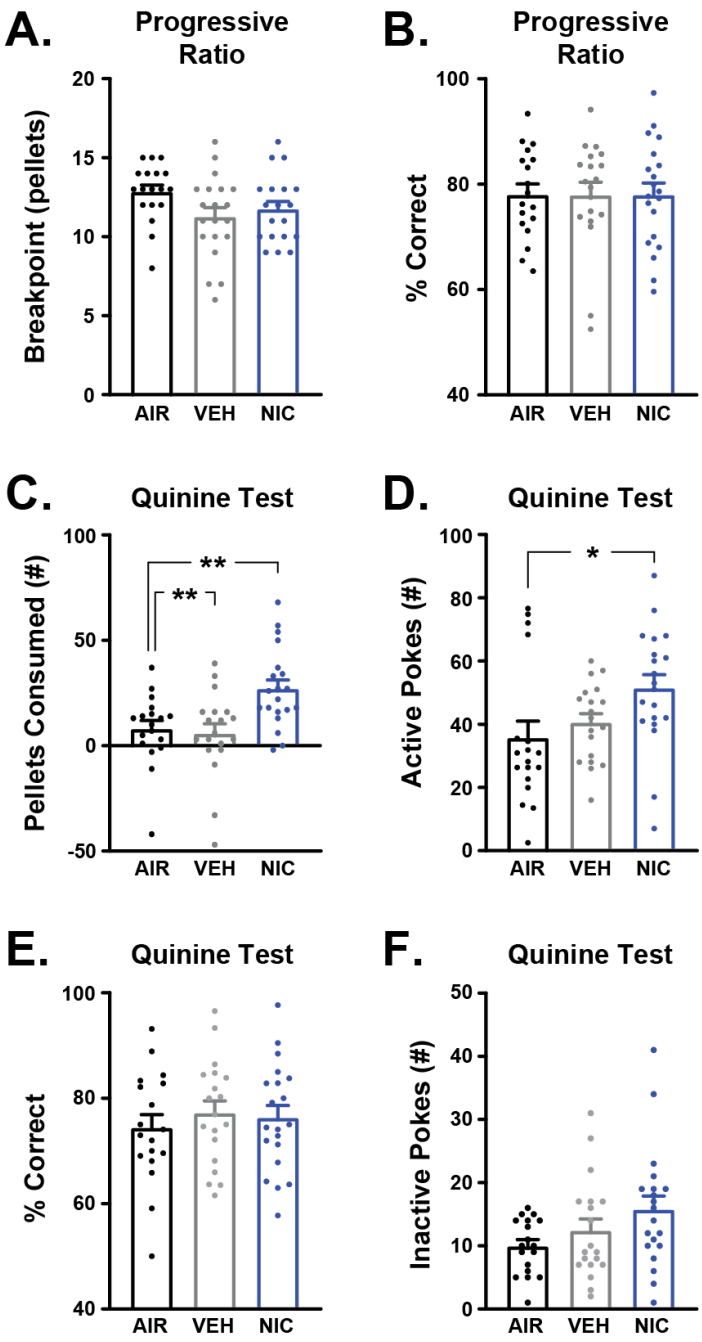

Figure 7: **Effects of nicotine CVE abstinence on sucrose motivation.** Motivation for sucrose was evaluated using the progressive ratio test (PRT) and the quinine test (QT), where sucrose pellets were adulterated with 0.44% quinine. Output measures for PRT included **(A)** breakpoint at the end of the session (4 hours) and **(B)** Response accuracy expressed as the percentage of correct nose pokes. Response to altered taste preference during QT included **(C)** number of quinine-adulterated sucrose pellets consumed, **(D)** the number of active nose pokes, **(E)** response accuracy,

and **(F)** inactive nose pokes. Data expressed as mean ± s.e.m., and statistical significance indicated by * $p<0.05$, ** $p<0.01$. PRT: n = 9-13 per group; QT: n =13-17 per group.

3.8 SUPPLEMENTAL MATERIAL

3.8a Supplemental Figures

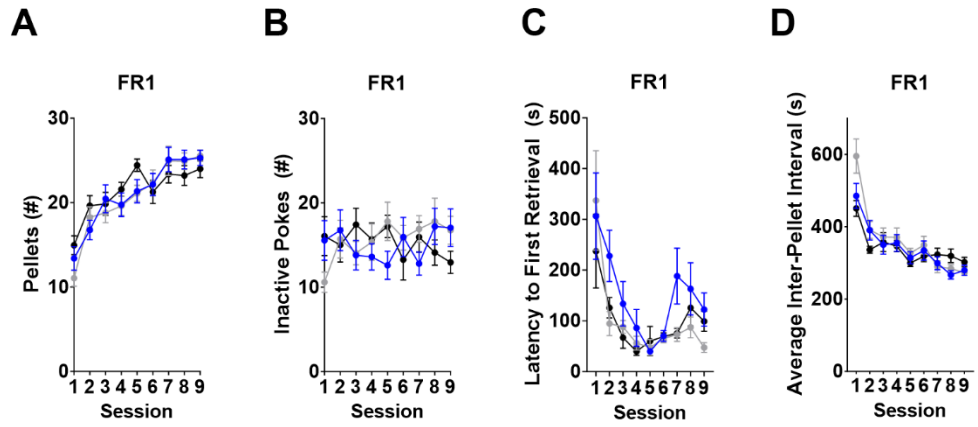

Figure S1: Effects of nicotine CVE abstinence on measures of operant sucrose self-administration. Acquisition of operant self-administration of sucrose pellets was evaluated during daily 2-hour sessions immediately following the last vapor exposure for nicotine CVE (NIC), vehicle CVE (VEH), or air controls (AIR). Output measures included **(A)** total sucrose pellets retrieved during each of the first 9 sessions, **(B)** number of inactive pokes during each of the first 9 sessions, **(C)** latency to remove the already-present sucrose pellet from the well during each of the first 9 sessions, and **(D)** average time between pellet dispensations during each of the first 9 sessions. Data expressed as mean ± s.e.m.. n=13-17 per group.

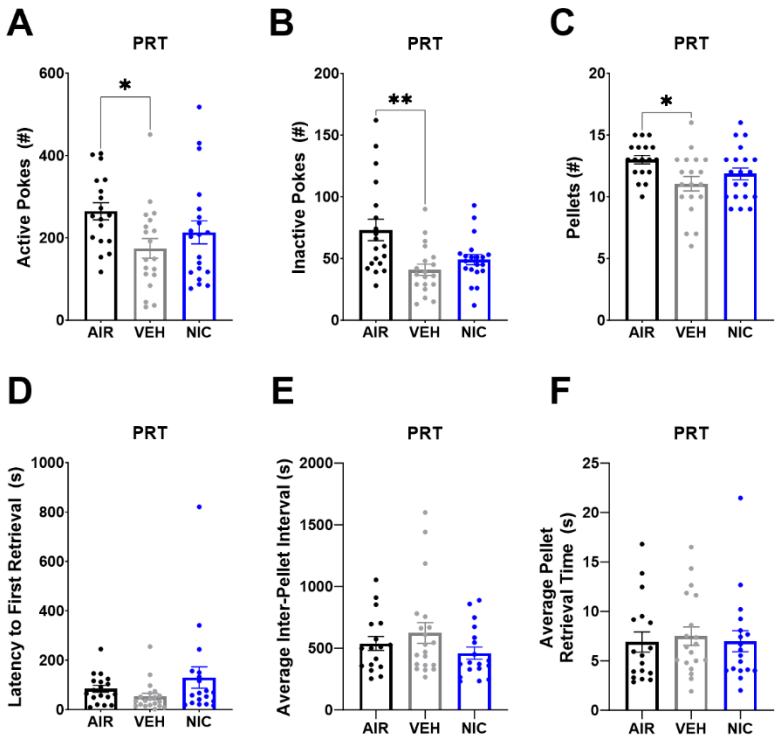

Figure S2: Effects of nicotine CVE abstinence on measures during a test of sucrose motivation. Motivation for sucrose was evaluated using a Progressive Ratio Test (PRT). Output measures for the PRT include **(A)** active nose pokes during the PRT, **(B)** inactive nose pokes during the PRT, **(C)** total sucrose pellets retrieved during the PRT, **(D)** latency to remove the already-present sucrose pellet from the well during the PRT, **(E)** average time between pellet dispensations during the PRT, and **(F)** mean time between the delivery and retrieval of the pellet during the PRT. Data expressed as mean ± s.e.m., and statistical significance indicated by * $p<0.05$, ** $p<0.01$. n = 9-13 per group.

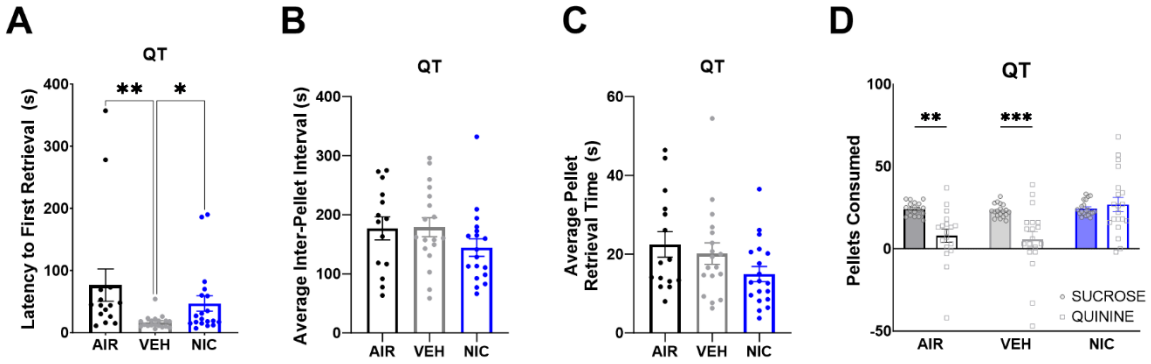

Figure S3: Effects of nicotine CVE abstinence on measures during a test of sucrose motivation and response to aversive reward. Motivation for sucrose and response to reward devaluation was evaluated using the quinine test (QT), where sucrose pellets were adulterated with 0.44% quinine. Output measures for the QT included **(A)** latency to remove the already present quinine-adulterated sucrose pellet during the QT, **(B)** average time between pellet dispensations during the QT, **(C)** mean time between the delivery and retrieval of the pellet during the QT, and **(D)** comparison of pellet consumption from prior sucrose days (filled) and QT (open) between groups. Data expressed as mean ± s.e.m., and statistical significance indicated by * $p<0.05$, ** $p<0.01$, *** $p<0.005$. n =13-17 per group.

3.8b Supplemental Tables

Supplemental Table 1 – Statistics for Dose-dependent effects of chronic vapor exposure (CVE) in mice (Figure 1)

Fig.	Task	Statistical Test	Factor	F-Value	P-Value	Post-Hoc (Displayed if P<0.1)
1B	Body Weight change (g) by Week of Vaping Dose Curve	Two-Way RM ANOVA	Interaction	F (15, 447) = 24.07	<0.0001	Dunnet's Multiple Comparisons test Week 1 AIR1 vs. NIC (2 min): P=<0.0001 ^^^^ AIR vs. NIC (5 min): P=<0.0001 #### AIR vs. NIC (10 min): P=<0.0001 **** AIR vs. NIC (15 min): P=<0.0001 + + + + AIR vs. NIC (60 min): P=<0.0001 $$$$ Week 2 AIR vs. NIC (2 min): P=<0.0001 ^^^^ AIR vs. NIC (5 min): P=<0.0001 #### AIR vs. NIC (10 min): P=.0004 *** AIR vs. NIC (15 min): P=<0.0001 + + + + Week 3 AIR vs. NIC (2 min): P=<0.0001 ^^^^ AIR vs. NIC (5 min): P=<0.0001 #### AIR vs. NIC (10 min): P=<0.0001 **** AIR vs. NIC (15 min): P=<0.0001 + + + + AIR vs. NIC (60 min): P=0.0173 $
			Weeks of CVE	F (3, 447) = 26.83	<0.0001	
			CVE Dose	F (5, 447) = 193.5	<0.0001	
1C	Locomotor Activity (m) Dose Curve	Two-Way RM ANOVA	Pre-Post x Dose	F (4, 90) = 4.480	0.0024	Bonferroni's Multiple Comparisons test BL – POST NIC (5 min): P<0.0001 **** NIC (10 min): P=0.0007 *** NIC (15 min): P=0.0031 ** NIC (60 min): P=0.0163 *
			Pre-Post	F (1, 90) = 44.05	<0.0001	
			CVE Dose	F (4, 90) = 3.968	0.0052	
			Subject	F (90, 90) = 2.090	0.0003	
1D	50% Response Threshold (g) Dose Curve	Two-Way RM ANOVA	Hours Post CVE x CVE Dose Factor	F (16, 340) = 2.885	0.0002	Dunnet's Multiple Comparisons test 1 hour AIR vs. NIC (10 min): P=0.0008 ***
			Hours Post CVE	F (3.211, 273.0) = 46.39	<0.0001	
			CVE Dose	F (4, 85) = 18.57	<0.0001	

			Subject	F (85, 340) = 2.549	<0.0001	2 hour AIR vs. NIC (5 min): P=0.0102 # AIR vs. NIC (10 min): P=<0.0001**** AIR vs. NIC (60 min): P=0.0372 $ 4 hour AIR vs. NIC (5 min): P=0.0001 ### AIR vs. NIC (10 min): P=<0.0001**** AIR vs. NIC (60 min): P=0.0063 $$ 16 hour AIR vs. NIC (10 min): P=0.0014** 24 hour AIR vs. NIC (10 min): P=0.0013**

Supplemental Table 2 – Statistics for the Effects of 10-minute CVE on Behavior (Figures 4-7)

4A	**OFT** Distance Traveled (m)	One-Way ANOVA	All Groups	F (2, 55) = 11.63	<0.0001	Tukey's Multiple Comparisons test AIR vs. NIC: P<0.0001 **** VEH vs. NIC: P=0.0014 **
4B	**OFT** Time Immobile (s)	One-Way ANOVA	All Groups	F (2, 55) = 8.334	0.0007	Tukey's Multiple Comparisons test AIR vs. NIC: P=0.0015 ** VEH vs. NIC: P=0.0038 **
4C	**OFT** Time in Center (s)	One-way ANOVA	All Groups	F (2, 55) = 2.732	0.0739	Tukey's Multiple Comparisons test VEH vs. NIC: P=0.0717
4D	**OFT** Center Entries (#)	One-Way ANOVA	All Groups	F (2, 55) = 2.757	0.0723	Tukey's Multiple Comparisons test AIR vs. NIC: P=0.0585
4E	**LDT** Exits from Dark (#)	Two-Way RM ANOVA	Hours Post CVE x Treatment	F (2, 50) = 5.221	0.0087	Tukey's Multiple Comparisons test 2 hour AIR vs. NIC: P=0.0003 *** VEH vs. NIC: P<0.0001 ****
			Hours Post CVE	F (1, 50) = 13.40	0.0006	
			Treatment	F (2, 50) = 7.576	0.0013	
			Subject	F (50, 50) = 1.530	0.0681	
4F	**LDT** Average Dark Visit (s)	Two-Way RM ANOVA	Hours Post CVE x Treatment	F (2, 50) = 4.900	0.0114	Tukey's Multiple Comparisons test 2 hour VEH vs. NIC: P=0.0171 *
			Hours Post CVE	F (1, 50) = 3.727	0.0592	
			Treatment	F (2, 50) = 1.627	0.2068	
			Subject	F (50, 50) = 2.486	0.0008	
4G	**LDT** Latency to Dark Exit (s)	Two-Way RM ANOVA	Hours Post CVE x Treatment	F (2, 50) = 5.818	0.0054	
			Hours Post CVE	F (1, 50) = 59.52	<0.0001	
			Treatment	F (2, 50) = 0.6739	0.5143	
			Subject	F (50, 50) = 2.359	0.0015	
4H	**LDT** Time in Dark (s)	Two-Way RM ANOVA	Hours Post CVE x Treatment	F (2, 50) = 8.163	0.0009	Tukey's Multiple Comparisons test 24 hour AIR vs. VEH: P=0.0026 **
			Hours Post CVE	F (1, 50) = 1.484	0.2289	
			Treatment	F (2, 50) = 1.104	0.3395	
			Subject	F (50, 50) = 2.453	0.0009	

Supplemental Table 2 cont. – Statistics for the Effects of 10-minute CVE on Behavior (Figures 4-7)

5A	**Splash Test** Grooming (s)	One-Way ANOVA		F (2, 57) = 4.908	0.0108	Tukey's Multiple Comparisons test AIR vs. VEH: P=0.0197 * AIR vs. NIC: P=0.0284 *
5B	**Sucrose Preference** Sucrose Preference (%)	Two-Way RM ANOVA	Hours Post CVE x Treatment	F (2, 45) = 0.7104	0.4969	
			Hours Post CVE	F (1, 45) = 4.267	0.0446	
			Treatment	F (2, 45) = 0.01634	0.9838	
			Subject	F (45, 45) = 1.761	0.0304	
6A	**FR1** Active Pokes (#) Per Day by Group	Two-Way RM ANOVA	Session × Treatment	F (16, 448) = 1.911	0.0178	Tukey's Multiple Comparisons test Session 1 AIR vs. VEH: P=0.0637
			Session	F (8, 448) = 47.18	<0.0001	
			Treatment	F (2, 56) = 0.1580	0.8542	
			Subject	F (56, 448) = 6.358	<0.0001	
6B	**FR1** Percent Correct (%) Per Day by Group	Two-Way RM ANOVA	Session × Treatment	F (16, 448) = 0.8757	0.5978	
			Session	F (8, 448) = 7.184	<0.0001	
			Treatment	F (2, 56) = 0.3412	0.7124	
			Subject	F (56, 448) = 2.801	<0.0001	
6C	**FR1** Average Pellet Retrieval Time (s) Per Day by Group	Mixed Effects Model (REML)	Session × Treatment	F (16, 440) = 4.337	<0.0001	Tukey's Multiple Comparisons test Session 1 AIR vs. VEH: P=0.0390 * AIR vs. NIC: P=0.0188 * Session 8: AIR vs. NIC: P=0.0089 **
			Session	F (1.742, 95.80) = 26.80	<0.0001	
			Treatment	F (2, 56) = 2.251	0.1147	
6D	**FR1** Sessions until Stable (#)	Kruskal-Wallis Test	All Groups	Kruskal-Wallis Statistic H(2) = 8.749	0.0126	Dunn's Multiple Comparisons test AIR vs. NIC: P=0.0093 **
6E	**FR1** Pellets Retrieved at Stability (#)	One-Way ANOVA	All Groups	F (2, 42) = 0.5653	0.5725	
7A	**PRT** Breakpoint (2 hours, Pellets, #)	Kruskal-Wallis Test	All Groups	Kruskal-Wallis Statistic H(2) = 5.223	0.0734	Dunn's Multiple Comparisons test AIR vs. VEH: P=0.0989
7B	**PRT** Percent Correct (%)	Kruskal-Wallis Test	All Groups	Kruskal-Wallis Statistic H(2) = 0.04870	0.9759	

Supplemental Table 2 cont. – Statistics for the Effects of 10-minute CVE on Behavior (Figures 4-7)

7C	**QT** Pellets Consumed (# Retrieved - # On Floor)	Kruskal-Wallis Test	All Groups	Kruskal-Wallis Statistic H(2) = 13.15	0.0014	Dunn's Multiple Comparisons test AIR vs. NIC: P=0.0098 ** VEH vs. NIC: P=0.0032 **
7D	**QT** Active Pokes (#)	Kruskal-Wallis Test	All Groups	Kruskal-Wallis Statistic H(2) = 8.499	0.0143	Dunn's Multiple Comparisons test AIR vs. NIC: P=0.0122 *
7E	**QT** Percent Correct (%)	Kruskal-Wallis Test	All Groups	Kruskal-Wallis Statistic H(2) = 0.6255	0.7314	
7F	**QT** Inactive Pokes (#)	Kruskal-Wallis Test	All Groups	Kruskal-Wallis Statistic H(2) = 4.972	0.0832	Dunn's Multiple Comparisons test AIR vs. NIC: P=0.0861

Supplemental Table 3 – Statistics for the Effects of 10-minute CVE on Behavior (Supplemental Figures 1-3)

S1A	**FR1** Pellets (#)	Two-Way RM ANOVA	Session × Treatment	F (16, 448) = 1.757	0.0345	
			Session	F (8, 448) = 45.23	<0.0001	
			Treatment	F (2, 56) = 0.1559	0.8561	
			Subject	F (56, 448) = 6.124	<0.0001	
S1B	**FR1** Inactive Pokes (#)	Two-Way RM ANOVA	Session × Treatment	F (16, 448) = 1.624	0.0591	
			Session	F (8, 448) = 0.4601	0.8840	
			Treatment	F (2, 56) = 0.08469	0.9189	
			Subject	F (56, 448) = 3.434	<0.0001	
S1C	**FR1** Latency to First Retrieval (s)	Mixed Effects Model (REML)	Session	F (2.874, 149.4) = 12.05	<0.0001	Tukey's Multiple Comparisons test Session 2 VEH vs. NIC: P=0.0639 Session 9 AIR vs. VEH: P=0.0639 VEH vs. NIC: P=0.0928
			Treatment	F (2, 56) = 4.831	0.0116	
			Session × Treatment	F (16, 416) = 0.9824	0.4750	
S1D	**FR1** Average Inter-pellet interval	Mixed Effects Model (REML)	Session	F (3.896, 212.3) = 40.71	<0.0001	Tukey's Multiple Comparisons test Session 1 AIR vs. VEH: P=0.0271 * Session 2 AIR vs. VEH: P=0.0959 Session 8 AIR vs. NIC: P=0.0596
			Treatment	F (2, 56) = 1.056	0.3547	
			Session × Treatment	F (16, 436) = 2.428	0.0016	
S2A	**PRT** Active Pokes (#)	Kruskal-Wallis Test	All Groups	Kruskal-Wallis Statistic H(2) = 7.288	0.0261	Dunn's Multiple Comparisons test AIR vs. VEH: P=0.0252 *
S2B	**PRT** Inactive Pokes (#)	Kruskal-Wallis Test	All Groups	Kruskal-Wallis Statistic H(2) = 11.11	0.0039	Dunn's Multiple Comparisons test AIR vs. VEH: P=0.0026 **
S2C	**PRT** Pellets (#)	Kruskal-Wallis Test	All Groups	Kruskal-Wallis Statistic H(2) = 7.143	0.0281	Dunn's Multiple Comparisons test AIR vs. VEH: P=0.0279 *

Supplemental Table 3 cont. – Statistics for the Effects of 10-minute CVE on Behavior (Supplemental Figures 1-3)

S2D	**PRT** Latency to First Retrieval (s)	Kruskal-Wallis Test	All Groups	Kruskal-Wallis Statistic H(2) = 8.495	0.0143	Dunn's Multiple Comparisons test AIR vs. VEH: P=0.0213 * VEH vs. NIC: P=0.0648
S2E	**PRT** Average Inter-pellet Interval (s)	Kruskal-Wallis Test	All Groups	Kruskal-Wallis Statistic H(2) = 1.995	0.3689	
S2F	**PRT** Average Pellet retrieval Time (s)	Kruskal-Wallis Test	All Groups	Kruskal-Wallis Statistic H(2) = 0.6888	0.7086	
S3A	**QT** Latency to First Retrieval (s)	Kruskal-Wallis Test	All Groups	Kruskal-Wallis Statistic H(2) = 13.44	0.0012	Dunn's Multiple Comparisons test AIR vs. VEH: P=0.0011 ** VEH vs. NIC: P=0.0455 *
S3B	**QT** Average Inter-pellet Interval (s)	Kruskal-Wallis Test	All Groups	Kruskal-Wallis Statistic H(2) = 2.956	0.2281	
S3C	**QT** Average Pellet retrieval Time (s)	Kruskal-Wallis Test	All Groups	Kruskal-Wallis Statistic H(2) = 3.815	0.1484	
S3D	**QT** Pellets Consumed	Two-Way RM ANOVA	Treatment x Session Type	F (2, 54) = 6.676	0.0026	Bonferroni's Multiple Comparisons test SUCROSE-QUININE AIR: P=0.0020 ** VEH: P=0.0006 ***
			Treatment	F (2, 54) = 7.747	0.0011	
			Session Type	F (1, 54) = 16.90	0.0001	
			Subject	F (54, 54) = 1.047	0.4335	

CHAPTER 4

Examining Cognitive Performance in Mice using the Novel Open-Source Operant Feeding Device FED3

Number of figures: 4; Number of tables: 1

ABBREVIATIONS:

Basolateral Amygdala (BLA), Discrimination Learning (DL), Discrimination and Reversal Learning (DL/RL), Ethanol (EtOH) Fatty Acid Amides (FAAs), Fatty Acid Amide Hydrolase (FAAH), Feeding Experiment Device 3 (FED3), Free Feeding (FF), Fixed Ratio (FR), Fixed Ratio 1 (FR1), Fixed Ratio 3 (FR3), Fixed Ratio 3 Reverse (FR3R), Fixed Ratio 5 (FR5), heterozygous (HET), ibotenic acid (IBO), knock-in (KI), Lateral orbitofrontal cortex (lOFC), medial orbitofrontal cortex (mOFC), medial prefrontal cortex (mPFC), orbitofrontal cortex (OFC), prefrontal cortex (PFC), phosphate buffered saline (PBS), Reversal Learning (RL), ventral orbitofrontal cortex (vOFC), wild-type (WT)

4.1 ABSTRACT

Executive dysfunction and alterations in goal-directed behavior are implicated in numerous psychiatric and neurological disorders. As researchers investigate the underlying neural mechanisms of disease states or therapeutics to treat executive dysfunction it is critical that they have access to the tools necessary to measure operant behaviors related to executive dysfunction including discrimination and reversal learning (DL/RL), progressive ratio (PR), and response to reward- or cue-devaluation. These tasks are conventionally performed in a limited number of expensive operant chambers, resulting in numerous labor-intensive short daily sessions where operant performance may be impacted by stressors associated with handling and a semi-novel environment. In this manuscript, we describe the use of an open-source, low-cost operant feeding device (Feeding Experimentation Device 3, FED3) and home-cage-like environment to conduct a 6-task operant test battery which can be completed in less than 20 daily 8-hour sessions. Our

battery consists of DL, RL, PR, reward devaluation via quinine, cue devaluation via extinction, and reinstatement. In the DL/RL portion of this test ibotenic acid lesions of the orbitofrontal cortex spare discrimination performance but impair reversal performance, demonstrating construct validity. Similarly, OFC lesions alter the response to increased instrumental effort and reward- and cue-devaluation. We then utilized this battery to investigate cognitive performance in a knock-in model of the P129T single nucleotide polymorphism of the fatty-acid amide hydrolase (FAAH) gene, associated with addiction, in male and female mice. Overall, we observed sex differences in the response to increased instrumental effort and reward devaluation, and that P129T KI animals demonstrated reduced activity in response to increased instrumental effort and cue devaluation. These KI animals also display decreased FAAH activity in many regions associated with cognitive dysfunction and addiction. Finally, we developed a Python-based database to collate and organize FED3 data across multiple sessions, allowing for experimenter modification of acquisition criterion. We believe that this short-duration, time- and cost-effective test battery presents an improvement on conventional operant tasks, thus encouraging the investigation of operant performance in mouse models of neurological and psychiatric diseases.

4.2 KEYWORDS

goal-directed behavior, mice, open-source, operant, orbitofrontal cortex, test battery

4.3 INTRODUCTION

Executive function comprises a cluster of cognitive abilities that allow an organism to plan, perform, alter, or inhibit goal-directed behavior [1–3]. These behaviors integrate information from multiple brain regions and neurotransmitter systems[3–5], dysregulation of which contributes to the symptomology of numerous psychiatric diseases[4,6,7], neurodegenerative disorders[8,9], and neurological disorders[10]. Clinical tests can quantify specific aspects of executive function and provide an important tool for understanding changes at the individual or population level[8,9]. As a therapeutic approach, clinical testing can facilitate treatment plans for patients experiencing cognitive impairments[3,11], and serve as endpoints for novel therapeutics in clinical trials[12,13] for psychiatric[14,15] and neurological disorders[16]. Executive measures thus provide information critical for understanding the development and impairment of executive function.

To study the mechanisms that underlie executive dysfunction in disease states, researchers in multiple fields need access to high-throughput operant tools to investigate goal-directed behaviors. These tools must be capable of collecting data from many animals at once or in a short period of time, and the data must be able to be analyzed quickly and efficiently. Historically, high throughput and low-cost methods of measuring executive function have included spatial learning tests like the Morris Water Maze[17,18] or Barnes Maze[19] in conjunction with recording and tracking software to measure escape latency or time to altered platform location. While these are important tools, their behavioral output is heavily influenced by hippocampal circuitry and thus may reflect mechanisms of spatial learning more than executive dysfunction, measures escape from an aversive environment rather than reward, and the results of such tests may be confounded by their inherently stressful nature. Alternatively, appetitive operant conditioning tests[20–23] using food as a reinforcer have been developed and widely implemented for evaluating distinct aspects of cognition, operant learning, and goal-directed behavior[24–29]. These approaches typically require high-cost commercial equipment and substantial dedicated research space[30–35], which creates a bottleneck in the total number of animals that can be tested. To account for these limitations, researchers often implement experimental conditions that facilitate high levels of operant responding in short (1-2 hour) behavioral sessions[34,35] such that each testing chamber can be used to evaluate multiple animals per day. However, performance under these conditions may be impacted by the stress of handling and a semi-novel environment[36–39], and this approach often takes weeks[31,32] to months[30,33] of

animal training before testing. Thus, such methods may not be suitable for implementation across all disease models or treatment methods, which may be temporally limited. For instance, prior research has demonstrated that pain can alter cognitive function[40], but many chemically-induced rodent pain models (e.g., Chemotherapy Induced Peripheral Neuropathy[41–43], Complete Freund's Adjuvant[44]) have a limited time frame which may result in difficulty or limitations to cognitive testing. Collectively, these challenges present a critical barrier to entry for many research groups outside of the traditional cognitive field who may be interested in evaluating executive function in rodents[27,45]. Further, it is possible that some behavioral effects may only be observed during extended-access sessions, as has been observed for certain drugs of abuse[46,47]. Thus, some nuanced behavioral patterns may not be observed when animals are limited to only a few hours of testing as in traditional cognitive tasks. While some have turned to using[27,48,49] home-cages with operant feeders or sippers to investigate such effects, these devices often necessitate singular housing, which may introduce stress and is thus typically avoided.

Here, we present a protocol for evaluating cognitive performance in mice using the Feeding Experimentation Device [50,51] version 3[52] (FED3) that addresses many of these challenges (**Figure 1**). The FED3 is an open-source device that can be constructed in-house or purchased commercially at a low cost, has a simple programmable interface, is battery-powered, and is small enough to be placed in a traditional mouse home-cage environment. Animals are tested for up to 8 hours in a dedicated testing chamber consisting of a FED3 placed in a traditional home-cage which is maintained with the animal's scent and bedding. These features reduce the influence of handling stress on behavior, reduce experimental footprint, and dramatically increase the number of mice that can be simultaneously evaluated. Additionally, these features allow for longer testing sessions, which may allow researchers to investigate more complex behavioral phenotypes such as the effects of circadian rhythm on feeding[53] or cognitive performance[54–56]. To make these procedures more broadly accessible to researchers, we further developed a customizable workflow that quickly identifies mice that have completed user-defined acquisition criteria and exports the results into a file that can be analyzed using traditional statistical analysis and/or graphing software. We validated our six-test cognitive battery using bilateral orbitofrontal cortical lesions targeting the lateral and ventral OFC to impact a select subset of cognitive behaviors, and show that the full testing battery can be completed in as few as 20 days. Prior research demonstrates that the OFC and these sub-regions

are involved in the flexible updating of behavior and outcome valuation. As such, lesioned animals should demonstrate impaired reversal learning[5,34,57] and perseverative activity[58] on the previously rewarded nose poke, a resistance to behavioral change in response reward[59–61] or cue devaluation[62]. We demonstrated that this FED3 testing protocol for evaluating executive function works equally well in both sexes, facilitating studies of sex differences, and can be used in aged mice with limited impact on testing length or performance, facilitating studies of neurodegenerative disorders which may require the use of aged mice[63–65].

Endocannabinoids and N-acylethanolamines (NAEs) have been implicated in numerous aspects of learning[66], memory[67], and reward[68,69]. The human single nucleotide polymorphism in the gene encoding for the Fatty Acid Amide Hydrolase protein (FAAH P129T) increases the likelihood of problematic drug use[70,71] and other neuropsychiatric disorders[72]. While many preclinical studies have investigated reward and addiction-related behavior via FAAH knockout[73,74] or inhibition[75–77], fewer preclinical studies have investigated the role of the FAAH P129T mutation. To address this gap and demonstrate the utility of this protocol, we used the above approach to identify sex- and genotype-dependent impairments in executive function in male and female P129T WT and KI animals. We demonstrate that P129T KI animals display distinct changes that may be associated with altered FAAH levels in regions implicated in cognition.

4.4 RESULTS

The FED3 has been successfully implemented in non-operant quantitative feeding studies[26], but published operant studies using the device have largely utilized basic fixed ratio motivated consumption tests[78]. More complex cognitive behavioral testing often requires larger group sizes than traditional feeding studies to achieve significance, and thus two major issues must be addressed for the FED3 to be a viable alternative to traditional operant behavioral apparatuses. First, data management becomes a limiting factor for cognitive behavioral studies that use multiple testing parameters. For example, the FED3 generates 800 individual data files for a n=40 mouse study performed over 20 sessions. Second, mice perform fewer operant responses and receive fewer food pellets per session in a low-stress home-cage environment using the FED3 than they do using traditional operant behavioral apparatus[52,79]. Thus, parameter optimization will be necessary to implement cognitive behavioral testing on the FED3 device.

Data pipeline for cognitive behavioral assessments

To address data management using FED3, we developed an open-source, Python-based data pipeline optimized for performing cognitive behavioral testing (**Figure 1C**). First, the SD card from each FED must be removed. After connecting the SD cards to a computer using a multi-port USB hub, a custom Python-based code imports files indicated by a user-updated reference file. It then appends the imported file names with several identification codes which are used to indicate the subject, test day, and test type. Users then upload these appended files to a custom database where each subject is assigned a unique ID, allowing for detailed organization of files by subject by test day. Users can then input their preferred analysis and acquisition parameters. For example, users can set a single-day acquisition of a minimum number of pellets retrieved and a minimum end-of-day percent correct, multi-day criteria which involves retrieving pellets within a specific window of stability to the prior day, or a criteria of percent correct in a user-defined rolling window. The database then generates a Microsoft Excel file containing the results of this analysis organized by subject and day, which users can download and reorganize for analysis via their preferred software. Using our semi-automated pipeline, we estimate that the complete data compilation and analysis for a 40-mouse study can be reduced to approximately

30 minutes per day. Furthermore, this approach can be scaled such that larger, high-throughput studies become feasible using FED3.

Fixed ratio impacts multiple parameters of operant performance using FED3

To establish optimal FED3 parameters for assessing cognitive function, we investigated the effect of reinforcement schedules on body weight, food consumption, and operant performance (**Figure 2A, B**). Male C57BL/6 mice (8-10 weeks) were group housed and given group magazine training for two sessions using the free feeding program (FF), which dispenses a food pellet each time a pellet is retrieved to allow continuous food access independent of operant behavior. Before session 3, mice were divided into one of four groups. For each daily session, mice were single-housed with their own FED3 for 8 hours before returning to the group-housed cage for 16 hours. Group 1 (FF) continued to use the FF program for the remainder of the experiment, while Groups 2-4 began operant conditioning using a fixed ratio 1 schedule of reinforcement (FR1) for sessions 3-9. At session 10, group 2 remained in FR1 while Group 3 and 4 increased to FR3 and FR5, respectively, for the remainder of the experiment. Using these four groups of reinforcement, we evaluated multiple parameters that may impact behavioral outcomes (complete statistics results compiled in **Supplemental Table 2**).

The fixed-ratio schedule significantly altered body weight. While the FF group increased weight over the course of 16 sessions, FR5 mice had significantly lower body weight by session 16 (**Figure 2C**). Accordingly, mice undergoing FR5 for 8 sessions exhibited a decrease in relative body mass (approximately 5%) compared with FF (**Figure 2D**). These weight changes were not observed among the FR1 or FR3 reinforcement schedules. Moreover, these changes in body mass could not be fully explained by food consumption. Although FF mice retrieved more pellets than any FR group, the FR5 mice retrieved a similar number of pellets as FR1 and FR3 (**Figure 2E**) and left a similar number of pellets on the floor of the cage (**Figure 2F**). For these reasons, we determined that FR5 was not appropriate for long-term cognitive testing using FED3.

The fixed-ratio schedule also had an impact on motivation and learning parameters. Compared to FR1, mice in the FR3 and FR5 groups required substantially fewer nose pokes to

acquire discrimination learning (DL), with all mice in these two groups reaching our threshold in less than 200 nose pokes and within two sessions (**Figure 2G**). Moreover, the time between when a pellet is dispensed by the FED3 and retrieved by the mouse is significantly reduced under both the FR3 and FR5 schedules of reinforcement (**Figure 2H**). Collectively these results indicate that FR1 did not produce sufficient goal-oriented behavior, while FR3 and FR5 both produce similar increases in operant performance. Thus, the cognitive behavioral testing in subsequent studies was performed using a FR3 schedule of reinforcement to reduce potentially confounding factors associated with the FR5-associated weight loss.

Validation of cognitive flexibility following bilateral lesion of OFC

To demonstrate the validity of using the FED3 for cognitive testing, we developed a 6-test operant battery to evaluate multiple aspects of cognitive behavior in mice (**Figure 3A**). Following two sessions magazine training under group housing conditions, male C57BL/6 mice (10-11 weeks) were tested in daily FR3 sessions until meeting DL acquisition criteria defined as meeting or exceeding 85% accuracy in a rolling window of 30 pokes[49,58]. Following acquisition, mice were tested for cognitive flexibility (Reversal Learning, RL), response to increased instrumental effort (Progressive Ratio, PR), response to reward devaluation (via Quinine adulteration, QU), response to cue devaluation (Extinction, EX), and response to cue re-valuation (Reinstatement, RE) over 20 8-hour sessions (**Figure 3B**). Following each test, mice met 3R acquisition and maintenance before beginning the next test. Importantly, these commonly used tasks investigate distinct but related aspects of cognitive and goal-directed behavior. Complete statistics results are compiled in **Supplemental Tables 3, 5-8**, arranged by graph.

To demonstrate that a subset of cognitive behaviors was driven by discrete cortical activity, we evaluated the effect of inactivating the orbital frontal cortex (OFC) on our behavioral test battery. Before the experiment, mice received bilateral injections of saline (SAL) or ibotenic acid (IBO, an excitotoxic agent) into the OFC and recovered for 7 to 10 days before testing **(Figure 3B)**. Immunohistological staining of the cortex performed post-study indicated that the lesioned regions consisted of large areas of the lateral and ventral OFC, but largely spared the medial and dorsolateral OFC regions with minimal impact on the medial prefrontal cortex (**Figure 3C**). While lesioned and sham mice needed a similar number of total pokes (**Figure 3D**) to acquire DL, the OFC-lesioned group required significantly more pokes than SAL to complete

RL and made more presses on the previously reinforced nose poke (**Figure 3E-F**). Compared with DL, both groups required substantially more nose pokes to reach criterion during RL, suggesting that this test presents a challenge in the flexible adjustment of previously learned behavior (**Figure S1B**, **S1C**). Collectively, these results demonstrate that the FED3 captures the OFC lesion-induced RL impairments previously identified in both human and rodent models[80] using traditional operant apparatus-based approaches.

The OFC is involved in numerous aspects of associative learning and goal-directed decision-making, including those related to reward valuation[81]. As such, we investigated the response to reward devaluation via the bitterant quinine in IBO-lesioned mice and SAL controls. Consistent with a role of the lateral and ventral OFC in the flexible updating of behavior in response to reward devaluation absent changes in quinine perception, we find that IBO lesioned animals did not demonstrate altered quinine consumption (**Figure 3G**), but maintained a higher Discrimination Index (**Figure 3H**) during the test than SAL controls. Thus, while there were no significant differences between groups in the number of active or inactive pokes at the end of the test (**Figure S2C-D**) or by repeated measures analysis in 30-minute bins (**Figure S2F-G**), IBO lesioned animals demonstrated a significantly higher correct poke bias (**Figure S2H**) and end of day percent correct (**Figure S2E**), unlike SAL animals who demonstrated non-significant increases in activity on the inactive noes poke in response to reward devaluation. Further consistent with the absence of a role of the OFC in innate taste aversion to quinine, both groups retrieved (**Figure S2A**) and left (**Figure S2B**) a similar number of pellets on the floor of the cage during the test. Collectively, the QU results suggest that lateral and ventral OFC lesions result in a failure to alter active poke activity in response to reward devaluation, absent changes in innate taste aversion, patterns of aversive reward retrieval, or aversive reward consumption,

Next, we investigated the effect of OFC inactivation on motivation and reward valuation. During the progressive ratio test (PR), IBO-lesioned mice made fewer active nose pokes (**Figure 3I**) and received fewer pellets (**Figure S3A**) than sham controls before reaching breakpoint. However, there was no difference in the number of active or inactive pokes at the end of the day (**Figure 3J**) or to the end of day percent correct responding during the PR test (**Figure S3C**). Subsequent tests of reward valuation during extinction learning (EX) and reinstatement (RE) demonstrated that OFC-lesioned and SAL control mice exhibited similar active pokes, inactive

pokes, and end of day responding on the active lever (**Figure S4A-C**) in a single-day EX test, which resulted in an extinction burst of increased activity compared to baseline performance (**Figure 3J**). Subsequent acquisition of operant performance for reward was similarly unaffected by treatment (**Figure 3K**). These findings indicate that the FED3 identified a role for the OFC in cognitive flexibility in response to increased instrumental effort.

FAAH P129T mutation produces cognitive deficits in both sexes

To demonstrate that the FED3 can be implemented for simultaneous and large scale rodent cognitive assessments, we implemented our test battery to evaluate FAAH P129T knock-in mice. The FAAH P129T mutation has been identified in clinical populations as a predictive biomarker for problematic drug use, as well as pro-analgesic and anxiolytic phenotypes (**Figure 4A**). A C57BL/6 mouse model of this single nucleotide polymorphism identified dysregulation of corticoamygdalar circuitry in the anxiolytic behavior. Despite the established role of cortical circuitry in these behavioral paradigms, the impact of P129T mutation in cognitive behaviors remains unexplored. Thus, we performed a complete cognitive assessment (**Figure 3B**) using wild-type (WT) and FAAH P129T knock-in (KI) mice of both sexes. Additionally, the mice used in these studies were 9-11 months old, allowing us to determine the robustness of this approach in aged mice, which show cognitive inflexibility as compared to young mice (**Figure S5G-H**). Using these four groups, we evaluated multiple goal-directed parameters that may impact behavioral outcomes (complete statistical results compiled in **Supplemental Tables 4, 9-12**).

Our study identified distinct genotypic effects on cognitive behavior in mice. No genotypic effects were revealed during acquisition of DL (**Figure 4B, S5A**) or RL (**Figure 4C, S5B-F**). During the QU test we observed significant effects of genotype on Discrimination Index (**Figure 4E**) and end of day percent correct (**Figure S6E**) absent changes in overall active or inactive (**Figure S6C-D**) pokes, suggesting that P129T KI animals may demonstrate increased behavioral flexibility in response to reward devaluation. There were no sex or genotype effects on quinine pellets eaten (**Figure 4D**), retrieved, or left on the floor (**Figure S6A-B**) suggesting these effects are not due to changes in the innate aversiveness of quinine. In response to increasing instrumental effort during the PR test, there was a main effect of genotype on the breakpoint as measured by active nose pokes (**Figure 4F**) and pellets (**Figure S7A**) , with KI animals making fewer total active pokes than their WT counterparts **(Figure S7B)**, but no

genotypic effect on inactive nose pokes (**Figure 4G**) or end of day percent correct (**Figure S7C**). On the first day of extinction, all groups increased active nose poke responding (extinction burst) compared with prior baseline FR3 performance once the FED3 stopped delivering food pellet, but the effect was stronger in WT animals **(Figure 4H).** As such, during the extinction burst, there was a main effect of genotype on the number of active **(Figure S8A)** and inactive (**Figure S8B**) nose pokes, with KI making fewer responses than WT mice. We further measured how long it took animals to extinguish learned behavior, however, there was no genotypic effect in the differences in the total number of nose pokes or sessions to reach extinction criteria **(Figure S8C-D)** or reinstatement (**Figure 4I**). We hypothesized that behavioral changes during PR and EX (but not DL/RL) could indicate dysregulation of other corticolimbic regions, such as the medial prefrontal cortex[82,83] and the dorsal striatum, and using activity-based protein profiling we confirmed that P129T exhibited diminished FAAH activity at both of these brain sites (**Figure 4J-L**), in addition to other brain regions broadly associated with reward, learning, and memory including the hippocampus, OFC, amygdala and VTA (**Figure S10**).

Additionally, we also identified multiple sex-specific effects that suggest females may use different cognitive strategies during testing. No sex-specific effects were revealed during acquisition of DL (**Figure 4B**), RL (**Figure 4C**), nor did they impact the number of pellets consumed during the QU test (**Figure 4D**) or the breakpoint in the PR test (**Figure 4F**). However, the females made more inactive nose pokes during DL (**Figure S5A**), and fewer inactive nose poke during QU (**Figure S5E**) and PR (**Figure 4G**) tests. While no effect of sex was measured on active (**Figure S8A**) or inactive (**Figure S8B**) nose pokes during the extinction burst, post hoc analysis revealed that the genotypic reduction of inactive nose pokes was driven largely by female KI mice. Collectively, these findings demonstrate that the FED3 can effectively compare cognitive tests in male and female mice using active nose pokes as an outcome measure, but sex-differences in inactive nose pokes during multiple tests may suggest that females may be less likely to alter habitual performance during some operant tasks.

4.5 MATERIALS AND METHODS

Reagents and Consumables

Materials were purchased as follows: **Behavioral Testing:** Cell Signaling: Braintree Scientific: Iso Pads, 6”x10” (#ISO); Bio-Serv: Dustless Precision Pellets, 20 mg, Rodent Purified Diet (#F0071); Dustless Precision Pellets, 20 mg, Rodent Purified Diet, Quinine (0.44% by weight) (#F07619). **Surgery:** MWI: Isoflurane (#NDC 13985-528-60): AbCam: Ibotenic Acid (ab146670-1001): Corning: Phosphate Buffered Saline, 1X (#21-040-CM). **Histology:** Millipore-Sigma: Xylenes (#534056); Cresyl Violet Acetate (#C5042); Eukitt® Quick-hardening mounting medium (#03989); Anhydrous Sodium Acetate (#S2889); Sigma Aldrich: Ultrapure Sucrose (#RES0928S-A102X), Sodium Hydroxide (#415413), Ethanol, Reagent Grade (#362808); Fisher Scientific: Acetic Acid, Glacial (#S70048); Corning: Phosphate Buffered Saline, 1X (#21-040-CM).

Animals

For experiments using only wild-type mice, C57BL/6J male mice (n=83) were purchased from Jackson Labs at 8-11 weeks and acclimated for 5-15 days before starting experimental procedures. All mice of both sexes (n=53) for experiments studying the FAAH P129T mutation were bred in-house using heterozygous × heterozygous breeding pairs of *Faah P129T* knock-in mice kindly provided by Dr. Benjamin Cravatt[110] (Scripps Research) and acclimated until the start of experimental procedures at 21 to 26 weeks of age. All mice were group-housed 2 to 5 per cage on a 12-hour reverse light cycle (21:00 on/09:00 off). Animals were given ad-libitum access to water, but food access was only given during daily 8-hour FED3 sessions or supplemental feeding (on weekends when testing was not performed) or in supplemental feeding as published[79]. Body weight was monitored twice weekly to ensure mice did not lose more than 15% of baseline body weight. All protocols and experiments were approved by the Virginia Tech (Blacksburg, VA, USA) Institutional Animal Care and Use Committee (IACUC).

EQUIPMENT AND SETUP

Feeding Experimentation Device 3 (FED3) Setup and Data Pipeline

FED3 Experimental Setup: Feeding and operant performance was measured using the open-source Feeding Experimentation Device 3 (FED3) [50,52]. The FED3 is a battery-powered operant device that consists of two nose pokes for operant training, a pellet dispenser, LEDs for visual reinforcement, a buzzer for auditory reinforcement, and a screen for experimenter observation

(**Figure 1A, B**). An internal microSD card logs interactions with the nose pokes and pellet well in real time for further analysis. Additionally, each device is outfitted with a 3D-printed shield to prevent animals from climbing on or behind the FED3 to prevent moisture from entering the device (**Supplemental Information**). Mice were tested in one 8h session per day, unless otherwise described in specific behavioral tests. During each test session, mice were single housed under red light in a standard cage containing a FED3, an empty food rack holding a water bottle, and an IsoPad for bedding (traditional bedding can enter the pellet well and interfere with data collection). At the end of each

FED3 Data Pipeline: Data collection and analysis for cognitive testing was streamlined using a Python-based data pipeline (**Figure 1C**). Session data was simultaneously retrieved from multiple SD cards using a multi-port USB hub equipped with micro-SD card readers using Python code (**Supplemental Information**) that utilized a reference file to append each FED3 data file name with mouse and study identifiers. Next, these files are uploaded to our custom Python-coded FED3 cognitive analysis database that allows users to modify acquisition criteria parameters as needed. Acquisition criterion can be set as meeting multiple criteria per day (number of pellets retrieved, stability to the previous day's number of pellets, end-of-day percent correct activity, etc.) or as reaching a minimum percent correct in a rolling window of pokes. The database will organize and calculate the data based on these user-set parameters, the results of which can be downloaded as a CSV file that can be further analyzed using traditional data analysis software (e.g. GraphPad Prism). All code described in the FED3 Data pipeline is freely available via GitHub https://github.com/mwblab/fed_database for implementation and further customization.

Cognitive Behavioral Procedures and Tests

The FED3 delivers pellet rewards based on user-defined programs written in Arduino. In the programs used for this study, all procedures and tests from a single FED3 record and time stamp the following parameters in a CSV file: active nose pokes, inactive nose pokes, pellets delivered, pellets retrieved, pellet retrieval time. The number of pellets found on the floor of each cage were determined by experimenter observation and included in the final data analysis.

Free Feeding: under this program, the FED3 delivers a pellet immediately after a pellet is removed from the pellet well. This results in continuous access to a pellet independent of operant responding and can be used for magazine training to acclimate mice to the FED3 and the food pellets[52].

Fixed Ratio Testing (FR): For all FR testing, every n^{th} correct response (non-chaining) was paired with a pellet delivery, audio tone (1 sec), and a visual LED cue (1 sec). The left nose poke was coded as the active lever for FR1, FR3, and FR5 testing; the right nose poke was coded as the active lever for FR3 reverse (FR3R). Acquisition of FR behavior was defined as reaching or exceeding 85% accuracy in a rolling window of 30 pokes (e.g., 26/30 pokes correct). These criteria were based on other long-access, in-cage operant feeding experiments[49,58]. The percent of correct pokes, the time until acquisition, the number of pokes (and pellets) until acquisition were calculated. While we did not investigate poke bias in these experiments, in other experiments where we collect poke data during extended sessions of FF we observe that daily poke bias is normally distributed, with the majority of sessions ending with 0.4 to 0.6% preference for the right poke (**Figure S9A**). We further find that during FF side preference can vary greatly by day, likely indicating that animals do not display strong preference for either poke (**Figure S9B**). Statistical results compiled in **Supplemental Table 13**.

Discrimination Learning (DL) and Reversal Learning (RL): DL was performed using a FR3 reinforcement schedule (active nose poke = left), and acquisition of DL behavior was defined as exceeding 85% accuracy in a rolling window of 30 pokes (e.g., 26/30 pokes correct). After meeting criterion, mice maintained the FR3 schedule for at least 2 additional sessions before moving on to the next test. The percent of correct pokes, the time until acquisition, the number of pokes (and pellets) until acquisition were calculated. RL was performed identical to DL, except that a FR3R reinforcement schedule (active nose poke = right) was implemented.

Quinine Test (QU): QU test was performed using a FR3R reinforcement schedule with grain pellets containing quinine (Dustless Precision Pellets, 20 mg, Rodent Purified Diet, Quinine (0.44% by weight), #F07619). This test was performed in a single 4h session, followed by access to standard chow for 4h. In the following session, mice returned to 3R and re-reached acquisition criterion before starting the next behavioral test. In addition to all previously described parameters, the number of pellets consumed was calculated as the number of pellets retrieved

minus the number of pellets on the floor of the cage at the completion of the QU test. Discrimination Index was calculated as (active nose pokes – inactive nose pokes)/(active nose pokes + inactive nose pokes)[127].

Progressive Ratio Test (PR): PR was performed using an escalating reinforcement schedule for grain pellets over a single 8-hour session. The number of responses on the active lever needed for reward dispensation increased exponentially based on the following equation: (ratio = ratio + round ((5 * exp (0.2 * PelletCount)) - 5))[52,128]. Breakpoint was defined as the highest number of reinforcers earned before a 30-minute break between pokes, or at end of session if no break of at least 30-minutes occurred[129]. In the following session, mice returned to F3R and re-reached acquisition criterion before starting the next behavioral test. In addition to all previously described parameters, the breakpoint and number of active/inactive nose pokes at the breakpoint were calculated.

Extinction (EX): EX was performed using a FR1 reverse reinforcement schedule (active nose poke = right) in 4h sessions, with active nose pokes paired with audio and visual cues but not food pellet. Following each 4h EX session, mice were given 8-hours of access to standard chow before returning to the fasted group-housed home-cage for 12 hours. Extinction burst was defined as the behavior that occurs during the first EX session. Acquisition of EX behavior was defined as ending a session with active pokes ≤20% of the average number of active pokes from the pre-extinction baseline (average of the preceding four FR3R sessions).

Reinstatement (RE): RE was performed using a FR3R reinforcement schedule (active nose poke = right), and acquisition of RE behavior was defined as exceeding 85% accuracy in a rolling window of 30 pokes (e.g., 26/30 pokes correct). The percent of correct pokes, the time until acquisition, the number of pokes (and pellets) until acquisition were calculated.

Intracranial Bilateral Lesions

Surgical Procedures: Animals were anesthetized with isoflurane via a low-flow vaporizer (Somnosuite, Kent Scientific) induced at 5% and maintained at 1-3% concentration. Animals were then secured in a stereotaxic frame (David Kopf Instruments) via ear bar. The skull was exposed and a Dremel was used to create holes in the skull at the injection site. Injections were

made with a 10-µl NanoFil Syringe (World Precision Instruments, Germany) with a 33 GA blunt needle (World Precision Instruments, Germany) mounted to a syringe pump (Pump 11 ELITE Nanomite, Harvard Apparatus) with an injection rate of 0.1 µl per minute with a 4-5 minute resting period before removal. Orbitofrontal cortex (OFC) lesions (AP: +2.55mm, ML: ±1.2mm, DV: +2.40mm from Brain OR +2.6mm from Skull) were made using established coordinates[130] in 26 mice by bilaterally injecting 0.4uL of ibotenic acid dissolved in 80:20 PBS and 1M NaOH. 17 sham-lesioned mice underwent the same procedure but were injected with sterile PBS. Mice were given 7-10 days to recover before beginning the experiment.

Histology: Mice that received OFC lesions were evaluated for accuracy and precision of lesion placement. Briefly, mice were sacrificed via cervical dislocation and decapitation for brain collection. Their brains were removed and drop-fixed in 4% w/v paraformaldehyde in PBS overnight at 4°C, followed by up to 36 hours each in a gradient of 10%/20%/30% Sucrose in PBS. Brains were coronally sectioned at 50um on a cryostat, mounted on glass slides, and stained with cresyl violet. Briefly, sections were mounted to slides and allowed to dry overnight. The following day sections were dehydrated in Xylene (10 m), rehydrated in 100%, 95% and then 70% ethanol (EtOH) followed by deionized distilled water (3 m each). Sections were then stained in 1% cresyl violet solution (8 to 16 m), dehydrated in 70% and 95% EtOH (1 to 2 m each), followed by saturation in Xylene (30+ m) before mounting with mounting medium and cover glass. Lesion size and location were examined under microscope and with images captured by 5MP USB digital camera (MU500, AmScope). Mice were excluded from the study if they failed to demonstrate substantial (>50%) lesioning of the lateral and ventral OFC on one or both sides of the brain from approximately +2.8mm to approximately +2.4mm bregma, or if injection track marks were substantially off target (AP: ±.5mm, ML: ±.2mm) (n = 8), if a majority of sections from these regions detached during the staining process (n = 2), or for hydrocephaly (n = 1), leaving a final n of 15 IBO animals.

4.6 STATISTICAL ANALYSIS

Statistical analyses were performed using GraphPad Prism (version 10.0.2). Data reported as mean ± SEM where applicable. Body weight over time was analyzed using two-way RM ANOVA followed by Tukey's post hoc, with ANOVA statistics and significant post hoc p-values reported in **Supplemental Tables 2-13**, arranged by graph. Number of pellets retrieved by session was analyzed using Mixed-Effects Model (REML), as hardware failures resulted in occasional data loss, with no follow-up post hoc tests. ANOVA statistics are reported in **Supplemental Table 2-13**, arranged by graph. Single variable tests between more than two groups (final body weight by reinforcement schedule, average pellets on floor by reinforcement schedule, etc.) were analyzed using one-way ANOVA followed by Bonferonni post hoc when appropriate with ANOVA statistics reported in **Supplemental Table 2-13**, arranged by graph. Single variable tests between two groups (pellets consumed by treatment group, active pokes by treatment group, etc.) were analyzed using unpaired t-Test, with statistics and p-values in **Supplemental Table 2-13**, arranged by graph. Single variable tests investigating sex × genotype effects (pellets consumed by sex × genotype, active pokes by sex × genotype, etc.) were analyzed using two-way ANOVA and Bonferroni post hoc when appropriate, with ANOVA statistics and relevant post hoc p-values reported in **Supplemental Table 2-13**, arranged by graph. Kaplan-Meier learning curves (pokes to acquisition during DL or RL) were analyzed using Log-Rank (Mantel-Cox) for differences between all groups. If significant differences were observed for experiments with more than two groups, pair-wise comparisons were made between each. In such cases the p-values reported (**Supplemental Table 2-13**, arranged by graph) have been multiplied by the number of comparisons made to account for Bonferroni's correction. Device failures during a single day test (QU, PR) resulted in either re-testing the mice during a new session or removing the mice from the final analysis. Statistical outliers were determined using Grubb's test across all related measures. In the event of multiple outliers within the same group, the individual with the higher z-value was removed.

4.7 DISCUSSION

Evaluation of cognitive behaviors using operant tests remains a critical component for understanding and treating a wide range of neurobiological disorders[5,11,84]. By addressing technical challenges related to experimental parameters and data management, we demonstrated that the open-source FED3 can be scaled to run large cohorts of mice simultaneously in low-stress, home-cage-like environments. Using this approach, we demonstrated that a 6-test operant battery can be completed in as few as 20 sessions and measure multiple dimensions of cognitive function including associative learning, cognitive flexibility, reward valuation and devaluation, and motivation. We validated this approach using site specific inactivation of the OFC and used the FED3 to identify genotypic and sex-specific changes in cognitive behaviors.

Our study supports an important role for stress in the underlying mechanisms of cognitive behaviors[85,86]. In this study, mice have unrestricted access to receive their daily food requirements during extended daily sessions and show no weight loss during FR1 and FR3 reinforcement schedules when compared with the free feeding group. However, mice exhibited a loss of weight during FR5 reinforcement that could not be explained by food consumption alone, as these animals ate the same number of food pellets as FR1 and FR3 mice. This suggests that the increased work needed for mice to receive sufficient food pellets during longer sessions may result in changes to metabolic or neuroendocrine systems. Accordingly, mice treated with the stress hormone corticosterone exhibit weight loss despite consuming more food[87]. By comparison, animals undergoing food reinforcement during short time-constrained paradigms may also be influenced by stress and anxiety-like reponses[36–39]. Studies show that mice may request more rewards than they actually consume during short reinforcement sessions under food-restricted conditions[88,89], suggesting that stress caused by perceived food instability may lead to observed hoarding behaviors and influence operant responding[90]. This stress may impinge on cognitive function as multiple lines of evidence support an inverted-U-shaped curve [91] for the influence of stress on learning and cognition, where moderate levels of stress enhance learning, while low or high stress impairs it. For instance, acute mild stressors increase performance during a paired associative learning task[92], and increase performance during a RL test[93,94]. However, other studies have found that acute or chronic stress results in strategy shifts associated with a switch to habitual activity at the expense of goal-directed behavior[91,95,96]. In our protocol each animal has a dedicated testing cage they inhabit for 8h, which may encourage familiarity

with the system and reduce the stress of testing. Thus, it is possible that a reduction in stress may facilitate learning and executive function, or be otherwise conducive to operant testing.

Our study using the FED3 demonstrates that the lateral and ventral OFC influences distinct aspects of executive functions. We found that inactivation of these regions of the OFC spared discrimination learning but impaired reversal learning performance[58,80,97] as measured by total pokes and errors to acquisition, reflecting the well-documented role of the OFC in flexible decision-making and perseverative behavior during reversal. Additionally, lesioned animals demonstrated a lower progressive ratio breakpoint without impacting error rate (captured by inactive nose pokes) during this test, supporting a previously described effect of lateral OFC inactivation in reducing motivated effortful behavior[83]. As others have reported, OFC lesioning had no effect on the number of quinine-infused pellets retrieved or consumed indicating that innate taste aversions are not controlled by these regions[98]. However, lesioned animals demonstrated a resistance to altering activity during the test, maintaining an overall active poke bias and higher discrimination index. These results are in line with other studies which find that OFC lesioned animals continue to approach cues associated with devalued rewards[99] and demonstrate a negative devaluation index[59]. Collectively, these results support the construct validity of our FED3 testing approach, demonstrating that it can be used to capture OFC-dependent behavioral changes. However, the OFC is also implicated in other aspects of decision-making broadly relating to value and outcome expectancies [100–102] and thus some studies report that inactivation of the OFC impairs extinction learning that were not seen in our study. This difference may be explained by the amount of time between lesion and testing [99,103], as neuronal plasticity and other compensatory mechanisms can lead to functional recovery in mice after a few weeks that mask the impact of the OFC during behavioral testing. Consistent with this, we performed extinction testing at least 20 days post-lesion and it is possible that OFC inactivation at an earlier timepoint may produce different results. It is also possible that the inclusion of cues after an active poke during this test may make it harder to compare to extinction tests where a cue is presented before action to illustrate operandum activity. Future studies could be done to examine the effect of OFC lesioning on cue-driven behavior by investigating un-cued extinction, cue reinstatement absent reward, and finally cue and reward reinstatement, as prior studies have demonstrated that the OFC is implicated in cue-induced reinstatement of cocaine seeking[104,105].

Despite these limitations, we demonstrate that the FED3 can be used to capture aspects of executive dysfunction commonly associated with OFC inactivation.

Many traditional appetitive operant tests find sex-differences [106–109] in reward consumption or operandum activity, which can preclude their comparison. We found no significant sex differences in the total number of pokes to discrimination or reversal learning, indicating that this protocol may be useful to investigate the interaction of genotype and sex on executive function in mouse lines, as we did for the FAAH P129T mice. While we did not observe differences in cognitive flexibility, during this investigation we observed that males increased activity on the inactive nose poke in response to both reward devaluation and increasing instrumental effort, an effect not observed in females. These differences may indicate that males employ a different response strategy than females in response to reward devaluation and increasing effort. Indeed, prior research has found that female rodents form habitual behavior more quickly than males[107], which may contribute to our observation that females maintained activity on the active poke in response to these tests. It is possible that stronger habitual activity or habit formation in females led to maintained performance on the active lever despite devaluation and increased effort, while males instead investigated whether the inactive lever may lead to typical reward dispensation.

While FAAH plays an important role in learning, memory, and executive function, this study represents the first evaluation of the human FAAH P129T polymorphism in this context. This mutation has been linked to problem drug use [70,71] and emotional-motivational reactivity [72] in humans, and enhanced fronto-amygdalar connectivity in the form of increased projections from the ventromedial PFC/Infralimbic area to the basolateral amygdala (BLA) in both humans and mice[110]. While behavioral regulation is a nuanced interaction between many brain regions, increased connectivity between the frontal cortex[111] and the BLA may impact effortful decision making and extinction. The PFC [112,113] and OFC [114] serve as important top-down regulators of BLA activity, and inactivation of the BLA is associated with decreased effortful activity for reward[115,116] and accelerated extinction behavior[117]. Accordingly, P129T KI mice, who have stronger connections between the PFC and the BLA made fewer pokes before reaching breakpoint during a progressive ratio test and were quicker to extinguish poking behavior on the first day of an extinction test. In contrast, FAAH knockout mice show increased motivation for

standard chow consumption[118], indicating that the P129T phenotype emerges as a result of incomplete inactivation or site-specific changes in motivational circuitry. However, it is possible that different results may be observed with stronger reinforcers, such as nicotine or other drugs of abuse. While there are various models for extinction of operant behavior accounting for differing reinforcer rates and contingencies, most account for the value or strength of the reinforcer, such that extinction can be considered a resistance to behavioral change, which is influenced by the relative value of the reinforcer[119,120]. As such, it has been demonstrated that higher sucrose solutions result in higher resistance to extinction[121]. Additionally, while drugs of abuse have been shown to be weak primary reinforcers, cues paired with drugs can be stronger than cues paired with non-drug reward[122]. It is possible that stronger reinforcers could result in more activation of the BLA-frontocortical circuit, elucidating different results.

Executive function is influenced by activity in numerous brain regions working in tandem. Prior studies demonstrate that the P129T mutation results in a FAAH protein with reduced cellular stability[71], which decreases local enzyme expression and facilitates endocannabinoid signaling. Our findings indicate that FAAH P129T KI mice have reduced FAAH activity in the mPFC, where endocannabinoids have been shown to regulate food motivation through glutamatergic plasticity[123]. In addition, we observed decreased FAAH activity in the dorsal striatum, a region that facilitates the performance of habitual activity[124] and effort-based decision making[125] in the absence of reward[126]. Thus, it is possible that alterations in striatal activity contributed to the observed results, whereby effortful behavior was decreased in response to increasing instrumental activity and to non-reward delivery in P129T KI animals. Taken together, these results provide further evidence that alterations in fronto-amygdalar and corticolimbic systems of FAAH P129T KI mice resulted in decreased effort-based decision-making in response to increasing effort or reward absence. Decreased FAAH activity was observed in other regions broadly relating reward, learning, and memory, including the hippocampus, OFC, amygdala, and VTA. Further investigation of the specific effects the P129T mutation on activity and connectivity between these regions may further elucidate their specific contributions to executive function and our observed results.

In conclusion, we demonstrate that the FED3 can function as an effective in-cage tool for evaluating cognition and learning behaviors in mice. The low cost of this approach allows for

high-throughput behavioral evaluations on a rapid timeline while maintaining the sensitivity of traditional approaches. To encourage broader implementation of this approach, we provided detailed methods for using a data pipeline as well as troubleshooting FED3 technical errors. Future studies will expand the variety and complexity of the behavioral tasks and apply these approaches to study the role of genetic and inducible models of neurological disorders that impact cognitive function.

4.8 REFERENCES

1. Mezzacappa, E. Executive Function ☆. in *Reference Module in Neuroscience and Biobehavioral Psychology* vol. 18 142–150 (Elsevier, 2017).

2. Best, J. R. & Miller, P. H. A Developmental Perspective on Executive Function. *Child Dev* **81**, 1641–1660 (2010).

3. Rabinovici, G. D., Stephens, M. L. & Possin, K. L. Executive Dysfunction. *CONTINUUM: Lifelong Learning in Neurology* **21**, 646–659 (2015).

4. Goldstein, R. Z. & Volkow, N. D. Dysfunction of the prefrontal cortex in addiction: neuroimaging findings and clinical implications. *Nat Rev Neurosci* **12**, 652–669 (2011).

5. Uddin, L. Q. Cognitive and behavioural flexibility: neural mechanisms and clinical considerations. *Nat Rev Neurosci* **22**, 167–179 (2021).

6. Warren, S. L., Heller, W. & Miller, G. A. The Structure of Executive Dysfunction in Depression and Anxiety. *J Affect Disord* **279**, 208–216 (2021).

7. Hill, E. L. Executive dysfunction in autism Elisabeth. *Trends Cogn Sci* **8**, 26–32 (2006).

8. Binetti, G. *et al.* Executive dysfunction in early Alzheimer's disease. *J Neurol Neurosurg Psychiatry* **60**, 91–93 (1996).

9. Dirnberger, G. & Jahanshahi, M. Executive dysfunction in Parkinson's disease: A review. *J Neuropsychol* **7**, 193–224 (2013).

10. B.C., M., L.A., F. & A.J., S. Executive dysfunction following traumatic brain injury: Neural substrates and treatment strategies. *NeuroRehabilitation* **17**, 333–344 (2002).

11. Medalla, A. & Lim, R. Treatment of Cognitive Dysfunction in Psychiatric Disorders. *J Psychiatr Pract* **10**, 17–25 (2004).

12. Keeney, J. T. R. *et al.* Doxorubicin-induced elevated oxidative stress and neurochemical alterations in brain and cognitive decline: Protection by MESNA and insights into mechanisms of chemotherapy-induced cognitive impairment ('chemobrain'). *Oncotarget* **9**, 30324–30339 (2018).

13. Cardoso, C. V. *et al.* Chemobrain in rats: Behavioral, morphological, oxidative and inflammatory effects of doxorubicin administration. *Behavioural Brain Research* **378**, 112233 (2020).

14. Cahill, K., Lindson-Hawley, N., Thomas, K. H., Fanshawe, T. R. & Lancaster, T. Nicotine receptor partial agonists for smoking cessation. *Cochrane Database of Systematic Reviews* vol. 2016 Preprint at https://doi.org/10.1002/14651858.CD006103.pub7 (2016).

15. Valentine, G. & Sofuoglu, M. Cognitive Effects of Nicotine: Recent Progress. *Curr Neuropharmacol* **16**, 403–414 (2018).

16. Chudasama, Y. Animal models of prefrontal-executive function. *Behavioral Neuroscience* **125**, 327–343 (2011).

17. Nunez, J. Morris water maze experiment. *Journal of Visualized Experiments* 12–13 (2008) doi:10.3791/897.

18. Vorhees, C. V. & Williams, M. T. Morris water maze: Procedures for assessing spatial and related forms of learning and memory. *Nat Protoc* **1**, 848–858 (2006).

19. Locklear, M. N. & Kritzer, M. F. Assessment of the effects of sex and sex hormones on spatial cognition in adult rats using the Barnes maze. *Horm Behav* **66**, 298–308 (2014).

20. Skinner, B. F. Can the Experimental Analysis of Behavior Rescue Psychology? *Behav Anal* **6**, 9–17 (1983).

21. Skinner, B. F. The experimental analysis of behavior. *Am Sci* **45**, 343–371 (1957).

22. Staddon, J. E. R. & Cerutti, D. T. Operant Conditioning. *Annu Rev Psychol* **54**, 115–144 (2003).

23. Fantino, E. & Stolarz-Fantino, S. Operant Conditioning. *Encyclopedia of Human Behavior: Second Edition* 749–756 (2012) doi:10.1016/B978-0-12-375000-6.00262-7.

24. Kirsch, I., Lynn, S. J., Vigorito, M. & Miller, R. R. The Role of Cognition in Classical and Operant Conditioning. *J Clin Psychol* **60**, 369–392 (2004).

25. Dalla, C. & Shors, T. J. Sex differences in learning processes of classical and operant conditioning. *Physiol Behav* **97**, 229–238 (2009).

26. Karlsson, R. M. & Cameron, H. A. Assessing reward preference using operant behavior in male and female mice. *PLoS One* **18**, e0291419 (2023).

27. Devarakonda, K., Nguyen, K. P. & Kravitz, A. V. ROBucket: A low cost operant chamber based on the Arduino microcontroller. *Behav Res Methods* **48**, 503–509 (2016).

28. Horner, A. E. *et al.* The touchscreen operant platform for assessing executive function in rats and mice. *Nat Protoc* **8**, (2013).

29. Horner, A. E. *et al.* The touchscreen operant platform for testing learning and memory in rats and mice. *Nat Protoc* **8**, 1961–1984 (2013).

30. Levine, T. E., Bornschein, R. L. & Arthur Michaelson, I. Technique for assessing visual discrimination learning in mice. *Pharmacol Biochem Behav* **7**, 567–570 (1977).

31. Heyser, C. J., Fienberg, A. A., Greengard, P. & Gold, L. H. DARPP-32 knockout mice exhibit impaired reversal learning in a discriminated operant task. *Brain Res* **867**, 122–130 (2000).

32. Graybeal, C. *et al.* Strains and Stressors: An Analysis of Touchscreen Learning in Genetically Diverse Mouse Strains. *PLoS One* **9**, e87745 (2014).

33. Brigman, J. L. *et al.* Impaired discrimination learning in mice lacking the NMDA receptor NR2A subunit. *Learning and Memory* **15**, 50–54 (2008).

34. Laughlin, R. E., Grant, T. L., Williams, R. W. & Jentsch, J. D. Genetic dissection of behavioral flexibility: Reversal learning in mice. *Biol Psychiatry* **69**, 1109–1116 (2011).

35. Aarde, S. M., Genner, R. M., Hrncir, H., Arnold, A. P. & Jentsch, J. D. Sex chromosome complement affects multiple aspects of reversal-learning task performance in mice. *Genes Brain Behav* **20**, 1–11 (2021).

36. Gallistel, C. R., King, A. P., Daniel, A. M., Papachristos, E. B. & Balci, F. Fully Automated 24 / 7 Behavioral Screening for Mutations in Targeted Cognitive Mechanisms in the Mouse. *Proceedings of Measuring Behavior 2008* **2008**, 55–56 (2008).

37. Balcombe, J. P., Barnard, N. D. & Sandusky, C. Laboratory routines cause animal stress. *Contemp Top Lab Anim Sci* **43**, 42–51 (2004).

38. Hurst, J. L. & West, R. S. Taming anxiety in laboratory mice. *Nat Methods* **7**, 825–826 (2010).

39. Chesler, E. J., Wilson, S. G., Lariviere, W. R., Rodriguez-Zas, S. L. & Mogil, J. S. Influences of laboratory environment on behavior [1]. *Nat Neurosci* **5**, 1101–1102 (2002).

40. Low, L. A. The impact of pain upon cognition: What have rodent studies told us? *Pain* **154**, 2603–2605 (2013).

41. Meade, J. *et al.* Molecular and behavioral mechanisms mediating paclitaxel-induced changes in affect-like behavior in mice. *The FASEB Journal* **33**, (2019).

42. Warncke, U. O. *et al.* Impact of Dose, Sex, and Strain on Oxaliplatin-Induced Peripheral Neuropathy in Mice. *Frontiers in Pain Research* **2**, 1–18 (2021).

43. Meade, J. A. *et al.* Effects of chemotherapy on operant responding for palatable food in male and female mice. *Behavioural Pharmacology* **32**, 422–434 (2021).

44. Chen, I. *et al.* NAPE-PLD regulates specific baseline affective behaviors but is dispensable for inflammatory hyperalgesia. *Neurobiology of Pain* **14**, 100135 (2023).

45. O'Leary, J. D., O'Leary, O. F., Cryan, J. F. & Nolan, Y. M. A low-cost touchscreen operant chamber using a Raspberry Pi^{TM}. *Behav Res Methods* **50**, 2523–2530 (2018).

46. Kitamura, O., Wee, S., Specio, S. E., Koob, G. F. & Pulvirenti, L. Escalation of methamphetamine self-administration in rats: A dose-effect function. *Psychopharmacology (Berl)* **186**, 48–53 (2006).

47. Mandyam, C. D. *et al.* Varied Access to Intravenous Methamphetamine Self-Administration Differentially Alters Adult Hippocampal Neurogenesis. *Biol Psychiatry* **64**, 958–965 (2008).

48. Adriani, W., Koot, S., Saso, L., Van Den Bos, R. & Laviola, G. Home cage testing of delay discounting in rats. *Behav Res Methods* **41**, 1169–1176 (2009).

49. Remmelink, E. *et al.* A 1-night operant learning task without food-restriction differentiates among mouse strains in an automated home-cage environment. *Behavioural Brain Research* **283**, 53–60 (2015).

50. Nguyen, K. P. *et al.* Feeding Experimentation Device (FED): A flexible open-source device for measuring feeding behavior. *J Neurosci Methods* **267**, 108–114 (2016).

51. Nguyen, K. P. *et al.* Feeding experimentation device (FED): Construction and validation of an open-source device for measuring food intake in rodents. *Journal of Visualized Experiments* **2017**, (2017).

52. Matikainen-Ankney, B. A. *et al.* An open-source device for measuring food intake and operant behavior in rodent home-cages. *Elife* **10**, (2021).

53. Koch, C. E. *et al.* Circadian regulation of hedonic appetite in mice by clocks in dopaminergic neurons of the VTA. *Nat Commun* **11**, 1–11 (2020).

54. Gritton, H. J., Sutton, B. C., Martinez, V., Sarter, M. & Lee, T. M. Interactions Between Cognition and Circadian Rhythms: Attentional Demands Modify Circadian Entrainment. *Behavioral Neuroscience* **123**, 937–948 (2009).

55. Valentinuzzi, V. S., Menna-Barreto, L. & Xavier, G. F. Effect of circadian phase on performance of rats in the Morris water maze task. *J Biol Rhythms* **19**, 312–324 (2004).

56. Hoffmann, H. J. & Balschun, D. Circadian differences in maze performance of C57BI/6 Ola mice. *Behavioural Processes* **27**, 77–83 (1992).

57. Ragozzino, M. E. The Contribution of the Medial Prefrontal Cortex, Orbitofrontal Cortex, and Dorsomedial Striatum to Behavioral Flexibility. *Ann. N.Y. Acad. Sci* **1121**, 355–375 (2007).

58. Remmelink, E., Smit, A. B., Verhage, M. & Loos, M. Measuring discrimination- and reversal learning in mouse models within 4 days and without prior food deprivation. *Learning & Memory* **23**, 660–667 (2016).

59. West, E. A., Forcelli, P. A., McCue, D. L. & Malkova, L. Differential effects of serotonin-specific and excitotoxic lesions of OFC on conditioned reinforcer devaluation and extinction in rats. *Behavioural Brain Research* **246**, 10–14 (2013).

60. Panayi, M. C. & Killcross, S. Functional heterogeneity within the rodent lateral orbitofrontal cortex dissociates outcome devaluation and reversal learning deficits. *Elife* **7**, 1–27 (2018).

61. Cetin, T., Freudenberg, F., Füchtemeier, M. & Koch, M. Dopamine in the orbitofrontal cortex regulates operant responding under a progressive ratio of reinforcement in rats. *Neurosci Lett* **370**, 114–117 (2004).

62. Hart, E. E., Sharpe, M. J., Gardner, M. P. H. & Schoenbaum, G. Responding to preconditioned cues is devaluation sensitive and requires orbitofrontal cortex during cue-cue learning. *Elife* **9**, 1–11 (2020).

63. Arulsamy, A., Corrigan, F. & Collins-Praino, L. E. Age, but not severity of injury, mediates decline in executive function: Validation of the rodent touchscreen paradigm for preclinical models of traumatic brain injury. *Behavioural Brain Research* **368**, 111912 (2019).

64. Young, J. W., Powell, S. B., Geyer, M. A., Jeste, D. V. & Risbrough, V. B. The mouse attentional-set-shifting task: A method for assaying successful cognitive aging? *Cogn Affect Behav Neurosci* **10**, 243–251 (2010).

65. Bizon, J. L., Foster, T. C., Alexander, G. E. & Glisky, E. L. Characterizing cognitive aging of working memory and executive function in animal models. *Front Aging Neurosci* **4**, 1–14 (2012).

66. Tsuboi, K., Uyama, T., Okamoto, Y. & Ueda, N. Endocannabinoids and related N-acylethanolamines: biological activities and metabolism. *Inflamm Regen* **38**, 28 (2018).

67. Blaskovits, F. Endocannabinoid function in hippocampal synaptic plasticity and spatial working memory. (2013).

68. Rademacher, D. J. & Hillard, C. J. Interactions between endocannabinoids and stress-induced decreased sensitivity to natural reward. *Prog Neuropsychopharmacol Biol Psychiatry* **31**, 633–641 (2007).

69. Tarragon, E. & Moreno, J. J. Role of endocannabinoids on sweet taste perception, food preference, and obesity-related disorders. *Chem Senses* **43**, 3–16 (2018).

70. Chiang, K. P., Gerber, A. L., Sipe, J. C. & Cravatt, B. F. Reduced cellular expression and activity of the P129T mutant of human fatty acid amide hydrolase: Evidence for a link between defects in the endocannabinoid system and problem drug use. *Hum Mol Genet* **13**, 2113–2119 (2004).

71. Sipe, J. C., Chiang, K., Gerber, A. L., Beutler, E. & Cravatt, B. F. A missense mutation in human fatty acid amide hydrolase associated with problem drug use. *Proc Natl Acad Sci U S A* **99**, 8394–8399 (2002).

72. Conzelmann, A. *et al.* A polymorphism in the gene of the endocannabinoid-degrading enzyme FAAH (FAAH C385A) is associated with emotional-motivational reactivity. *Psychopharmacology (Berl)* **224**, 573–579 (2012).

73. Basavarajappa, B. S., Yalamanchili, R., Cravatt, B. F., Cooper, T. B. & Hungund, B. L. Increased ethanol consumption and preference and decreased ethanol sensitivity in female FAAH knockout mice. *Neuropharmacology* **50**, 834–844 (2006).

74. Merritt, L. L., Martin, B. R., Walters, C., Lichtman, A. H. & Damaj, M. I. The endogenous cannabinoid system modulates nicotine reward and dependence. *Journal of Pharmacology and Experimental Therapeutics* **326**, 483–492 (2008).

75. Cippitelli, A. *et al.* Endocannabinoid regulation of acute and protracted nicotine withdrawal: Effect of FAAH inhibition. *PLoS One* **6**, (2011).

76. Cippitelli, A. *et al.* Increase of brain endocannabinoid anandamide levels by FAAH inhibition and alcohol abuse behaviours in the rat. *Psychopharmacology (Berl)* **198**, 449–460 (2008).

77. Zhou, Y. *et al.* Blockade of alcohol escalation and “relapse” drinking by pharmacological FAAH inhibition in male and female C57BL/6J mice. *Psychopharmacology (Berl)* **234**, 2955–2970 (2017).

78. London, T. D. *et al.* Coordinated ramping of dorsal striatal pathways preceding food approach and consumption. *Journal of Neuroscience* **38**, 3547–3558 (2018).

79. Winstanley, C. A. *et al.* ΔFosB induction in orbitofrontal cortex mediates tolerance to cocaine-induced cognitive dysfunction. *Journal of Neuroscience* **27**, 10497–10507 (2007).

80. Izquierdo, A., Brigman, J. L., Radke, A. K., Rudebeck, P. H. & Holmes, A. The neural basis of reversal learning: An updated perspective. *Neuroscience* **345**, 12–26 (2017).

81. Bissonette, G. B. & Roesch, M. R. Neurophysiology of Reward-Guided Behavior: Correlates Related to Predictions, Value, Motivation, Errors, Attention, and Action. in *Brain Imaging in Behavioral Neuroscience* 199–230 (2015). doi:10.1007/7854_2015_382.

82. Bouton, M. E., Maren, S. & McNally, G. P. Behavioral and neurobiological mechanisms of pavlovian and instrumental extinction learning. *Physiol Rev* **101**, 611–681 (2021).

83. Gourley, S. L., Lee, A. S., Howell, J. L., Pittenger, C. & Taylor, J. R. Dissociable regulation of instrumental action within mouse prefrontal cortex. *European Journal of Neuroscience* **32**, 1726–1734 (2010).

84. Marquardt, K. & Brigman, J. L. The impact of prenatal alcohol exposure on social, cognitive and affective behavioral domains: Insights from rodent models. *Alcohol* **51**, 1–15 (2016).

85. Gargiulo, A. T. *et al.* Sex differences in cognitive flexibility are driven by the estrous cycle and stress-dependent. *Front Behav Neurosci* **16**, (2022).

86. Bergamini, G. *et al.* Mouse psychosocial stress reduces motivation and cognitive function in operant reward tests: A model for reward pathology with effects of agomelatine. *European Neuropsychopharmacology* (2016) doi:10.1016/j.euroneuro.2016.06.009.

87. Peng, B. *et al.* Corticosterone attenuates reward-seeking behavior and increases anxiety via D2 receptor signaling in ventral tegmental area dopamine neurons. *Journal of Neuroscience* **41**, 1566–1581 (2021).

88. Haluk, D. M. & Wickman, K. Evaluation of study design variables and their impact on food-maintained operant responding in mice. *Behavioural Brain Research* **207**, 394–401 (2010).

89. Heath, C. J., Phillips, B. U., Bussey, T. J. & Saksida, L. M. Measuring motivation and reward-related decision making in the rodent operant touchscreen system. *Curr Protoc Neurosci* **2016**, 8.34.1-8.34.20 (2016).

90. Júnior, A. R. F., Castelli, M. C. Z. & Oliveira, E. C. A. de. Effects of chronic mild stress on operant discrimination learning. *Behavior Analysis: Research and Practice* **15**, 20–27 (2015).

91. Arnsten, A. F. T. Stress signalling pathways that impair prefrontal cortex structure and function. *Nat Rev Neurosci* **10**, 410–422 (2009).

92. Roebuck, A. J., Liu, M. C., Lins, B. R., Scott, G. A. & Howland, J. G. Acute stress, but not corticosterone, facilitates acquisition of paired associates learning in rats using touchscreen-equipped operant conditioning chambers. *Behavioural Brain Research* **348**, 139–149 (2018).

93. Graybeal, C. *et al.* Paradoxical reversal learning enhancement by stress or prefrontal cortical damage: rescue with BDNF. *Nat Neurosci* **14**, 1507–1509 (2011).

94. Hurtubise, J. L. & Howland, J. G. Effects of stress on behavioral flexibility in rodents. *Neuroscience* **345**, 176–192 (2017).

95. Dias-Ferreira, E. *et al.* Chronic Stress Causes Frontostriatal Reorganization and Affects Decision-Making. *Science (1979)* **325**, 621–625 (2009).

96. Schwabe, L. & Wolf, O. T. Stress modulates the engagement of multiple memory systems in classification learning. *Journal of Neuroscience* **32**, 11042–11049 (2012).

97. Bissonette, G. B. & Powell, E. M. Reversal learning and attentional set-shifting in mice. *Neuropharmacology* **62**, 1168–1174 (2012).

98. Ramírez-Lugo, L., Peñas-Rincón, A., Ángeles-Durán, S. & Sotres-Bayon, F. Choice behavior guided by learned, but not innate, taste aversion recruits the orbitofrontal cortex. *Journal of Neuroscience* **36**, 10574–10583 (2016).

99. Gallagher, M., McMahan, R. W. & Schoenbaum, G. Orbitofrontal cortex and representation of incentive value in associative learning. *Journal of Neuroscience* **19**, 6610–6614 (1999).

100. Zhou, J., Gardner, M. P. & Schoenbaum, G. Is the core function of orbitofrontal cortex to signal values or make predictions? *Curr Opin Behav Sci* **41**, 1–9 (2021).

101. Schoenbaum, G. & Roesch, M. Orbitofrontal Cortex, Associative Learning, and Expectancies. *Neuron* **47**, 633–636 (2005).

102. Schoenbaum, G., Takahashi, Y., Liu, T. L. & Mcdannald, M. A. Does the orbitofrontal cortex signal value? *Ann N Y Acad Sci* **1239**, 87–99 (2011).

103. Pickens, C. L. *et al.* Different Roles for Orbitofrontal Cortex and Basolateral Amygdala in a Reinforcer Devaluation Task. *Journal of Neuroscience* **23**, 11078–11084 (2003).

104. Fuchs, R. A., Evans, K. A., Parker, M. P. & See, R. E. Differential involvement of orbitofrontal cortex subregions in conditioned cue-induced and cocaine-primed reinstatement of cocaine seeking in rats. *Journal of Neuroscience* **24**, 6600–6610 (2004).

105. Arguello, A. A. *et al.* Role of a Lateral Orbital Frontal Cortex-Basolateral Amygdala Circuit in Cue-Induced Cocaine-Seeking Behavior. *Neuropsychopharmacology* **42**, 727–735 (2017).

106. Tapia, M. A., Lee, J. R., Weise, V. N., Tamasi, A. M. & Will, M. J. Sex differences in hedonic and homeostatic aspects of palatable food motivation. *Behavioural Brain Research* **359**, 396–400 (2019).

107. Schoenberg, H. L., Sola, E. X., Seyller, E., Kelberman, M. & Toufexis, D. J. Female rats express habitual behavior earlier in operant training than males. *Behavioral Neuroscience* **133**, 110–120 (2019).

108. Wong, P. T. P. A behavioral field approach to general activity: Sex differences and food deprivation in the rat. *Anim Learn Behav* **7**, 111–118 (1979).

109. van Hest, A., van Haaren, F. & van de Poll, N. E. Operant conditioning of response variability in male and female Wistar rats. *Physiol Behav* **45**, 551–555 (1989).

110. Dincheva, I. *et al.* FAAH genetic variation enhances fronto-amygdala function in mouse and human. *Nat Commun* **6**, 6395 (2015).

111. Wassum, K. M. Amygdala-cortical collaboration in reward learning and decision making. *Elife* **11**, 1–29 (2022).

112. Manoocheri, K. & Carter, A. G. Rostral and caudal basolateral amygdala engage distinct circuits in the prelimbic and infralimbic prefrontal cortex. *Elife* **11**, 1–23 (2022).

113. McGarry, L. M. & Carter, A. G. Prefrontal Cortex Drives Distinct Projection Neurons in the Basolateral Amygdala. *Cell Rep* **21**, 1426–1433 (2017).

114. Zeeb, F. D. & Winstanley, C. A. Functional disconnection of the orbitofrontal cortex and basolateral amygdala impairs acquisition of a rat gambling task and disrupts animals' ability to alter decision-making behavior after reinforcer devaluation. *Journal of Neuroscience* **33**, 6434–6443 (2013).

115. Hart, E. E. & Izquierdo, A. Basolateral amygdala supports the maintenance of value and effortful choice of a preferred option. *European Journal of Neuroscience* **45**, 388–397 (2017).

116. Hosking, J. G., Cocker, P. J. & Winstanley, C. A. Dissociable contributions of anterior cingulate cortex and basolateral amygdala on a rodent cost/benefit decision-making task of cognitive effort. *Neuropsychopharmacology* **39**, 1558–1567 (2014).

117. Sun, N. & Laviolette, S. R. Inactivation of the basolateral amygdala during opiate reward learning disinhibits prelimbic cortical neurons and modulates associative memory extinction. *Psychopharmacology (Berl)* **222**, 645–661 (2012).

118. Touriño, C., Oveisi, F., Lockney, J., Piomelli, D. & Maldonado, R. FAAH deficiency promotes energy storage and enhances the motivation for food. *Int J Obes* **34**, 557–568 (2010).

119. Nevin, J. A. & Grace, R. C. Behavioral momentum and the law of effect. *Behavioral and Brain Sciences* **23**, 73–130 (2000).

120. Nevin, J. A. Resistance to extinction and behavioral momentum. *Behavioural Processes* **90**, 89–97 (2012).

121. McCloskey, J. L. & Tombaugh, T. N. Sucrose concentration, constant delay of reward, and resistance to extinction. *J Exp Psychol* **88**, 128–132 (1971).

122. Tunstall, B. J. & Kearns, D. N. Cocaine can generate a stronger conditioned reinforcer than food despite being a weaker primary reinforcer. *Addiction Biology* **21**, 282–293 (2016).

123. Domingo-Rodriguez, L. *et al.* A specific prelimbic-nucleus accumbens pathway controls resilience versus vulnerability to food addiction. *Nat Commun* **11**, 1–16 (2020).

124. Hilario, M., Holloway, T., Jin, X. & Costa, R. M. Different dorsal striatum circuits mediate action discrimination and action generalization. *European Journal of Neuroscience* **35**, 1105–1114 (2012).

125. Balleine, B. W., Delgado, M. R. & Hikosaka, O. The role of the dorsal striatum in reward and decision-making. *Journal of Neuroscience* **27**, 8161–8165 (2007).

126. Schouppe, N., Demanet, J., Boehler, C. N., Richard Ridderinkhof, K. & Notebaert, W. The role of the striatum in effort-based decision-making in the absence of reward. *Journal of Neuroscience* **34**, 2148–2154 (2014).

127. Spencer, S. *et al.* A Model of Δ9-Tetrahydrocannabinol Self-administration and Reinstatement That Alters Synaptic Plasticity in Nucleus Accumbens. *Biol Psychiatry* **84**, 601–610 (2018).

128. Richardson, N. R. & Roberts, D. C. S. <1996 - Richardson & Roberts - J Neurosci Methods (Progressive Ration).pdf>. *J Neurosci Methods* **66**, 1–11 (1996).

129. Golden, S. A. *et al.* Compulsive Addiction-like Aggressive Behavior in Mice. *Biol Psychiatry* **82**, 239–248 (2017).

130. Paxinos, G. & Franklin, K. B. J. *The Mouse Brain in Stereotaxic Coordinates*. (Elsevier Science).

4.9 FIGURES

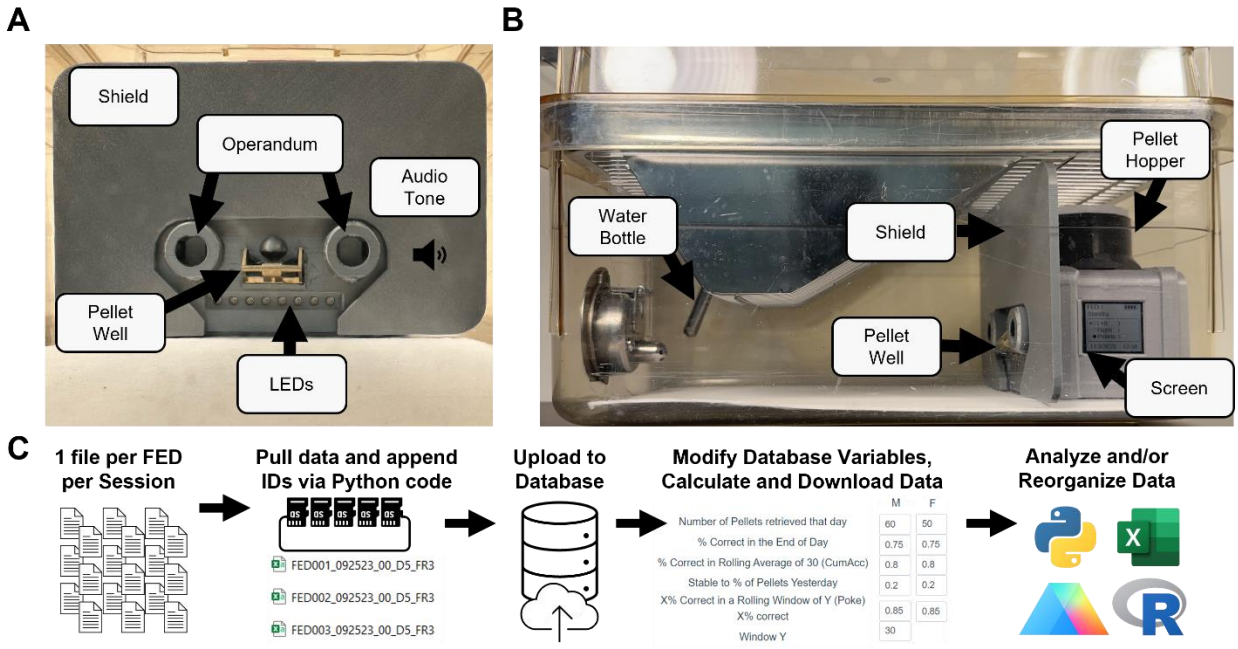

Figure 1. Description of FED3 setup and data analysis pipeline. (A) Front-view of the FED3 in a standard mouse home-cage demonstrating the main mouse-interaction features including two operandum, a pellet well, and LED and audio cues. **(B)** Side-view of FED3 in a standard home-cage demonstrating the additional features including the FED pellet hopper and screen, a custom-printed shield to prevent the mouse from climbing on the device, and the bottle for water consumption. **(C)** Data pipeline optimized for high throughput data cognitive behavioral analysis of cognitive behavioral tests using the FED3 including: bulk file collection from individual SD cards using Python code, data upload to a Python-based database followed by data analysis via user-defined experimental thresholds, and downloading of the compiled results as a XSLX file for statistical analysis using preferred software. A detailed guide to the pipeline and all custom code can be found in the Supplemental Information.

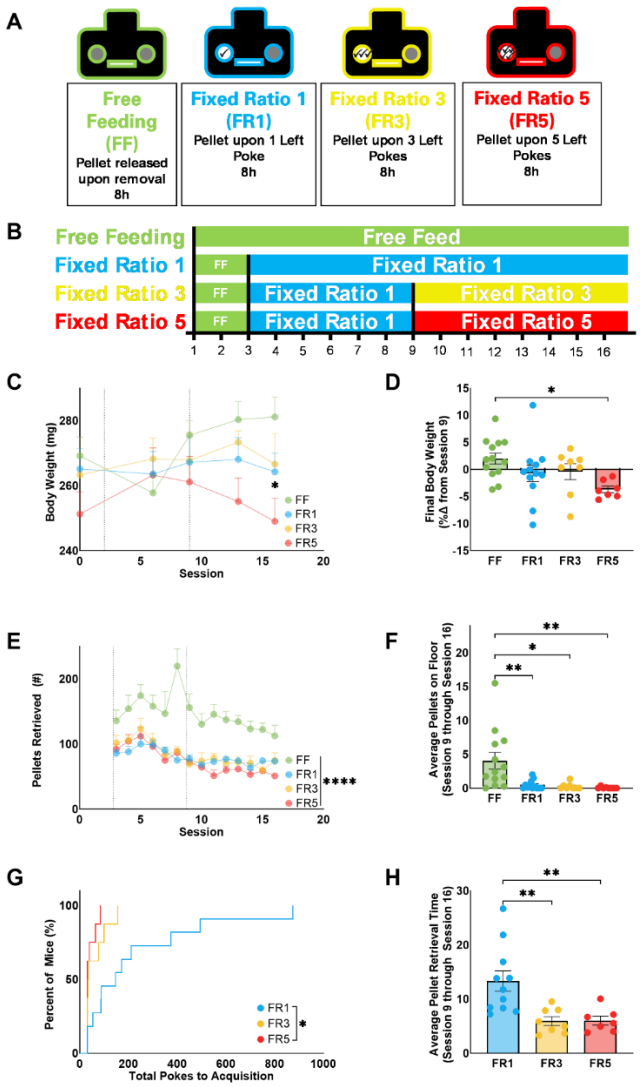

Figure 2. Fixed ratio impacts multiple parameters of operant performance using FED3. (A) Description of FED3 programs used to determine the optimal parameters for operant performance including Free Feeding (FF), Fixed-Ratio 1 (FR1), Fixed-Ratio 3 (FR3), and Fixed-Ratio 5 (FR1). **(B)** Experimental timeline for evaluating parameters of operant performance and goal-directed behaviors of four groups of male mice: FF (green, n=13), FR1 (blue, n=11), FR3 (yellow, n=8), FR5 (red, n=8). All four groups started with 2 sessions of group-housed FF before being single housed for FF, FR1, FR3, and/or FR5 as outlined for 14 additional sessions. **(C)** Mouse body weight (mg) was evaluated after session 7, 9, 14, and 16. **(D)** Bodyweight on session 16 displayed as the percent change from session 9, when group 3 and 4 started FR3 and FR5, respectively. **(E)** Number of Pellets dispensed by the FED3 per day. **(F)** Number of pellets

found on the floor of the testing cage (average of sessions 9 through 16). **(G)** Kaplan-Meier curve of the total number of nose pokes required for animals to reach acquisition criterion: 85% correct in a rolling window of 30 pokes (starting at session 9). **(H)** Average time to retrieve a pellet from the pellet well (average of sessions 9 through 16). Data displayed as mean ± SEM (except G). Statistical significance indicated by *P<0.05, ** P<0.01, ****P<0.0001.

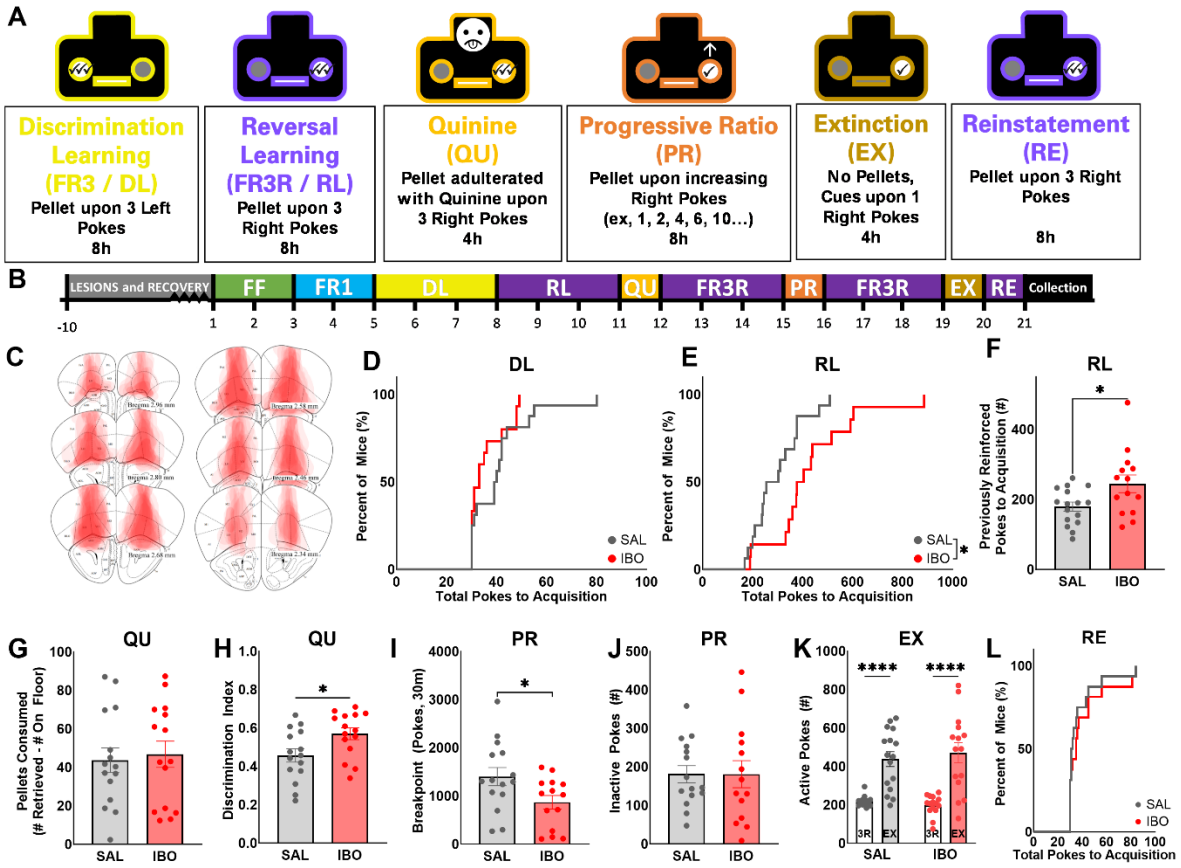

Figure 3. Bilateral OFC lesions reduce reversal learning behavior using FED3. (A) Description of FED3 programs used to evaluate cognitive performance including Discrimination Learning (DL, also FR3), Reversal Learning (RL, also FR3R), Quinine Test (QU), Progressive Ratio Test (PR), Extinction (EX), and Reinstatement (RE). **(B)** Experimental timeline for a typical mouse undergoing this behavioral battery, demonstrating lesion and recovery time followed by daily progression through tests. Male mice received bilateral injection of saline (SAL, n=16) or ibotenic acid (IBO, n=15) into the orbitalfrontal cortex (OFC), and were given 7 days to recover before initiating the 6 test behavioral battery. Tissue collection for histological verification of lesion efficacy and location occurred 27 to 32 days post-injection. **(C)** Schematic demonstrating lesioning of the lateral and ventral OFC across subjects, with each subject represented on a separate stacked layer. **(D,E)** Kaplan-Meier curve of the total nose pokes required for animals to reach the acquisition criterion of 85% during DL and RL. **(F)** Number of nose pokes on the previously reinforced nose poke until reaching acquisition criterion during RL. **(G)** Number of Quinine-adulterated pellets consumed during QU test. Consumption is calculated as pellets retrieved during the test minus pellets found on the floor. **(H)** Discrimination Index

during QU test. **(I)** Number of active pokes made before reaching a breakpoint, defined as 30 minutes of inactivity during PR test, or final number of pokes. **(J)** Number of inactive pokes made during the PR test. **(K)** Number of active pokes made during prior four days of 3R (3R) or on the initial EX session demonstrating extinction burst. **(L)** Kaplan-Meier curve of the total nose pokes required for animals to reach acquisition criterion of 85% during Reinstatement (RE). Data displayed as mean ± SEM (except D and E). Statistical significance indicated by *P<0.05. Diagrams modified from Paxinos and Franklin (2001).

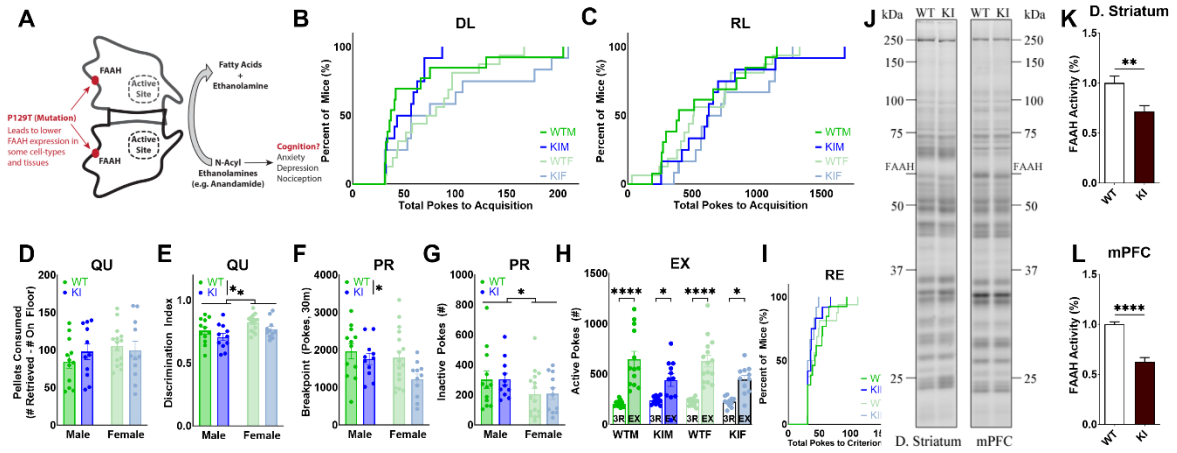

Figure 4. Both FAAH P129T genotype and sex influence cognitive performance in aged mice. (A) Fatty acid amide hydrolase (FAAH) plays a critical role in corticolimbic signaling and influence multiple behaviors including nociception, anxiety, depression, and cognition. The P129T single nucleotide polymorphism occurs outside the FAAH active site, yet it can dysregulate corticoamygdalar circuitry and increase problematic drug use in clinical populations. For this study, we evaluated wild-type (WT) and FAAH P129T knock in (KI) mice of both sexes for cognitive impairments using FED3. **(B)** Kaplan-Meier curve of the total nose pokes required for animals to reach the acquisition criterion of 85% correct in a rolling window of 30 pokes during DL. **(C)** Kaplan-Meier curve of the total nose pokes required for animals to reach the acquisition criterion of 85% correct in a rolling window of 30 pokes during RL. **(D)** Number of Quinine-adulterated pellets consumed during the Quinine (QU) test. Consumption is calculated as pellets retrieved during the test minus pellets found on the floor. **(E)** Discrimination Index during the QU test. **(F)** Number of pokes made before reaching a breakpoint, defined as 30 minutes of inactivity during the Progressive Ratio (PR) test. **(G)** Number of inactive pokes made during the PR test. **(H)** Number of active pokes made during prior four days of 3R (3R) or on the first Extinction (EX) session demonstrating extinction burst. **(I)** Kaplan-Meier curve of the total nose pokes required for animals to reach the acquisition criterion of 85% correct in a rolling window of 30 pokes during Reinstatement (RE). **(J)** ABPP gel demonstrating FAAH activity in the dorsal striatum (D. Striatum) and medial prefrontal cortex (mPFC) in representative WT and KI animals. **(K)** Quantification of active FAAH enzyme levels in the D. Striatum of WT and KI mice. **(L)** Quantification of active FAAH enzyme levels in the mPFC of WT and KI mice. Data

displayed as mean ± SEM where applicable from four groups: WT males (n=12-13), KI males (n=11-12), WT females (n=15-16), and KI females (n=11-12). Statistical significance indicated by. *P<0.05, ** P<0.01**,** ****P<0.0001.

4.10 SUPPLEMENTAL MATERIAL

4.10a Supplemental Figures

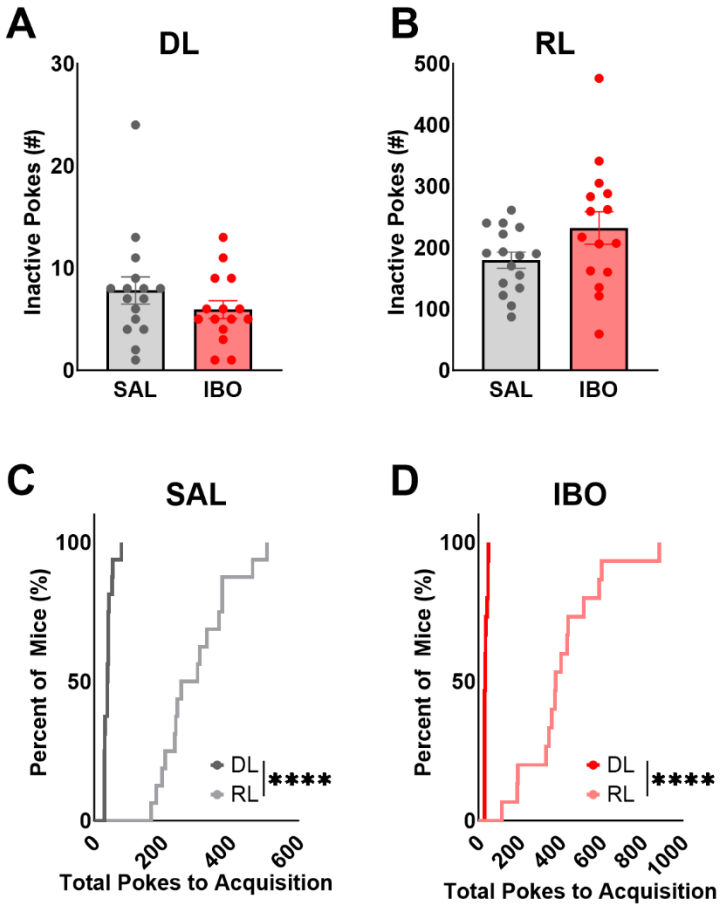

Supplemental Figure 1. Effects of OFC lesion on discrimination and reversal learning.

(A) Number of inactive pokes made before reaching the acquisition criterion of 85% correct in a rolling window of 30 pokes during DL. **(B)** Number of inactive pokes made before reaching the acquisition criterion of 85% correct in a rolling window of 30 pokes during RL. **(C)** Kaplan-Meier curve of the total nose pokes required for SAL animals to reach the acquisition criterion of 85% correct in a rolling window of 30 pokes) during DL and RL. **(D)** Kaplan-Meier curve of the total nose pokes required for IBO animals to reach the acquisition criterion of 85% correct in a rolling window of 30 pokes) during DL and RL. Data displayed as mean ± SEM where applicable (SAL n=15-16, IBO n=14-15). Statistical significance indicated by ****P<0.0001.

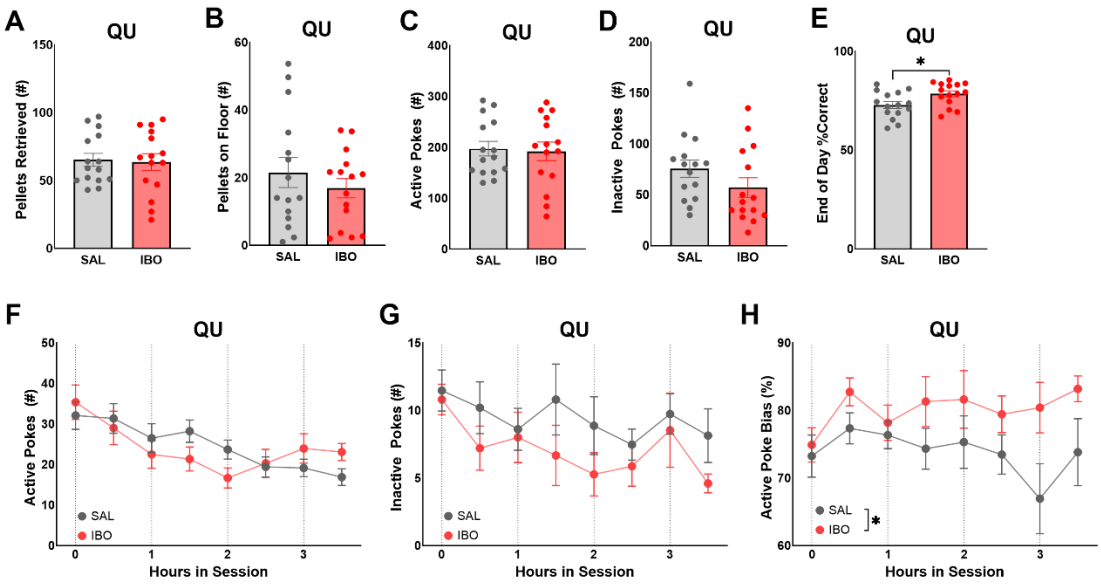

Supplemental Figure 2. Effects of OFC lesion on response to aversive reward.

(A) Number of Quinine-adulterated pellets retrieved from the device during a 4-hour Quinine (QU) task. **(B)** Number of Quinine-adulterated pellets found on the floor of the cage at the end of the QU task. **(C)** Number of active pokes made during the QU task. **(D)** End-of-day performance during a 4-hour QU task, displayed as percent correct at the end of the day. **(F)** Number of active pokes made by 30-minute bins during the QU task. **(G)** Number of inactive pokes made by 30-minute bins during the QU task **(H)** Active poke bias by 30-minute bins during the QU task. Data displayed as mean ± SEM (SAL n=15-16, IBO n=14-15). Statistical significance indicated by *P<0.05.

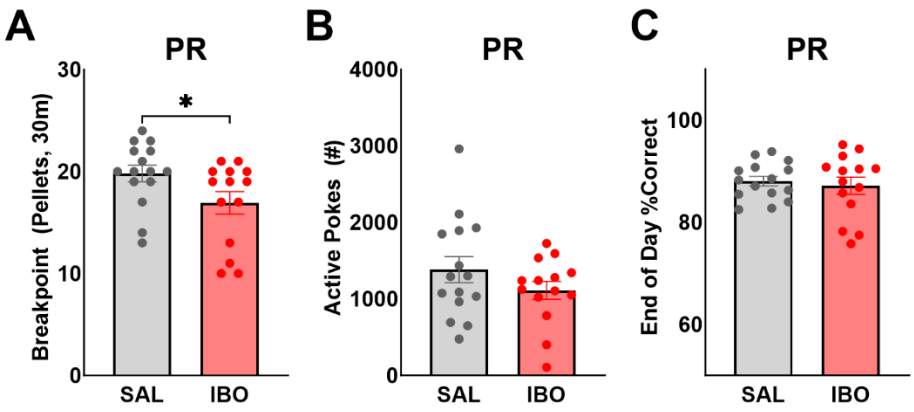

Supplemental Figure 3. Effects of OFC lesion on response to increasing instrumental effort. (A) Pellets retrieved before reaching a breakpoint, defined as 30 minutes of inactivity during an 8-hour Progressive Ratio (PR) task. **(B)** Number of active pokes made during an 8-hour PR task. **(C)** End-of-day performance during an 8-hour PR task, displayed as percent correct at the end of the day. Data displayed as mean ±SEM (SAL n=15-16, IBO n=14-15). Statistical significance indicated by *P<0.05.

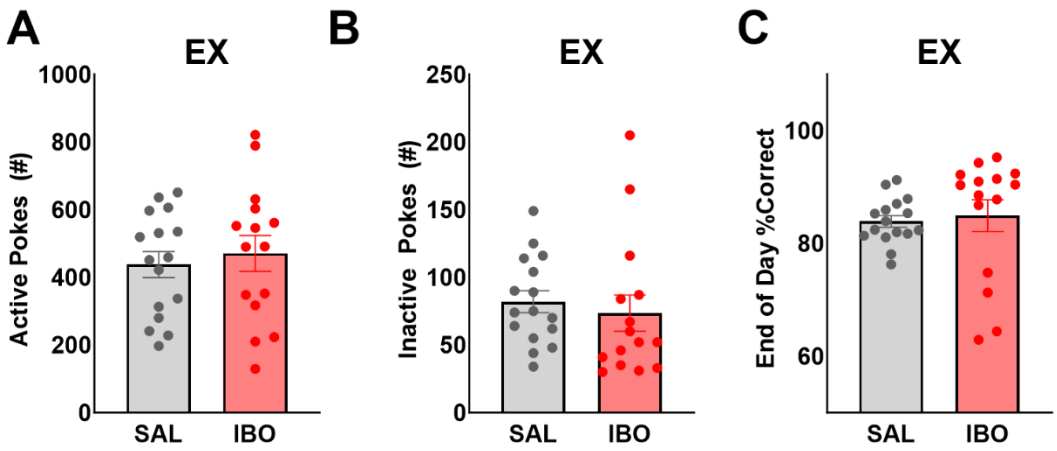

Supplemental Figure 4. Effects of OFC lesion on response to cue devaluation and reinstatement. (A) Active nose pokes made over a 4-hour extinction (EX) trial. **(B)** Inactive nose pokes made over a 4-hour extinction (EX) trial. **(C)** End-of-day performance during a 4-hour EX task, displayed as percent correct at the end of the day. Data displayed as mean ± SEM (SAL n=15-16, IBO n=14-15) where applicable. Statistical significance indicated by ****P<0.0001.

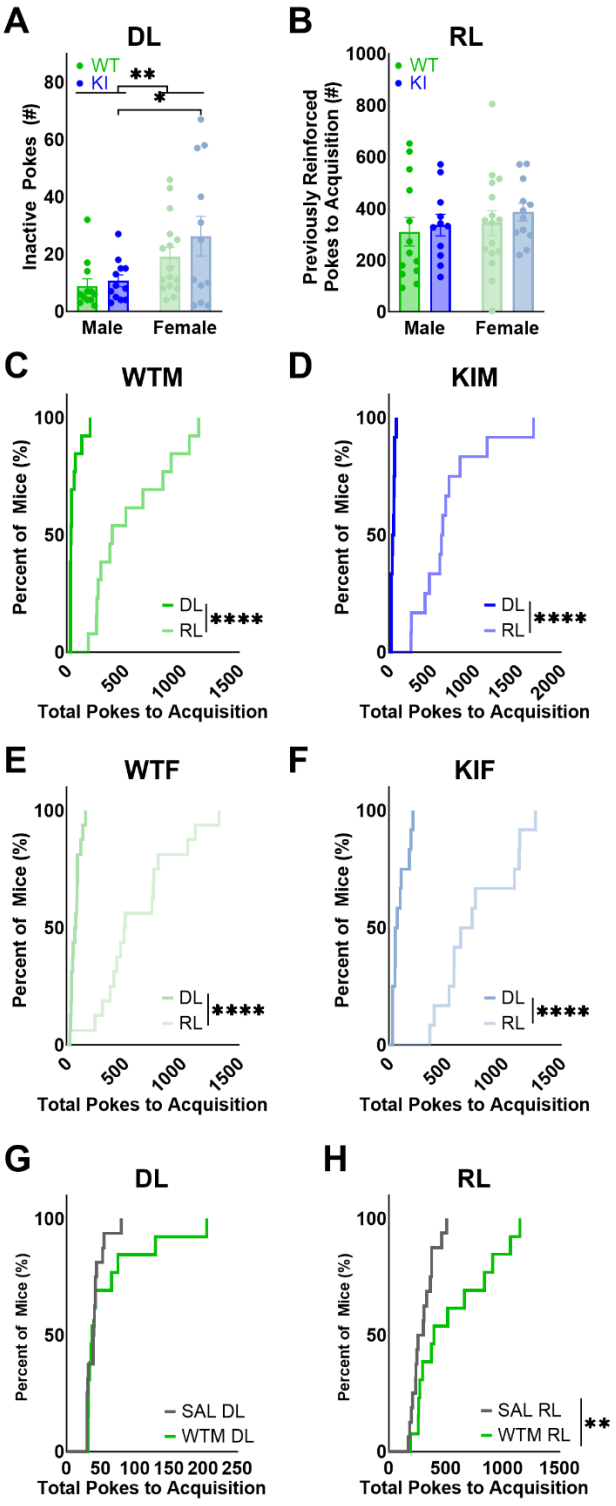

Supplemental Figure 5. Contribution of Sex, P129T genotype, and Age to cognitive flexibility. Number of inactive pokes made before reaching acquisition criterion (85% correct in a rolling window of 30 pokes) during **(A)** discrimination learning (DL) and **(B)** reversal learning

(RL). Kaplan-Meier curves of the total nose pokes required to reach the acquisition criterion during DL and RL by **(C)** wild-type males (WTM, n=12-13), **(D)** P129T knock-in males (KIM, n=11-12), **(E)** wild-type females (WTF, n=15-16), and **(F)** P129T knock-in females (KIF, n=11-12). **(G)** Kaplan-Meier curves of the total nose pokes required to reach acquisition criterion between aged P129T WTM (21+ weeks old) and SAL lesioned controls (10+ weeks old) during **(G)** DL and **(H)** RL. Data displayed as mean ± SEM where applicable. Statistical significance indicated by *P<0.05, **P<0.01, ****P<0.0001.

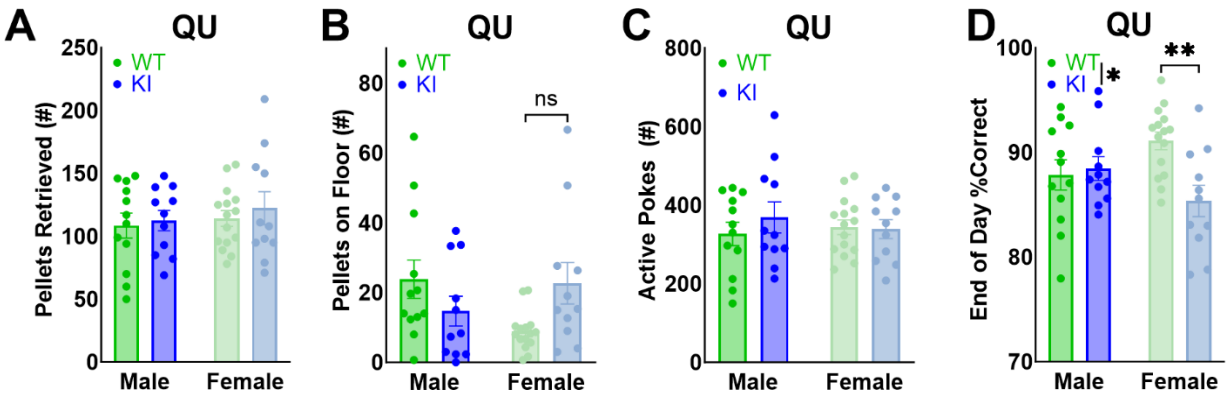

Supplemental Figure 6. Contribution of Sex and P129T Genotype to response to aversive reward. (A) Number of Quinine-adulterated pellets retrieved from the device during a 4-hour Quinine (QU) task. **(B)** Number of Quinine-adulterated pellets found on the floor of the cage at the end of the QU task. **(C)** Number of active pokes made during the QU task. **(D)** End-of-day performance during the QU task, displayed as percent correct at the end of the day. Data displayed as mean ± SEM from four groups: wild-type males (WTM, n=12-13), P129T knock-in males (KIM, n=11-12), wild-type females (WTF, n=15-16), and P129T knock-in females (KIF, n=11-12). Statistical significance indicated by *P<0.05, ** P<0.01.

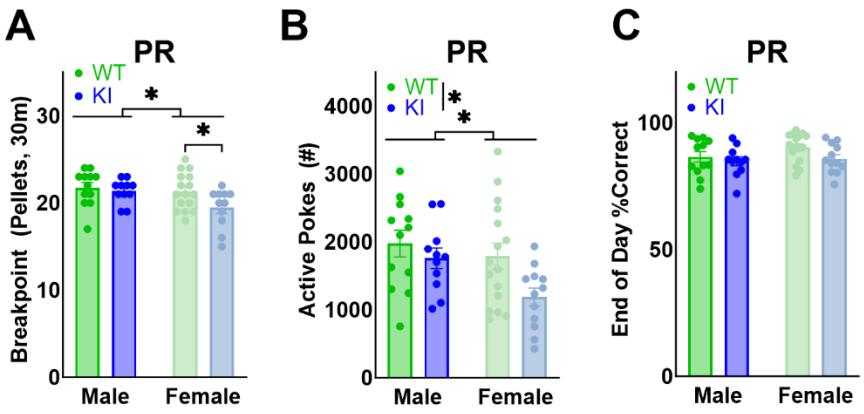

Supplemental Figure 7. Contribution of Sex and P129T genotype to response to increasing instrumental effort. (A) Pellets retrieved before reaching a breakpoint, defined as 30 minutes of inactivity during an 8-hour Progressive Ratio (PR) task. **(B)** Number of active pokes made during PR task. **(C)** End-of-day performance during the PR task, displayed as percent correct at the end of the day. Data displayed as mean ± SEM from four groups: wild-type males (WTM, n=12-13), P129T knock-in males (KIM, n=11-12), wild-type females (WTF, n=15-16), and P129T knock-in females (KIF, n=11-12). Statistical significance indicated by *P<0.05, ** P<0.01.

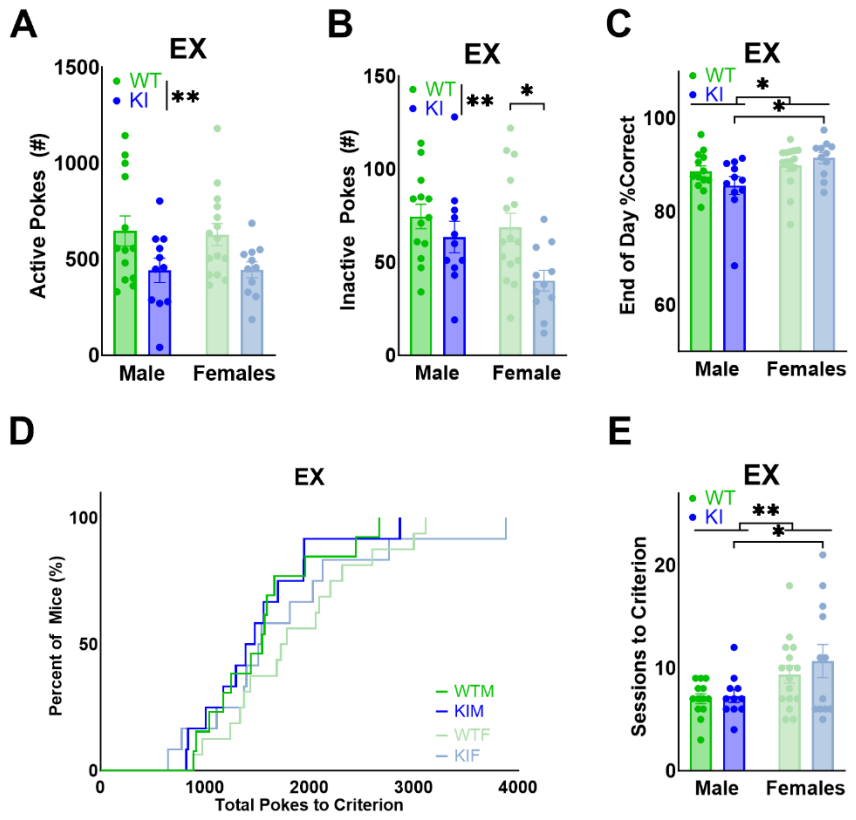

Supplemental Figure 8. Contribution of Sex and P129T Genotype to response to cue devaluation, extinction, and reinstatement. (A) Active pokes made during the first day of a 4-hour extinction (EX) task **(B)** Inactive pokes made during the first day of a 4-hour extinction (EX) task. **(C)** End-of-day performance during a single 4-hour EX task, displayed as percent correct at the end of the day. **(D)** Kaplan-Meier curve of the total number of nose pokes needed to reach the acquisition criterion of ending a session with active pokes ≤20% of the average number of active pokes from the preceding 4 3R sessions. **(E)** Number of sessions for animals to meet EX acquisition. Kaplan-Meier curve of the total nose pokes required for animals to reach the acquisition criterion (85% correct in a rolling window of 30 pokes) during reinstatement (RE) Data displayed as mean ± SEM from four groups: wild-type males (WTM, n=12-13), P129T knock-in males (KIM, n=11-12), wild-type females (WTF, n=15-16), and P129T knock-in females (KIF, n=11-12). Statistical significance indicated by *P<0.05, **P<0.01, ****P<0.0001.

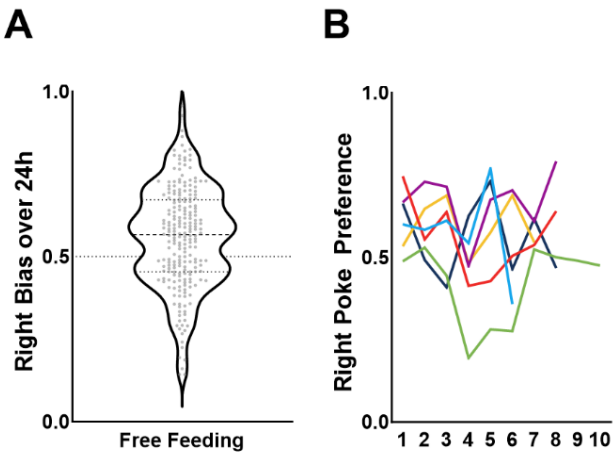

Supplemental Figure 9. Visualization of Side Preference During Free Feeding. (A) End of day Right Bias of 222 daily sessions from 18+ animals during Free Feeding. **(B)** Right Bias by day of select animals.

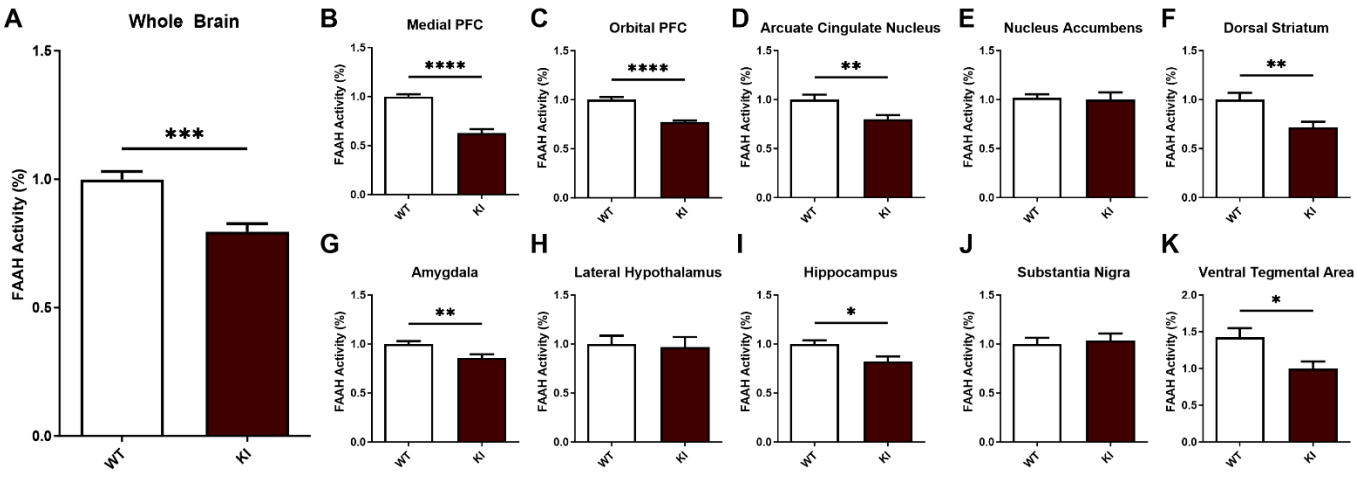

Supplemental Figure 10. Quantification of active FAAH enzyme levels in WT and KI animals. Quantification of active FAAH enzyme levels in the **(A)** whole brain, **(B)** medial PFC, **(C)** OFC, **(D)** Arcuate Cingulate Nucleus, **(E)** Nucleus Accumbens, **(F)** Dorsal Striatum, **(G)** Amygdala, **(H)** Lateral Hypothalamus, **(I)** Hippocampus, **(J)** Substantia Nigra, **(K)** Ventral Tegmental Area. Statistical significance indicated by. *P<0.05, ** P<0.01**,** ****P<0.0001.

4.10b Supplemental Tables

Supplemental Table 1. Troubleshooting FED3 Errors during Cognitive Testing

Issue	Effect on Data	Cause	Solution
Pellet Well Ghost: FED3 senses a pellet when the food well is empty	Stops all collection of pellet-related data	Debris on the pellet well IR sensor	**Step 1:** Visually inspect the IR sensor, and carefully remove any large debris from the diodes using a small gauge needle. **Step 2:** Remove the following parts from the FED3: RTC, Arduino, Motor Chip, Battery. **Step 3:** Clean the IR beam diodes using a waterpik (filled with double distilled water) on a medium-to-high setting for four to eight seconds. **Step 4:** Remove water from IR sensor and PCB using a fan-powered air gun. *Caution*: Using "canned air" in place of an air gun may deposit chemicals potentially damaging the IR sensor. **Step 5:** Allow device to dry overnight, and reassemble FED3 in morning. **Step 6:** Test device to see if this Step 1-5 fixed ghosting errors. If cleaning does not address this issue, resolder and/or replace the faulty IR sensor and associated resistor (Left:R1, Well:R2, Right:R3). If problem persists replace entire PCB board.
		Damage to the pellet well IR sensor	
		Faulty pellet well soldering to the PCB	
Nose poke Ghost: FED3 senses an active left or right nose poke when the mouse is not interacting with the operandum	Produces over-estimation of nose-poke-related data May lead to program switching mid experiment	Debris on the pellet well IR sensor	
		Damage to the pellet well IR sensor	
		Faulty pellet well soldering to the PCB	
Blind Pellet Well: FED3 fails to sense a pellet in the food well	Stops accurate collection of pellet-related data Increased pellet dispensation and risk of Pellet Jam	Improperly positioned pellet well or PCB	Ends of IR sensor should be <0.6mm from internal edge of pellet well. Tighten screws holding the PCB down or remove and reposition pellet well to achieve. *Note:* If FED3 consistently delivers two pellets before sensing, place a single drop of epoxy, super glue, or solder along bottom of pellet well.
Blind Nose Poke: FED3 fails to sense a nose poke when the mouse is interacting with the operandum	Stops all collection of nose-poke-related data May prevent pellet release if on active poke	Faulty Soldering	Resolder all five points of contact between the IR sensor, associated resistor (Left:R1, Well:R2, Right:R3), and the PCB. If problem persists, replace entire PCB board.

Supplemental Table 1 (cont). Troubleshooting FED3 Errors during Cognitive Testing

Issue	Effect on Data	Cause	Solution
Pellet Jam: FED3 develops a clog in the chute that prevents pellet dispensing	Prevents pellet dispensation and stops accurate collection of pellet-related data	Moisture	Remove moisture from FED3 and home cage • Address any leaks in the cage from water dispensation devices. • Ensure cages have sufficient air circulation. • Dry out the chute using a fan-powered air gun.
		Debris	Dislodge debris and clean the pellet chute: • Remove the pellet wheel. • Push two entwined pipe cleaners through the chute to the pellet well, then pull back and forth to dislodge any pellet blockages. Repeat, entering from the pellet well. • Use a waterpik (filled with double distilled water) on a medium-to-high setting for ten to fifteen seconds at chute entry and chute exit to remove any remaining debris. • Remove water from the pellet chute using a fan-powered air gun. • Allow device to dry overnight, and re-attach pellet wheel in morning. *Note:* Sifting pellets to remove broken pieces prior to filling will help reduce debris buildup in FED3.
		Pellet Disk	Make sure the pellet disk is properly attached to the motor on the FED3 • Screwing too tight leads to non-spinning • Screw too loose leads to slipping
Jumping/Hopping: Pellet is released but does not remain in pellet well.	Increased pellet dispensation and risk of Pellet Jam Inaccurate number of pellets on floor of cage	Improperly positioned pellet well or PCB	Some amount of jumping/hopping is acceptable (<5 hops in 100 releases). If significantly more, check that well is placed properly and not angled. Ends of IR sensor should be <0.6mm from internal edge of pellet well. Tighten screws holding the PCB down or remove and reposition pellet well to achieve.

Supplemental Table 1 (cont). Troubleshooting FED3 Errors during Cognitive Testing

Issue	Effect on Data	Cause	Solution
SD Card Error: Upon start displays a warning that SD card is not inserted despite presence of SD card	FED3 will not boot into experimental programs	Debris	Repeatedly remove and reinsert SD card • Turn off FED3 and remove SD card • Dislodge any debris from SD slot using soft paint brush, air gun, or manually blowing air into slot • Replace SD card • Repeat in quick succession five to ten times
		Faulty Feather M0 Adalogger	Replace Feather M0 Adalogger
RTC Error: Upon start displays an incorrect or impossible date and time	Timestamps may be incorrect, impossible, or fail to progress through time Collected data may need manual modification or be completely unusable ***Note:*** Upon booting if the date is incorrect but six values (ex 151481 or 010000) the data will likely be usable. If it contains non-numerical values (@5@5@5) or more than six values (1651652165) the data will not be usable.	Improperly positioned RTC	Inspect that the RTC board is fully seated into but not bending the PCB header. If it is not: • Press on or reposition RTC board • Turn device on to check for proper time • Reflash time clock and device code

		Low button cell battery	Measure Button Cell Battery Level
			
			• **Option 1: With RTC in device:**
			  ○ Place positive lead of multimeter on positive side of battery or metal holding it to the RTC
			  ○ Place negative lead on flat surface of the SD card slot
			• **Option 2: Button Cell Battery out of RTC or RTC out of device:**
			  ○ Place positive lead of multimeter on positive side of battery or metal holding it to the RTC.
			  ○ Place negative lead on negative side of battery
			
			Readings <1.5V indicate battery needs replacing
			
			After replacing, reflash time clock and device code

		Dead button cell battery	

Supplemental Table 2. Statistics for all Behavioral Tests in Figure 2.

Fig.	Test	Statistical Test	Factor	Test Statistic	P-Value	Post-Hoc (Displayed if P<0.1)
2C	Body Weight (mg) by Session for Reinforcement Study	Two-way RM ANOVA	Session x Reinforcement	F(12,148) = 4.493	<0.0001	Bonferroni's multiple comparisons test Session 16 FF vs FR5: P=0.0170
			Session	F(3.134,116.0) = 3.935	0.0093	
			Reinforcement	F(3, 37) = 1.238	0.3099	
			Subject	F(37, 148) = 21.79	<0.0001	
2D	Final Body Weight (%Δ from Session 9) for Reinforcement Study	One-way ANOVA	-----	F(3,36) = 2.946	0.0458	Bonferroni's multiple comparisons test FF vs FR5: P=0.0349
2E	Pellets Retrieve (#) by Session for Reinforcement Study	Mixed-Effects Model (REML)	Session	F(4.965,168.4) = 12.05	<0.0001	No Post-Hoc Analysis performed
			Reinforcement	F(3,35) = 17.81	<0.0001	
			Session x Reinforcement	F(39,441) = 1.995	0.0005	
2F	Average Pellets on Floor (Session 9 through Session 16) for Reinforcement Study	One-way ANOVA	-----	F(3,37) = 6.503	0.0012	No Post-Hoc Analysis performed
2G	Total Number of Pokes to Acquisition during Discrimination Learning by Reinforcement Schedule for Reinforcement Study	Log-Rank (Mantel-Cox)	All Groups	χ^2 = 12.1, df = 2	0.0024	-----
			FR1 vs FR3	χ^2 = 5.425, df = 1	0.0594	Bonferroni's correction
			FR1 vs FR5	χ^2 = 10.72, df = 1	0.0033	
			FR3 vs FR5	χ^2 = 1.2, df = 1	0.8199	
2H	Average Pellet Retrieval Time (Session 9 through 16)	One-way ANOVA	-----	F(2,23) = 8.534	0.0017	Tukey's multiple comparisons test FR1 vs FR3: P=0.0047 FR1 vs FR5: P=0.0072

Supplemental Table 3. Statistics for all Behavioral Tests in Figure 3.

Fig.	Test	Statistical Test	Factor	F-Value etc	P-Value	Post-Hoc (Displayed if P<0.1)
3D	**DL** Total Pokes to Acquisition during Discrimination Learning for Saline or Ibotenic Lesioned Animals	Log-Rank (Mantel-Cox)	-----	$\chi^2 = 1.701$, df = 1	0.1922	-----
3E	**RL** Total Pokes to Acquisition during Reversal Learning for Saline or Ibotenic Lesioned Animals	Log-Rank (Mantel-Cox)	-----	$\chi^2 = 6.535$, df = 1	0.0106	-----
3F	**RL** Previously Reinforced Pokes to Acquisition (#) during Reversal Learning for Saline or Ibotenic Lesioned Animals	Unpaired t-Test	-----	t(28) = 2.377	0.0245	-----
3G	**QU** Pellets consumed (# Retrieved - # On Floor) for Saline or Ibotenic Lesioned Animals	Unpaired t-Test	-----	t(28) = 0.3234	0.7488	-----
3H	**QU** Discrimination Index for Saline or Ibotenic Lesioned Animals	Unpaired t-Test	-----	t(28) = 2.445	0.0210	-----
3H	**PR** Breakpoint (Pokes, 30m) for Saline or Ibotenic Lesioned Animals	Unpaired t-Test	-----	t(27) = 2.249	0.0329	-----
3I	**PR** Inactive Pokes (#) over entire session for Saline or Ibotenic Lesioned Animals	Unpaired t-Test	-----	t(27) = 0.003478	0.9973	-----
3J	**EX** Active Pokes (#) During Previous Four days of 3R (3R) compared to Single day Extinction (EX) for Saline or Ibotenic Lesioned Animals	Two-way RM ANOVA	Session x Lesion	F (1, 29) = 0.6830	0.4153	Bonferroni's multiple comparisons test 3R – EX SAL: P=<0.0001 IBO: P=<0.0001
			Session	F (1, 29) = 58.60	<0.0001	
			Lesion	F (1, 29) = 0.03756	0.8477	
			Subject	F (29, 29) = 1.139	0.3640	
3K	**RE** Total Pokes to Acquisition during Reinstatement for	Log-Rank (Mantel-Cox)	-----	$\chi^2 = 0.3958$, df = 1	0.5293	-----

	Saline or Ibotenic Lesioned Animals					

Supplemental Table 4. Statistics for all Behavioral Tests in Figure 4.

Fig.	Test	Statistical Test	Factor	F-Value etc	P-Value	Post-Hoc (Displayed if P<0.1)
4B	**DL** Total Number of Pokes to Acquisition during Discrimination Learning for P129T Animals	Log-Rank (Mantel-Cox)	All Groups	$\chi^2 = 6.350$, df = 3	0.0958	-----
			WTM v KIM	$\chi^2 = 0.05262$, df = 1	<0.9999	Bonferroni's correction
			WTM v WTF	$\chi^2 = 1.219$, df = 1	<0.9999	
			KIM v KIF	$\chi^2 = 3.870$, df = 1	0.1968	
			WTF v KIF	$\chi^2 = 1.122$, df = 1	<0.9999	
4C	**RL** Total Number of Pokes to Acquisition during Reversal Learning for P129T Animals	Log-Rank (Mantel-Cox)	All Groups	$\chi^2 = 1.602$, df = 3	0.6589	-----
4D	**QU** Pellets consumed (# Retrieved - # On Floor) for P129T Animals	Two-way ANOVA	Interaction	F (1, 45) = 0.9896	0.3252	-----
			Sex	F (1, 45) = 1.410	0.2414	
			Genotype	F (1, 45) = 0.1529	0.6977	
4E	**QU** Discrimination Index for P129T Animals	Two-way ANOVA	Interaction	F (1, 45) = 0.03921	0.8439	Bonferroni's multiple comparisons test
			Sex	F (1, 45) = 6.502	0.0143	
			Genotype	F (1, 45) = 3.228	0.0791	Male - Female WT: P=0.1742 KI: P=0.1400
4F	**PR** Breakpoint (Pokes, 30m) for P129T Animals	Two-way ANOVA	Interaction	F (1, 46) = 1.027	0.3161	Bonferroni's multiple comparisons test
			Sex	F (1, 46) = 3.836	0.0562	
			Genotype	F (1, 46) = 4.548	0.0383	WT - KI Male: P=0.8937 Female: P=0.0522
4G	**PR** Inactive Pokes (#) over entire session for P129T Animals	Two-way ANOVA	Interaction	F (1, 46) = 0.0001492	0.9903	Bonferroni's multiple comparisons test
			Sex	F (1, 46) = 4.636	0.0366	
			Genotype	F (1, 46) = 0.01079	0.9177	Male - Female WT: P=0.2229 KI: P=0.3150
4H	**EX** Active Pokes (#) During Previous Four days of 3R (3R) compared to Single day Extinction (EX) for	Three-way ANOVA	Session	F (1, 46) = 88.51	<0.0001	Bonferroni's multiple comparisons test
			Sex	F (1, 46) = 0.009461	0.9229	
			Genotype	F (1, 46) = 8.142	0.0065	3R – EX WTM: P<0.0001 KIM: P=0.0781 WTF: P<0.0001 KIF: P=0.0404
			Session x Sex	F (1, 46) = 0.01854	0.8923	
			Session x Genotype	F (1, 46) = 9.765	0.0031	
			Sex x Genotype	F (1, 46) = 0.004652	0.9459	
			Session x Sex x Genotype	F (1, 46) = 0.1535	0.6971	EX – EX WTM – KIM: P=0.0294 WTF - KIF: P=0.0619

Supplemental Table 4 cont.. Statistics for all Behavioral Tests in Figure 4.

4I	**RE** Total Pokes to Acquisition during Reinstatement for	Log-Rank (Mantel-Cox)	All Groups	$\chi^2 = 5.982$, df = 3	0.1125	-----
4H	**EX** Active Pokes (#) for P129T Animals	Two-way ANOVA	Interaction	F (1, 46) = 0.03052	0.8621	Bonferroni's multiple comparisons test Male (WT vs KI) P=0.0607 ns Female (WT vs KI) P=0.0912 ns
			Sex	F (1, 46) = 0.01420	0.9057	
			Genotype	F (1, 46) = 9.210	0.0040	
4I	**EX** Inactive Pokes (#) for P129T Animals	Two-way ANOVA	Interaction	F (1, 46) = 1.444	0.2356	Bonferroni's multiple comparisons test Male (WT vs KI) P=0.6018 Female (WT vs KI) P=0.0146
			Sex	F (1, 46) = 4.018	0.0509	
			Genotype	F (1, 46) = 7.315	0.0096	
4K	**D. Striatum** FAAH Activity (%)	Unpaired t-Test	-----	t(16)=3.140	0.0063	-----
4L	**mPFC** FAAH Activity (%)	Unpaired t-Test	-----	t(15)=7.917	<0.0001	-----

Supplemental Table 5. Statistics for all Behavioral Tests in Figure S1.

Fig.	Test	Statistical Test	Factor	F-Value etc	P-Value	Post-Hoc (Displayed if P<0.1)
S1A	**DL** Inactive Pokes to Acquisition during Discrimination Learning for Saline or Ibotenic Lesioned Animals	Unpaired t-Test	-----	t(28)=0.6673	0.5101	-----
S1B	**SAL** Total Pokes to Acquisition during Discrimination and Reversal Learning or Saline Lesioned Animals	Log-rank (Mantel-Cox) test	-----	χ^2 = 36.79, df 1	<0.0001	-----
S1C	**IBO** Total Pokes to Acquisition during Discrimination and Reversal Learning or Ibotenic Lesioned Animals	Log-rank (Mantel-Cox) test	-----	χ^2 = 34.15, df 1	<0.0001	-----

Supplemental Table 6. Statistics for all Behavioral Tests in Figure S2.

Fig.	Test	Statistical Test	Factor	F-Value etc	P-Value	Post-Hoc (Displayed if P<0.1)
S2A	**QU** Pellets Retrieved (#) for Saline or Ibotenic Lesioned Animals	Unpaired t-Test	-----	t(28)=0.2058	0.8384	-----
S2B	**QU** Pellets On Floor of Cage (#) for Saline or Ibotenic Lesioned Animals	Unpaired t-Test	-----	t(28)=0.8807	0.3860	-----
S2C	**QU** Active Pokes (#) for Saline or Ibotenic Lesioned Animals	Unpaired t-Test	-----	t(28)=0.2180	0.8290	-----
S2D	**QU** Inactive Pokes (#) for Saline or Ibotenic Lesioned Animals	Unpaired t-Test	-----	t(28)=1.436	0.1620	-----
S2E	**QU** End of Day Percent Correct (%) for Saline or Ibotenic Lesioned Animals	Unpaired t-Test	-----	t(28)=2.445	0.0210	-----
S2F	**QU** Active Pokes (#) in 30 minute bins for Saline or Ibotenic Lesioned Animals	Two-way RM ANOVA	Time x Lesion	F (7, 196) = 2.095	0.0458	-----
			Time	F (7, 196) = 8.343	<0.0001	
			Lesion	F (1, 28) = 0.04752	0.8290	
			Subject	F (28, 196) = 5.287	<0.0001	
S2G	**QU** Inactive Pokes (#) in 30 minute bins for Saline or Ibotenic Lesioned Animals	Two-way RM ANOVA	Time x Lesion	F (7, 196) = 0.4482	0.8706	-----
			Time	F (7, 196) = 2.127	0.0425	
			Lesion	F (1, 28) = 2.055	0.1628	
			Subject	F (28, 196) = 4.479	<0.0001	
S2H	**QU** Active Poke Bias (%) in 30 minute bins for Saline or Ibotenic Lesioned Animals	Mixed-Effects Model (REML)	Time x Lesion	F (7, 189) = 0.8258	0.5670	-----
			Time	F (4.868, 131.4) = 1.115	0.3554	
			Lesion	F (1, 28) = 7.311	0.0115	

Supplemental Table 7. Statistics for all Behavioral Tests in Figure S3.

Fig.	Test	Statistical Test	Factor	F-Value etc	P-Value	Post-Hoc (Displayed if P<0.1)
S3A	**PR** Breakpoint (Pellets, 30m) for Saline or Ibotenic Lesioned Animals	Unpaired t-Test	-----	t(27)=2.118	0.0435	-----
S3B	**PR** Active Pokes (#) for Saline or Ibotenic Lesioned Animals	Unpaired t-Test	-----	t(27)=1.292	0.2073	-----
S3C	**PR** End of Day Percent Correct (%) for Saline or Ibotenic Lesioned Animals	Unpaired t-Test	-----	t(27)=0.4875	0.6298	-----

Supplemental Table 8. Statistics for all Behavioral Tests in Figure S4.

Fig.	Test	Statistical Test	Factor	F-Value etc	P-Value	Post-Hoc (Displayed if P<0.1)
S4A	**EX** Active Pokes (#) for Saline or Ibotenic Lesioned Animals	Unpaired t-Test	-----	t(29)=0.5121	0.6125	-----
S4B	**EX** Inactive Pokes (#) for Saline or Ibotenic Lesioned Animals	Unpaired t-Test	-----	t(29)=0.5494	0.5870	-----
S4C	**EX** End of Day Percent Correct (%) for Saline or Ibotenic Lesioned Animals	Unpaired t-Test	-----	t(29)=0.3507	0.7283’	-----

Supplemental Table 9. Statistics for all Behavioral Tests in Figure S5.

Fig.	Test	Statistical Test	Factor	F-Value etc	P-Value	Post-Hoc (Displayed if P<0.1)
S5A	**DL** Inactive Pokes (#) to Acquisition during Discrimination Learning for P129T animals	Two-way ANOVA	Interaction	F (1, 48) = 0.4377	0.5114	Bonferroni's multiple comparisons test Male - Female WT: P=0.1540 KI: P=0.0249
			Sex	F (1, 48) = 9.801	0.0030	
			Genotype	F (1, 48) = 1.183	0.2823	
S5B	**RL** Previously Reinforced Pokes (#) to Acquisition during Discrimination Learning for P129T animals	Two-way ANOVA	Interaction	F (1, 48) = 0.03076	0.8615	-----
			Sex	F (1, 48) = 0.8103	0.3725	
			Genotype	F (1, 48) = 0.5229	0.4731	
S5C	**WTM** Total Pokes to Acquisition during Discrimination and Reversal Learning for WTM P129T	Log-rank (Mantel-Cox) test	-----	$\chi^2 = 28.08$, df = 1	<0.0001	-----
S5D	**KIM** Total Pokes to Acquisition during Discrimination and Reversal Learning for KIM P129T	Log-rank (Mantel-Cox) test	-----	$\chi^2 = 26.29$, df = 1	<0.0001	-----
S5E	**WTF** Total Pokes to Acquisition during Discrimination and Reversal Learning for WTF P129T	Log-rank (Mantel-Cox) test	-----	$\chi^2 = 28.97$, df = 1	<0.0001	-----
S5F	**KIF** Total Pokes to Acquisition during Discrimination and Reversal Learning for KIF P129T	Log-rank (Mantel-Cox) test	-----	$\chi^2 = 27.00$, df = 1	<0.0001	-----
S5G	**DL** Total Number of Pokes to Acquisition during Discrimination Learning for Saline Lesioned Animals and aged WTM P129T	Log-rank (Mantel-Cox) test	-----	$\chi^2 = 1.128$, df = 1	0.2882	-----
S5H	**RL** Total Number of Pokes to Acquisition during Discrimination Learning for Saline Lesioned Animals and aged WTM P129T	Log-rank (Mantel-Cox) test	-----	$\chi^2 = 7.422$, df = 1	0.0064	-----

Supplemental Table 10. Statistics for all Behavioral Tests in Figure S6.

Fig.	Test	Statistical Test	Factor	F-Value etc	P-Value	Post-Hoc (Displayed if P<0.1)
S6A	**QU** Pellets Retrieved (#) for P129T Animals	Two-way ANOVA	Interaction	F (1, 45) = 0.05014	0.8238	-----
			Sex	F (1, 45) = 0.6836	0.4127	
			Genotype	F (1, 45) = 0.4188	0.5208	
S6B	**QU** Pellets Left on Floor (#) for P129T Animals	Two-way ANOVA	Interaction	F (1, 45) = 6.922	0.0116	Bonferroni's multiple comparisons test WT – KI M: P=0.3115 F: P=0.0523
			Sex	F (1, 45) = 0.6391	0.4282	
			Genotype	F (1, 45) = 0.2902	0.5928	
S6C	**QU** Active Pokes (#) for P129T Animals	Two-way ANOVA	Interaction	F (1, 45) = 0.6931	0.4095	-----
			Sex	F (1, 45) = 0.05228	0.8202	
			Genotype	F (1, 45) = 0.4392	0.5109	
S6D	**QU** Inactive Pokes (#) for P129T Animals	Two-way ANOVA	Interaction	F (1, 45) = 0.03921	0.8439	Bonferroni's multiple comparisons test Male - Female WT: P=0.1742 KI: P=0.1400
			Sex	F (1, 45) = 6.502	0.0143	
			Genotype	F (1, 45) = 3.228	0.0791	
S6E	**QU** End of Day Percent Correct (%) for P129T Animals	Two-way ANOVA	Interaction	F (1, 45) = 6.714	0.0129	Bonferroni's multiple comparisons test WT - KI M: P>0.9999 F: P=0.0028
			Sex	F (1, 45) = 0.003896	0.9505	
			Genotype	F (1, 45) = 4.406	0.0414	

Supplemental Table 11. Statistics for all Behavioral Tests in Figure S7.

Fig.	Test	Statistical Test	Factor	F-Value etc	P-Value	Post-Hoc (Displayed if P<0.1)
S7A	**PR** Breakpoint (Pellets, 30m) for Saline or Ibotenic Lesioned Animals	Two-way ANOVA	Interaction	F (1, 46) = 1.680	0.2014	Bonferroni's multiple comparisons test WT – KI M: P>0.9999 F: P=0.0418
			Sex	F (1, 46) = 4.272	0.0444	
			Genotype	F (1, 46) = 3.908	0.0541	
S7B	**PR** Active Pokes (#) for Saline or Ibotenic Lesioned Animals	Two-way ANOVA	Interaction	F (1, 46) = 0.9791	0.3276	Bonferroni's multiple comparisons test WT – KI M: P=0.8328 F: P=0.0497
			Sex	F (1, 46) = 4.038	0.0504	
			Genotype	F (1, 46) = 4.776	0.0340	
S7C	**PR** End of Day Percent Correct (%) for Saline or Ibotenic Lesioned Animals	Two-way ANOVA	Interaction	F (1, 46) = 0.6130	0.4377	-----
			Sex	F (1, 46) = 1.876	0.1774	
			Genotype	F (1, 46) = 3.138	0.0831	

Supplemental Table 12. Statistics for all Behavioral Tests in Figure S8.

Fig.	Test	Statistical Test	Factor	F-Value etc	P-Value	Post-Hoc (Displayed if P<0.1)
S8A	**EX** Active Pokes (#) on Day 1 of EX for P129T Animals	Two-way ANOVA	Interaction	F (1, 46) = 0.03052	0.8621	Bonferroni's multiple comparisons test WT - KI M: P=0.0607 F: P=0.0912
			Sex	F (1, 46) = 0.01420	0.9057	
			Genotype	F (1, 46) = 9.210	0.0040	
S8B	**EX** Inactive Pokes (#) on Day 1 of EX for P129T Animals	Two-way ANOVA	Interaction	F (1, 46) = 1.444	0.2356	Bonferroni's multiple comparisons test WT - KI M: P=0.06018 F: P=0.0146
			Sex	F (1, 46) = 4.018	0.0509	
			Genotype	F (1, 46) = 7.315	0.0096	
S8C	**EX** End of Day Percent Correct (%) on Day 1 of EX for P129T Animals	Two-way ANOVA	Interaction	F (1, 46) = 2.879	0.0965	Bonferroni's multiple comparisons test Male - Female WT: P>0.9999 KI: P=0.0129
			Sex	F (1, 46) = 6.608	0.0135	
			Genotype	F (1, 46) = 0.2692	0.6063	
S8D	**EX** Total Pokes to Extinction Criterion for P129T Animals	Log-Rank (Mantel-Cox)	-----	$\chi^2 = 3.040$, df = 3	0.3856	-----
S8E	**EX** Sessions to Extinction Criterion (#) for P129T Animals	Two-way ANOVA	Interaction	F (1, 48) = 0.2681	0.6070	Bonferroni's multiple comparisons test Male - Female WT: P=0.1530 KI: P=0.0500
			Sex	F (1, 48) = 8.594	0.0052	
			Genotype	F (1, 48) = 0.6320	0.4305	

Supplemental Table 13. Statistics for all Behavioral Tests in Figure S9.

Fig.	Test	Statistical Test	Factor	F-Value etc		P-Value	Post-Hoc (Displayed if P<0.1)
S9A	Right Poke Bias over 24h	D'Agostino & Pearson test	Normal Distribution	K2 = 1.313		0.4457	
		Descriptive Statistics		Number of values	222		
				Minimum	0.1429		
				25% Percentile	0.4539		
				Median	0.5668		
				75% Percentile	0.6722		
				Maximum	0.9577		
				Range	0.8149		
				Mean	0.5566		
				Std. Deviation	0.1542		
				Std. Error of Mean	0.01035		

Supplemental Table 14. Statistics for all Molecular Tests in Figure S10.

Fig.	Test	Statistical Test	Factor	F-Value etc	P-Value	Post-Hoc (Displayed if P<0.1)
S10A	**Whole Brain** FAAH Activity (%)	Unpaired t-Test	-----	t(19)=4.593	0.0002	-----
S10B	**mPFC** FAAH Activity (%)	Unpaired t-Test	-----	t(15)=7.917	<0.0001	-----
S10C	**OFC** FAAH Activity (%)	Unpaired t-Test	-----	t(16)=7.114	<0.0001	-----
S10D	**Arcuate Cingulate Nucleus** FAAH Activity (%)	Unpaired t-Test	-----	t(18)=3.046	0.0070	-----
S10E	**Nucleus Accumbens** FAAH Activity (%)	Unpaired t-Test	-----	t(12)=0.2168	0.8320	-----
S10F	**Dorsal Striatum** FAAH Activity (%)	Unpaired t-Test	-----	t(16)=3.140	0.0063	-----
S10G	**Amygdala** FAAH Activity (%)	Unpaired t-Test	-----	t(18)=3.032	0.0072	-----
S10H	**Lateral Hypothalamus** FAAH Activity (%)	Unpaired t-Test	-----	t(18)=0.2275	0.8226	-----
S10I	**Hippocampus** FAAH Activity (%)	Unpaired t-Test	-----	t(16)=2.848	0.0116	-----
S10J	**Substantia Nigra** FAAH Activity (%)	Unpaired t-Test	-----	t(17)=0.3826	0.7067	-----
S10K	**Ventral Tegmental Area** FAAH Activity (%)	Unpaired t-Test	-----	t(11)=2.724	0.0198	-----

4.11C Supplemental Text

DETAILED GUIDE FOR PULLING DATA FROM THE FED3

PHYSICAL MATERIALS NEEDED

1. Multi-port USB hub
    a. Examples (Amazon ASIN)
    b. Amazon Basics USB 3.0 10 Port HUB (B07V6MXF3C)
    c. SABRENT 13 port High Speed USB 2.0 HUB (B00HL7Z46K)
2. Micro-SD readers
    a. Examples (Amazon ASIN)
    b. USB SD Card Reader for PC, 3 Packs Micro SD Card to USB Adapter, Card Reader for Camera Memory Card Reader, Wansurs Card Reader for Laptop (3 Pack USB2.0) (B0B9R7H765)
    c. SanDisk MobileMate USB 3.0 microSD Card Reader- SDDR-B531-GN6NN (B07G5JV2B5)
3. Multi-card SD holder
    a. Examples (Amazon ASIN)
    b. 10 Slots Micro SD Card Case Holder Storage Organizer (B07T6SWXK5)
    c. BANDC Micro SD/SDHC/SDXC Card Storage Holder Case (B0196PR0H0)

CUSTOMIZING THE PYTHON CODE

1. Download and install Python using default settings. All libraries used by this code are included in Python's default settings.
2. Open the supplied python code (Pulling_Data_From_SD_Cards.py) in your preferred code editor (Atom, Notepad++, Serris, etc).
3. Lines 36 and 52 of the code denote where extracted files will be saved to. Alter these lines as needed, making sure to use double backslashes. These values must match. At the location specified a new main folder and sub folders will be created based on values specified in the reference file.

FILLING IN THE REFERENCE FILE

The reference file is how the Python code searches through the FED3 data to identify which files to copy to the computer. The reference file can be written at the beginning of the study or written day-by-day, saved as one file, or as daily files. Once data for one animal or one day has been written the data can be copied and pasted for the rest of the studies, with only the details in B, E, G, H, and sometimes C needing updating. Leaving cells in columns other than F will result in the python code encountering an error or malfunctioning.

Column A- FED_Name: Populate with ‘FED’ followed by the three digit identifier.

- This identifier is determined by a file on the SD card itself, named “Fed_Number”

Column B- Date_Code: Populate with the date code written as mmddyy with a preceding apostrophe.

- If the FED3 has a working real time clock this will be the date the test was run. If the FED3’s real time clock has stopped working, the date is displayed when the file is written and in the lower left hand corner of the screen.
- A date can have more than one file if the FED3 was turned off, restarted, or if the real time clock is malfunctioning. In these instances the FED3 file names will end with an underscore followed by several digits. These digits will increase as new files are created (e.g., _00, _01, _02). The python code collects all files that match the Date_Code. If the file number is known the Date_Code can be written as mmddyy_## to limit to the specific file.

Column C- SD_Card: Populate with the letter identifying the drive location the specific SD card will be placed.

- In our experience so long as the multi-hub remains powered through an external source, few if any of these values will change during the experiment. Despite this, we suggest physically writing the drive order on or near the multi-hub, plugging a

single SD card in, waiting for a pop-up window to verify the drive location, and then repeating this step for the other SD cards.

Column D- Cohort: Populate with a title for the main folder the data will be saved to.

- If this folder does not exist, a new folder with this name will be created at the location specified in python code lines 36 and 52.

Column E- Day: Populate with a title for the sub-folder the data will be saved to.

- If this folder does not exist, a new folder with this name will be created at the location specified in python code lines 36 and 52 and Column D.

Column F- New_Fed: In the event that multiple SD cards have the same FED_Name value, and you do not wish to rename the SD card itself, this column can be used to change the FED_Name value after copying te file, but before it is pasted to its new location.

Column G- Test_Date: Populate with the session/day number. Must be written with a CAPITAL D. e.g., session/day 1 = D1.

Column H- Test_Type: Populate with identifiers that our database used to organize the data. This should be changed to correspond to the type of test that is occurring, as follows:

a. FF – Free Feeding
b. FR1 – Fixed Ratio 1 – Left Active
c. FR3 – Fixed Ratio 3 - Left Active
d. FR5 - Fixed Ratio 5 - Left Active
e. 3R - Fixed Ratio 3 Reverse – Right Active
f. PR – Progressive Ratio - Right Active
g. PR_X – Progressive Ratio which had a hardware failure during the test – Right Active
    i. Informs the database that this data should be calculated, but not used for determining stability etc.
h. 3R_PR – A return to 3R after a PR test -Right Active
i. 3R_PR_X – A return to 3R after a PR test with a hardware failure - Right Active
    i. Informs the database that this data should be calculated, but not used for determining stability etc.
j. QU – Quinine – Right Active

k. QU_X – Quinine which had a hardware failure during the test – Right Active
    i. Informs the database that this data should be calculated, but not used for determining stability etc.
l. 3R_QU – A return to 3R after a QU test – Right Active
m. 3R_QU_X – A return to 3R after a QU test with a hardware failure – Right Active
    i. Informs the database that this data should be calculated, but not used for determining stability etc.
n. E – Extinction
o. RE – Return to 3R after Extinction

	A	B	C	D	E	F	G	H
1	FED_Name	Date_Code	SD_Card	Cohort	Day	New_FED	Test_Date	Test_Type
2	FED036	081323	F	FEEDING\\DLRL	d10		D10	E
3	FED000	081323	I	FEEDING\\DLRL	d10	FED099	D10	E
4	FED005	081323	L	FEEDING\\DLRL	d10		D10	E
5	FED023	081323	M	FEEDING\\DLRL	d10		D10	E
6	FED030	081323	D	FEEDING\\DLRL	d10		D10	E
7	FED033	081323	J	FEEDING\\DLRL	d10		D10	E
8	FED039	081323	E	FEEDING\\DLRL	d10		D10	E
9	FED041	081323	G	FEEDING\\DLRL	d10		D10	3R

DAILY TASKS

1. Manually record the information displayed on the FED3 screen (left and right nose pokes, pellets dispensed, etc)
    a. Though this information is typically written to the SD card, errors can occur where the internal date of the FED3 is incorrect, and the user does not catch it when turning the device on or off. In this case the manually recorded numbers can be cross-referenced with the final row of values in various files to find the correct file. In rare cases unknown errors can result in the writing of a blank file for the day. In such cases, the numbers from the screen can be used to estimate operant performance.

AS NEEDED TASKS

- These As Needed Tasks should minimally be performed the first day of each new task, and at the end of every single-day task. An individual's data typically does not need to be puled during the post-acquisition maintenance phase.

If using a criterion based on reaching a minimum amount correct in a rolling average of pokes these tasks should be completed after the first day of each task, and the end of every single-day

task. Once an animal has reached acquisition it is typically unnecessary to pull the data durin ghte post-acquisition maintenance phase.
If using a multi-day criterion the data should be collected every two to three days. The data that is manually recorded at the end of each session can be used to estimate acquisition. Before moving an animal to the next testing stage that animals data should be pulled and analyzed.

Pulling Data From the SD Cards

2. Physically remove the SD card from the FED3 and place it into multi-card holder. Repeat steps 1 and 2 for all devices.
3. Plug SD cards one by one into the multi-hub port, double checking that the letter location matches what is written in the reference file. If the multi-hub port has renamed any locations ensure that you change the reference file as needed
4. Ensure the Reference File is properly populated with the necessary information.
5. Run the supplied python code [name]. The code uses the reference file to search through the SD cards for files based on the following logic:

Search at location ‘SD_Card’ for files that matches ‘FED_Name’. Search through these for files also matching ‘Date_Code’. For files that match this, place the in a good_list.

   a. If a file matching that row is not found, print an error in the python window.
   b. For all files in good_list, append the file name with _ ‘Test_Date’_’Test_Type’
   c. If the row has a value in New_FED, replace FED_Name with New_FED
   d. Paste all files to the location specified in the python code, in a folder called COHORT in a sub folder called DAY.

6. Double check that all files have been pulled. So long as you did not have to restart a FED3 during the session the number of files in location\Cohort\Day should increase by the number of SD cards plugged into the multi-hub. If this number is too low, it indicated a file was not found, which will also be indicated by the python command window printing an error message. Common reasons for a file not being found include:
   a. The SD card was not fully plugged into the SD card reader, or the reader was not plugged into the multi-port hub.
   b. The date code was entered incorrectly.

i. Ensure the date code is written as ‘mmddyy

c. The FED3’s real time clock is incorrect and the filename is under a different date.
    i. Use the manually recorded values to check the SD card for data matching what was recorded. If a file is found you can either change the file name to match what is written in the reference file, or change the reference file to match the file name.

d. A random error occurred, and the file was not written correctly.
    i. In a 40-aimal 20-day study which generated ~800 files we had this occur approximately 5 times, giving this error a <1% chance of occurring.

7. Repeat steps 3 to 6 for all remaining groups of SD cards.
8. Upload the files to the database. 100 files can be uploaded to the database at once, and multiple days of data can be uploaded at once. When the data is uploaded a message will appear at the bottom of the screen.
9. Change the databases’ calculation variables as needed, then press the calculate button to analyze the data based on these criteria. When the data has finished calculating [how it shows that the thing is done].

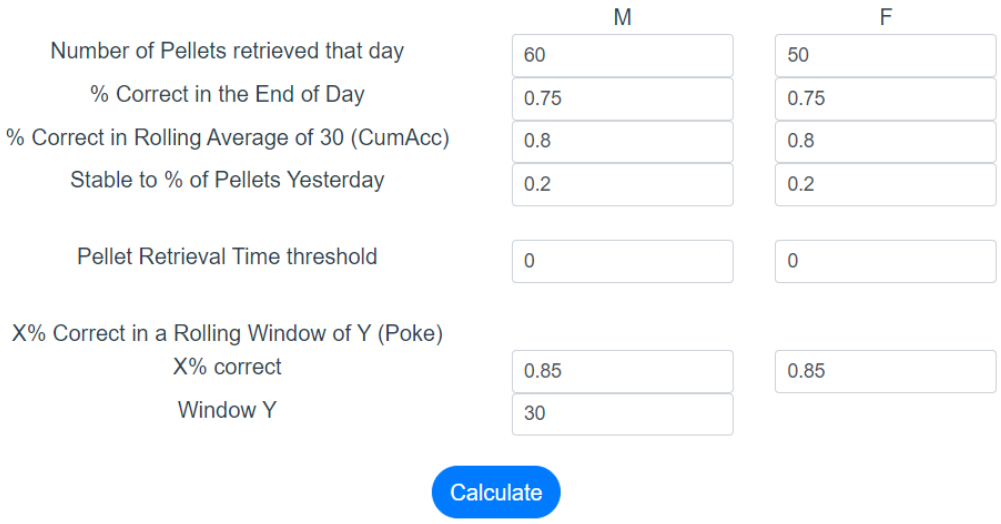

a. Number of pellets retrieved that day
    i. Any numerical value.

ii. The minimum number of pellets in an 8 hour session that an animal must retrieve from the FED3, with different variables based on sex.

b. % correct in the end of day
    i. From 0 to 1
    ii. The minimum percentage correct at the end of the day.
    iii. Calculated as (# active pokes/# Total pokes)

c. % correct in rolling average of 30
    i. From 0 to 1
    ii. The minimum percent correct in a rolling average of 30 cumulative averages that an animal must have met.

d. Stable to % of pellets yesterday
    i. From 0 to 1
    ii. The maximum percent deviation from the prior days number of pellets

e. Pellet Retrieval Time Threshold
    i. Any numerical value.
    ii. Pellet Retrieval Times over this value will be excluded from the Pellet Retrieval calculations.

f. X% correct in a rolling window of Y (Poke): X% correct
    i. From 0 to 1
    ii. The minimum percent correct that must be met in a rolling window of size Y.

g. X% correct in a rolling window of Y (Poke): Window Y
    i. Any numerical value
    ii. The size of the rolling window.

10. Once the data has finished calculating, name and download the .csv file containing the calculated data.

THE CSV FILE

11. The .csv file is arranged into three sheets containing the relevant data.
    a. All_Data1: Acquisition table based on the first four criteria specified. Each column refers to one test day, specified by the Test_Date identifier. Below this

is listed a binary 0/False or 1/True for whether an animal met all 4 criteria for that day. These criteria can be modified in the open source database code.

i. To the right of this acquisition table data are the total number of criteria an animal met for that day.
ii. Below the acquisition table is a table denoting the daily test type for each animal.

b. All_Data2: Individual acquisition criteria based on the criteria specified. Each column refers to one test day, specified by the Test_Date identifier. Each criteria is grouped together, with an animal getting a binary 0/false 1/true score for the criterion. The criterion are arranged as follows and identified in the data_type column. To the right of the binary table the actual values are displayed
    i. Num_p_day: Number of pellets retrieved that day.
    ii. Stab_yesterday: Whether the number of pellets retrieved that day is within the specified stability range to the number of pellets retrieved the previous day.
        1. This will ignore single-day test types like QU and PR. Instead, on the first 3R_QU or 3R_PR will be compared to the last 3R.
    iii. End_day_Acc: Whether the end of day accuracy is above the specified value
    iv. max10_rolling_30: Whether the maximum value for a rolling average of 30 pokes is a
    v. left_pokes_per_day:
    vi. right_pokes_per_day
    vii. Test_type
c. All_data3: Data regarding the pellet retrieval time and when an animal first met the rolling average X in window of Y pokes.
    i. Rt_avg: The animals average retrieval time over the entire session
    ii. Rt_sem: Standard error of the mean for the animals average pellet retrieval time over the entire session.

iii. Rt_Pellet_count: The total number of pellet retrievals that were included in the retrieval time.
iv. Rt_Raw: comma separated cell with each pellet retrieval time listed in it.
v. Rolling_left_poke_30: comma separated cell containing (in order): time elapsed from session start to first time the animal met a rolling average for the left pokes . Timestamp at first time the animal met the rolling average. The total number of left pokes at first time the animal met the rolling average. The total number of right pokes at first time the animal met the rolling average.
vi. Rolling_right_poke_30: Same as above, except calculated for a right poke rolling average.

12. This .csv file can be used as-is, or re-organized.

Custom Python Code for pulling data from the SD cards

```
1  #Pulling_Data_From_SD_Cards.py
2  # Made by Jeremy Decker and Laura Murdaugh on 5/19/2022
3  import numpy as np
4  import pandas as pd
5  from tkinter import filedialog
6  from tkinter import *
7  import datetime
8  import re
9  import math
10 import os
11 import glob
12 import shutil
13 import win32com.client
14
15 def main():
16     # Create a pop-up window that asks you to specify your reference file
17     refroot = Tk()
18     refroot.filename = filedialog.askopenfilename()
19     ref_file = pd.read_excel(refroot.filename)
20     # When reading the reference file, indicate which row the program is working on
21     print(ref_file.shape)
22     for i in range(0, ref_file.shape[0]):
23         print("Processing " + ref_file.FED_Name[i])
24         # Create a "good_list", where files that meet search criterion are temporarily stored
25         good_list = []
26         # search at location SD_Card for files that are .csv, which contain the FED_Name,
   the Date_Code, and are larger than 0kb.
27         for files in glob.glob(ref_file.SD_Card[i] + ':\\*.csv'):
```

```
28          if re.search(ref_file.FED_Name[i], files):
29              if re.search(str(ref_file.Date_Code[i]), files):
30                  fs = os.stat(files)
31                  if fs.st_size > 0:
32                      # For files that meet the criterion, add to good_list.
33                      good_list.append(files)
34      # Check that the below location exists. If not, create it.
35      # When filling the location out, ensure that you use double backslashes. This must match the values in line 52. Further organization can be added here, or by including subfolder location in the Cohort section of the reference file.
36      os.makedirs('C:\\USERS\\USER\\LOCATION\\MAINFOLDER1\\' + ref_file.Cohort[i] + '\\' + str(ref_file.Day[i]), exist_ok=True)
37      # If a file for a row cannot be found, print a line in the command to indicate that.
38      if not good_list:
39          print(f"              File not found:{ref_file.Day[i]}, {ref_file.FED_Name[i]}, {ref_file.Date_Code[i]},{ref_file.Test_Date[i]}")
40      # For files in the good_list append the name with the identifiers from the refernce file.
41      for files in good_list:
42          file_name = os.path.basename(files)
43          test_date = str(ref_file.Test_Date[i])
44          test_type = str(ref_file.Test_Type[i])
45          new_file_name = file_name.rsplit('.', 1)[0] + "_" + test_date + "_" + test_type + "." + file_name.rsplit('.', 1)[1]
46          # If the value for New_FED is not empty, then replace the original FED_Name with the value from New_FED.
47          if pd.notnull(ref_file.New_FED[i]):
48              new_fed = str(ref_file.New_FED[i])
49              new_file_name = new_fed + new_file_name[len(ref_file.FED_Name[i]):]
50          # Move the files from the good_list to the location below.
```

```
51          # When filling the location out, ensure that you use double backslashes. This must match the values in line 35. Further organization can be added here, or by including subfolder location in the Cohort section of the reference file.
52              destination = os.path.join('C:\\USERS\\USER\\LOCATION\\MAINFOLDER1\\' + ref_file.Cohort[i] + '\\' + str(ref_file.Day[i]), new_file_name)
53              shutil.copy(files, destination)
54
55  if __name__ == '__main__':
56      main()
```

SUMMARY AND CONCLUSIONS

GENERAL SUMMARY

In summary, the ability to efficiently and comprehensively investigate rodent behavior is of paramount importance for multiple fields, including neuroscience. Utilization of a single behavioral test may result in inaccurate conclusions or an incomplete understanding of the effects of manipulation. Thus, researchers should utilize multiple related tests in the form of a test battery to more comprehensively capture and understand behavioral changes. In this dissertation I have presented results utilizing standard test batteries and documented a novel operant test battery with a broad focus on pain-like, affective, and operant behaviors. Together, the information in this dissertation demonstrates the utility of multi-faceted behavioral assays and the combination of traditional and novel approaches to collect more comprehensive behavioral data, which will allow researchers to better investigate neural circuitry underlying behaviors or the behavioral changes associated with novel therapeutics.

While not the sole focus of my work, two chapters (Chapter 2 and Chapter 4) investigated the role of n-acyl-ethanolamines (NAEs) on aspects of affective, pain-like, and cognitive behavior. Chapter 2 focused on disruption of NAE synthesis which results in decreased level of specific NAEs, while Chapter 4 focused on a mutation in the Fatty Acid Amide Hydrolase (FAAH) gene, which results in increased NAE levels in specific regions. From these complementary studies I found evidence that further supports the role of NAEs in these behaviors, as has been suggested from previous research.

SUMMARY AND FUTURE DIRECTIONS OF CHAPTER 2:

In this study we used a combination of affective and pain-like behavioral test batteries to investigate the role of N-acylphosphatidylethanolamine Phospholipase D (NAPE-PLD) on behavior in male and female mice. NAPE-PLD is an enzyme important for the biosynthesis of n-acyl-ethanolamines (NAEs), key lipid mediators of the endocannabinoid system (ECS). The ECS is implicated in numerous behaviors and physiological processes including affective, stress, and inflammatory responses, and has thus been the focus of numerous preclinical studies. However, many of these studies have focused on fatty acid amide hydrolase (FAAH), the primary enzyme for NAE metabolization, overlooking the potential effects of modulating NAE biosynthesis. As

such, we investigated the effects of global NAPE-PLD knockout in both sexes to investigate the effects of chronic and systemic NAPE-PLD inactivation.

We found that NAPE-PLD KO mice exhibited a subset of behaviors associated with FAAH manipulation. NAPE-PLD KO resulted in reduced sucrose preference, a measure of anhedonia. However, the KO mice displayed otherwise normal anxiety- and depression-like behaviors. These findings support a role of NAPE-PLD in mediating an interaction between stress and anhedonic behavior. These results further suggest that while NAPE-PLD inactivation may not serve as a likely candidate for novel psychiatric therapeutics, it would likely be well-tolerated. Indeed, the ECS is often implicated in inflammation and the pain response. We found that NAPE-PLD KO did not alter mechanical allodynia or functional grip force during a model of inflammatory arthritis, but did alter baseline thermal response sensitivity. Overall, these results suggest that NAPE-PLD would likely not be a high-value target for treating inflammatory arthritis, but did not preclude the involvement of NAPE-PLD in other aspects pain, like neuropathic pain. Future directions of this study may include the investigation of NAPE-PLD in other disease mechanisms or the effects of NAPE-PLD KO on other affective or cognitive behaviors.

SUMMARY AND FUTURE DIRECTIONS OF CHAPTER 3:

In this study we used a combination of physiological, affective, pain-like, and operant measures to investigate the effects of a novel chronic vapor exposure (CVE) model in mice. Nicotine dependence is among the leading causes of preventable death worldwide, with high relapse rates in those attempting to quit. Electronic Nicotine Delivery Systems (ENDS) represent a novel approach to create preclinical animal models of nicotine dependence via inhalation. The aim of this study was to validate a new model of chronic nicotine exposure in mice using an ENDS and measure changes in affective behavior and operant responding. First, we validated vapor chambers (La Jolla Vapor) by performing a pharmacokinetic study using ultra performance liquid chromatography tandem mass spectrometry (UPLC-MS/MS) to quantify nicotine in blood. Next, we assessed the effect of different exposure doses on body weight, locomotor activity, and mechanical allodynia to determine an inter vape interval for further testing. At a dose that produces signs of nicotine dependence (10 min frequency), no effect of nicotine abstinence on anxiety-like (open field test and light/dark box) or depressive-like behaviors (splash test and sucrose preference test) were observed. In measures of operant responding, abstinence from

nicotine increased the number of sessions until acquisition, decreased number of rewards before breakpoint in a progressive ratio task, and increased consumption of quinine pellets during an aversive reward task. These results inform the ongoing investigation of effects of CVE and present a novel vapor-based method of exposure and demonstrate the utility of the FED3 to perform operant tasks in models of addiction-like behavior.

SUMMARY AND FUTURE DIRECTIONS OF CHAPTER 4:

Understanding how and why an organism makes goal-directed decisions is crucial to multiple fields, including psychology and neuroscience. While this can be studied using traditional operant chambers, aspects of the chambers prevent high throughput investigations, limiting our knowledge. In this manuscript I described the protocol for investigating behaviors related to goal-based decision-making and executive function (EF). This protocol allows for the efficient investigation of 6 operant tests in as few as 19 sessions. I demonstrated construct validity of the discrimination and reversal learning (DL/RL) aspect of this protocol using orbitofrontal cortex (OFC) lesions, additionally finding that lesions reduced responding in a progressive ratio (PR) test. Using this protocol I identified sex- and genotype-specific differences in an aged P129T mouse model. These mice contain a mutation associated with addictive behavior in humans, demonstrating that this protocol can be used to investigate altered decision-making in addiction-related models. Finally, to encourage the uptake of this protocol we designed a custom Python-based database and described a data pipeline for efficient analysis of operant behavior.

The work shared in this manuscript allows for the more cost- and labor-efficient investigation of goal-directed behavior and EF. The protocol developed could improve the comprehensive investigation of decision-making behavior across multiple disciplines, increasing our understanding of executive dysfunction and opening the field to new researchers. This protocol could allow researchers to evaluate the neural mechanisms underlying decision-making more comprehensively or increase pre-clinical investigation of cognitive effects of novel therapeutics.

For instance, the Buczynski-Gregus lab is broadly interested in behavioral pharmacology with a focus on novel therapeutics focusing on pain states and addiction. We are particularly excited by this protocol, as it will allow for more comprehensive behavioral investigation during temporally limited states. For instance, we are interested in investigating the effects of a novel therapeutic targets on chemotherapy-induced peripheral neuropathy (CIPN). While the duration of

paclitaxel-based CIPN models may vary in response to dose and delivery schedule, our model resolves within 30 day. To investigate the cognitive effects of this novel therapeutic in a traditional operant chamber, we would either need to induce CIPN after initial DL and/or limit our investigation to a few key behaviors; either of these decisions could result in key cognitive effects being overlooked. If we wished to perform a full investigation of all 6 behaviors captured in my test, we would need to run multiple cohorts of animals, which would limit our ability to compare results between groups. Instead, the protocol detailed in this manuscript will allow us to investigate multiple aspects of cognitive behavior before the resolution of CIPN, or allow us to investigate potential effects of novel therapeutics to reduce or prevent the onset of cognitive deficits associated with CIPN. This protocol could be applied to other temporally limited models, including CFA pain models, TBI models, or aging models. The challenges presented by attempting multi-test cognitive batteries with temporally limited models may have presented an additional critical barrier to entry for research groups outside of the traditional cognitive field, a barrier which is rectified by the FED3 model proposed here.